2018

Topics in generalized linear mixed models and spatial subgroup analysis

Xin Wang
Iowa State University

Topics in generalized linear mixed models and spatial subgroup analysis

by

Xin Wang

A dissertation submitted to the graduate faculty

in partial fulfillment of the requirements for the degree of

DOCTOR OF PHILOSOPHY

Major: Statistics

Program of Study Committee:
Zhengyuan Zhu, Co-major Professor
Vivekananda Roy, Co-major Professor
Emily Berg
Alicia Carriquiry
Huaiqing Wu

The student author, whose presentation of the scholarship herein was approved by the program of study committee, is solely responsible for the content of this dissertation. The Graduate College will ensure this dissertation is globally accessible and will not permit alterations after a degree is conferred.

Iowa State University

Ames, Iowa

2018

DEDICATION

To my husband Lanfeng and my brother Chong.

TABLE OF CONTENTS

Page

LIST OF TABLES

Page

LIST OF FIGURES

Page

ACKNOWLEDGEMENTS

I would like to take opportunity to thank my advisors Dr. Zhengyuan Zhu and Dr. Vivekananda Roy for their guidance, patience, encouragement and support during my five years study and research. Without their help, I cannot complete this work and pursue my career. From them, I have learned the way and the attitude of doing research.

I would also like to thank my committee members for their efforts and contributions to this work: Dr. Emily Berg, Dr. Alicia Carriquiry and Dr. Huaiqing Wu. Thank Dr. Emily Berg for all her kind and great help in my research assistant work. I would also like to thank Dr. Kenneth Koehler for his guidance of teaching. Additionally, I would like to thank Dr. Dongchu Sun and Dr. Helen Hao Zhang for their suggestions of my research work.

I would like to thank my parents for their endless love and support. Especially my mother, she tries to understand my life that is far away from her. I would also like to thank my friends both in China and USA. Thanks Hailan for her smile, support and help.

ABSTRACT

In this thesis, two topics are studied, generalized linear mixed models and spatial subgroup analysis.

Within the topic of generalized linear mixed models, this thesis focuses on three aspects. First, estimation of link function in generalized linear models is studied. We propose a new algorithm that uses P-spline for nonparametrically estimating the link function which is guaranteed to be monotone. We also conduct extensive simulation studies to compare our nonparametric approach with various parametric approaches. Second, a spatial hierarchical model based on generalized Dirichlet distribution is developed to construct small area estimators of compositional proportions in the National Resources Inventory survey. At the observation level, the standard design based estimators of the proportions are assumed to follow the generalized Dirichlet distribution. After proper transformation of the design based estimators, beta regression is applicable. We consider a logit mixed model for the expectation of the beta distribution, which incorporates covariates through fixed effects and spatial effect through a conditionally autoregressive process. Finally, convergence rates of Markov chain Monte Carlo algorithms for Bayesian generalized linear mixed models are studied. For Bayesian probit linear mixed models, we construct two-block Gibbs samplers using the data augmentation (DA) techniques and prove the geometric ergodicity of the Gibbs samplers under both proper priors and improper priors. We also provide conditions for posterior propriety when the design matrices take commonly observed forms. For Bayesian logistic regression models, we establish that the Markov chain underlying Polson et al.'s (2013) DA algorithm is geometrically ergodic under a flat prior. For Bayesian logistic linear mixed models, we construct a two-block Gibbs sampler using Polson et al.'s (2013) DA technique under proper priors and prove the uniform ergodicity of this Gibbs sampler.

The other topic is spatial subgroup analysis with repeated measures. We use pairwise concave penalties for the differences among group regression coefficients based on smoothly clipped absolute deviation penalty. We also consider pairwise weights associated with each paired penalty based on spatial information. We show that the oracle estimator based on weighted least square is a local minimizer of the objective function with probability approaching 1 under some conditions. In the simulation study, we compare the performances of different weights as well as equal weights, which shows that the spatial information will help when the minimal group difference is small or the number of repeated measures is small.

CHAPTER 1. OVERVIEW

Analyzing non-Gaussian data is an important topic in Statistics. Generalized linear models (GLMs) and Generalized linear mixed models (GLMMs) are often used. This topic is studied in both methodological and theoretical aspects. Besides that, spatial subgroup analysis is also studied.

In Chapter 2, we propose a new algorithm to estimate the unknown link function with monotone constraints in GLMs. In classical GLMs, the link function is assumed to be a known function. Examples of traditional link functions include logit, probit and the complementary log-log (cloglog) links. Czado and Santner (1992) showed that misspecification of link function can introduce bias and increase mean squared error of regression coefficient estimates and the predicted probabilities for binary data. Flexible families of link functions have been proposed in the literature to address the misspecification problem. These link functions usually have parameters to control the skewness of link functions, such as robit link function (Liu, 2004), GEV link function (Wang and Dey, 2010) and symmetric power link family (Jiang et al., 2013). Besides parametric link functions, Muggeo and Ferrara (2008) proposed a generalized single index model (GSIM), which assumed an unknown link function with linear predictors. In Muggeo and Ferrara (2008), the link function is estimated by P-spline (Eilers and Marx, 1996; Eilers et al., 2015) and the monotone assumption is dealt with by introducing a very large penalty term. The algorithm we propose can be applied to models with more than one covariate and can estimate the link function and the regression coefficients simultaneously. The algorithm is an iterative procedure with two steps. The first step is to estimate the unknown link function. The transformation in Wang and Yang (2009) is used to restrict the domain of the index. The quadratic optimization based method is then applied to estimate the monotone link function when fixing the estimates of the regression coefficients, which can guarantee that we have a monotone link function. The second step is to estimate the regression coefficients when fixing the link function. We also conduct a simulation study to compare logit,

probit, robit, GEV, splogit, generalized additive model with our proposed algorithm in binary data. The simulation study shows that the nonparametric link function model estimated by our proposed algorithm has the best overall performance, and can approximate different parametric link functions very well when the data is simulated from these link functions.

In Chapter 3, a spatial hierarchical model is developed to produce county level estimates for the National Resources Inventory (NRI) survey. The proposed model is based on a generalized Dirichlet (GD) distribution to construct small area estimators of compositional proportions in several mutually exclusive and exhaustive land cover categories. Because of small sample sizes, standard NRI estimators can have relatively large estimated coefficients of variation at the county level. Additional sources of information, particularly auxiliary variables and explicit model assumptions, are needed to improve the precision of the county level estimators. The proposed model has several characteristics. First, estimators based on the model respect the parameter space for the proportions and satisfy a sum-to-one constraint. Second, the model allows incorporation of covariates and spatial dependence structures to provide more information to improve the estimators. Additionally, it can incorporate the estimated variance of the original NRI estimators to appropriately reflect NRI sample design and estimation procedures. To specify a model appropriate for the NRI application, we begin with an assumption that the observed county level compositional proportions are realizations from the GD distribution, which is a flexible distribution for vectors of compositional proportions. The GD assumption permits a transformation of the county level proportions to independent beta random variables with distinct mean and dispersion parameters. The expectation of the beta distribution is modeled as a logit-linear mixed model with covariates describing large scale structure and spatially correlated random effects for counties. The spatial structure is specified through a spatial conditionally autoregressive (CAR) model, as in Banerjee et al. (2014). Our variance model exploits both the chi-square distribution and the lognormal distribution, which extends that of Maiti et al. (2014) to incorporate covariates. In a design based evaluation study, the proposed model based estimators are shown to have smaller root mean squared error and relative root mean squared error than design based estimators and multinomial model based estimators

(López-Vizcaíno et al., 2013). We also apply the proposed models to estimate the proportions of area in several broaduses for Iowa counties in 2012.

In Chapter 4, we consider Markov chain Monte Carlo (MCMC) algorithms for exploring the intractable posterior densities associated with Bayesian probit linear mixed models under both proper and improper priors on the regression coefficients and variance components. In particular, we construct two-block Gibbs samplers using the data augmentation (DA) techniques. In order to provide valid standard errors, we need to establish a central limit theorem (CLT) for the time average estimators. The only standard method of establishing CLT for MCMC estimators, is to prove that the underlying Markov chain is *geometrically ergodic* (Jones and Hobert, 2001). Geometric ergodicity is also needed for consistently estimating the asymptotic variance in the Markov chain CLT (Flegal and Jones, 2010). Under proper priors, the Gibbs sampler Markov chain is geometrically ergodic under truncated priors on precision parameters. While under improper priors, the conditions for geometric convergence are similar to those guaranteeing posterior propriety. We also provide conditions for posterior propriety when the design matrices take commonly observed forms. DA algorithms are known to suffer from slow convergence (Meng and Van Dyk, 1999; Van Dyk and Meng, 2001). The Haar parameter expanded data augmentation (PX-DA) algorithm (Liu and Wu, 1999) is an improvement of the DA algorithm and it has been shown that it is theoretically at least as good as the DA algorithm (Hobert and Marchev, 2008) in both efficiency and operator norm ordering. We propose corresponding Haar PX-DA algorithms, which have essentially the same computational cost as the two-block Gibbs samplers. An example is used to show the efficiency gain of the Haar PX-DA algorithm over the block Gibbs sampler and the full Gibbs sampler.

In Chapter 5, the MCMC algorithm for Bayesian logistic linear model is studied. Logistic regression model is the most popular model for analyzing binary data, which is due to the fact that the expectation of observing 1 has a closed form as a function of linear predictors, and it is also easy to interpret the coefficients in terms of odds ratio. In Bayesian framework, when there is no prior information available about the parameters, noninformative priors are generally used. A popular method of analyzing binary data is by fitting a Bayesian logistic regression model with a

flat prior on unknown coefficients. The resulting intractable posterior density can be explored by running Polson et al.'s (2013) DA algorithm. We establish that the Markov chain underlying Polson et al.'s (2013) DA algorithm is geometrically ergodic under the necessary and sufficient conditions for propriety of the posterior density (Chen and Shao, 2001). Proving this theoretical result is practically important as it ensures the existence of central limit theorems for sample averages under a finite second moment condition. The CLT in turn allows users of the DA algorithm to calculate standard errors for posterior estimates. In Chapter 6, we construct a two-block Gibbs sampler using Polson et al.'s (2013) DA technique for Bayesian logistic linear mixed models with normal priors on regression parameters and truncated Gamma priors on precision parameters. Furthermore, we prove the uniform ergodicity of this Gibbs sampler.

In Chapter 7, spatial subgroup analysis with repeated measures is studied. Spatial clustering or spatial boundaries detection is an important problem in disease mapping, spatial epidemiology and population genetics (Hegarty and Barry, 2008; Reich and Bondell, 2011; Lawson, 2013; Li et al., 2015). Ma and Huang (2016) and Ma and Huang (2017) considered the problem in linear regression settings and used the smoothly clipped absolute deviation penalty (Fan and Li, 2001) and the minimax concave penalty (Zhang, 2010). In spatial data analysis, observations near each other could share similar patterns. So spatial dependence information should be considered in models to find homogeneous groups. We consider a spatial clustering or spatial subgroup analysis problem based on regression coefficients for spatial areal data with repeated measures. We use pairwise concave penalties for the differences among group (cluster) regression coefficients. We also consider pairwise weights associated with each paired penalty based on spatial information. Theoretical properties of the proposed estimators are proved. Besides that, several different pairwise weights are studied in the simulation study according to the estimated number of groups, root mean square error and adjusted Rand index. The results show that the spatial information will help when the minimal group difference is small, or the number of repeated measures is small. An example is also used to illustrate our proposed estimators.

Bibliography

Banerjee, S., Carlin, B. P., and Gelfand, A. E. (2014). *Hierarchical modeling and analysis for spatial data*. Crc Press.

Chen, M.-H. and Shao, Q.-M. (2001). Propriety of posterior distribution for dichotomous quantal response models. *Proceedings of the American Mathematical Society*, 129(1):293–302.

Czado, C. and Santner, T. J. (1992). The effect of link misspecification on binary regression inference. *Journal of statistical planning and inference*, 33(2):213–231.

Eilers, P. H. and Marx, B. D. (1996). Flexible smoothing with B-splines and penalties. *Statistical science*, 11(2):89–121.

Eilers, P. H., Marx, B. D., and Durbán, M. (2015). Twenty years of P-splines. *SORT-Statistics and Operations Research Transactions*, 39(2):149–186.

Fan, J. and Li, R. (2001). Variable selection via nonconcave penalized likelihood and its oracle properties. *Journal of the American statistical Association*, 96(456):1348–1360.

Flegal, J. M. and Jones, G. L. (2010). Batch means and spectral variance estimators in Markov chain Monte Carlo. *The Annals of Statistics*, 38(2):1034–1070.

Hegarty, A. and Barry, D. (2008). Bayesian disease mapping using product partition models. *Statistics in medicine*, 27(19):3868–3893.

Hobert, J. P. and Marchev, D. (2008). A theoretical comparison of the data augmentation, marginal augmentation and PX-DA algorithms. *The Annals of Statistics*, 36(2):532–554.

Jiang, X., Dey, D. K., Prunier, R., Wilson, A. M., and Holsinger, K. E. (2013). A new class of flexible link functions with application to species co-occurrence in cape floristic region. *The Annals of Applied Statistics*, 7(4):2180–2204.

Jones, G. L. and Hobert, J. P. (2001). Honest exploration of intractable probability distributions via Markov chain Monte Carlo. *Statistical Science*, 16(4):312–334.

Lawson, A. B. (2013). *Bayesian disease mapping: hierarchical modeling in spatial epidemiology*. CRC press.

Liu, C. (2004). Robit regression: a simple robust alternative to logistic and probit regression. In *Applied Bayesian modeling and causal inference from incomplete-data perspectives*, pages 227–238. Wiley: London.

Liu, J. S. and Wu, Y. N. (1999). Parameter expansion for data augmentation. *Journal of the American Statistical Association*, 94(448):1264–1274.

López-Vizcaíno, E., Lombardía, M. J., and Morales, D. (2013). Multinomial-based small area estimation of labour force indicators. *Statistical modelling*, 13(2):153–178.

Ma, S. and Huang, J. (2016). Estimating subgroup-specific treatment effects via concave fusion. *arXiv preprint arXiv:1607.03717*.

Ma, S. and Huang, J. (2017). A concave pairwise fusion approach to subgroup analysis. *Journal of the American Statistical Association*, 112(517):410–423.

Maiti, T., Ren, H., and Sinha, S. (2014). Prediction error of small area predictors shrinking both means and variances. *Scandinavian Journal of Statistics*, 41(3):775–790.

Meng, X.-L. and Van Dyk, D. A. (1999). Seeking efficient data augmentation schemes via conditional and marginal augmentation. *Biometrika*, 86:301–320.

Muggeo, V. M. and Ferrara, G. (2008). Fitting generalized linear models with unspecified link function: A P-spline approach. *Computational Statistics & Data Analysis*, 52(5):2529–2537.

Polson, N. G., Scott, J. G., and Windle, J. (2013). Bayesian inference for logistic models using Pólya-Gamma latent variables. *Journal of the American statistical Association*, 108(504):1339–1349.

Reich, B. J. and Bondell, H. D. (2011). A spatial Dirichlet process mixture model for clustering population genetics data. *Biometrics*, 67(2):381–390.

Van Dyk, D. A. and Meng, X.-L. (2001). The art of data augmentation (with discussion). *Journal of Computational and Graphical Statistics*, 10:1–50.

Wang, L. and Yang, L. (2009). Spline estimation of single-index models. *Statistica Sinica*, 19(2):765–783.

Wang, X. and Dey, D. K. (2010). Generalized extreme value regression for binary response data: an application to B2B electronic payments system adoption. *The Annals of Applied Statistics*, 4(4):2000–2023.

Zhang, C.-H. (2010). Nearly unbiased variable selection under minimax concave penalty. *The Annals of statistics*, 38(2):894–942.

CHAPTER 2. A NEW ALGORITHM TO ESTIMATE MONOTONE NONPARAMETRIC LINK FUNCTIONS AND A COMPARISON WITH PARAMETRIC APPROACH

Modified from a paper accepted by *Statistics and Computing*

Xin Wang[1], Vivekananda Roy and Zhengyuan Zhu

Department of Statistics, Iowa State University

Abstract

The generalized linear model (GLM) is a class of regression models where the means of the response variables and the linear predictors are joined through a link function. Standard GLM assumes the link function is fixed, and one can form more flexible GLM by either estimating the flexible link function from a parametric family of link functions or estimating it nonparametically. In this paper, we propose a new algorithm that uses P-spline for nonparametrically estimating the link function which is guaranteed to be monotone. It is equivalent to fit the generalized single index model with monotonicity constraint. We also conduct extensive simulation studies to compare our nonparametric approach for estimating link function with various parametric approaches, including traditional logit, probit and robit link functions, and two recently developed link functions, the generalized extreme value link and the symmetric power logit link. The simulation study shows that the link function estimated nonparametrically by our proposed algorithm performs well under a wide range of different true link functions and outperforms parametric approaches when they are misspecified. A real data example is used to illustrate the results.

key words: Generalized linear model; Monotone link functions; P-spline; Single index model; Skewed link functions

[1]Corresponding author

2.1 Introduction

In the generalized linear model (GLM) setup, a link function is used to link the predictors and the expectation of the response variable (McCullagh and Nelder, 1989). In classical GLMs, the link function is assumed to be a known function. Examples of traditional link functions include logit, probit and the complementary log-log (cloglog) links. Czado and Santner (1992) showed that misspecification of link function can introduce bias and increase mean squared error of regression coefficient estimates and the predicted probabilities for binary data. Flexible families of link functions have been proposed in the literature to address the misspecification problem. Pregibon (1980) considered tests and estimation of link function through model linearization. Aranda-Ordaz (1981) considered two families of link functions for both symmetric and asymmetric cases. Mallick and Gelfand (1994) used a mixture beta cumulative distribution with fixed number of components as a link function. Liu (2004) proposed the robit link function which assumes the link function to be the inverse cumulative distribution function (CDF) of a t distribution with the degrees of freedom as a parameter. Several algorithms are proposed in the literature to estimate the parameters of the robit model, see, e.g., Liu (2004) and Roy (2014). The robit link function can approximate both the logit link and the probit link with different values of degrees of freedom. One limitation of the robit link function is that it is symmetric in the sense that the probabilities going to 0 and 1 have the same rates (Jiang et al., 2013). Kim et al. (2008) proposed a flexible class of link functions based on a generalized skewed t distribution. Another skewed link function based on the generalized extreme value distribution (GEV) was introduced by Wang and Dey (2010), in which a shape parameter is used to control the skewness of the link function. They used simulation study to show that GEV link is a more flexible link function by comparing it with logit, probit and cloglog links in a Bayesian framework. An undesirable property of the GEV link is that the support of GEV distribution is not the whole real line. Jiang et al. (2013) proposed a symmetric power link family, which has a parameter to control the skewness, to analyze a species co-occurrence data set. One of the members of this family is the splogit link function, which has logistic distribution as the base

function. Both t distribution and exponential distribution can also be used as base functions in Jiang et al. (2013)'s symmetric power links.

Instead of using flexible link functions, alternately, one can use a simple link function and fit a more flexible regression model. Hastie and Tibshirani (1990) and Wood (2006) developed the generalized additive model (GAM), in which they used a traditional fixed link function and fitted an additive model for the covariates. Some extensions are reviewed in Härdle et al. (2012). When there is one covariate, GAM can be viewed as a GLM with nonparametric link function. When having more than one covariate, single index model (SIM) can be built. In SIM, the expectation of the response is modeled as $h(\boldsymbol{X}\boldsymbol{\beta})$, where h is an unknown function and $\boldsymbol{X}\boldsymbol{\beta}$ is the index. The inverse of h is equivalent to the link function in GLMs when h is monotone. Ichimura (1993) and Klein and Spady (1993) discussed SIM estimators for binary data. However, these approaches cannot guarantee the monotonicity of h. Weisberg and Welsh (1994) proposed a way to estimate unknown link function in GLM using kernel functions, which does not have monotone constraints for link function. Muggeo and Ferrara (2008) proposed a generalized single index model (GSIM), which assumed an unknown link function with linear predictor. In Muggeo and Ferrara (2008), the link function is estimated by P-spline (Eilers and Marx, 1996; Eilers et al., 2015) and the monotone assumption is dealt with by introducing a very large penalty term.

The problem of estimating monotone functions have been studied in the literature for a long time. Ramsay (1988) proposed to estimate nondecreasing functions by using linear combination of integrated splines with nonnegative coefficients. Ramsay (1998) estimated the monotone function based on differential equations by using spline base functions in estimation. Wang (2000) extended Ramsay (1998)'s method to estimate monotone link function in GLMs. B-spline (De Boor, 2001) is also a tool to estimate monotone functions (He and Shi, 1998; Leitenstorfer and Tutz, 2007). A new algorithm to estimate monotone link function in GLMs via P-spline, which is based on Taylor expansion and quadratic optimization, was introduced in Wang and Small (2015). However, these results are all limited to univariate predictor only. Bollaerts et al. (2006) introduced the monotone constraints based on the derivative of B-splines in estimating a quantile regression, which is similar

in Muggeo and Ferrara (2008). This idea is also applied in Eilers et al. (2009) and Marx et al. (2011).

In this paper, we propose a new algorithm to estimate the unknown link function with monotone constraints in GLMs. This algorithm can be applied to models with more than one covariate and can estimate the link function and the regression coefficients simultaneously. The algorithm is an iterative procedure with two steps. The first step is to estimate the unknown link function. The transformation in Wang and Yang (2009) is used to restrict the domain of the index. Quadratic optimization based method is then applied to estimate the monotone link function when fixing the estimates of the regression coefficients, which can guarantee that we have a monotone link function. The second step is to estimate the regression coefficients when fixing the link function.

As mentioned above, a lot of parametric link functions have been proposed in the literature. Unfortunately, there does not seem to be any comprehensive studies comparing these parametric link functions and our nonparametric link functions when fitting GLMs. One of the goals of the current paper is to undertake an extensive simulation study to compare the performance of traditional link functions, the recently proposed flexible parametric link functions and nonparametric link function in terms of prediction accuracy. We use simulation study to compare logit, probit, robit, GEV, splogit, GAM with our proposed algorithm in binary data. The simulation study shows that the nonparametric link function model estimated by our proposed algorithm has the best overall performance, and can approximate different parametric link functions very well when the data are simulated from these link functions.

The rest of the paper is organized as follows. In Section 2.2, different parametric link functions are reviewed. In Section 2.3, we review existing nonparametric methods for estimating link functions. In Section 2.4, we describe the new algorithm to estimate monotone unknown link functions in GLMs. Simulation study results are presented in Section 2.5, where the performances of a variety of link functions are compared under different true links. The results from a real data analysis are in Section 2.6. Some concluding remarks are given in Section 2.7.

2.2 Parametric link functions

Let Y_i be the response variable for the ith observation, $\boldsymbol{x}_i$ be the vector of covariates, $\boldsymbol{\beta}$ be the regression coefficients and $\eta_i = \boldsymbol{x}_i'\boldsymbol{\beta}$ for $i = 1, \ldots, n$. We assume that Y_i's are independent with density,

$$f(y_i|\theta_i, \psi_i) = d(y_i, \psi_i) \exp[(\theta_i y_i - b(\theta_i))/a(\psi_i)],$$

where θ_i and ψ_i are unknown parameters, and ψ_i could be constant in one parameter distributions, such as the Bernoulli distribution and the binomial distribution (McCullagh and Nelder, 1989). The functions $a(\cdot)$ and $b(\cdot)$ are known functions and,

$$\begin{aligned} \mu_i &\equiv E(Y_i) = b'(\theta_i), \\ \text{var}(Y_i) &= \frac{b''(\theta_i)}{a(\psi_i)} = \frac{V(\mu_i)}{a(\psi_i)}. \end{aligned}$$

A link function $g(\cdot)$ links the expectation μ_i and the covariates $\boldsymbol{x}_i$ through,

$$g(\mu_i) = \eta_i \equiv \boldsymbol{x}_i'\boldsymbol{\beta}. \tag{2.1}$$

When $g(\cdot) = b'^{-1}(\cdot)$, then $\theta_i = \boldsymbol{x}_i'\boldsymbol{\beta}$ and in this case $g(\cdot)$ is called the canonical link for the model.

2.2.1 Symmetric link functions

Jiang et al. (2013) provided an interpretation of symmetric and asymmetric link functions. For symmetric link functions, the probabilities of going to 0 and 1 have the same rates for binary or binomial variables. Logit, probit and robit link functions are all symmetric link function. Figure 2.1 shows the CDFs corresponding to logit, probit and robit with degrees of freedom 1 and 2. All of them go through the point $(0, 0.5)$. And they are symmetric with respect to $(0, 0.5)$.

For logit link function, we have $g(\mu_i) = \log(\mu_i/(1 - \mu_i))$, which is a closed form and is easy to deal with. If $g(\mu_i) = \Phi^{-1}(\mu_i)$, then we have the probit regression model, where $\Phi(\cdot)$ is the CDF of the standard normal distribution. Both logit and probit link functions are completely known; there is no parameter to estimate in these link functions. On the other hand, the robit link with $g(\mu_i) = F_\nu^{-1}(\mu_i)$, where $F_\nu(\cdot)$ is the CDF of t distribution with degrees of freedom ν, has a

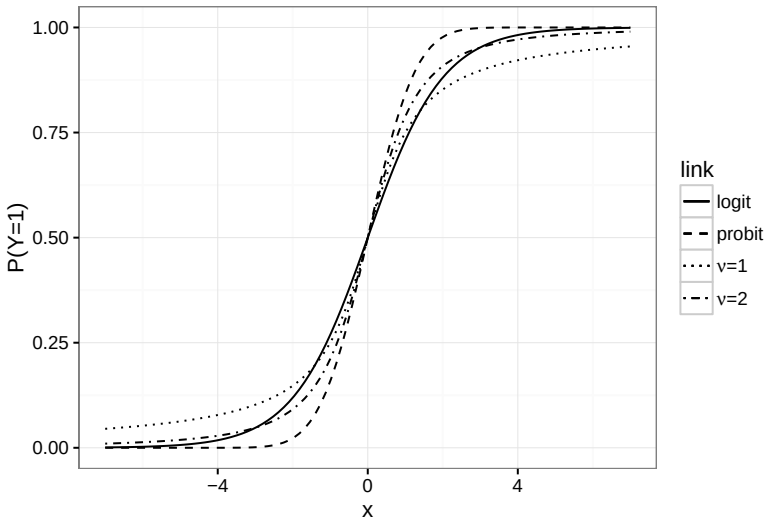

Figure 2.1: Symmetric link functions

parameter ν. EM-type algorithms can be used to estimate both the value of degrees of freedom parameter and the regression coefficients (Liu, 2004).

2.2.2 Asymmetric link functions

An example of traditional asymmetric link function is cloglog link, $g(\mu_i) = -\log(-\log(\mu_i))$, which does not have any parameters to control the skewness of the link function. By introducing parameters in the link function, we can have flexible asymmetric link functions, such as the generalized skewed t link in Kim et al. (2008), the GEV link in Wang and Dey (2010) and the splogit link in Jiang et al. (2013).

Wang and Dey (2010)'s GEV link is given by,

$$g^{-1}(\eta_i) = 1 - G_\xi(-\eta_i), \tag{2.2}$$

where $G_\xi(\cdot)$ is the cumulative distribution function of the GEV distribution with center parameter 0, scale parameter 1 and shape parameter ξ, i.e., $G_\xi(x) = \exp[-\{1+\xi x\}_+^{-1/\xi}]$, where $\{z\}_+ = \max\{z, 0\}$. In Wang and Dey (2010), the parameters of the model are estimated under Bayesian framework. In our simulation study, we calculate maximum likelihood estimates of the parameters

instead of using a Bayesian method. Since the support of GEV is $\{x : 1+\xi x \geq 0\}$, we use R package *nloptr* (Ypma, 2014) to solve the optimization problem with constraints $\{\boldsymbol{\beta} : 1-\xi \boldsymbol{x}_i'\boldsymbol{\beta} \geq 0\}$. Wang and Dey (2010) used the definition of skewness of a random variable as $\gamma_M = 1 - 2F(M_x)$, where F is the CDF of the random variable and M_x is the mode. The GEV link in (2.2) is negatively skewed when $\xi < \log 2 - 1$ and positively skewed when $\xi > \log 2 - 1$. They used simulation study and a real data set to show that GEV link function can approximate probit and logit links well. Besides that, GEV can improve the results of cloglog for imbalanced data.

For the symmetric power link, we have $g(\mu_i) = F_r^{-1}(\mu_i)$ (Jiang et al., 2013) with

$$F_r(x) \quad = \quad F_0^r\left(\frac{x}{r}\right)\boldsymbol{I}_{(0,1]}(r) + [1 - F_0^{1/r}(-rx)]\boldsymbol{I}_{(1,+\infty)}(r),$$

where $F_0(x)$ is a base function, and r is the parameter which controls the skewness of the link function. The function $F_0(x)$ can be the CDF of the logistic distribution, t distribution or the exponential distribution. Jiang et al. (2013) considered a Bayesian analysis of binomial data using the symmetric power links. Here we consider logistic distribution only and the corresponding splogit links. One problem of this link function is that splogit link is continuous at $r = 1$, but it is not differentiable. In this paper, we maximize the profile likelihood of r to do estimation, that is, we estimate r by,

$$\begin{aligned} \hat{r} &= \arg\max_r p(r), \text{ where,} \\ p(r) &= \arg\max_{\boldsymbol{\beta}} \sum_{i=1}^{n} y_i \log \frac{F_r(\boldsymbol{x}_i'\boldsymbol{\beta})}{1 - F_r(\boldsymbol{x}_i'\boldsymbol{\beta})} + \sum_{i=1}^{n} \log(1 - F_r(\boldsymbol{x}_i'\boldsymbol{\beta})). \end{aligned}$$

Jiang et al. (2013) compared splogit link and GEV link when simulating data from logit, cloglog and log-log link models. Splogit performs better than GEV when the true link function is logit or log-log and GEV link performs better when the true link is cloglog.

Figure 2.2 shows the CDFs of GEV link function and the splogit link function with different values of ξ and r. They do not go through the point $(0, 0.5)$ and the rate at which they go to 0 is different from the rate going to 1. For example, the GEV link with $\xi = 0.5$ goes to 1 at faster rate than to 0.

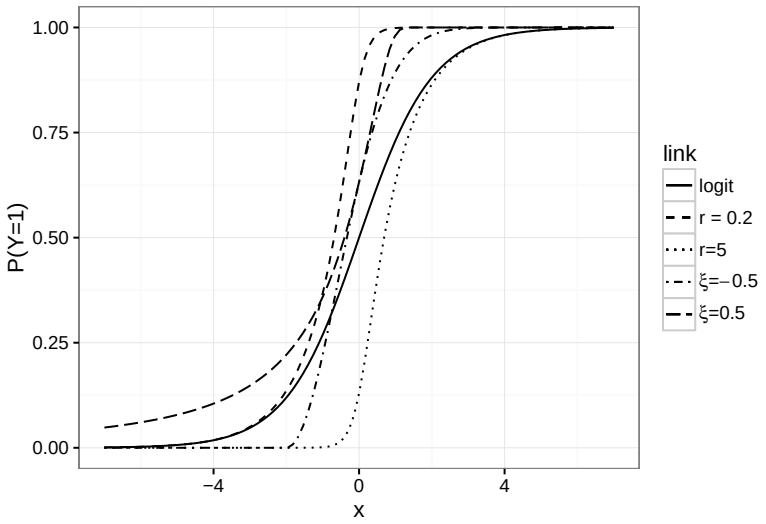

Figure 2.2: Asymmetric link functions

2.3 Nonparametric link functions

In section 2.2, we discussed several parametric link functions. In many cases, it is not clear which parametric link function is more suitable, then one can estimate the link function nonparametrically. Weisberg and Welsh (1994) used kernel method to estimate the unknown link function. They started from the expectation and variance structure with the following form,

$$\begin{aligned} E(Y_i) &= g^*(\boldsymbol{x}_i^T\boldsymbol{\beta}), \\ \mathrm{Var}(Y_i) &= \sigma^2 V(g^*(\boldsymbol{x}_i^T\boldsymbol{\beta})). \end{aligned}$$

The algorithm is a two-step iteration procedure. The first step is to update $\boldsymbol{\beta}$ when fixing $g^*(\cdot)$. The second step is to update the $g^*(\cdot)$ when fixing $\boldsymbol{\beta}$. In fact, the estimated function is the inverse of the link function $g(\cdot)$ defined in (2.1). Since the kernel smoothing method is used to do the estimation, the monotonicity cannot be guaranteed.

We now describe the generalized single index model (GSIM) proposed in Muggeo and Ferrara (2008) for binary data. They considered,

$$\mathrm{logit}(\mu_i) = \phi(\boldsymbol{x}_i'\boldsymbol{\beta}), \tag{2.3}$$

where $\text{logit}(\mu_i) = \log(\mu_i/(1-\mu_i))$ and $\phi(\cdot)$ is an unknown function, which is estimated by P-spline. The link function for this model is $g(\mu_i) = \phi^{-1}(\text{logit}(\mu_i))$. They used a two steps algorithm to fit the GSIM. When fixing $g(\cdot)$, the estimation problem becomes a common GLM problem, where iterative weighted least squares (McCullagh and Nelder, 1989) is used to update the estimates of $\boldsymbol{\beta}$. When fixing $\boldsymbol{\beta}$, the unknown function $g(\cdot)$ is estimated by P-spline (Eilers and Marx, 1996). More specially, Muggeo and Ferrara (2008) considered

$$\text{logit}(\mu_i) = \phi(\boldsymbol{x}_i'\boldsymbol{\beta}) = \boldsymbol{B}(\boldsymbol{x}_i'\boldsymbol{\beta})\boldsymbol{\delta},$$

where $\boldsymbol{B}(\cdot)_{n\times(K+1)}$ is the B-spline basis matrix with the ith row $\boldsymbol{B}(\boldsymbol{x}_i'\boldsymbol{\beta}) = (B_{0,p}(\boldsymbol{x}_i'\boldsymbol{\beta}), \ldots, B_{K,p}(\boldsymbol{x}_i'\boldsymbol{\beta}))$, p is the degree of the basis functions and $\boldsymbol{\delta} = (\delta_0, \delta_1, \ldots, \delta_K)'$. The number K is the sum of p and the number of interior knots.

Iterative weighted least squares is used to update the estimation of $\boldsymbol{\delta}$, which is similar to Eilers and Marx (1996). Besides the set of constraints for $\boldsymbol{\delta}$ in P-spline with second order, they used another set of constraints for the monotone functions. The monotone constraints are obtained by assuming nonnegative or nonpositive derivative of a function. Based on the properties of B-spline (De Boor, 2001), we can write the derivative of $\boldsymbol{B}\boldsymbol{\delta}$ as,

$$\frac{d}{dx}\sum_{k=0}^{K}\delta_k B_{k,p}(x) = \frac{1}{h}\sum_{k=0}^{K-1} B_{k,p-1}(x)(\delta_{k+1}-\delta_k),$$

where $\boldsymbol{B}$ is based on equally spaced knots with h as the distance between consecutive interior knots.

Since all the values of B-spline basis functions are nonnegative, the nonnegative monotonic constraints for $\boldsymbol{\delta}$ are $\delta_{k+1} - \delta_k \geq 0$, which can be written as,

$$A\boldsymbol{\delta} = \begin{pmatrix} -1 & 1 & 0 & \cdots & 0 & 0 \\ 0 & -1 & 1 & \cdots & 0 & 0 \\ 0 & 0 & -1 & \cdots & 0 & 0 \\ \vdots & \vdots & \vdots & \vdots & \vdots & \vdots \\ 0 & 0 & 0 & 0 & -1 & 1 \end{pmatrix} \boldsymbol{\delta} \geq 0.$$

Muggeo and Ferrara (2008) dealt with the monotone constraints by including a very large penalty value $\kappa = 10^6$ on the penalty term as $\kappa\boldsymbol{\delta}'A'VA\boldsymbol{\delta}$, where $V = \text{diag}(I(\delta_1 - \delta_0 < 0), \ldots, I(\delta_K -$

$\delta_{K-1} < 0)$) and $I(\cdot)$ is the indicator function. Here κ is a tuning parameter which controls the cost of violating the monotonicity constraints. But, we found that the monotonicity may not be satisfied in some cases, which may depend on the tuning parameter λ and the sample size n. The new algorithm we propose in the next section does not suffer from such problem.

2.4 A new algorithm for estimating monotone link functions

The new algorithm contains two steps, which is similar to the algorithm in Muggeo and Ferrara (2008). But there are two main differences. The first one is the constraint for $\boldsymbol{\beta}$. Muggeo and Ferrara (2008) standardized $\boldsymbol{x}'\boldsymbol{\beta}$ in every iteration. Here we follow the constraints $||\boldsymbol{\beta}|| = 1$ and the transformation in Wang and Yang (2009) before using the P-spline to estimate $\phi(\cdot)$, where $\boldsymbol{\beta} = (\beta_1, \ldots, \beta_d)^T$. No intercept is included in $\boldsymbol{\beta}$. The transformation is defined as $U(\cdot)$, which is the rescaled centered beta cumulative distribution function with,

$$U(\eta) = F_d(\eta) = \int_{-1}^{\frac{\eta}{a}} \frac{\Gamma(d+1)}{\Gamma(\frac{d+1}{2})^2 2^d}(1-t^2)^{\frac{d-1}{2}} dt,$$

where $\eta \in [-a, a]$, d is the dimension of $\boldsymbol{\beta}$. As mentioned in Wang and Yang (2009), the transformation U has a quasi-uniform $[0, 1]$ distribution, which makes it reasonable to use equally spaced knots. Then, (2.3) becomes,

$$g_0(\mu_i) = \phi(U(\eta_i)) = \boldsymbol{B}(U(\eta_i))\boldsymbol{\delta}.$$

where $\eta_i = \boldsymbol{x}_i'\boldsymbol{\beta}$, g_0 is a known function which can define the range of μ_i. In particular, g_0 can be the canonical link function. For example, in binary data, we can use logit as g_0, which can make sure that the value of μ_i is between 0 and 1. $\boldsymbol{B}(x)_{n\times(K+1)}$ corresponds to spline functions. The transformation considered can make the values of $U(\boldsymbol{x}_i'\boldsymbol{\beta})$ not too extreme. In Wang and Yang (2009), they used 95th percentile of $\{||\boldsymbol{x}_i||\}_{i=1}^n$ as the value of a. Since we use the constraints $||\boldsymbol{\beta}|| = 1$, we have $||\boldsymbol{x}_i'\boldsymbol{\beta}|| \leq ||\boldsymbol{x}_i||$. We use the maximum value of $||\boldsymbol{x}_i||$ as a in simulation study and real data analysis. Also, the continuous variables are centered and scaled.

The second difference is that instead of using a large penalty to force the estimated function to be close to a monotone function, we use Taylor expansion and iterative quadratic optimization described in Wang and Small (2015) to solve the constrained optimization problem directly.

In the first step, $\boldsymbol{\beta}$ is fixed, and then, the problem becomes fitting a generalized linear model

$$g_0(\mu_i) = \boldsymbol{B}\boldsymbol{\delta} \tag{2.4}$$

with constraints and penalties on $\boldsymbol{\delta}$. The monotone constraint for the link function is denoted as $A\boldsymbol{\delta} \geq 0$ in section 2.3. The penalty is P-spline associated with D,

$$D = \begin{pmatrix} 1 & -2 & 1 & \cdots & 0 \\ 0 & 1 & -2 & \cdots & 0 \\ \vdots & \vdots & \vdots & \vdots & \vdots \\ 0 & 0 & -2 & 1 & 0 \\ 0 & 0 & 1 & -2 & 1 \end{pmatrix}.$$

In Muggeo and Ferrara (2008), the $\boldsymbol{\delta}$ is updated by,

$$\hat{\boldsymbol{\delta}} = (\boldsymbol{B}'\tilde{\boldsymbol{W}}^{\delta}\boldsymbol{B} + \lambda D'D + \kappa A'VA)^{-1}\boldsymbol{B}'\tilde{\boldsymbol{W}}^{\delta}y. \tag{2.5}$$

We update $\boldsymbol{\delta}$ by solving the iterative quadratic optimization. The problem in (2.4) with monotone constraints can be solved by,

$$\min_{\boldsymbol{\delta}} \quad - \quad \left[(\boldsymbol{y} - \tilde{\boldsymbol{\mu}})\tilde{\boldsymbol{d}} + \tilde{\boldsymbol{W}}^{\delta}\boldsymbol{B}\tilde{\boldsymbol{\delta}}\right]' \boldsymbol{B}\boldsymbol{\delta} + \frac{1}{2}\boldsymbol{\delta}'(\boldsymbol{B}'\tilde{\boldsymbol{W}}^{\delta}\boldsymbol{B} + \lambda D'D)\boldsymbol{\delta}, \tag{2.6}$$

where $\tilde{\boldsymbol{d}}, \tilde{\boldsymbol{\mu}}, \tilde{\boldsymbol{W}}^{\delta}$ and $\tilde{\boldsymbol{\delta}}$ are from previous step, $(\boldsymbol{y} - \tilde{\boldsymbol{\mu}})\tilde{\boldsymbol{d}}$ are coordinate-wise product and $\tilde{\boldsymbol{W}}^{\delta} = \text{diag}(w_1^{\delta}, \ldots, w_n^{\delta})$, $\tilde{\boldsymbol{d}} = (\tilde{d}_1, \ldots, \tilde{d}_n)'$, where,

$$\begin{aligned} w_i^{\delta} &= \left[\left(\frac{d\eta_i}{d\mu_i}\right)^2 V(\mu_i)\right]^{-1}\Bigg|_{\mu_i=\tilde{\mu}_i}, \\ \tilde{d}_i &= \left(V(\mu_i)\frac{d\eta_i}{d\mu_i}\right)^{-1}\Bigg|_{\mu_i=\tilde{\mu}_i}. \end{aligned}$$

Note that (2.6) can be solved by quadratic programming. For example, let $g_0(\mu_i) = \eta_i$ and $g_0(\cdot) = \text{logit}(\cdot)$, for binary data, we have,

$$\begin{aligned} \frac{d\eta_i}{d\mu_i} &= \frac{1}{\mu_i(1-\mu_i)}, \\ V(\mu_i) &= \mu_i(1-\mu_i). \end{aligned}$$

So in this case $w_i^{\delta} = \tilde{\mu}_i(1-\tilde{\mu}_i)$ and $\tilde{d}_i = 1$.

In the second step, $\boldsymbol{\delta}$ is fixed. Then, the problem becomes fitting a GLM with a fixed link function

$$q^{-1}(g_0(\mu_i)) = x_i'\boldsymbol{\beta},$$

where $q(\cdot) = \phi(U(\cdot))$. We use the revised Newton method (Boyd and Vandenberghe, 2004) mentioned below to update $\boldsymbol{\beta}$ in Algorithm 2.1.

Algorithm 2.1 Revised Newton method for updating $\boldsymbol{\beta}$

1: 1: Compute $\Delta_\beta = (\boldsymbol{X}'\tilde{\boldsymbol{W}}^\beta\boldsymbol{X})^{-1}\boldsymbol{X}'\tilde{\boldsymbol{W}}^\beta\boldsymbol{z}^\beta$, where $\tilde{\boldsymbol{W}}^\beta = \text{diag}(w_1^\beta, \ldots, w_n^\beta)$, $\boldsymbol{z}^\beta = (z_1^\beta, \ldots, z_n^\beta)'$, and w_i^β, z_i^β are defined as,

$$\begin{aligned} w_i^\beta &= \left[\left(\frac{d\eta_i}{d\mu_i}\right)^2 V(\mu_i)\right]^{-1} (\phi')^2(U')^2\Big|_{\mu_i=\tilde{\mu}_i} \\ z_i^\beta &= (y_i - \tilde{\mu}_i)\frac{d\eta_i}{d\mu_i}\cdot[\phi'U']^{-1}. \end{aligned}$$

2: 2: Let $\nabla_l = \boldsymbol{X}'\tilde{\boldsymbol{W}}^\beta\boldsymbol{z}^\beta$ and choose the step size t by backtracking line search (Boyd and Vandenberghe, 2004).

3: 2.1: Start from $t = 1$, let $t = \gamma t$.

4: 2.2: Set $\boldsymbol{\beta}^{\text{new}} = \boldsymbol{\beta}^{\text{old}} + t\Delta_\beta$.

5: 2.3: Standardize $\boldsymbol{\beta}^{\text{new}}$ to make $||\hat{\boldsymbol{\beta}}^{\text{new}}|| = 1$.

6: 2.4: Repeat previous steps until $l(\boldsymbol{\beta}^{\text{new}}) < l(\boldsymbol{\beta}) + \alpha t(\nabla l)^T\Delta_\beta$, where l is the negative log-likelihood and $\alpha \in (0, 0.5)$, $\gamma \in (0, 1)$.

7: 3: Update $\boldsymbol{\beta}$.

Remark 2.1. *In Algorithm 2.1, when $t = 1$, $\boldsymbol{\beta}$ is updated with size 1 in the Δ_β direction. This is equivalent to the results based on the weighted least square, that is ,*

$$\boldsymbol{\beta}^{new} = (\boldsymbol{X}'\tilde{\boldsymbol{W}}^\beta\boldsymbol{X})^{-1}\boldsymbol{X}'\tilde{\boldsymbol{W}}^\beta\boldsymbol{z},$$

where $\boldsymbol{z} = \boldsymbol{X}'\boldsymbol{\beta}^{old} + \boldsymbol{z}^{\beta}$. *But in the simulation study, we find that the moving size 1 could be too large to have numeric issues with small* λ. *So we use a backtracking line search method to find a small size* t. *The results based on backtracking line search and weighted least square are the same with same* λ *if both can be evaluated.*

Based on the previous two steps, the proposed algorithm which we call MPS has the following steps in Algorithm 2.2.

Algorithm 2.2 The MPS algorithm for estimating unknown link function

1: Start with initial values for $\hat{\boldsymbol{\beta}}$ and $\hat{\boldsymbol{\delta}}$.
2: Given current $\hat{\boldsymbol{\beta}}^{(m)}$ and $\hat{\boldsymbol{\delta}}^{(m)}$, calculate $\boldsymbol{x}_i'\hat{\boldsymbol{\beta}}^{(m)}$. Then update $\boldsymbol{\delta}$ by solving (2.6).
3: Given current $\hat{\boldsymbol{\beta}}^{(m)}$ and $\hat{\boldsymbol{\delta}}^{(m+1)}$, update $\boldsymbol{\beta}$ using the revised Newton method.
4: Repeat previous two steps until some convergence criterion is met.

Initial values for $\boldsymbol{\beta}$ can be chosen by fitting a logistic regression model without intercept and standardizing it such that $||\boldsymbol{\beta}|| = 1$. The initial values for $\boldsymbol{\delta}$ are 0's. Boyd and Vandenberghe (2004) suggest to choose α between 0.01 and 0.3, γ between 0.1 and 0.8. In our simulation study and the real data example, we choose $\alpha = 0.25$ and $\gamma = 0.5$, and the convergence criterion is $||\boldsymbol{\theta}^{(m+1)} - \boldsymbol{\theta}^{(m)}|| < \epsilon$, where $\boldsymbol{\theta} = (\boldsymbol{\beta}', \boldsymbol{\delta}')'$ and ϵ is a small value. Here we use $\epsilon = 10^{-8}$.

As in Muggeo and Ferrara (2008), the variability of the regression coefficients and the link function can be obtained from a bootstrap approach. That means the MPS is fitted for each bootstrap sample $b = 1, \ldots, B$ to obtain the bootstrap sample distribution of the regression coefficients and the link function.

2.5 Simulation study

In this section, we use simulation study to compare different parametric link functions and nonparametric link function estimated by our proposed algorithm MPS. We simulate binary data from the Bernoulli distribution under different link functions, including logit, probit, robit, GEV and splogit with different parameters. Models with parametric link functions (logit, probit, robit, GEV, splogit), our algorithm MPS described in section 2.4 are considered. As mentioned in Section

2.1, a flexible regression model is also a choice to extend the GLM. So the GAM with logit link (Wood, 2006) is also considered in the simulation study. We compare the performance of different link functions based on the prediction performance.

2.5.1 Simulation settings

The sample sizes we consider are $n = 100$, 200 and 500. Let $\boldsymbol{\beta} = (0, 1, 1)'$, and $\eta_i = \beta_0 + x_{1i}\beta_1 + x_{2i}\beta_2$, where x_1 is continuous and simulated from $N(-0.5, 1)$ satisfying $|x_1 + 0.5| \leq 3$, the other variable x_2 is a binary variable drawn from Bernoulli(0.5). We assume that Y_i's are independent Bernoulli(μ_i) random variables with $g(\mu_i) = \eta_i$, where we vary the true link function $g(\cdot)$. The simulation procedure is as follows.

For $m = 1, \ldots, M$,

1. Simulate $x_{1i} \sim N(-0.5, 1)I(|x_{1i} + 0.5| \leq 3)$ and $x_{2i} \sim \text{Bern}(0.5)$ for $i = 1, \ldots, n$.

   Let $\boldsymbol{x}_i = (1, x_{1i}, x_{2i})'$. Obtain the sequence x_{1i}^{new} from $\min(x_1)$ to $\max(x_1)$ with length 200 on a regular grid. Combine x_{1i}^{new} with $\{0, 1\}$ for all combinations. That means, for each x_{1i}^{new}, we can create two vectors with $(1, x_{1i}^{\text{new}}, 0)'$ and $(1, x_{1i}^{\text{new}}, 1)'$. Denoted these vectors as $\boldsymbol{x}_{j,\text{new}}, j = 1, \ldots, 400$. This data set is used to compare the prediction performances of different link functions.

2. Calculate $\mu_i^{(m)} = g^{-1}(\boldsymbol{x}_i^T\boldsymbol{\beta})$ for $i = 1, \ldots, n$ and $\mu_{j,\text{new}}^{(m)} = g^{-1}(\boldsymbol{x}_{j,\text{new}}^T\boldsymbol{\beta})$ for $j = 1, \ldots n_1$, where $n_1 = 400$ and g is the specified link function.

3. Simulate $y_i^{(m)} \sim \text{Bern}(\mu_i^{(m)})$ under specified link function for $i = 1, \ldots, n$.

4. Estimate parameters under different link functions based on data sets with different sample size n.

   In P-spline method, 9 equally spaced knots are used. Generalized cross validation(Wood, 2008) is used to select the penalty parameter λ, which is given by

$$V_g(\lambda) = nD(\hat{\boldsymbol{\delta}}_\lambda, \hat{\boldsymbol{\beta}}_\lambda)/(n - \gamma\tau)^2,$$

where $\tau = \text{trace}(C)$, $C = (\boldsymbol{B}'\boldsymbol{W}^{\delta}\boldsymbol{B} + \lambda D'D)^{-1}\boldsymbol{B}'\boldsymbol{W}^{\delta}\boldsymbol{B}$ and $D(\hat{\boldsymbol{\delta}}_\lambda, \hat{\boldsymbol{\beta}}_\lambda)$ is the deviance, which is defined as $2(l_{\max} - l(\hat{\boldsymbol{\delta}}_\lambda, \hat{\boldsymbol{\beta}}_\lambda))$, where l is the log-likelihood, $l_{\max}$ is the maximum possible log-likelihood. In binary setting, $l_{\max} = 0$.

For the estimation of logit and probit, we use the maximum likelihood. For robit, we use PX-EM algorithm in Liu (2004). For GEV and splogit, we use the methods mentioned in section 2.2.

5. Predict $\hat{\mu}^{(m)}_{j,\text{new}} = \hat{g}^{-1}(\boldsymbol{x}^T_{j,\text{new}}\hat{\boldsymbol{\beta}})$, $j = 1, \ldots, n_1$, based on the estimated parameters.

Based on the previous results, we calculate the following three statistics for $M = 100$,

$$\text{RMSE} = \sqrt{\frac{1}{Mn_1}\sum_{m=1}^{M}\sum_{j=1}^{n_1}(\hat{\mu}^{(m)}_{j,\text{new}} - \mu^{(m)}_{j,\text{new}})^2}, \tag{2.7}$$

$$\text{WRMSE} = \sqrt{\frac{1}{M}\sum_{m=1}^{M}\sum_{j=1}^{n_1} w_j(\hat{\mu}^{(m)}_{j,\text{new}} - \mu^{(m)}_{j,\text{new}})^2}, \tag{2.8}$$

and

$$TC = \frac{1}{Mn_1}\sum_{m=1}^{M}\sum_{j=1}^{n_1} |\max(0.75, \hat{\mu}^{(m)}_{j,\text{new}}) - \max(0.75, \mu^{(m)}_{j,\text{new}})|. \tag{2.9}$$

In (2.8), $w_j \propto f_{\text{norm}}(x^{\text{new}}_{1j}; -0.5, 1)$, where $f_{\text{norm}}(\cdot)$ is the pdf of the standard normal distribution and $\sum_{j=1}^{n_1} w_j = 1$. The reason we consider the unequal weights is that normal distribution is a popular assumption in real data analysis. (2.9) measures the tail behavior of the link function which borrows the idea from survival data analysis (Yuan, 2008). It is used to see how well different models predict the extreme probabilities.

Besides the linear case in η, we also compare the performances of different link functions in nonlinear case. Here we consider a simple case with one covariate. Three scenarios are considered, including both monotone and nonmonotonic functions, which we could have in real data examples. The first one is $\eta = 0.2(x_1 + 1)^3 - 2$, the second one is $\eta = x_1^2 + x_1 - 3$, and the third one is $\eta = -0.2(x_1 - 3)^2 - 0.15x_1^2 + 3$. The covariate x_1 is from the same distribution as in the linear case. Figure (2.3) shows the plot of η under these three different scenarios. The second one is not

monotone. The other two are monotone curves. And the third one is more like a linear line than the third one. In these three cases, the algorithm is just the first part of the algorithm in section 2.4 with updating $\boldsymbol{\delta}$ in (2.6), which is just the algorithm in Wang and Small (2015).

For robit link, we consider the degrees of freedom with values 0.6, 1 and 2. When considering the GEV link function, the shape parameter controls the skewness of the link function. Since the support of the GEV distribution depends on the unknown location parameter and shape parameter, different location parameters are taken to avoid the values of η too far away from the support of the GEV distributions with different shape parameters. In linear case, the location parameters are -1.5, -1, 0 and 1.2 corresponding to the shape parameters 1, 0.5, -0.5 and -1. For nonlinear cases, the location parameters are -2, -1, 1 and 1.5 for the same shape parameters. For splogit link, the considered r values are 0.2 and 5 in linear case and 0.6 and 1.5 in nonlinear case. For choosing the penalty parameter λ, we use 100 values between 10^{-5} and 10^{12} in $\log_{10}$ scale.[2]

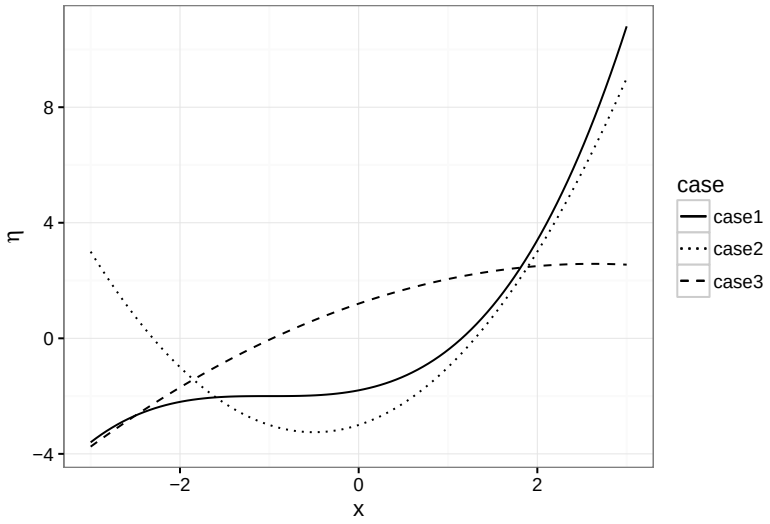

Figure 2.3: Shape of the predictor function in different scenarios

[2]In nonlinear case 1, when the true model is probit, the boundary values are 10^{-5} and 10^{11}, since there are nonpositive definite problem in solve.QR() when the λ are too large.

2.5.2 Simulation results

This section shows the results of the simulation study. Table 2.1 gives the abbreviations of different link functions. Tables 2.2, 2.3 and 2.4 show the simulation results of linear case and nonlinear case 1. Tables 2.5, 2.6 and 2.7 show the results for nonlinear case 2 and case 3. In each row, the results are based on different link functions with data simulated from the true corresponding link function. For example, robit(0.6) row means that the simulated data sets are simulated under robit link with parameter $\nu = 0.6$. Then, we estimate parameters under different assumptions of link function. If the assumed link function has additional parameter, then the parameter is estimated as in Section 2.2. Figures 2.4 and 2.5 show the details of RMSE for selected true link functions for linear case and nonlinear case 1 with sample size 500.

Table 2.1: Considered link functions

Abbreviation	Link function
L	logit
P	probit
R	robit
G	GEV
S	splogit
A	GAM
MPS	Monotone nonparametric link
PS	Without monotone constraints

"PS" can be estimated by the algorithm in (2.5) without the large penalty term and assuming $||\boldsymbol{\beta}|| = 1$ and $\beta_1 > 0$. In each cell, the three link functions are the first three link functions with smaller value in (2.7), (2.8) and (2.9). For example in the cell with output L/P/MPS, it means that the model with logit link provides the best result, probit is the second best, and MPS is the third best.

In most cases of Tables 2.2, 2.3 and 2.4, MPS is in the top three, especially for large sample sizes. Below we summarize our observations:

1. If the true link function is symmetric, use of asymmetric link function can lead to poor performance.

2. If the true link function is skewed, then a symmetric link function cannot provide correct relationship between covariates and the dependent variable.

3. The GEV distribution is approximate symmetric with $\xi = -0.5$. This is why for linear case and nonlinear case 1, some symmetric link functions can approximate it well when sample size is 500. For that case, the results of MPS are close to the top three results even though it is not in the top three (see Supplemental materials). Under both symmetric and asymmetric true link functions, MPS approach provides reasonable results according to different criteria.

4. For nonlinear case 2, it is quite different from linear function, so the nonparametric method without constraints performs much better than other parametric link functions.

5. In nonlinear case 3, it is quite similar to linear function,; thus the nonparametric link function does not have much advantage over the parametric link functions.

Table 2.2: Summary of simulation results with sample size 100

True link	Linear case			Nonlinear case 1		
	RMSE	WRMSE	TC	RMSE	WRMSE	TC
logit	L/P/**MPS**	P/L/**MPS**	**MPS**/L/P	G/R/S	G/R/**MPS**	G/S/**MPS**
probit	P/L/**MPS**	P/L/**MPS**	L/P/**MPS**	S/G/**MPS**	G/S/**MPS**	G/S/**MPS**
robit(0.6)	**MPS**/L/P	**MPS**/L/P	R/**MPS**/L	R/G/S	G/R/**MPS**	P/L/R
robit(1)	L/**MPS**/P	L/P/**MPS**	**MPS**/R/L	R/G/S	G/R/**MPS**	G/R/S
robit(2)	L/**MPS**/P	L/P/**MPS**	**MPS**/L/P	G/R/S	G/R/**MPS**	G/S/R
gev(1)	G/S/R	G/S/L	G/S/PS	G/R/**MPS**	G/R/**MPS**	G/**MPS**/S
gev(0.5)	S/G/L	S/G/L	G/S/PS	G/R/S	G/R/**MPS**	G/PS/S
gev(-0.5)	P/L/**MPS**	P/L/**MPS**	L/P/**MPS**	G/S/PS	G/S/**MPS**	G/S/PS
gev(-1)	S/L/**MPS**	S/L/**MPS**	S/L/P	G/S/**MPS**	G/S/**MPS**	G/PS/S
splogit(0.2/0.6)	S/P/L	P/S/L	S/P/PS	G/R/S	G/R/**MPS**	G/PS/S
splogit(5/1.5)	S/P/L	S/P/L	S/P/G	G/S/R	G/S/**MPS**	G/S/**MPS**

Table 2.3: Summary of simulation results with sample size 200

True link	Linear case			Nonlinear case 1		
	RMSE	WRMSE	TC	RMSE	WRMSE	TC
logit	L/P/**MPS**	P/L/**MPS**	L/P/**MPS**	G/R/**MPS**	G/R/**MPS**	G/S/PS
probit	P/L/**MPS**	P/L/G	P/L/G	S/**MPS**/R	S/**MPS**/R	S/**MPS**/G
robit(0.6)	R/**MPS**/L	L/**MPS**/P	R/**MPS**/L	R/G/PS	R/G/**MPS**	R/S/**MPS**
robit(1)	**MPS**/L/R	**MPS**/L/P	**MPS**/L/R	R/G/PS	R/G/**MPS**	G/R/**MPS**
robit(2)	L/**MPS**/P	L/**MPS**/P	L/**MPS**/P	R/G/**MPS**	**MPS**/R/G	G/**MPS**/R
gev(1)	G/S/PS	G/S/**MPS**	G/S/PS	G/R/PS	G/R/**MPS**	G/PS/**MPS**
gev(0.5)	S/G/**MPS**	S/G/L	G/S/PS	G/R/PS	R/G/**MPS**	G/PS/**MPS**
gev(-0.5)	P/L/**MPS**	P/L/**MPS**	L/P/**MPS**	G/S/PS	G/PS/S	G/S/PS
gev(-1)	S/**MPS**/L	S/G/L	S/L/G	PS/**MPS**/S	PS/G/**MPS**	G/PS/S
splogit(0.2/0.6)	S/P/**MPS**	S/P/**MPS**	S/PS/P	**MPS**/G/R	**MPS**/R/G	G/PS/S
splogit(5/1.5)	S/**MPS**/P	S/**MPS**/P	S/**MPS**/G	G/R/**MPS**	G/R/**MPS**	G/S/R

Table 2.4: Summary of simulation results with sample size 500

True link	Linear case			Nonlinear case 1		
	RMSE	WRMSE	TC	RMSE	WRMSE	TC
logit	L/**MPS**/P	L/P/**MPS**	L/**MPS**/P	G/**MPS**/PS	**MPS**/G/R	G/**MPS**/PS
probit	P/L/R	P/L/R	P/L/G	**MPS**/PS/S	**MPS**/R/PS	**MPS**/PS/S
robit(0.6)	R/**MPS**/L	**MPS**/R/L	R/**MPS**/L	R/G/**MPS**	R/**MPS**/PS	**MPS**/G/PS
robit(1)	R/**MPS**/L	**MPS**/L/R	R/L/**MPS**	**MPS**/R/G	**MPS**/R/PS	**MPS**/G/PS
robit(2)	**MPS**/L/R	L/**MPS**/R	**MPS**/L/R	**MPS**/R/PS	**MPS**/R/PS	**MPS**/PS/G
gev(1)	G/S/PS	G/S/PS	S/G/PS	PS/R/**MPS**	R/**MPS**/PS	PS/G/**MPS**
gev(0.5)	S/G/**MPS**	S/G/**MPS**	S/G/PS	**MPS**/PS/G	**MPS**/R/PS	PS/**MPS**/G
gev(-0.5)	S/P/L	P/L/S	L/R/P	**MPS**/PS/S	**MPS**/PS/G	PS/S/**MPS**
gev(-1)	S/PS/**MPS**	S/**MPS**/PS	S/L/A	PS/**MPS**/S	PS/**MPS**/G	PS/G/**MPS**
splogit(0.2/0.6)	S/**MPS**/PS	S/**MPS**/PS	S/PS/**MPS**	**MPS**/PS/G	**MPS**/PS/R	PS/**MPS**/G
splogit(5/1.5)	S/**MPS**/PS	S/**MPS**/PS	S/**MPS**/PS	**MPS**/G/R	**MPS**/R/G	G/**MPS**/S

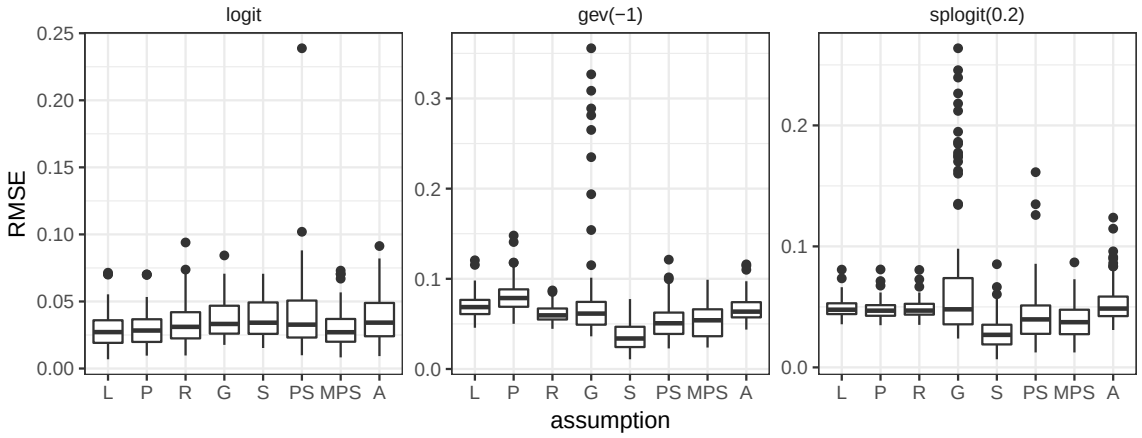

Figure 2.4: RMSE of linear case with sample size 500

Table 2.5: Summary of simulation results with sample size 100 for nonlinear case 2 and case 3

True link	Nonlinear case 2			Nonlinear case 3		
	RMSE	WRMSE	TC	RMSE	WRMSE	TC
logit	PS/R/G	PS/**MPS**/R	G/**MPS**/S	S/G/L	S/L/**MPS**	S/L/G
probit	PS/R/G	PS/R/**MPS**	PS/G/R	L/P/**MPS**	L/P/**MPS**	L/**MPS**/P
robit(0.6)	PS/R/G	PS/R/G	R/**MPS**/G	R/L/S	S/R/L	R/S/G
robit(1)	PS/R/G	PS/R/**MPS**	G/R/**MPS**	R/S/L	S/L/**MPS**	R/S/G
robit(2)	PS/R/G	PS/R/G	**MPS**/S/L	S/**MPS**/L	S/**MPS**/L	S/L/R
gev(1)	R/G/PS	R/G/**MPS**	G/S/**MPS**	G/S/**MPS**	G/S/L	G/S/PS
gev(0.5)	PS/R/G	R/G/PS	PS/G/R	G/S/P	G/S/P	G/S/PS
gev(-0.5)	PS/**MPS**/R	PS/**MPS**/R	PS/**MPS**/G	S/L/G	S/L/G	S/L/G
gev(-1)	PS/**MPS**/R	PS/**MPS**/R	PS/**MPS**/R	S/**MPS**/PS	S/**MPS**/L	S/L/**MPS**
splogit(0.6)	PS/R/**MPS**	PS/R/**MPS**	PS/G/R	L/P/**MPS**	L/P/**MPS**	L/**MPS**/P
splogit(1.5)	PS/G/R	PS/**MPS**/G	G/**MPS**/S	S/G/L	S/G/L	S/G/R

Table 2.6: Summary of simulation results with sample size 200 for nonlinear case 2 and case 3

True link	Nonlinear case 2			Nonlinear case 3		
	RMSE	WRMSE	TC	RMSE	WRMSE	TC
logit	PS/R/**MPS**	PS/**MPS**/R	PS/G/R	S/G/L	S/G/L	S/L/R
probit	PS/R/**MPS**	PS/**MPS**/R	PS/R/**MPS**	L/**MPS**/P	L/**MPS**/P	L/S/**MPS**
robit(0.6)	PS/R/**MPS**	PS/R/**MPS**	R/G/PS	R/S/L	R/S/PS	R/S/G
robit(1)	PS/R/**MPS**	PS/**MPS**/R	PS/R/G	R/S/L	R/S/**MPS**	R/S/G
robit(2)	PS/R/G	PS/R/**MPS**	R/S/L	S/**MPS**/R	S/**MPS**/R	S/R/L
gev(1)	PS/R/G	PS/R/G	PS/G/R	G/S/**MPS**	G/S/PS	G/S/PS
gev(0.5)	PS/R/G	PS/R/**MPS**	PS/G/R	G/S/**MPS**	G/S/P	G/S/PS
gev(-0.5)	PS/**MPS**/R	PS/**MPS**/R	PS/**MPS**/R	S/**MPS**/L	S/**MPS**/L	S/L/R
gev(-1)	PS/**MPS**/R	PS/**MPS**/R	PS/**MPS**/R	S/**MPS**/PS	S/**MPS**/PS	S/R/**MPS**
splogit(0.6)	PS/R/**MPS**	PS/**MPS**/R	PS/**MPS**/R	L/**MPS**/R	L/**MPS**/R	L/S/**MPS**
splogit(1.5)	PS/R/**MPS**	PS/**MPS**/R	G/R/PS	S/G/**MPS**	S/G/**MPS**	S/R/G

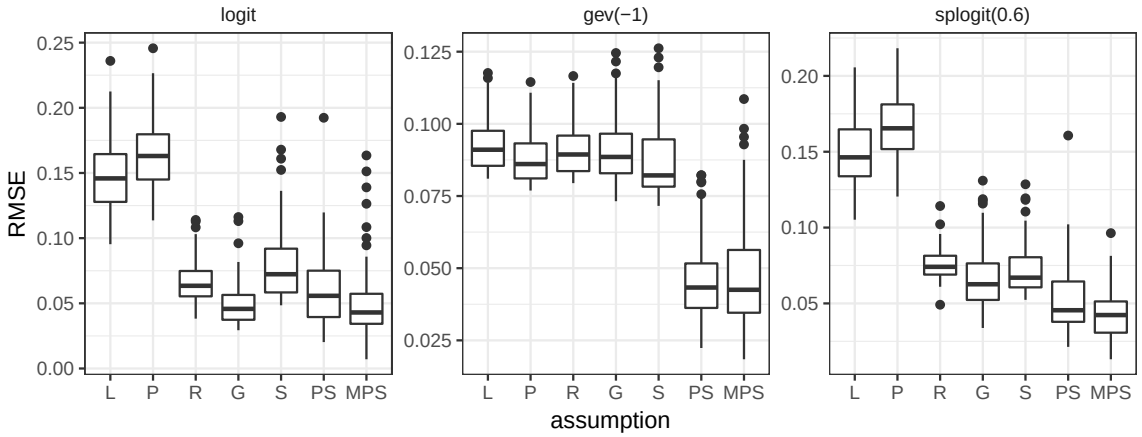

Figure 2.5: RMSE of nonlinear case 1 with sample size 500

Table 2.7: Summary of simulation results with sample size 500 for nonlinear case 2 and case 3

True link	Nonlinear case 2			Nonlinear case 3		
	RMSE	WRMSE	TC	RMSE	WRMSE	TC
logit	PS/**MPS**/R	PS/**MPS**/R	PS/**MPS**/R	S/G/**MPS**	S/G/PS	S/R/PS
probit	PS/**MPS**/R	PS/**MPS**/R	PS/**MPS**/R	S/L/**MPS**	S/L/R	S/L/R
robit(0.6)	PS/**MPS**/R	PS/**MPS**/R	PS/**MPS**/R	R/S/PS	R/PS/S	R/PS/S
robit(1)	PS/**MPS**/R	PS/**MPS**/R	PS/**MPS**/R	R/S/**MPS**	R/PS/S	R/S/PS
robit(2)	PS/**MPS**/R	PS/**MPS**/R	**MPS**/R/G	S/R/**MPS**	S/R/**MPS**	R/S/**MPS**
gev(1)	PS/**MPS**/R	PS/**MPS**/R	PS/**MPS**/G	S/G/PS	S/G/PS	S/G/PS
gev(0.5)	PS/**MPS**/R	PS/**MPS**/R	PS/**MPS**/G	S/G/**MPS**	G/S/PS	G/S/PS
gev(-0.5)	PS/**MPS**/R	PS/**MPS**/R	PS/**MPS**/R	S/**MPS**/PS	S/**MPS**/PS	S/R/**MPS**
gev(-1)	PS/**MPS**/R	PS/**MPS**/R	PS/**MPS**/R	S/**MPS**/PS	S/**MPS**/PS	S/R/**MPS**
splogit(0.6)	PS/**MPS**/R	PS/**MPS**/R	PS/**MPS**/R	L/**MPS**/R	L/**MPS**/R	S/L/**MPS**
splogit(1.5)	PS/**MPS**/R	PS/**MPS**/R	PS/**MPS**/R	S/**MPS**/PS	S/PS/**MPS**	S/PS/R

2.6 Real data analysis

In this section, we use the data from Muggeo and Ferrara (2008) with sample size $n = 683$ to compare the models considered in section 2.5.2. The data set is available at http://www.econ.uiuc.edu/~roger/courses/471/data/weco.dat, which is used to study the quit behavior of production workers. The response variable is binary with $y_i = 1$ if the worker quits within six months of starting a new job, 0 otherwise.

The model we fit in MPS is,

$$\text{logit}(\mu_i) = \phi(U(\beta_1 x_1 + \beta_2 x_2)),$$

where $\phi(\cdot)$ is an unknown function which is estimated by P-spline, $U(\cdot)$ is the rescaled centered beta cumulative distribution function given in section 2.4, and the constraint for coefficients is $\beta_1^2 + \beta_2^2 = 1$. The variable x_1 denotes sex with 1 for males and 0 for females and the variable x_2 denotes the dexterity test score.

A fivefold cross-validation is conducted to compare the performance of different models. The average misclassification rates for logit, probit, robit, GEV, splogit, the monotone nonparametric link (MPS) and GAM are 0.253, 0.252, 0.243, 0.253. 0.248, 0.243 and 0.251, respectively. The additional parameter in link function is estimated together with the regression coefficients according to Section 2.2. We can see that the robit link and MPS link provide similar results. Figure 2.6

shows the estimated link functions for the two levels of "sex." The bottom and top bars are the distributions of the dexterity test score. Robit and MPS links have similar patterns, that is why they have similar results. Logit and probit have almost the same curve, so probit is not shown here. Logit, probit, splogit and GEV have big differences from the MPS link in the tails. When using MPS link function, the estimated coefficients for sex and dex are 0.5899 (se 0.1498) and -0.8075 (se 0.1049), which means that males tend to quit the job more than females when they have the same dexterity score and the higher the dexterity score the smaller the probability to quit the job within six months. The standard errors in the parentheses are based on bootstrap samples with $B = 100$. Figure 2.7 shows the estimated link function in black lines and 100 estimated link functions based on bootstrap samples in gray lines.

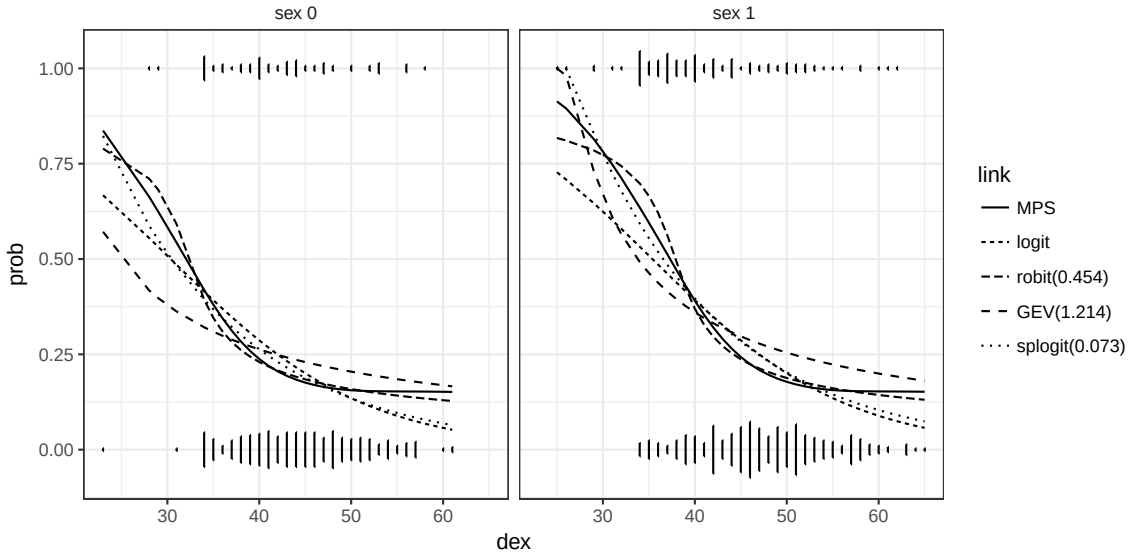

Figure 2.6: The plot of $P(y_i = 1)$ under different link functions

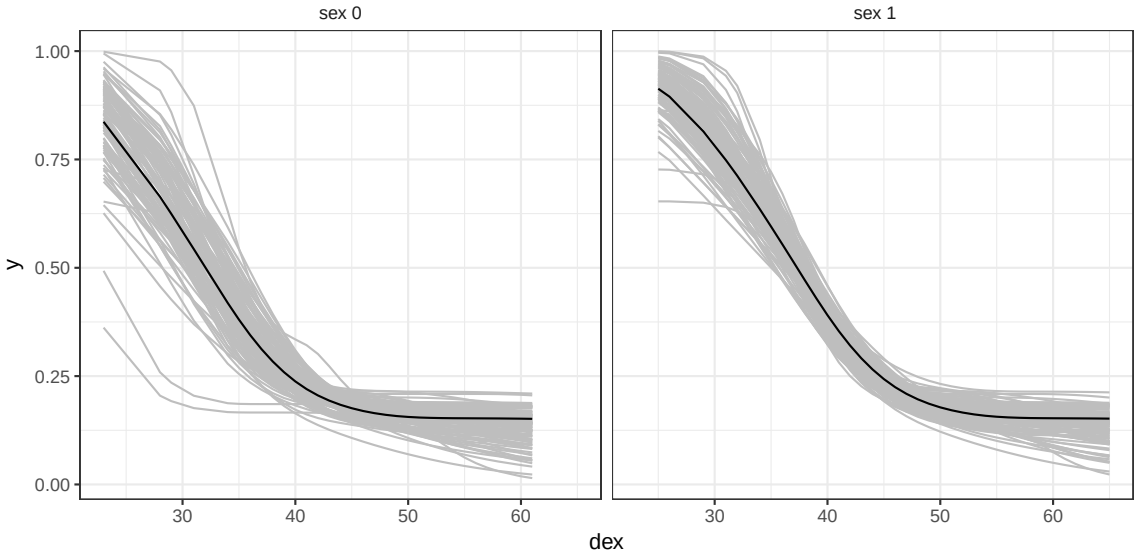

Figure 2.7: Estimated link function from bootstrap samples

2.7 Conclusion and discussion

As mentioned in Section 2.3, algorithm of (2.5) may not satisfy the monotonicity constraint $\boldsymbol{A\delta} \geq 0$ for some λ. As an example, we simulate a data set with sample size 100 with $GEV(1)$ link. We estimate the model with $\lambda = 20$ and calculate $A\boldsymbol{\delta}$, which has negative values. Thus, the monotone constraint is not satisfied. And the precision may depend on the value of κ. If the value of κ increases to 10^{14} or larger, it would have numeric issue when calculating the matrix inverse. If the sample size increases to 500 with the first 100 the same as before, then the estimated $\boldsymbol{\delta}$ satisfies the constraint. However, when using (2.6), the constraint is satisfied automatically for any λ, at least at machine zero level (2.220446^{-16}).

The new algorithm estimates the unknown monotone link function in GLMs by P-spline. It guarantees that the estimated link function is monotone and it can handle multiple covariates. The algorithm contains two steps to update the regression coefficients and the link function separately. It ensures the monotone constraints through solving a quadratic optimization problem. In the simulation study, we compare several traditional link functions as well as recently developed skewed

link functions with those estimated nonparametrically. The results show that the nonparametric link function fitted using the proposed algorithm can approximate the true link functions very well in most cases. If the sample size is not very small, in the absence of prior knowledge on the true link function, we recommend the use of nonparametric link function, which provides a robust alternative for fitting GLMs.

Supplemental materials

Supplemental materials include extra details on our simulation study.

Bibliography

Aranda-Ordaz, F. J. (1981). On two families of transformations to additivity for binary response data. *Biometrika*, 68(2):357–363.

Bollaerts, K., Eilers, P. H., and Aerts, M. (2006). Quantile regression with monotonicity restrictions using P-splines and the l_1-norm. *Statistical Modelling*, 6(3):189–207.

Boyd, S. and Vandenberghe, L. (2004). *Convex optimization*. Cambridge university press.

Czado, C. and Santner, T. J. (1992). The effect of link misspecification on binary regression inference. *Journal of statistical planning and inference*, 33(2):213–231.

De Boor, C. (2001). *A practical guide to splines*. Springer-Verlag, New York.

Eilers, P. H., Li, B., and Marx, B. D. (2009). Multivariate calibration with single-index signal regression. *Chemometrics and Intelligent Laboratory Systems*, 96(2):196–202.

Eilers, P. H. and Marx, B. D. (1996). Flexible smoothing with B-splines and penalties. *Statistical science*, 11(2):89–121.

Eilers, P. H., Marx, B. D., and Durbán, M. (2015). Twenty years of P-splines. *SORT-Statistics and Operations Research Transactions*, 39(2):149–186.

Härdle, W. K., Müller, M., Sperlich, S., and Werwatz, A. (2012). *Nonparametric and semiparametric models*. Springer.

Hastie, T. and Tibshirani, R. (1990). *Generalized additive models*. CRC Press.

He, X. and Shi, P. (1998). Monotone B-spline smoothing. *Journal of the American statistical Association*, 93(442):643–650.

Ichimura, H. (1993). Semiparametric least squares (SLS) and weighted SLS estimation of single-index models. *Journal of Econometrics*, 58(1):71–120.

Jiang, X., Dey, D. K., Prunier, R., Wilson, A. M., and Holsinger, K. E. (2013). A new class of flexible link functions with application to species co-occurrence in cape floristic region. *The Annals of Applied Statistics*, 7(4):2180–2204.

Kim, S., Chen, M.-H., and Dey, D. K. (2008). Flexible generalized t-link models for binary response data. *Biometrika*, 95(1):93–106.

Klein, R. W. and Spady, R. H. (1993). An efficient semiparametric estimator for binary response models. *Econometrica*, 61(2):387–421.

Leitenstorfer, F. and Tutz, G. (2007). Generalized monotonic regression based on B-splines with an application to air pollution data. *Biostatistics*, 8(3):654–673.

Liu, C. (2004). Robit regression: a simple robust alternative to logistic and probit regression. In *Applied Bayesian modeling and causal inference from incomplete-data perspectives*, pages 227–238. Wiley: London.

Mallick, B. K. and Gelfand, A. E. (1994). Generalized linear models with unknown link functions. *Biometrika*, 81(2):237–245.

Marx, B. D., Eilers, P. H., and Li, B. (2011). Multidimensional single-index signal regression. *Chemometrics and Intelligent Laboratory Systems*, 109(2):120–130.

McCullagh, P. and Nelder, J. A. (1989). *Generalized linear models*. CRC press.

Muggeo, V. M. and Ferrara, G. (2008). Fitting generalized linear models with unspecified link function: A P-spline approach. *Computational Statistics & Data Analysis*, 52(5):2529–2537.

Pregibon, D. (1980). Goodness of link tests for generalized linear models. *Journal of the Royal Statistical Society. Series C (Applied Statistics)*, 29(1):15–23.

Ramsay, J. O. (1988). Monotone regression splines in action. *Statistical science*, 3(4):425–441.

Ramsay, J. O. (1998). Estimating smooth monotone functions. *Journal of the Royal Statistical Society. Series B, Statistical Methodology*, 60(2):365–375.

Roy, V. (2014). Efficient estimation of the link function parameter in a robust Bayesian binary regression model. *Computational Statistics & Data Analysis*, 73:87–102.

Wang, L. and Yang, L. (2009). Spline estimation of single-index models. *Statistica Sinica*, 19(2):765–783.

Wang, W. and Small, D. S. (2015). Monotone B-spline smoothing for a Generalized linear Model Response. *The American Statistician*, 69(1):28–33.

Wang, X. and Dey, D. K. (2010). Generalized extreme value regression for binary response data: an application to B2B electronic payments system adoption. *The Annals of Applied Statistics*, 4(4):2000–2023.

Wang, Z. (2000). An algorithm for generalized monotonic smoothing. *Journal of Applied Statistics*, 27(4):495–507.

Weisberg, S. and Welsh, A. (1994). Adapting for the missing link. *The Annals of Statistics*, 22(4):1674–1700.

Wood, S. (2006). *Generalized additive models: an introduction with R*. CRC press.

Wood, S. N. (2008). Fast stable direct fitting and smoothness selection for generalized additive models. *Journal of the Royal Statistical Society: Series B, Statistical Methodology*, 70(3):495–518.

Ypma, J. (2014). Introduction to nloptr: an R interface to NLopt. Technical report.

Yuan, Y. (2008). *Prediction performance of survival models*. University of Waterloo.

CHAPTER 3. SMALL AREA ESTIMATION OF PROPORTIONS WITH CONSTRAINT FOR NATIONAL RESOURCES INVENTORY SURVEY

Xin Wang [1], Emily Berg[1], Zhengyuan Zhu[1], Dongchu Sun[2] and Gabriel Demuth[1]

[1]Department of Statistics, Iowa State University

[2]Department of Statistics, University of Missouri-Columbia and East China Normal University

Abstract

Motivated by the need to produce small area estimates for the National Resources Inventory survey, we develop a spatial hierarchical model based on a generalized Dirichlet distribution to construct small area estimators of compositional proportions in several mutually exclusive and exhaustive land cover categories. At the observation level, the standard design based estimators of the proportions are assumed to follow the generalized Dirichlet distribution. After proper transformation of the design based estimators, beta regression is applicable. We consider a logit mixed model for the expectation of the beta distribution, which incorporates covariates through fixed effects and spatial effect through a conditionally autoregressive process. In a design based evaluation study, the proposed model based estimators are shown to have smaller root mean squared error and relative root mean squared error than design based estimators and multinomial model based estimators.

key words: Generalized Dirichlet distribution; Spatial hierarchical model; Sampling variance modeling; Small area estimation; Survey statistics

3.1 Introduction

The National Resources Inventory (NRI) is a longitudinal survey that monitors status and trend in numerous characteristics, primarily related to natural resources and agriculture, on nonfederal

US land. It is the largest and one of the longest longitudinal surveys in US and provides critical information on soil erosion, land management and landcover change, which is important for the evaluation of climate change and effects of land conservation practices. One of the parameters of interest in the NRI is the proportion of area for a set of mutually exclusive and exhaustive land categories termed broaduses. Examples of broaduses are cultivated cropland, pasture, forest, and developed land. The NRI sample design is a two-phase stratified design, and data collection is largely through interpretation of aerial photography. Section 3.2 reviews the essential features of the NRI sample design, data collection, and estimation procedures for our application. Nusser and Goebel (1997) and Breidt and Fuller (1999) provide further detail. Traditionally, the NRI publishes estimates of broaduse proportions at state and national levels.

Accurate information on local land-cover compositions is essential for developing conservation policies and land management plans. In particular, monitoring cultivated cropland is important for agricultural planning and ensuring a sustainable food supply. Motivated by such demand, Natural Resources Conservation Service (NRCS) asked us to develop county level estimates of broaduse proportions for NRI. Because of small sample sizes, standard NRI estimators can have relatively large estimated coefficient of variation at the county level. Additional sources of information, particularly auxiliary variables and explicit model assumptions, are needed to improve the precision of the county level estimators.

We would like the model applied to NRI estimators of county level broaduse proportions to have several characteristics. Estimators based on the model should respect the parameter space for the proportions and satisfy a sum-to-one constraint. The model should allow incorporation of covariates and spatial dependence structures to provide more information to improve the estimators. As we will demonstrate in Section 3.3, including spatial dependence as well as auxiliary information is important because the auxiliary variables do not fully explain the spatial structure in the data. Additionally, it is desirable to incorporate the estimated variance of the original NRI estimators (design based), since the NRI is a complex survey, variance estimator can reflect the complexity of

the design. The NRI county level estimation application is an example of a more general problem of estimating a vector of proportions that sum to one for each small area.

Fay and Herriot (1979) and Battese et al. (1988) introduce the approach of using linear mixed effects models to obtain more precise small area estimators. Rao and Molina (2015), Jiang and Lahiri (2006b), and Pfeffermann (2013) review extensions to more complex models, including models with correlated random components and nonlinear expectation functions. One approach for binary response variables is to model the small area counts (Rao and Molina, 2015). For example, He and Sun (2000) use a hierarchical Bayesian model with spatial correlations that treats the realized counts as binomial random variables to estimate hunting success rates. An alternative method is to model the proportions directly (Datta et al., 1999). Jiang and Lahiri (2006a) use a beta linking model for the expectation of design based estimators of proportions. Liu et al. (2007) compare several hierarchical Bayesian models for proportions in the context of small area estimation. In particular, models where the design based estimators are assumed to have beta distributions are compared to models where the design based estimators are assumed to have normal distributions. The models of Liu et al. (2007) respect the sampling design and include covariates, but they do not incorporate spatial dependence structures. These methods for binary data do not apply readily to a vector of proportions with a sum to one constraint.

Analyzing a vector of proportions with a constraint can start from a multinomial or Dirichlet distribution. Agresti and Hitchcock (2005) and Congdon (2005) review Bayesian estimation of multinomial parameters. Molina et al. (2007) and López-Vizcaíno et al. (2013) use multinomial-based mixed models to analyze labor force participation without considering spatial dependence. In López-Vizcaíno et al. (2015), the model was extended to a time correlated model with area random effects. Jin et al. (2013) use spatial multinomial regression models for the purpose of understanding relationships between land ownership history and forest landscape structure, an objective that is analytical in nature and differs from small area prediction. Berg and Fuller (2014) use the covariance structure of the Dirichlet distribution as a working model for small area prediction of vectors of proportions that satisfy a restriction.

Models based on the multinomial or Dirichlet distribution assume negative correlations between different categories, a structure that the real data may not satisfy. The relationships between means and variances of different categories for these two distributions may not hold for the survey estimators. The generalized Dirichlet (GD) distribution is a flexible model for vectors of proportions that satisfy a sum-to-one constraint. We can incorporate the sampling variances and preserve the sampling variance structure. Connor and Mosimann (1969) discuss general properties of the GD distribution. Wong (1998) discusses the use of the GD distribution as a prior for the multinomial distribution. One convenient property of the GD distribution is that independent beta distributions with different parameters are obtained after proper transformation. Ferrari and Cribari-Neto (2004) propose beta regression to model rates and proportions. In their model, they reparameterize the beta density so that the parameters of the beta density function are an expectation parameter and a dispersion parameter. Simas et al. (2010) extend beta regression to allow a nonlinear term in the regression and model the dispersion parameter as well. Gamerman and Cepeda-Cuervo (2013) considers spatial effects in both the mean and dispersion models for beta regression models.

To specify a model appropriate for the NRI application, we begin with an assumption that the observed county level proportions are realizations from the GD distribution. The GD assumption permits a transformation of the county level proportions to independent beta random variables with distinct mean and dispersion parameters. Spatial information can also be considered in small area estimation problems (Petrucci and Salvati, 2006; Lawson et al., 2012). Spatial hierarchical Bayesian models are specified for the transformed variables here. The expectation of the beta distribution is modeled as a logit-linear mixed model with covariates describing large scale structure and spatially correlated random effects for counties. The spatial structure is specified through a spatial conditionally autoregressive (CAR) model, as in Banerjee et al. (2014). The complexities of the NRI design and the availability of the auxiliary information make area-level modeling preferable to unit-level models. We discuss how the NRI motivates our model choice in more detail in Sections 3.2-3.3.

Modeling the sampling variances of the survey estimators is essential in many small area estimation applications because the survey based variance estimators often provide approximately unbiased variance estimators but can have large variances due to small sample sizes. Appropriately specified variance models can retain the information about the sample design and estimation procedures contained in the design based variance estimator, while reducing the variance of the variance estimator by borrowing information across areas. Cho et al. (2002) model the sampling variances with lognormal distributions. Maples et al. (2009), Dass et al. (2012) and Maiti et al. (2014) discuss the use of chi-squared distributions to model sampling variance. Gomez-Rubio et al. (2010) discuss both spatial models and modeling the variance in small areas in a Bayesian setting.

Our model for the design based estimators of the variances, described in more detail in Section 3.3, accomplishes two goals. The first is to treat the survey based variance estimators as approximately unbiased. The second is to incorporate auxiliary information. Our variance model exploits both the chi-square distribution and the lognormal distribution to achieve these two ends. Our sampling variance model extends that of Maiti et al. (2014) to incorporate covariates and uses Bayesian instead of frequentist procedures for inference.

A design based simulation study is conducted in section 3.4 to compare our proposed model based estimators to design based estimators and the estimators based on the multinomial model proposed in López-Vizcaíno et al. (2013). We treat the NRI "foundation sample," the sample obtained in the first phase of the NRI's two phase design, as the finite population for the design based simulation study, and use a sample design similar to the NRI sample design to select subsamples for the Monte Carlo (MC) study. The MC relative root mean squared error and mean squared error are computed for both design based estimators and estimators based on the hierarchical GD model, using the complete foundation sample as the reference for constructing true parameters. The results show that our proposed model based estimators can reduce relative RMSE and RMSE by 15% or more on average compared with design based estimators, and performs better than the estimators based on the multinomial model.

In Section 3.2, we introduce the National Resources Inventory survey in detail. In Section 3.3, the proposed hierarchical GD model is described. Then, we compare design based and model based estimators through a design based Monte Carlo study, in which we treat the foundation data as the target finite population and sample it using a sampling design that reflects the properties of the NRI sampling design in Section 3.4. In Section 3.5, proposed models are applied to estimate the proportions of area in several broaduses for Iowa counties in 2012. Section 3.6 summarizes and identifies areas for future work.

3.2 National Resources Inventory

The NRI is supported by the US Department of Agriculture Natural Resources Conservation Service and conducted in cooperation with Iowa State University. The NRI sample design is a two-phase sample (Nusser and Goebel, 1997). The first phase sample, called the "foundation sample," consists of approximately 300,000 segments (primary sampling units), each of which contains 2 or 3 sampled points (secondary sampling units). From 1982- 1997, the full NRI foundation sample was observed in five-year intervals (1982, 1987, 1992 and 1997). In 2000, the NRI transitioned to an annual sample design to facilitate special studies and spread the workload more evenly. Because observing all 300,000 segments in the foundation sample on an annual basis is too expensive, the annual samples are subsamples of original foundation sample. In the annual samples, approximately 40,000 segments, called "core" segments, are observed every year. The rest of the foundation sample is divided into several supplemental panels, each with approximately 30,000 segments that are observed periodically. That means, about 70,000 segments are observed every year since 2000.

Data collection in the NRI is primarily through visual interpretation of aerial photography supplemented by local data collection and integration of administrative records. Some information is collected at the point level, such as the type of crop planted in the field containing a point. Other information is collected at the segment level, such as the urban area in the segment. An estimation procedure creates imputed points to represent segment information and imputes data to create a complete time series for points not observed in a particular year. All the information is

transformed to points with associated weights to represent the sample design and adjustments to administrative control totals. In the final data set, each record corresponds to a real or imputed point, each of which contains a complete time series and an associated weight. Weighted sums of characteristics for points are considered approximately unbiased for the corresponding population parameters.

Each year, a point y_j is classified into a set of mutually exclusive and exhaustive land cover categories called broaduses. The standard NRI design based estimator of the proportion of area in broaduse k ($k = 1, \ldots, 12$) for the state in a particular year is defined as

$$\hat{p}_k = \frac{\sum_{j=1}^{n_{state}} w_j I[y_j = k]}{\sum_{j=1}^{n_{state}} w_j}, \tag{3.1}$$

where w_j is the weight for point j in the state, $I[y_j = k]$ is the indicator that point j is classified in category k, n_{state} is the number of points in the state, and the subscript for year is omitted because we focus on a single time point. Because the NRI uses the area of the state as control, $\sum_{j=1}^{n_{state}} w_j$ is equal to the area of the state. Similarly, the NRI design based estimator of the proportion of county i in broaduse k is defined as

$$\hat{p}_{ki} = \frac{\sum_{j=1}^{n_i} w_{ij} I[y_{ij} = k]}{\sum_{j=1}^{n_i} w_{ij}}, \tag{3.2}$$

where n_i is the number of points in county i, and ij indexes the j^{th} point in the i^{th} county. Because the first phase strata are contained in counties, it is reasonable to treat the sampling errors for estimators for two different counties as independent. Because of the complexity of the NRI design, jackknife method is used for variance estimation. The jackknife variance estimator for category k and county i is defined

$$\hat{V}(\hat{p}_{ki}) = \frac{B-1}{B} \sum_{b=1}^{B} (\hat{p}_{ki}^{(b)} - \hat{p}_{ki}^{est})^2 \tag{3.3}$$

where $\hat{p}_{ki}^{(b)}$ is the estimate based on the b^{th} set of replicate weights, $\hat{p}_{ki}^{est}$ is the mean of the B replicate estimates, and in the NRI, $B = 29$. To define the replicate weights, the NRI sample is sorted geographically and divided into 29 groups. The weight for an element assigned to group b is set to zero in replicate b, and ratio adjustments similar to those used to construct the original weights are repeated to construct the replicate weights.

The design based county estimates defined in (3.2) are not published. Since the survey is designed for state level estimates, the summation of all weights in one county may not match the area of the county. In addition, due to relatively small sample sizes for counties, particularly in the annual samples, the county level estimators are often judged unreliable in terms of estimated coefficient of variation (CV). For example, the estimated CV for cultivated cropland at the state level is 0.57% in 2012. However, estimates of CV for counties range from 10% to 30%. For pastureland, the average estimated CV across counties is 40%. Thus, we consider model based estimators to improve the precision of the county level estimators.

The Cropland data layer (CDL) is a classification of square pixels into several mutually exclusive and exhaustive land cover categories, which classified satellite readings into land cover categories using NASS survey data and administrative data as ground truth. See Han et al. (2012) for further detail on the CDL. The CDL has been released annually from 2006 through the present. We decided to obtain auxiliary information from the Cropland Data Layer because it is nationally consistent and timely. NRI and CDL categories are similar enough that we are able to build a map between CDL and NRI categories based on the definitions. And CDL contains categories that are relatively straightforward to map to NRI categories. However the goals of the NRI and CDL projects are different, and a one to one mapping between the NRI and CDL does not exist. After mapping NRI categories to CDL categories, the specific covariate used in the models is the proportion of pixels in a county classified in a particular NRI broaduse. Because of the NRI and CDL use different definitions and data collection procedures, the correlations between the covariate and the NRI estimators defined in (3.2) vary across categories. For example, the linear correlation is 0.9651 for cultivated cropland, but for pastureland, the linear correlation is 0.5029. For pastureland, the spatial dependence has potential to help to improve the model based estimators, even after considering auxiliary information.

3.3 Spatial Bayesian hierarchical models for proportions

As mentioned in Section 3.2, the NRI county level estimates have large values of estimated coefficient of variation. Thus in this section, we propose the spatial Bayesian hierarchical models used for small area estimation of NRI county level proportions. In Section 3.3.1, we introduce the generalized Dirichlet (GD) distribution and present the transformation to independent beta random variables. In Section 3.3.2, we specify the hierarchical models used for small area estimation, which begin with an assumption that the NRI estimators of proportions are realizations from GD distributions and variance estimators are realizations from chi-squared distributions. Section 3.3.3 presents specific details required for Bayesian inference.

3.3.1 Generalized Dirichlet distribution

Let $p_k, k = 1, \ldots, K$ be the proportion of the kth category with $\sum_{k=1}^{K} p_k = 1$. The probability density function of the generalized Dirichlet distribution (Connor and Mosimann, 1969) is

$$f(\boldsymbol{p}, |\boldsymbol{\eta}_1, \boldsymbol{\eta}_2) = \left[\prod_{k=1}^{K-1} B(\eta_{1k}, \eta_{2k})\right]^{-1} p_K^{\eta_{2,K-1}-1} p_1^{\eta_{11}-1} \prod_{k=2}^{K-1} \left[p_i^{\eta_{1k}-1} \left(\sum_{j=k}^{K} p_j\right)^{\eta_{2,k-1}-(\eta_{1k}+\eta_{2k})}\right], \quad (3.4)$$

where $\boldsymbol{p} = (p_1, \ldots, p_{K-1}, p_K)^T$, $p_K = 1 - \sum_{k=1}^{K-1} p_k$, $\boldsymbol{\eta}_1 = (\eta_{11}, \ldots, \eta_{1,K-1})^T$, $\boldsymbol{\eta}_2 = (\eta_{21}, \ldots, \eta_{2,K-1})^T$, and $B(\eta_{1i}, \eta_{2i})$ is the beta function. We denote $f(\boldsymbol{p}, |\boldsymbol{\eta}_1, \boldsymbol{\eta}_2)$ as $GD(\boldsymbol{\eta}_1, \boldsymbol{\eta}_2)$. From Connor and Mosimann (1969), the GD distribution has a useful connection to a collection of independent beta random variables. To define this relationship, let

$$z_k = \frac{p_k}{\sum_{j=k}^{K} p_j}, \text{for } k = 1, \ldots, K-1. \quad (3.5)$$

It can be shown (Connor and Mosimann, 1969) that $\{z_k, k = 1, \ldots, K-1\}$ is a collection of independent random variables with beta distributions, where the parameters governing the distribution of z_k are η_{1k} and η_{2k}.

Let $\alpha_k = E(z_k)$, from the transformation in (3.5) and the independence of z_k's, the expectations of p_k's are given by

$$E(p_k) = \begin{cases} \alpha_1 & k = 1, \\ \alpha_k \prod_{j=1}^{k-1} (1 - \alpha_j) & k = 2, \ldots, K-1, \\ \prod_{j=1}^{K-1} (1 - \alpha_j) & k = K. \end{cases} \tag{3.6}$$

The properties of the GD distribution are useful for the NRI application. Compared with the Dirichlet distribution, the GD distribution has more parameters, permitting greater flexibility. If $\eta_{2,k-1} = \eta_{1k} + \eta_{2k}$ for $i = 2, \ldots, K-1$, the GD distribution becomes the standard Dirichlet distribution. For Dirichlet distribution, the variance and the mean has a specific relationship, this relationship can be more flexible and is controlled by an extra parameter for GD distribution. The functional restrictions of the Dirichlet distribution also lead us to prefer the flexibility that the GD distribution allows.

3.3.2 Model specification

Let $i = 1, \ldots I$ be the index for area and $k = 1, \ldots K$ be the index for category. In the NRI application, the categories correspond to different land cover classes (broaduses), and the small areas are counties. Let $\hat{p}_{ki}$ be the design based estimator of the proportion of the kth category in county i. Assume that a design based estimator of the sampling variance, denoted $\hat{V}(\hat{p}_{ki})$, is available. In the NRI, $\hat{V}(\hat{p}_{ki})$ is obtained by jackknife variance.

Assume $(\hat{p}_{1i}, \ldots, \hat{p}_{Ki})^T$ follows $\mathrm{GD}(\boldsymbol{\eta}_{1i}, \boldsymbol{\eta}_{2i})$, where $\boldsymbol{\eta}_{1i} = (\eta_{1,1i}, \ldots, \eta_{1,(K-1)i})^T$ and $\boldsymbol{\eta}_{2i} = (\eta_{2,11}, \ldots, \eta_{2,(K-1)i})^T$. Based on the properties of the GD distribution, we use the following transformations,

$$z_{ki} = \frac{\hat{p}_{ki}}{\hat{p}_{ki} + \cdots + \hat{p}_{Ki}}, \tag{3.7}$$

where $z_{ki} \overset{ind}{\sim} \mathrm{Beta}(\eta_{1,ki}, \eta_{2,ki})$ for $k = 1, \ldots, K-1$. Then the problem becomes a beta regression problem. In a beta regression problem, expectation parameters $\alpha_{ki} = E(z_{ki}) = \eta_{1,ki}/(\eta_{1,ki} + \eta_{2,ki})$ and dispersion parameters $\phi_{ki} = \eta_{1,ki} + \eta_{2,ki}$ are modeled (Ferrari and Cribari-Neto, 2004; Simas et al., 2010).

The model structure we consider for the transformed expectation α_{ki} has following form,

$$\text{logit}(\alpha_{ki}) = \beta_{k0} + x_{ki}\beta_{k1} + U_{ki}. \tag{3.8}$$

Since $0 < \alpha_{ki} < 1$, we use a logit link function, that is $\text{logit}(x) = \log(x/(1-x))$. x_{ki} is a covariate, which can have more than one dimension in general. β_{k0} and β_{k1} are regression coefficients. We also consider the spatial information U_{ki}, since adjacent counties may have similar land cover characteristics and the auxiliary information does not fully explain the spatial structure in the response variables.

In NRI, the covariate is obtained from the CDL, as discussed in Section 3.2. To define the covariate x_{ki}, we begin by defining a set of CDL proportions to have the same categories as the NRI proportions. The same transformation defined in (3.7) is applied to the CDL proportions to obtain $K-1$ proportions, $\hat{p}_{c,ki}$. The covariate x_{ki}, for $k = 1, \ldots, K-1$, is obtained by applying a logit transformation to the $\hat{p}_{c,ki}$, $k = 1, \ldots K-1$. The CAR model (Banerjee et al., 2014) is used to model the spatial effect in (3.8), which is defined by conditional distributions $(U_{ki}|U_{kj}, j \neq i) \sim N(\rho_k \sum_{j \neq i} C_{ij}U_{kj}/C_{i+}, \delta_k/C_{i+})$, where ρ_k is the spatial dependence parameter, δ_k is the variance component of category k, $\boldsymbol{C}$ is the adjacency matrix with diagonal element $C_{ii} = 0$ and ijth off-diagonal element $C_{ij} = I[$ county i and j share a common boundary$]$, and $C_{i+} = \sum_{j \neq i} C_{ij}$. The joint distribution of $\boldsymbol{U}_k = (U_{k1}, \ldots, U_{kI})'$ is $N(0, \delta_k(\boldsymbol{D} - \rho_k \boldsymbol{C})^{-1})$, where $\boldsymbol{D} = \text{diag}(C_{1+}, \ldots, C_{n+})$. In order to guarantee $\boldsymbol{D} - \rho_k \boldsymbol{C}$ is positive definite, ρ_k should satisfy $\lambda_{\min}^{-1} < \rho_k < \lambda_{\max}^{-1}$, where $\lambda_{\min}$ and $\lambda_{\max}$ are the minimal negative and maximal positive eigenvalues of $\boldsymbol{D}^{-1/2}\boldsymbol{C}\boldsymbol{D}^{-1/2}$, respectively. The ability of this formulation to accommodate different spatial dependence parameters and different regression parameters is particularly important for the NRI application. As explained in Section 3.2, the correlations between NRI proportions and CDL proportions vary by category, as well as the strength of the spatial dependence. To allow this flexibility, we consider the general model in which different categories have different spatial dependence parameters ρ_k.

Next, we will build a model on the dispersion parameters ϕ_{ki}. The most general assumption for dispersion parameter allows a different ϕ_{ki} for each area and category. Under this assumption,

one approach of estimating ϕ_{ki} is to estimate ϕ_{ki} with the design based estimators and variance estimators of the proportions and then treat the estimated ϕ_{ki} as fixed quantities in the models. Treating a design based estimate of the variance as the true variance is an approach that has been used in the small area estimation literature (Jiang and Lahiri, 2006a). For this approach, according to the definition of beta distribution, we have

$$\hat{\phi}_{ki} = \frac{z_{ki}(1-z_{ki})}{\hat{V}(z_{ki})} - 1, \tag{3.9}$$

where z_{ki} is obtained from the estimators of proportions as defined in (3.7), and $\hat{V}(z_{ki})$ can be approximated by Taylor series approximation for the proportions and the estimates of the sampling variances of the proportions $\hat{V}(\hat{p}_{ki})$ given in (3.10),

$$\begin{aligned}\hat{V}(z_{ki}) = &\left(\frac{\sum_{j=k+1}^{K}\hat{p}_{ji}}{(\sum_{j=k}^{K}\hat{p}_{ji})^2}\right)^2 \hat{V}(\hat{p}_{ki}) + \sum_{j=k+1}^{K}\left(\frac{\hat{p}_{ki}}{(\sum_{j=k}^{K}\hat{p}_{ji})^2}\right)^2 \hat{V}(\hat{p}_{ji}) \\ &-2\sum_{j=k+1}^{K}\frac{\hat{p}_{ki}\sum_{j=k+1}^{K}\hat{p}_{ji}}{(\sum_{j=k}^{K}\hat{p}_{ji})^4}\widehat{Cov}(\hat{p}_{ki},\hat{p}_{ji}) + \sum_{j=k+1}^{K}\sum_{g\neq j}\frac{\hat{p}_{ki}^2}{(\sum_{j=k}^{K}\hat{p}_{ji})^4}\widehat{Cov}(\hat{p}_{ji},\hat{p}_{gi}).\end{aligned} \tag{3.10}$$

The covariance is calculated as $\widehat{Cov}(\hat{p}_{ki},\hat{p}_{ji}) = \rho_{kj,i}\sqrt{\hat{V}(\hat{p}_{ki})\cdot\hat{V}(\hat{p}_{ji})}$, where $\rho_{kj,i}$ is replaced by the sample correlation between $\hat{\boldsymbol{p}}_k$ and $\hat{\boldsymbol{p}}_j$ with $\hat{\boldsymbol{p}}_k = (\hat{p}_{k1},\ldots,\hat{p}_{kI})^T$. The model based on fixed quantities of ϕ_{ki} in (3.9) is denoted as "M1". That is, In "M1", the expectation model is $\text{logit}(\alpha_{ki}) = \beta_{k0} + x_{ki}\beta_{k1} + U_{ki}$, for $k = 1,\ldots,K-1$ and ϕ_{ki}'s are estimated from (3.9).

The other approach is to model ϕ_{ki} through modeling the sampling variance. As in Maiti et al. (2014), we can build a joint model with both means and variances. The variance model is built through using both chi-squared and lognormal distributions in (3.11) and (3.12), allowing us assume that the NRI variance estimators are unbiased, respect the mean-variance relationship in the beta distribution, and incorporate covariates. For the variance model, assume

$$\hat{V}(z_{ki}) \sim \frac{V(z_{ki})}{q_i}\chi^2(q_i), \tag{3.11}$$

where $V(z_{ki}) = \alpha_{ki}(1-\alpha_{ki})/(\phi_{ki}+1)$. The dispersion parameter ϕ_{ki} is modeled as

$$\log(\phi_{ki}) = \gamma_{k0} + \gamma_{k1}u_{ki} + e_{ki}, \tag{3.12}$$

where γ_{k0} and γ_{k1} are coefficients to estimate, u_{ki} is a covariate, and $e_{ki} \overset{\text{iid}}{\sim} N(0, \delta_{\phi k})$. Here we use the same covariate in both mean model and variance model. In the NRI, we use the number of the primary sampling units (PSUs) in a county as the value of q_i, where we use the number of PSUs instead of the number of sampled points because we expect that a positive intracluster correlation would cause the variance estimate based on the number of sampled points to be too small. The model combining variance model in (3.11) is denoted as "M2". In our application, we prefer to use the model "M2", which combines the mean model in (3.8) and the variance model (3.11) together. That is, in "M2", the expectation model is $\text{logit}(\alpha_{ki}) = \beta_{k0} + x_{ki}\beta_{k1} + U_{ki}$, and ϕ_{ki}'s are modeled through the variance model $\hat{V}(z_{ki}) \sim \chi^2(q_i)V(z_{ki})/q_i$.

3.3.3 Bayesian estimation

We specify the following priors: $\pi(\boldsymbol{\beta}) \propto 1$, $\pi(\boldsymbol{\gamma}) \propto 1$ and $\rho_k \sim \text{Uniform}(\lambda_{\min}^{-1}, \lambda_{\max}^{-1})$. As in Gelman (2006) and Polson and Scott (2012), the inverted-beta prior is used as the prior distribution for variance parameters, which is equvilant to use the half-Cauchy prior for the stanadard deviation parameter. We use Gibbs sampling to simulate from the posterior distributions. Because the full conditional distribution for $v_{ki} = \text{logit}(\alpha_{ki})$ does not have a closed form, Metropolis Hastings is used to sample from the posterior distributions of these parameters using the techniques in Diggle et al. (1998). For ρ_k, since the posterior distribution of ρ_k is proportional to a logconcave function, adaptive rejection sampling (Gilks and Wild, 1992) is used here. To diagnose convergence, we use the scale reduction factor (Gelman and Rubin, 1992). The burn in value is 5000 iterations and the next 5000 iterations are used to approximate the posterior distributions in the simulation study. In real data analysis, the 50000 iterations after burn-in size 10000 iterations are used.

3.4 Design based simulation study

In this section, we conduct a design based Monte Carlo (MC) study to evaluate the properties of the estimators under conditions reflective of the NRI. The first phase NRI sample (the foundation sample) serves as the finite population for the simulation study. The parameters of interest are the

county level proportions in the categories cultivated cropland, pastureland, and the remainder (a combined category contains all other 9 categories) for the year 1997, the last year in which the full foundation sample was observed. The full foundation sample is considered as the finite population. Samples are drawn from the population. For each sample, we calculate the design based estimates and model based estimates. We compare estimators based on the models proposed in Section 3.3 ("M1" and "M2") to design based estimators in (3.2) and estimators based on the multinomial model of López-Vizcaíno et al. (2013).

The sample design for the simulation study is a stratified single-stage cluster sample with counties as strata. The primary sampling unit is an NRI segment, and all points in a selected segment are included in the sample. Iowa has 99 counties, and the number of segments per county in the finite population for Iowa ranges from 46 to 259. We use pivotal sampling (Deville and Tille, 1998) implemented in the `R` package Tille and Matei (2016) (*sampling*) to select a without-replacement sample of segments with specified selection probabilities. The initial inclusion probability for each segment is proportional to the weight of the segment, which is the summation of all the point weights in the segment. For each county, the sampling fraction is 0.2, which is close to that in the NRI annual sample. The design based estimators (Horvitz-Thompson estimator) (Särndal et al., 2003) and the corresponding variance estimators (Stehman and Overton, 1989) are calculated. The estimation procedure is implemented by the `R` package Lumley (2011) (*survey*) .

In the foundation sample (the finite population for the simulation), the area of each of the three categories (Cultivated Cropland, Pastureland and other) that we consider is greater than zero in every county. A design based estimate for a random sample, however, may equal zero. Because the support of the beta distribution does not contain zero, we use a simple procedure to replace zero estimates with positive values. The weight of each point is rounded to 100 acres, and we know the area of each county. A zero estimate for a category therefore means that estimate of the area of that category in the county, without rounding the weights, would fall between 0 and $1/T_i$ acres, where T_i is the known area of county i in units of 100 acres, which is range from 2523 to 6331. We replace a zero design based estimate with the small proportion $0.5/T_i$, which is the midpoint

between the lower bound of 0 and the upper bound of $1/T_i$. The percentage of zero estimates is around 4% .

Figure 3.1 and Figure 3.2 show the MC root mean squared error (RMSE) and the MC relative root mean squared error (RRMSE), respectively, for model based estimators and the design based estimator. The relative RMSE is calculated as RMSE_{ki}/p_{ki}, where $\text{RMSE}_{ki} = \sqrt{R^{-1}\sum_{r=1}^{R}(\hat{p}_{ki}^{(r)} - p_{ki})^2}$, $\hat{p}_{ki}^{(r)}$ is the estimator (model or design based) of the proportion in category k and county i in MC sample r, and p_{ki} is the finite population proportion for the simulation. The number of MC samples is $R = 200$. The estimator based on the multinomial model of López-Vizcaíno et al. (2013) is denoted "Mult".

Figure 3.1: Design RMSE of small area estimators based on different models

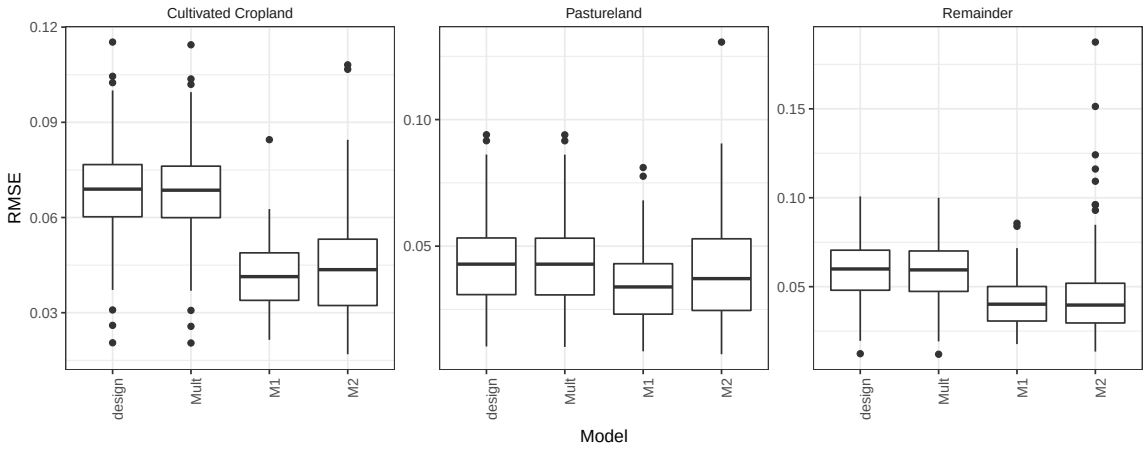

In terms of mean and median RMSE and relative RMSE, the proposed model based estimators perform better than the design based estimators and the estimators based on the multinomial model. As mentioned above, all the components in multinomial distribution are assumed negatively correlated. For the GD distribution, only the first component is negatively correlated with other components. For this finite population, the estimators for cultivated cropland are negatively correlated with other two categories, while the estimators for pasture and the remainder are positively correlated with each other. The ability of the GD distribution to describe this correlation structure may explain why the estimators based on the GD distribution are more efficient than

Figure 3.2: Design relative RMSE of small area estimators based on different models

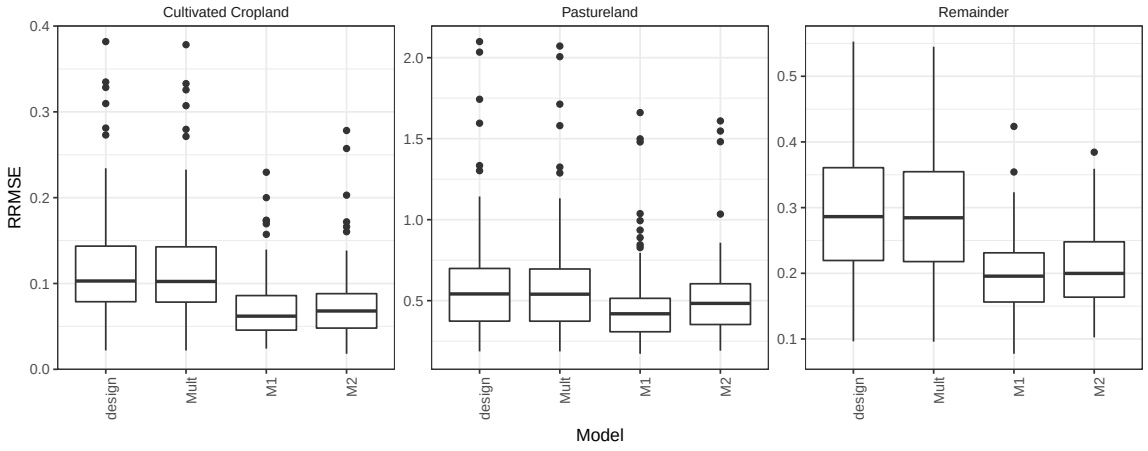

estimators based on the multinomial distribution. Estimators based on M1 have the smallest mean and median relative RMSE and RMSE. The estimators for the pasture domain have larger relative RMSE than the estimators for the remainder categories because the finite population proportions for pasture are typically small.

We also evaluate the posterior variance as an estimator of the MC variance. The MC variance is defined as the variance of R estimates, $V(\hat{p}_{ki}) = \sum_{r=1}^{R} \left(\hat{p}_{ki}^{r} - \hat{p}_{ki}^{\text{avg}}\right)^2 / (R-1)$, where $\hat{p}_{ki}^{\text{avg}}$ is the mean of the R estimates. In order to evaluate the bias of the posterior variance as an estimator of the MC variance, we calculate the MC relative bias as $E(\hat{V}(\hat{p}_{ki}))/V(\hat{p}_{ki}) - 1$, where $E(\hat{V}(\hat{p}_{ki}))$ is the MC mean of the posterior variance. For "M1", posterior variances of the GD-based have positive bias for cultivated cropland and remainder categories but a negative bias for pastureland. The posterior variance based on the "M2" model has a positive bias for the MC variance for all categories. Even though, the posterior variance is not expected to be an unbiased estimator of the design-variance of the estimators, the average of posterior variances is smaller than the variance of the design based estimators, demonstrating that the posterior variance captures the efficiency gain due to the use of the spatial hierarchical Bayesian model.

3.5 Application to 2012 NRI

In this section, we apply models M1 and M2 to 2012 NRI data to obtain estimates of county level proportions. The parameters of interest in the application are the proportion of area in each of Iowa's 99 counties in the categories of Cultivated Cropland, Pastureland, and the Remainder, which is a set containing all other 9 categories, in 2012. All of these three categories have nonzero estimates. As discussed in Section 3.2, the estimated coefficient of variation for design based NRI estimates at the county level are often large. Model based estimates are considered here to improve the reliability of the estimators. The estimated variance of z_{ik} is calculated using jackknife replicate weights prepared for the 2012 NRI.

Model assessment is based on the posterior predictive distribution (Gelman et al., 2014). Because state level estimates are considered stable in the NRI, we choose state level estimates as the characteristics of the data to which we compare data generated from the model. The following method is used to assess the model.

1. Calculate state level proportions $\hat{p}_k$ for $k = 1, \ldots, 3$, using the design based NRI estimates.
2. Simulate $z_{ki}^{(m)}$ from the posterior predictive distribution for $i = 1, \ldots, I, m = 1, \ldots, M$ from M1 and M2, where m denotes the Gibbs iteration.
3. Transform $z_{ki}^{(m)}$ back to $\hat{p}_{ki}^{(m)}$.
4. Calculate state level proportions $\hat{p}_k^{(m)} = \sum_{i=1}^{n} \hat{p}_{ki}^{(m)} \sum_{j=1}^{n_i} w_{ij} / \sum_{i=1}^{n} \sum_{j=1}^{n_i} w_{ij}$.
5. Calculate p-values as $\frac{1}{M} \sum_{m=1}^{M} I(\hat{p}_k^{(m)} > \hat{p}_k)$.

where n is the number of counties, n_i is the number of points in county i and w_{ij} is the weight of point ij. If we have really small p values or really large p values, that means the county level estimates based on models cannot capture the characteristics, state level estimates, of the data set. We also use DIC (Spiegelhalter et al., 2002) to compare different models. The model with smaller DIC is preferred.

Table 3.1 shows the results of the model assessment for the models considered. In terms of p-values, M2 is better, while M1 is better according to DIC. Based on these results, M2 reproduces the state level proportions better than M1. The predictive posterior distribution and DIC give different preferred models. In our application, we want the selected model to respect the original data structure and characteristics. Thus, we prefer M2 over M1 for this application, since we consider the state level estimates as important characteristics.

Table 3.1: Model assessment p-values and DIC values

	p-value			
	Cultivated Cropland	Pastureland	Others	DIC
M1	0.0470	0.8802	0.9501	-357.8808
M2	0.2204	0.2387	0.9087	-340.8546

Table 3.2 shows posterior means and standard deviations for different parameters. For the spatial effect ρ_k, the 95% credible intervals based on 2.5% and 97.5% quantiles are (-1.575, 0.967) and (0.799, 0.999) for cultivated cropland and pastureland, respectively. For cultivated cropland ($k = 1$), the spatial effect does not differ significantly from zero. The reason is that the covariate CDL itself has a strong spatial effect (Moran's I $p-$values less than 2^{-16}), and the NRI and CDL cropland also have a strong correlation (95% credible interval of β_1 is (0.833,1.116) in Table 3.2). Thus, the CDL explains the spatial structure in the NRI cultivated cropland estimates. In contrast, for pastureland ($k = 2$), the relationship between the NRI and CDL is not very strong (95% credible interval of β_1 is (-0.106, 0.687), and the spatial effect becomes highly significant, which is used to reduce the uncertainty in county estimates.

Because of the assumption of generalized Dirichlet distribution, the sum to one constraint is satisfied automatically. Since NRI is designed for state estimates, we also want that the aggregated county level model based estimates are equal to the design based survey state estimates. Thus, benchmarked estimates are considered, which satisfy both the sum-to-one constraint and the aggregated state level estimates based on the county level estimates equal to the NRI state level

Table 3.2: Estimates of parameters

	$k=1$ est (sd)	$k=2$ est (sd)
β_0	0.234 (0.062)	-1.033 (0.48)
β_1	0.973 (0.072)	0.288 (0.201)
γ_0	2.822 (0.072)	2.963 (0.101)
γ_1	-1.041 (0.086)	-0.708 (0.206)
δ	0.071 (0.06)	0.756 (0.238)
ρ	-0.075 (0.755)	0.952 (0.056)
δ_ϕ	0.271 (0.047)	0.575 (0.096)

estimates. Specifically, the benchmarking constraints are,

$$\sum_{k=1}^{3} \hat{p}_{ki} = 1, \qquad \text{for } i = 1, \ldots, n, \tag{3.13}$$

$$\sum_{i=1}^{n} \hat{p}_{ki} A_i = A_0 \hat{p}_k, \qquad \text{for } k = 1, \ldots, 3, \tag{3.14}$$

where A_i is the known area of county i, and $A_0 = \sum_{i=1}^{n} A_i$, which is the administrative state area. (3.13) and (3.14) are for the sum-to-one constraint and state level estimates constraint respectively. We use raking method (Kalton, 1983) to benchmark the estimates. Figure 3.3 shows the estimates of different categories.

Figure 3.3: Estimated maps

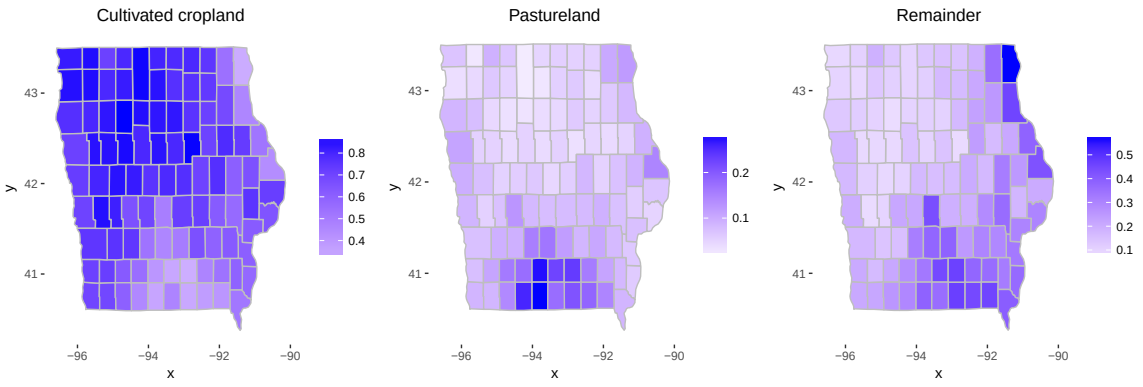

According to You et al. (2004), the posterior mean square error (PMSE) of the benchmarked estimator can be calculated as,

$$\widehat{PMSE}(\hat{p}_{ki}^{(bench)}) = \hat{V}(\hat{p}_{ki}^{post}) + (\hat{p}_{ki}^{post} - \hat{p}_{ki}^{(bench)})^2, \tag{3.15}$$

where $\hat{p}_{ki}^{post}$ is the model based estimator, $\hat{V}(\hat{p}_{ki}^{post})$ is the posterior variance of $\hat{p}_{ki}$, and $\hat{p}_{ki}^{(bench)}$ is the benchmarked estimator. The PMSE includes the corrections due to the benchmarking process. The benchmarked estimates do not differ much from the original model based estimates. For cultivated cropland and pastureland, the benchmarked estimates are larger than the original model based estimates. But for the remainder, the benchmarked estimates are smaller.

Figure 3.4 shows the estimates and 95% confidence intervals of the design based estimates and 95% posterior intervals of the benchmarked model based estimates for cultivated cropland. The confidence intervals are defined as $\hat{p}_{ki} \pm 1.96\sqrt{\hat{V}(\hat{p}_{ki})}$, where $\hat{p}_{ki}$ is the NRI design based estimate, $\hat{V}(\hat{p}_{ki})$ is the jackknife variance. And the posterior intervals are defined as $\hat{p}_{ki}^{(bench)} \pm 1.96\sqrt{\widehat{PMSE}(\hat{p}_{ki}^{(bench)})}$. Figure 3.4 demonstrates the efficiency gain due to the spatial hierarchical Bayesian model. This has important implication for policy because county estimates with better accuracy can provide better guides for land management planning at county level.

Figure 3.4: Intervals of cultivated cropland for NRI design based estimates and benchmarked estimates at county level

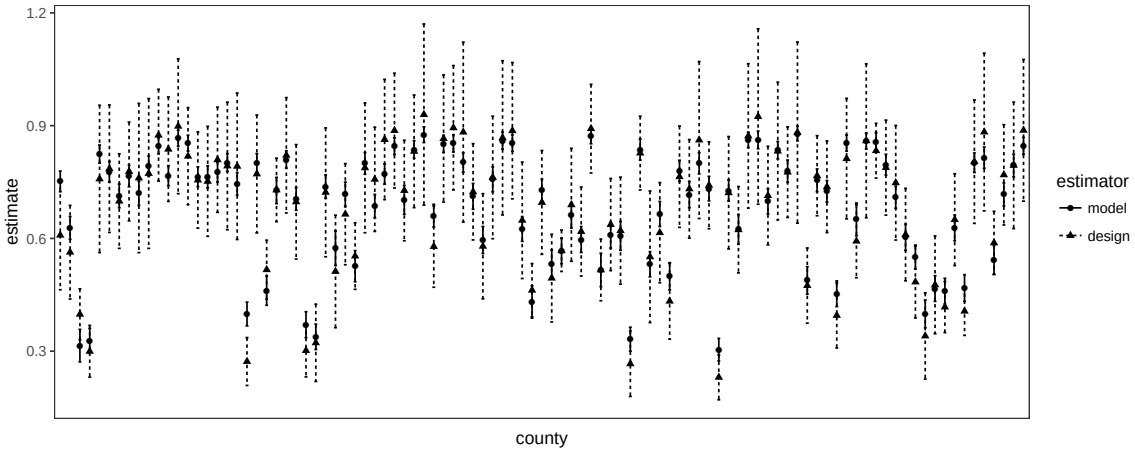

3.6 Discussion

This paper uses the generalized Dirichlet distribution to model design based estimates of proportions and obtain small area estimators of proportions. Based on the relationship between the

GD distribution and the beta distribution, a spatial Bayesian hierarchical model with beta regression is formulated and applied to NRI data. Another innovation is the introduction of a model for the dispersion parameter of the beta distribution that utilizes both chi-squared and lognormal distributions. In a design-based Monte Carlo study that represents the NRI data, the model based estimators are superior to design based estimators and multinomial model estimators in terms of RMSE and relative RMSE. The use of the posterior predictive distribution validates the use of the variance model for the NRI application.

The approach based on the GD distribution has several advantages for the NRI application. The GD distribution allows greater flexibility than both the multinomial distribution and the Dirichlet distribution. The variance model allows us to incorporate auxiliary information in the design based variance estimators. The model allows different covariate, regression parameters and spatial effects for different categories.

The study generates several questions for future work. The proposed models assume that all proportions are greater than 0. While this is not an important limitation for this application, in the future we will consider a zero-inflated model that allows zeros for both estimated proportions and true values. An extension to include a temporal component has potential utility for forecasting and estimation of change.

Bibliography

Agresti, A. and Hitchcock, D. B. (2005). Bayesian inference for categorical data analysis. *Statistical Methods and Applications*, 14(3):297–330.

Banerjee, S., Carlin, B. P., and Gelfand, A. E. (2014). *Hierarchical modeling and analysis for spatial data*. Crc Press.

Battese, G. E., Harter, R. M., and Fuller, W. A. (1988). An error-components model for prediction of county crop areas using survey and satellite data. *Journal of the American Statistical Association*, 83(401):28–36.

Berg, E. J. and Fuller, W. A. (2014). Small area prediction of proportions with applications to the Canadian Labour Force Survey. *Journal of Survey Statistics and Methodology*, 2(3):227–256.

Breidt, F. J. and Fuller, W. A. (1999). Design of supplemented panel surveys with application to the National Resources Inventory. *Journal of Agricultural, Biological, and Environmental Statistics*, 4(4):391–403.

Cho, M. J., Eltinge, J. L., Gershunskaya, J., and Huff, L. (2002). Evaluation of generalized variance function estimators for the US Current Employment Survey. In *Proceedings of the American Statistical Association, Survey Research Methods Section*, pages 534–539.

Congdon, P. (2005). *Bayesian models for categorical data*. John Wiley & Sons.

Connor, R. J. and Mosimann, J. E. (1969). Concepts of independence for proportions with a generalization of the Dirichlet distribution. *Journal of the American Statistical Association*, 64(325):194–206.

Dass, S. C., Maiti, T., Ren, H., and Sinha, S. (2012). Confidence interval estimation of small area parameters shrinking both means and variances. *Survey Methodology*, 38(2):173–187.

Datta, G. S., Lahiri, P., Maiti, T., and Lu, K. L. (1999). Hierarchical Bayes estimation of unemployment rates for the states of the US. *Journal of the American Statistical Association*, 94(448):1074–1082.

Deville, J.-C. and Tille, Y. (1998). Unequal probability sampling without replacement through a splitting method. *Biometrika*, 85(1):89–101.

Diggle, P. J., Tawn, J., and Moyeed, R. (1998). Model-based geostatistics. *Journal of the Royal Statistical Society: Series C (Applied Statistics)*, 47(3):299–350.

Fay, R. E. and Herriot, R. A. (1979). Estimates of income for small places: an application of James-Stein procedures to census data. *Journal of the American Statistical Association*, 74(366a):269–277.

Ferrari, S. and Cribari-Neto, F. (2004). Beta regression for modelling rates and proportions. *Journal of Applied Statistics*, 31(7):799–815.

Gamerman, D. and Cepeda-Cuervo, E. (2013). Generalized Spatial Dispersion Models. In *Technical report, Universidade Federal do Rio de Janeiro*.

Gelman, A. (2006). Prior distributions for variance parameters in hierarchical models (comment on article by Browne and Draper). *Bayesian analysis*, 1(3):515–534.

Gelman, A., Carlin, J. B., Stern, H. S., and Rubin, D. B. (2014). *Bayesian data analysis*, volume 2. Taylor & Francis.

Gelman, A. and Rubin, D. B. (1992). Inference from iterative simulation using multiple sequences. *Statistical science*, 7(4):457–472.

Gilks, W. R. and Wild, P. (1992). Adaptive rejection sampling for Gibbs sampling. *Journal of the Royal Statistical Society. Series C (Applied Statistics)*, 41(2):337–348.

Gomez-Rubio, V., Best, N., Richardson, S., Li, G., and Clarke, P. (2010). Bayesian statistics small area estimation. Technical report, Imperial College London (Unpublished). http://eprints.ncrm.ac.uk/1686/.

Han, W., Yang, Z., Di, L., and Mueller, R. (2012). CropScape: A Web service based application for exploring and disseminating US conterminous geospatial cropland data products for decision support. *Computers and Electronics in Agriculture*, 84:111–123.

He, Z. and Sun, D. (2000). Hierarchical Bayes estimation of hunting success rates with spatial correlations. *Biometrics*, 56(2):360–367.

Jiang, J. and Lahiri, P. (2006a). Estimation of finite population domain means: A model-assisted empirical best prediction approach. *Journal of the American Statistical Association*, 101(473):301–311.

Jiang, J. and Lahiri, P. (2006b). Mixed model prediction and small area estimation. *Test*, 15(1):1–96.

Jin, C., Zhu, J., Steen-Adams, M. M., Sain, S. R., and Gangnon, R. E. (2013). Spatial multinomial regression models for nominal categorical data: a study of land cover in Northern Wisconsin, USA. *Environmetrics*, 24(2):98–108.

Kalton, G. (1983). Compensating for Missing Survey Data. Technical report.

Lawson, A. B., Choi, J., Cai, B., Hossain, M., Kirby, R. S., and Liu, J. (2012). Bayesian 2-stage space-time mixture modeling with spatial misalignment of the exposure in small area health data. *Journal of agricultural, biological, and environmental statistics*, 17(3):417–441.

Liu, B., Lahiri, P., and Kalton, G. (2007). Hierarchical Bayes modeling of survey-weighted small area proportions. In *Proceedings of the Survey Research Methods Section, American Statistical Association*, pages 3181–3186.

López-Vizcaíno, E., Lombardía, M. J., and Morales, D. (2013). Multinomial-based small area estimation of labour force indicators. *Statistical modelling*, 13(2):153–178.

López-Vizcaíno, E., Lombardía, M. J., and Morales, D. (2015). Small area estimation of labour force indicators under a multinomial model with correlated time and area effects. *Journal of the Royal Statistical Society: Series A (Statistics in Society)*, 178(3):535–565.

Lumley, T. (2011). *Complex surveys: a guide to analysis using R*. John Wiley & Sons.

Maiti, T., Ren, H., and Sinha, S. (2014). Prediction error of small area predictors shrinking both means and variances. *Scandinavian Journal of Statistics*, 41(3):775–790.

Maples, J., Bell, W., and Huang, E. T. (2009). Small area variance modeling with application to county poverty estimates from the American community survey. In *Proceedings of the Section on Survey Research Methods Section, American Statistical Association*, pages 5056–5067.

Molina, I., Saei, A., and José Lombardía, M. (2007). Small area estimates of labour force participation under a multinomial logit mixed model. *Journal of the Royal Statistical Society: Series A (Statistics in Society)*, 170(4):975–1000.

Nusser, S. and Goebel, J. (1997). The National Resources Inventory: a long-term multi-resource monitoring programme. *Environmental and Ecological Statistics*, 4(3):181–204.

Petrucci, A. and Salvati, N. (2006). Small area estimation for spatial correlation in watershed erosion assessment. *Journal of agricultural, biological, and environmental statistics*, 11(2):169.

Pfeffermann, D. (2013). New important developments in small area estimation. *Statistical Science*, 28(1):40–68.

Polson, N. G. and Scott, J. G. (2012). On the half-Cauchy prior for a global scale parameter. *Bayesian Analysis*, 7(4):887–902.

Rao, J. N. and Molina, I. (2015). *Small area estimation*. John Wiley & Sons.

Särndal, C.-E., Swensson, B., and Wretman, J. (2003). *Model assisted survey sampling*. Springer Science & Business Media.

Simas, A. B., Barreto-Souza, W., and Rocha, A. V. (2010). Improved estimators for a general class of beta regression models. *Computational Statistics & Data Analysis*, 54(2):348–366.

Spiegelhalter, D. J., Best, N. G., Carlin, B. P., and Van Der Linde, A. (2002). Bayesian measures of model complexity and fit. *Journal of the Royal Statistical Society: Series B (Statistical Methodology)*, 64(4):583–639.

Stehman, S. and Overton, W. (1989). Pairwise inclusion probability formulas in random-order, variable probability, systematic sampling. *Oregon State University, Technical Report*, 131:28.

Tille, Y. and Matei, A. (2016). *sampling: Survey Sampling. R package version 2.8.* https://cran.r-project.org/package=sampling.

Wong, T.-T. (1998). Generalized Dirichlet distribution in Bayesian analysis. *Applied Mathematics and Computation*, 97(2):165–181.

You, Y., Rao, J., and Dick, P. (2004). Benchmarking hierarchical Bayes small area estimators in the Canadian census undercoverage estimation. *Statistics in Transition*, 6(5):631–640.

CHAPTER 4. CONVERGENCE ANALYSIS OF BLOCK GIBBS SAMPLERS FOR BAYESIAN PROBIT LINEAR MIXED MODELS

Xin Wang and Vivekananda Roy

Department of Statistics, Iowa State University

Abstract

In this article, we consider Markov chain Monte Carlo (MCMC) algorithms for exploring the intractable posterior densities associated with Bayesian probit linear mixed models under both proper and improper priors on the regression coefficients and variance components. In particular, we construct two-block Gibbs samplers using the data augmentation (DA) techniques. Furthermore, we prove geometric ergodicity of the Gibbs samplers, which is the foundation for building central limit theorems for MCMC based estimators and subsequent inferences. Under improper priors, the conditions for geometric convergence are similar to those guaranteeing posterior propriety. We also provide conditions for posterior propriety when the design matrices take commonly observed forms. In general, the Haar parameter expansion for DA (PX-DA) algorithm is an improvement of the DA algorithm and it has been shown that it is theoretically at least as good as the DA algorithm. For probit linear mixed models, we propose corresponding Haar PX-DA algorithms, which have essentially the same computational cost as the two-block Gibbs samplers. An example is used to show the efficiency gains of the Haar PX-DA algorithms over the block Gibbs samplers and full Gibbs samplers.

key words: Data augmentation, Drift condition, Geometric ergodicity, Haar PX-DA algorithm, Markov chains, Posterior propriety

4.1 Introduction

Generalized linear mixed models (GLMMs) are generalized linear models with random terms in the linear predictor. The random effects in the GLMM can accommodate for overdispersion often present in non-Gaussian data, and dependence among correlated observations arising from longitudinal or repeated measures studies. GLMM is one of the most frequently used statistical models. Here, we consider a popular Bayesian GLMM for binary data, namely, the probit linear mixed model.

Let $(Y_1, Y_2, \ldots, Y_n)$ denote the vector of Bernoulli random variables. Let $\boldsymbol{x}_i$ and $\boldsymbol{z}_i$ be the $p \times 1$ and $q \times 1$ known covariates and random effect design vectors respectively associated with the ith observation for $i = 1, \ldots, n$. Let $\boldsymbol{\beta} \in \mathbb{R}^p$ be the unknown vector of regression coefficients and $\boldsymbol{u} \in \mathbb{R}^q$ be the random effects vector. A GLMM can be built (McCulloch et al., 2011; Breslow and Clayton, 1993) with a link function that connects the expectation of Y_i with $\boldsymbol{x}_i$ and $\boldsymbol{z}_i$. One of the very popular link functions is the probit link function, Φ^{-1}, resulting in

$$P(Y_i = 1) = \Phi(\boldsymbol{x}_i^T\boldsymbol{\beta} + \boldsymbol{z}_i^T\boldsymbol{u}),$$

where Φ is the cumulative distribution function of the standard normal random variable. Assume that we have r random effects with $\boldsymbol{u} = (\boldsymbol{u}_1^T, \ldots, \boldsymbol{u}_r^T)^T$, where $\boldsymbol{u}_j$ is a $q_j \times 1$ vector with $q_j > 0$, $q_1 + \cdots + q_r = q$, and $\boldsymbol{u}_j \overset{\text{ind}}{\sim} N(0, \boldsymbol{I}_{q_j} 1/\tau_j)$, where $\tau_j \in \mathbb{R}_+ \equiv (0, \infty)$ is the precision parameter associated with $\boldsymbol{u}_j$ for $j = 1, \ldots, r$. Let $\boldsymbol{\tau} = (\tau_1, \ldots, \tau_r)$, thus, the data model for the probit GLMM is

$$\begin{aligned} Y_i|\boldsymbol{\beta}, \boldsymbol{u} &\overset{\text{ind}}{\sim} \text{Bern}(\alpha_i) \text{ for } i = 1, \ldots, n \text{ with} \\ \alpha_i &= \Phi(\boldsymbol{x}_i^T\boldsymbol{\beta} + \boldsymbol{z}_i^T\boldsymbol{u}) \text{ for } i = 1, \ldots, n, \\ \boldsymbol{u}_j|\boldsymbol{\tau} &\overset{\text{ind}}{\sim} N\Big(0, \frac{1}{\tau_j}\boldsymbol{I}_{q_j}\Big), \; j = 1, \ldots, r. \end{aligned} \tag{4.1}$$

Let $\boldsymbol{y} = (y_1, y_2, \ldots, y_n)^T$ be the observed Bernoulli response variables. Note that, the likelihood function for $(\boldsymbol{\beta}, \boldsymbol{\tau})$ is

$$L(\boldsymbol{\beta}, \boldsymbol{\tau}|\boldsymbol{y}) = \int_{\mathbb{R}^q} \prod_{i=1}^{n} \Big[\Phi(\boldsymbol{x}_i^T\boldsymbol{\beta} + \boldsymbol{z}_i^T\boldsymbol{u})\Big]^{y_i} \Big[1 - \Phi(\boldsymbol{x}_i^T\boldsymbol{\beta} + \boldsymbol{z}_i^T\boldsymbol{u})\Big]^{1-y_i} \phi_q(\boldsymbol{u}; \boldsymbol{0}, \boldsymbol{D}(\boldsymbol{\tau})^{-1}) d\boldsymbol{u}, \tag{4.2}$$

which is not available in closed form. Here, $\phi_q(s; a, B)$ denotes the probability density function of the $q-$dimensional normal distribution with mean vector a, covariance matrix B and evaluated at s, and $\boldsymbol{D}(\boldsymbol{\tau}) = \oplus_{j=1}^{r} \tau_j \boldsymbol{I}_{q_j}$.

In Bayesian framework, one needs to specify the prior distributions of $\boldsymbol{\beta}$ and $\boldsymbol{\tau}$. Assume $\boldsymbol{\beta}$ and $\boldsymbol{\tau}$ are apriori independent. Let $\pi(\boldsymbol{\beta})$ and $\pi(\boldsymbol{\tau})$ be the prior densities of $\boldsymbol{\beta}$ and $\boldsymbol{\tau}$ respectively. Thus, the joint posterior density of $(\boldsymbol{\beta}, \boldsymbol{\tau})$ is

$$\pi(\boldsymbol{\beta}, \boldsymbol{\tau}|\boldsymbol{y}) = \frac{1}{c(\boldsymbol{y})} L(\boldsymbol{\beta}, \boldsymbol{\tau}|\boldsymbol{y}) \pi(\boldsymbol{\beta}) \pi(\boldsymbol{\tau}), \tag{4.3}$$

where

$$c(\boldsymbol{y}) = \int_{\mathbb{R}_+^r} \int_{\mathbb{R}^p} L(\boldsymbol{\beta}, \boldsymbol{\tau}|\boldsymbol{y}) \pi(\boldsymbol{\beta}) \pi(\boldsymbol{\tau}) d\boldsymbol{\beta} d\boldsymbol{\tau},$$

is the marginal density of $\boldsymbol{y}$. Since the likelihood function $L(\boldsymbol{\beta}, \boldsymbol{\tau}|\boldsymbol{y})$ is not available in closed form, the posterior density is intractable for any choice of the prior distributions of $\boldsymbol{\beta}$ and $\boldsymbol{\tau}$. In this article, we consider both of the two popular choices of priors for $\boldsymbol{\beta}$, namely a normal prior and the improper flat prior. When the prior distribution of $\boldsymbol{\beta}$ is normal (section 4.2), we do not assume any specific form of the prior distribution of $\boldsymbol{\tau}$ except that the support of $\boldsymbol{\tau}$ is bounded away from zero. On the other hand, if $\pi(\boldsymbol{\beta}) \propto 1$ (section 4.3), our results hold under popular gamma priors and power priors on $\boldsymbol{\tau}$. Generally, Markov chain Monte Carlo (MCMC) algorithms are used for exploring the posterior density (4.3).

Even in the absence of random effects, for the probit regression model, the posterior distribution of $\boldsymbol{\beta}$ is difficult to sample from (Roy and Hobert, 2007). Albert and Chib's (1993) MCMC algorithm for sampling from the posterior distribution associated with the probit regression model is the most widely used data augmentation (DA) algorithm. The DA technique used in Albert and Chib (1993) can also be applied to the probit linear mixed model. Following Albert and Chib (1993), let $v_i \in \mathbb{R}$ be the continuous latent variable corresponding to the ith binary observation Y_i, such that $Y_i = I(v_i > 0)$, where $v_i|\boldsymbol{\beta}, \boldsymbol{u} \overset{\text{ind}}{\sim} N(\boldsymbol{x}_i^T\boldsymbol{\beta} + \boldsymbol{z}_i^T\boldsymbol{u}, 1)$ for $i = 1, \ldots, n$. Then

$$P(Y_i = 1) = P(v_i > 0) = \Phi(\boldsymbol{x}_i^T\boldsymbol{\beta} + \boldsymbol{z}_i^T\boldsymbol{u}), \tag{4.4}$$

that is, $Y_i|\boldsymbol{\beta}, \boldsymbol{u} \overset{\text{ind}}{\sim} \text{Bern}(\alpha_i)$ as in (4.1). Let $\boldsymbol{v} = (v_1, \ldots, v_n)^T$, then $\boldsymbol{v}|\boldsymbol{\beta}, \boldsymbol{u} \sim N(\boldsymbol{X}\boldsymbol{\beta} + \boldsymbol{Z}\boldsymbol{u}, \boldsymbol{I}_n)$, where $\boldsymbol{X}_{n\times p} = (\boldsymbol{x}_1, \ldots, \boldsymbol{x}_n)^T$ and $\boldsymbol{Z}_{n\times q} = (\boldsymbol{z}_1, \ldots, \boldsymbol{z}_n)^T$.

Using the latent variables $\boldsymbol{v}$, we can introduce a joint density $\pi(\boldsymbol{\beta}, \boldsymbol{u}, \boldsymbol{v}, \boldsymbol{\tau}|\boldsymbol{y})$ (see section 4.2.1 for details) such that

$$\int_{\mathbb{R}^q} \int_{\mathbb{R}^n} \pi(\boldsymbol{\beta}, \boldsymbol{u}, \boldsymbol{v}, \boldsymbol{\tau}|\boldsymbol{y}) d\boldsymbol{v} d\boldsymbol{u} = \pi(\boldsymbol{\beta}, \boldsymbol{\tau}|\boldsymbol{y}), \tag{4.5}$$

where $\pi(\boldsymbol{\beta}, \boldsymbol{\tau}|\boldsymbol{y})$ is the posterior density defined in (4.3). If all the full conditionals of the joint density $\pi(\boldsymbol{\beta}, \boldsymbol{u}, \boldsymbol{v}, \boldsymbol{\tau}|\boldsymbol{y})$ are easy to sample from, then a Gibbs sampler can be run and it can be used to make inferences on the posterior density (4.3). Indeed this full Gibbs sampler is traditionally used in the analysis of Bayesian probit linear mixed models (Baragatti, 2011). In this article, instead of using full conditional distributions, we construct two-block Gibbs samplers with $(\boldsymbol{\beta}^T, \boldsymbol{u}^T)^T$ as one block and $(\boldsymbol{v}^T, \boldsymbol{\tau}^T)^T$ as the other block — which is our first contribution. In general, block Gibbs samplers are known to be better than the Gibbs samplers based on full conditional distributions in terms of having smaller operator norm (Liu et al., 1994). On the other hand, generally by combining multiple parameters, it may be computationally inefficient to draw them simultaneously in each iteration. From section 4.2.1 and Appendix F, we see that in terms of computational cost the difference between the two-block Gibbs sampler developed here and the corresponding full Gibbs sampler is that in every iteration, the former requires inversion of a $(p+q)\times(p+q)$ matrix, while the later needs a $p \times p$ and a $q \times q$ matrix inversion. The difference in the computational cost can be reduced by using the methods of Bhattacharya et al. (2016) for drawing from the conditional Gaussian distributions of these algorithms. In a real data example in section 4.4, we observe that the two-block Gibbs sampler is more efficient than the full Gibbs sampler in terms of having higher effective sample sizes per unit time.

The above mentioned block Gibbs sampler has an everywhere strictly positive Markov transition density, implying that the underlying Markov chain is Harris ergodic (Asmussen and Glynn, 2011; Meyn and Tweedie, 1993). Thus, the time average estimators based on the block Gibbs sampler can be used to consistently estimate the (posterior) means with respect to the joint density $\pi(\boldsymbol{\beta}, \boldsymbol{u}, \boldsymbol{v}, \boldsymbol{\tau}|\boldsymbol{y})$. In practice, it is crucial to know whether the Monte Carlo errors associated with

these estimates are sufficiently small. However, in order to provide valid standard errors, we need to establish a central limit theorem (CLT) for the time average estimators. Unlike for the ordinary Monte Carlo methods based on iid samples, mere existence of the finite second moment does not guarantee a CLT for MCMC estimators. The only standard method of establishing a CLT for MCMC estimators is to prove that the underlying Markov chain is *geometrically ergodic* (Jones and Hobert, 2001). Geometric ergodicity is also needed for consistently estimating the asymptotic variance in the Markov chain CLT (Flegal and Jones, 2010). Roy and Hobert (2007) and Chakraborty and Khare (2017) proved geometric ergodicity of Albert and Chib's (1993) DA algorithm for the Bayesian probit regression model under improper and proper priors on the regression coefficients. For linear models, Jones and Hobert (2004) and Tan and Hobert (2009) analyzed the Gibbs sampler for one-way random effects models under proper priors and improper priors respectively. Johnson and Jones (2010) analyzed the block Gibbs sampler for Bayesian linear mixed models under the assumption $\boldsymbol{X}^T\boldsymbol{Z} = \boldsymbol{0}$. Román and Hobert (2012) and Román and Hobert (2015) established geometric rate of convergence of the Gibbs samplers for Bayesian linear mixed models under improper and proper priors without the assumption of $\boldsymbol{X}^T\boldsymbol{Z} = \boldsymbol{0}$. However, *no such* convergence analysis of the Gibbs samplers for any Bayesian generalized linear mixed model is available in the literature. Our second contribution, in this paper, is establishing geometric convergence rates for the block Gibbs sampler for Bayesian probit linear mixed models.

DA algorithms are known to suffer from slow convergence (Meng and Van Dyk, 1999; Van Dyk and Meng, 2001). Liu and Wu (1999) proposed the *parameter expansion for data augmentation* (PX-DA) algorithm, which can converge faster than the DA algorithm without much extra computational effort (Van Dyk and Meng, 2001; Roy, 2014). Hobert and Marchev (2008) proved that the Haar PX-DA algorithm, that is based on a Haar measure, is better than any other PX-DA algorithm and the original DA algorithm in both the efficiency ordering and the operator norm ordering. For the probit regression model, Roy and Hobert (2007), through an example, showed that the Haar PX-DA algorithm can lead to huge gains in efficiency over the DA algorithm of Albert and Chib (1993). Our third contribution is to construct Haar PX-DA algorithms improving the block Gibbs

samplers mentioned before. Since geometric ergodicity of the Haar PX-DA algorithm follows from geometric ergodicity of the DA algorithm (Hobert and Marchev, 2008), we have CLTs for the Haar PX-DA algorithm based estimators as well.

The article is organized as follows. In section 4.2, we construct the two-block Gibbs sampler for the Bayesian probit linear mixed model under proper priors, provide its geometric convergence results and present a corresponding Haar PX-DA algorithm. In section 4.3, we construct a similar two-block Gibbs sampler under improper priors and prove geometric ergodicity of the underlying Markov chain. We also establish conditions for propriety of the posterior distribution under improper priors, when $\boldsymbol{X}$ and $\boldsymbol{Z}$ take commonly observed forms. A real data example is given in section 4.4. Section 4.5 contains some conclusions and discussions. Finally, the proofs of geometric convergence of the Gibbs samplers and posterior propriety appear in the appendices.

4.2 Geometric ergodicity of the two-block Gibbs sampler under proper priors

In this section, we first construct a two-block Gibbs sampler for the Bayesian probit linear mixed model. Then, in section 4.2.2, we describe its geometric rate of convergence. Finally, in section 4.2.3, the proposed Haar PX-DA algorithm is presented.

4.2.1 A two-block Gibbs sampler

We begin with deriving the joint density $\pi(\boldsymbol{\beta}, \boldsymbol{u}, \boldsymbol{v}, \boldsymbol{\tau}|\boldsymbol{y})$ mentioned in the introduction. We consider multivariate normal priors for regression coefficients $\boldsymbol{\beta}$. In particular, given $\boldsymbol{\tau}$, we assume that $\boldsymbol{u}$ and $\boldsymbol{\beta}$ are independent with

$$\boldsymbol{\beta}|\boldsymbol{\tau} \sim N_p(\boldsymbol{Q}^{-1}\boldsymbol{\mu}_0, \boldsymbol{Q}^{-1}),$$

where $\boldsymbol{Q}$ is a $p \times p$ known positive definite matrix, $\boldsymbol{\mu}_0 \in \mathbb{R}^p$ is a known p dimensional vector. As mentioned in Chakraborty and Khare (2017), any vector $\tilde{\boldsymbol{\mu}} \in \mathbb{R}^p$ can be written as $\tilde{\boldsymbol{\mu}} = \boldsymbol{Q}^{-1}\boldsymbol{Q}\tilde{\boldsymbol{\mu}} = \boldsymbol{Q}^{-1}\boldsymbol{\mu}_0$ with $\boldsymbol{\mu}_0 = \boldsymbol{Q}\tilde{\boldsymbol{\mu}}$. Thus, it is not restrictive to assume the above form of the prior mean for

$\boldsymbol{\beta}$. Define

$$\pi(\boldsymbol{\beta},\boldsymbol{u},\boldsymbol{v},\boldsymbol{\tau}|\boldsymbol{y}) = \frac{1}{c(\boldsymbol{y})}\left[\prod_{i=1}^{n}\phi(v_i;\boldsymbol{x}_i^T\boldsymbol{\beta}+\boldsymbol{z}_i^T\boldsymbol{u},1)\left[1_{(0,\infty)}(v_i)\right]^{y_i}\left[1_{(-\infty,0]}(v_i)\right]^{1-y_i}\right]$$
$$\times\,\phi_q(\boldsymbol{u};\boldsymbol{0},\boldsymbol{D}(\boldsymbol{\tau})^{-1})\phi_p(\boldsymbol{\beta};\boldsymbol{Q}^{-1}\boldsymbol{\mu}_0,\boldsymbol{Q}^{-1})\pi(\boldsymbol{\tau}). \tag{4.6}$$

From (4.2) and (4.4) it follows that (4.5) holds. For the precision parameters $\boldsymbol{\tau}$, we assume that $\pi(\boldsymbol{\tau})$ is a proper density and the support of the prior density $\pi(\boldsymbol{\tau})$ is bounded away from zero. Thus we assume that there exists a positive constant τ_0, such that $\pi(\boldsymbol{\tau}) = 0$ when $\tau_j < \tau_0$ for some $j = 1, 2, \ldots, r$. As we discuss later, although no specific functional form for $\pi(\boldsymbol{\tau})$ is assumed (beyond truncation) here, the $\boldsymbol{\tau}$ conditional distribution from (4.6) needs to be easy to sample from.

Since

$$\begin{aligned}\pi(\boldsymbol{\beta},\boldsymbol{u},\boldsymbol{v},\boldsymbol{\tau}|\boldsymbol{y}) \;\propto\; & \exp\left[-\frac{1}{2}\sum_{i=1}^{n}\left(v_i-\boldsymbol{x}_i^T\boldsymbol{\beta}-\boldsymbol{z}_i^T\boldsymbol{u}\right)^2\right]\cdot\prod_{i=1}^{n}\left[1_{(0,\infty)}(v_i)\right]^{y_i}\left[1_{(-\infty,0]}(v_i)\right]^{1-y_i}\\ & \cdot\prod_{j=1}^{r}\tau_j^{\frac{q_j}{2}}\cdot\exp\left[-\frac{1}{2}\tau_j\boldsymbol{u}_j^T\boldsymbol{u}_j\right]\cdot\exp\left[-\frac{1}{2}\left(\boldsymbol{\beta}-\boldsymbol{Q}^{-1}\boldsymbol{\mu}_0\right)^T\boldsymbol{Q}\left(\boldsymbol{\beta}-\boldsymbol{Q}^{-1}\boldsymbol{\mu}_0\right)\right]\cdot\pi(\boldsymbol{\tau}),\end{aligned}$$

letting $\boldsymbol{\eta} \equiv (\boldsymbol{\beta}^T, \boldsymbol{u}^T)^T$ and $\boldsymbol{W}_{n\times(p+q)} \equiv (\boldsymbol{X}, \boldsymbol{Z})$, standard calculations show that the conditional density of $\boldsymbol{\eta}$ is

$$\pi(\boldsymbol{\eta}|\boldsymbol{v},\boldsymbol{\tau},\boldsymbol{y}) \propto \exp\left[-\frac{1}{2}(\boldsymbol{v}-\boldsymbol{W}\boldsymbol{\eta})^T(\boldsymbol{v}-\boldsymbol{W}\boldsymbol{\eta})\right]\cdot\exp\left[-\frac{1}{2}\boldsymbol{\eta}^T\boldsymbol{A}(\boldsymbol{\tau})\boldsymbol{\eta}+\boldsymbol{\eta}^T\boldsymbol{l}\right], \tag{4.7}$$

where

$$\boldsymbol{l} = \left(\boldsymbol{\mu}_0^T, \boldsymbol{0}_{q\times1}^T\right)^T \;\text{ and }\; \boldsymbol{A}(\boldsymbol{\tau}) = \begin{pmatrix}\boldsymbol{Q} & \boldsymbol{0}_{p\times q}\\ \boldsymbol{0}_{q\times p} & \boldsymbol{D}(\boldsymbol{\tau})\end{pmatrix}.$$

Thus,

$$\boldsymbol{\eta}|\boldsymbol{v},\boldsymbol{\tau},\boldsymbol{y} \sim N_{p+q}\left(\boldsymbol{\Sigma}^{-1}\boldsymbol{\mu},\boldsymbol{\Sigma}^{-1}\right), \tag{4.8}$$

where

$$\boldsymbol{\Sigma} = \begin{pmatrix}\boldsymbol{X}^T\boldsymbol{X}+\boldsymbol{Q} & \boldsymbol{X}^T\boldsymbol{Z}\\ \boldsymbol{Z}^T\boldsymbol{X} & \boldsymbol{Z}^T\boldsymbol{Z}+\boldsymbol{D}(\boldsymbol{\tau})\end{pmatrix} = \boldsymbol{W}^T\boldsymbol{W}+\boldsymbol{A}(\boldsymbol{\tau}) \;\text{ and }\; \boldsymbol{\mu} = \boldsymbol{W}^T\boldsymbol{v}+\boldsymbol{l}. \tag{4.9}$$

Similarly, the conditional density of $(\boldsymbol{v}, \boldsymbol{\tau})$ is

$$\begin{aligned}\pi(\boldsymbol{v}, \boldsymbol{\tau}|\boldsymbol{\eta}, \boldsymbol{y}) \quad \propto \quad & \prod_{i=1}^{n} \phi\left(v_i - \boldsymbol{w}_i^T\boldsymbol{\eta}; 0, 1\right)\left[1_{(0,\infty)}\left(v_i\right)\right]^{y_i}\left[1_{(-\infty,0]}\left(v_i\right)\right]^{1-y_i} \\ & \cdot \prod_{j=1}^{r} \tau_j^{\frac{q_j}{2}} \cdot \exp\left[-\frac{1}{2}\tau_j \boldsymbol{u}_j^T\boldsymbol{u}_j\right] \cdot \pi(\boldsymbol{\tau}),\end{aligned}$$

where $\boldsymbol{w}_i^T$ is the ith row of $\boldsymbol{W}$ for $i = 1, \ldots, n$. Thus, conditional on $(\boldsymbol{\eta}, \boldsymbol{y})$, v_i, $i = 1, \ldots, n$ and $\boldsymbol{\tau}$ are independent. We have

$$v_i|\boldsymbol{\eta}, \boldsymbol{y} \overset{\text{ind}}{\sim} \text{TN}(\boldsymbol{w}_i^T\boldsymbol{\eta}, 1, y_i),\ i = 1, \ldots, n, \tag{4.10}$$

where $\text{TN}(\mu, \sigma^2, \omega)$ denotes the distribution of the normal random variable with mean μ and variance σ^2, that is truncated to have only positive values if $\omega = 1$, and only nonpositive values if $\omega = 0$.

The conditional density of $\boldsymbol{\tau}$ is

$$\pi(\boldsymbol{\tau}|\boldsymbol{\eta}, \boldsymbol{y}) \propto \prod_{j=1}^{r} \tau_j^{\frac{q_j}{2}} \exp\left[-\frac{1}{2}\tau_j \boldsymbol{u}_j^T\boldsymbol{u}_j\right] \cdot \pi(\boldsymbol{\tau}). \tag{4.11}$$

As mentioned before we assume that there exists $\tau_0 > 0$ such that $\pi(\boldsymbol{\tau}) = 0$ if $\tau_j < \tau_0$ for some $j = 1, 2, \ldots, r$. In the special case, if $\pi(\boldsymbol{\tau}) = \prod_{j=1}^{r} \pi(\tau_j)$, and for each j, $\pi(\tau_j)$ is the density of truncated Gamma random variable with parameters a_j and b_j, that is

$$\pi(\tau_j) \propto \tau_j^{a_j - 1} e^{-b_j\tau_j} I(\tau_j \geq \tau_0), \tag{4.12}$$

then conditional on $\boldsymbol{\eta}, \boldsymbol{y}$, τ_j's are independent and τ_j follows truncated Gamma distribution with parameter $a_j + q_j/2$ and $b_j + \boldsymbol{u}_j^T\boldsymbol{u}_j/2$. Since the Gibbs sampler alternates between draws from the conditional densities of $\boldsymbol{\eta}$ and $(\boldsymbol{v}, \boldsymbol{\tau})$, it is necessary that the conditional density $\pi(\boldsymbol{\tau}|\boldsymbol{\eta}, \boldsymbol{y})$ given in (4.11) is easy to sample from.

Thus, one single iteration of the block Gibbs sampler $\{\boldsymbol{\eta}^{(m)}, \boldsymbol{v}^{(m)}, \boldsymbol{\tau}^{(m)}\}_{m=0}^{\infty}$ has the following two steps in Algorithm 4.1.

4.2.2 Geometric ergodicity of the block Gibbs sampler

In this section, we establish the geometric rate of convergence of the block Gibbs sampler $\{\boldsymbol{\eta}^{(m)}, \boldsymbol{v}^{(m)}, \boldsymbol{\tau}^{(m)}\}_{m=0}^{\infty}$. Since it is a two-block Gibbs sampler, it has the same rate of convergence

Algorithm 4.1 The $(m+1)$st iteration of the two-block Gibbs sampler

1: Draw $\boldsymbol{\tau}^{(m+1)}$ from (4.11) with $\boldsymbol{u} = \boldsymbol{u}^{(m)}$, and independently draw $v_i^{(m+1)}|\boldsymbol{\eta}^{(m)}, \boldsymbol{y} \overset{\text{ind}}{\sim} \text{TN}(\boldsymbol{w}_i^T\boldsymbol{\eta}^{(m)}, 1, y_i)$ for $i = 1, \ldots, n$.
2: Draw $\boldsymbol{\eta}^{(m+1)}$ from (4.7), that is,

$$\boldsymbol{\eta}^{(m+1)} \sim N\left(\left(\boldsymbol{W}^T\boldsymbol{W} + \boldsymbol{A}(\boldsymbol{\tau}^{(m+1)})\right)^{-1}\left(\boldsymbol{W}^T\boldsymbol{v}^{(m+1)} + \boldsymbol{l}\right), \left(\boldsymbol{W}^T\boldsymbol{W} + \boldsymbol{A}(\boldsymbol{\tau}^{(m+1)})\right)^{-1}\right).$$

as the $\boldsymbol{\eta}$-marginal Markov chain $\{\boldsymbol{\eta}^{(m)}\}_{m=0}^{\infty}$ (Roberts and Rosenthal, 2001). Below we analyze this $\boldsymbol{\Psi} \equiv \{\boldsymbol{\eta}^{(m)}\}_{m=0}^{\infty}$ chain.

Let $\boldsymbol{\eta}'$ be the current state and $\boldsymbol{\eta}$ be the next state of the Markov chain $\boldsymbol{\Psi}$, then the Markov transition density (Mtd) of $\boldsymbol{\Psi}$ is

$$k(\boldsymbol{\eta}|\boldsymbol{\eta}') = \int_{\mathbb{R}_+^r}\int_{\mathbb{R}^n} \pi(\boldsymbol{\eta}|\boldsymbol{v}, \boldsymbol{\tau}, \boldsymbol{y})\pi(\boldsymbol{v}, \boldsymbol{\tau}|\boldsymbol{\eta}', \boldsymbol{y})d\boldsymbol{v}d\boldsymbol{\tau}, \tag{4.13}$$

where $\pi(\cdot|\cdot, \boldsymbol{y})$'s are the conditional densities from section 4.2.1. Routine calculations show that $k(\boldsymbol{\eta}|\boldsymbol{\eta}')$ is reversible and thus is invariant with respect to the marginal density of $\boldsymbol{\eta}$ denoted as $\pi(\boldsymbol{\eta}|\boldsymbol{y}) \equiv \int_{\mathbb{R}_+^r}\int_{\mathbb{R}^n} \pi(\boldsymbol{\eta}, \boldsymbol{v}, \boldsymbol{\tau}|\boldsymbol{y})d\boldsymbol{v}d\boldsymbol{\tau}$. Let $h : \mathbb{R}^{p+q} \mapsto \mathbb{R}$ be a real valued function. Suppose our interest is to estimate the (posterior) mean $E(h(\boldsymbol{\eta})|\boldsymbol{y}) \equiv \int_{\mathbb{R}^{p+q}} h(\boldsymbol{\eta})\pi(\boldsymbol{\eta}|\boldsymbol{y})d\boldsymbol{\eta}$. Since $k(\boldsymbol{\eta}|\boldsymbol{\eta}')$ is strictly positive, the Markov chain $\boldsymbol{\Psi}$ is Harris ergodic (Meyn and Tweedie, 1993). Thus if $E(|h(\boldsymbol{\eta})||\boldsymbol{y}) < \infty$, then $E(h(\boldsymbol{\eta})|\boldsymbol{y})$ can be consistently estimated by

$$\bar{h}_m = \frac{1}{m}\sum_{i=0}^{m-1} h(\boldsymbol{\eta}^{(i)}).$$

As mentioned in the introduction, in order to provide an asymptotically valid confidence interval for $E(h(\boldsymbol{\eta})|\boldsymbol{y})$ based on $\bar{h}_m$, we need to establish a CLT for $\bar{h}_m$. We say a CLT exists for $\bar{h}_m$ if there exists a constant $\sigma_h^2 \in (0, \infty)$ such that,

$$\sqrt{m}\left(\bar{h}_m - E(h(\boldsymbol{\eta})|\boldsymbol{y})\right) \xrightarrow{d} N\left(0, \sigma_h^2\right) \text{ as } m \to \infty. \tag{4.14}$$

If (4.14) holds and a consistent estimator $\hat{\sigma}_h^2$ of σ_h^2 is available, then the standard errors $\hat{\sigma}_h/\sqrt{m}$ can be used to provide an asymptotic confidence interval for $E(h(\boldsymbol{\eta})|\boldsymbol{y})$ (Roy and Hobert, 2007). Unfortunately, Harris ergodicity of $\boldsymbol{\Psi}$ does not guarantee (4.14), although it ensures consistency of

$\bar{h}_m$. One method of proving (4.14) is to establish the geometric rate of convergence for the Markov chain $\boldsymbol{\Psi}$ (Jones and Hobert, 2001). Geometric ergodicity of $\boldsymbol{\Psi}$ also allows for consistent estimation of σ_h^2 using batch means or spectral variance methods (Flegal and Jones, 2010).

Let $\mathscr{B}$ denote the Borel σ-algebra of $\mathbb{R}^{p+q}$ and $K(\cdot,\cdot)$ be the Markov transition function corresponding to the Mtd $k(\cdot,\cdot)$ in (4.13), that is, for any set $O \in \mathscr{B}$, $\boldsymbol{\eta}' \in \mathbb{R}^{p+q}$ and any $j = 0, 1, \ldots,$

$$K(\boldsymbol{\eta}', O) = \Pr(\boldsymbol{\eta}^{(j+1)} \in O | \boldsymbol{\eta}^{(j)} = \boldsymbol{\eta}') = \int_O k(\boldsymbol{\eta}|\boldsymbol{\eta}')d\boldsymbol{\eta}. \tag{4.15}$$

Then the m-step Markov transition function is $K^m(\boldsymbol{\eta}', O) = \Pr(\boldsymbol{\eta}^{(m+j)} \in O | \boldsymbol{\eta}^{(j)} = \boldsymbol{\eta}')$. Let $\Pi(\cdot|\boldsymbol{y})$ be the probability measure with density $\pi(\boldsymbol{\eta}|\boldsymbol{y})$. The Markov chain $\boldsymbol{\Psi}$ is geometrically ergodic if there exists a constant $0 < t < 1$ and a function $J : \mathbb{R}^{p+q} \mapsto \mathbb{R}^+$ such that for any $\boldsymbol{\eta} \in \mathbb{R}^{p+q}$,

$$||K^m(\boldsymbol{\eta}, \cdot) - \Pi(\cdot|\boldsymbol{y})||_{\text{TV}} := \sup_{O \in \mathscr{B}} |K^m(\boldsymbol{\eta}, O) - \Pi(O|\boldsymbol{y})| \leq J(\boldsymbol{\eta})t^m. \tag{4.16}$$

Harris ergodicity of $\boldsymbol{\Psi}$ implies that $||K^m(\boldsymbol{\eta}, \cdot) - \Pi(\cdot|\boldsymbol{y})||_{\text{TV}} \downarrow 0$ as $m \to \infty$, while (4.16) guarantees its exponential rate of convergence. Roberts and Rosenthal (1997) showed that since $\boldsymbol{\Psi}$ is reversible, if (4.16) holds then there exists a CLT, that is (4.14) holds, for all h with $E(h^2(\boldsymbol{\eta})|\boldsymbol{y}) < \infty$. A proof of Theorem 4.1 by establishing a *drift condition* for $\boldsymbol{\Psi}$ is given in the Appendix A.

Theorem 4.1. *The Markov chain $\boldsymbol{\Psi}$ underlying the block Gibbs sampler in Algorithm 4.1 is geometrically ergodic.*

Remark 4.1. *In this section, we assume that the support of the precision parameters $\boldsymbol{\tau}$ is bounded away from zero. This assumption is crucially used in the proof of Theorem 1. We prove this theorem by establishing a drift condition using the drift function $V(\boldsymbol{\eta}) = \sum_{i=1}^n (\boldsymbol{\omega}_i^T \boldsymbol{\eta})^2 + \boldsymbol{\beta}^T \boldsymbol{Q} \boldsymbol{\beta} + \tau_0 \boldsymbol{u}^T \boldsymbol{u}$. We believe that removal of the truncated support assumption from Theorem 1 would require using a different drift function and thus starting from scratch to establish a drift condition.*

Remark 4.2. *Theorem 4.1 does not make any assumptions on the dimensions p, q or the sample size n. Thus, it is applicable to the modern high dimensional data sets where p (and/or q) can be much larger than n.*

4.2.3 A Haar PX-DA algorithm

As mentioned in section 4.1, DA algorithms often suffer from slow convergence and high autocorrelations. Liu and Wu (1999) proposed parameter expansion for data augmentation (PX-DA) algorithms for speeding up the convergence of DA algorithms. Hobert and Marchev (2008) compared the performance of PX-DA algorithms based on a Haar measure (called Haar PX-DA algorithms) with PX-DA algorithms based on a probability measure and DA algorithms. In particular, they showed that, under some mild conditions, the Haar PX-DA algorithms are better than the general PX-DA algorithms and the DA algorithms in both the efficiency ordering and the operator norm ordering. As shown in Hobert and Marchev (2008), compared to the DA algorithm, in PX-DA, an extra step is added (sandwiched) between the two steps of the original DA algorithm. In order to construct this extra step, we derive the marginal density

$$\begin{aligned} \pi\left(\boldsymbol{v}, \boldsymbol{\tau} | \boldsymbol{y}\right) &= \int_{\mathbb{R}^{p+q}} \pi(\boldsymbol{\eta}, \boldsymbol{v}, \boldsymbol{\tau} | \boldsymbol{y}) d\boldsymbol{\eta} \\ &\propto \prod_{i=1}^{n} \left[1_{(0,\infty)}\left(v_i\right)\right]^{y_i} \left[1_{(-\infty,0]}\left(v_i\right)\right]^{1-y_i} \prod_{j=1}^{r} \tau_j^{\frac{q_j}{2}} \\ &\cdot \quad |\boldsymbol{\Sigma}|^{-1/2} \exp\left\{-\frac{1}{2}\left[\boldsymbol{v}^T M_1 \boldsymbol{v} - 2\boldsymbol{v}^T M_2 - \boldsymbol{l}^T \boldsymbol{\Sigma} \boldsymbol{l}\right]\right\} \pi(\boldsymbol{\tau}), \end{aligned} \tag{4.17}$$

where

$$M_1 = \left[\boldsymbol{I} - \boldsymbol{W}\left(\boldsymbol{W}^T\boldsymbol{W} + \boldsymbol{A}(\boldsymbol{\tau})\right)^{-1}\boldsymbol{W}^T\right] \text{ and } M_2 = \boldsymbol{W}\left(\boldsymbol{W}^T\boldsymbol{W} + \boldsymbol{A}(\boldsymbol{\tau})\right)^{-1}\boldsymbol{l}.$$

Let $\mathcal{Z}$ denote the subset of $\mathbb{R}^n$ where $\boldsymbol{v}$ lives, that is, $\mathcal{Z}$ is the Cartesian product of n half (positive or nonpositive) lines, where the ith component is $(0, \infty)$ (if $y_i = 1$) or $(-\infty, 0]$ (if $y_i = 0$). Let G be the unimodular multiplicative group on $\mathbb{R}_+$ with Haar measure $\nu(dg) = dg/g$, where dg is Lebesgue measure on $\mathbb{R}_+$. For constructing an efficient extra step, as in Roy (2014), we let the group G act on $\mathcal{Z} \times \mathbb{R}_+^r$ through a group action $T(\boldsymbol{v}, \boldsymbol{\tau}) = (g\boldsymbol{v}, \boldsymbol{\tau}) = (gv_1, gv_2, \ldots, gv_n, \boldsymbol{\tau})$. With the group action defined this way, it can be shown that the Lebesgue measure on $\mathcal{Z} \times \mathbb{R}_+^r$ is relatively left invariant with multiplier $\chi(g) = g^n$ (Roy, 2014; Hobert and Marchev, 2008). Following Hobert

and Marchev (2008), consider a probability density function $\vartheta(g)$ on G where

$$\begin{aligned} \vartheta(g)\, dg &\propto \pi(g\boldsymbol{v}, \boldsymbol{\tau}|\boldsymbol{y})\, \chi(g)\, \nu(dg) \\ &\propto g^{n-1} \exp\left\{-\frac{1}{2}\left[g^2 \boldsymbol{v}^T M_1 \boldsymbol{v} - 2g\boldsymbol{v}^T M_2\right]\right\} dg. \end{aligned} \tag{4.18}$$

Given $(\boldsymbol{v}, \boldsymbol{\tau})$, $\vartheta(g)$ is a valid density since M_1 is a positive definite matrix. From Hobert and Marchev (2008), it follows that the transition $(\boldsymbol{v}, \boldsymbol{\tau}) \to (\boldsymbol{v}', \boldsymbol{\tau}) \equiv T(\boldsymbol{v}, \boldsymbol{\tau}) = (g\boldsymbol{v}, \boldsymbol{\tau})$ where $g \sim \vartheta(g)$, is reversible with respect to $\pi(\boldsymbol{v}, \boldsymbol{\tau}|\boldsymbol{y})$ defined in (4.17). Since $\vartheta(g)$ in (4.18) is log-concave, the adaptive rejection sampling algorithm (Gilks and Wild, 1992) can be used to efficiently sample from $\vartheta(g)$. Given $\boldsymbol{\eta}^{(m)}$, below are the three steps involved in the $(m+1)$st iteration of the Haar PX-DA algorithm to move to the new state $\boldsymbol{\eta}^{(m+1)}$.

Algorithm 4.2 The $(m+1)$st iteration of the Haar PX-DA algorithm

1: Draw $\boldsymbol{\tau}$ from (4.11) with $\boldsymbol{u} = \boldsymbol{u}^{(m)}$, and independently draw $v_i|\boldsymbol{\eta}^{(m)}\boldsymbol{y} \overset{\text{ind}}{\sim} \text{TN}(\boldsymbol{w}_i^T\boldsymbol{\eta}^{(m)}, 1, y_i)$, $i = 1, \ldots, n$.
2: Draw g from (4.18).
3: Calculate $v_i' = gv_i$ for $i = 1, \ldots, n$, and draw $\boldsymbol{\eta}^{(m+1)}$ from (4.7) conditional on $\boldsymbol{v}' = (v_1', \ldots, v_n')$ and $\boldsymbol{\tau}$, that is, draw

$$\boldsymbol{\eta}^{(m+1)} \sim N\left(\left(\boldsymbol{W}^T\boldsymbol{W} + \boldsymbol{A}(\boldsymbol{\tau})\right)^{-1}\left(\boldsymbol{W}^T\boldsymbol{v}' + \boldsymbol{l}\right), \left(\boldsymbol{W}^T\boldsymbol{W} + \boldsymbol{A}(\boldsymbol{\tau})\right)^{-1}\right).$$

The Mtd of the above Haar PX-DA algorithm can be written as

$$k^*(\boldsymbol{\eta}|\boldsymbol{\eta}') = \int_{\mathbb{R}^n}\int_{\mathbb{R}_+^r}\int_{\mathbb{R}^n} \pi(\boldsymbol{\eta}|\boldsymbol{v}', \boldsymbol{\tau}, \boldsymbol{y})\, F(\boldsymbol{v}, d\boldsymbol{v}')\, \pi(\boldsymbol{v}, \boldsymbol{\tau}|\boldsymbol{\eta}', \boldsymbol{y})\, d\boldsymbol{v} d\boldsymbol{\tau} d\boldsymbol{v}', \tag{4.19}$$

where $F(\cdot, \cdot)$ is the Markov transition function corresponding to the move $(\boldsymbol{v}, \boldsymbol{\tau}) \to (\boldsymbol{v}', \boldsymbol{\tau}) = T(\boldsymbol{v}, \boldsymbol{\tau})$. Let K^* and K be the Markov operators associated with the Mtds k^* and k defined in (4.19) and (4.13) respectively. From Hobert and Marchev (2008), we have $\|K^*\|_{\text{OP}} \leq \|K\|_{\text{OP}}$, where $\|K\|_{\text{OP}}$ denotes the norm of the operator K (see also Roy, 2012b). Since the block Gibbs sampler is geometrically ergodic, we have $\|K^*\|_{\text{OP}} \leq \|K\|_{\text{OP}} < 1$ (Roberts and Rosenthal, 1997). Thus we have the following corollary.

Corollary 4.1. *Under the conditions of Theorem 4.1, the Markov chain underlying the Haar PX-DA algorithm described in Algorithm 4.2 is geometrically ergodic.*

The extra step of Algorithm 4.2 is a single draw from the univariate density $\vartheta(g)$, which is easy to sample from. Thus, the computational burden, per iteration, for the Haar PX-DA algorithm is similar to that of the block Gibbs sampler described in section 4.2.1. Two other Haar PX-DA algorithms can be constructed by using group actions $T_1(\boldsymbol{v}, \boldsymbol{\tau}) = (\boldsymbol{v}, g\boldsymbol{\tau})$ and $T_2(\boldsymbol{v}, \boldsymbol{\tau}) = (g\boldsymbol{v}, g\boldsymbol{\tau})$. However, the corresponding $\vartheta(g)$'s are not easy to sample from, thus we do not consider them here.

4.3 Geometric ergodicity of the two-block Gibbs sampler under improper priors

In this section we consider an improper flat prior for $\boldsymbol{\beta}$, that is, $\pi(\boldsymbol{\beta}) \propto 1$ and τ_j's, $j = 1, \ldots, r$, are apriori independent with

$$\pi(\tau_j) \propto e^{-b_j \tau_j} \tau_j^{a_j - 1}, \tag{4.20}$$

which can be proper or improper. Note that, in this section, the prior distributions of τ_j's are *not* assumed to be truncated. Since we are using improper priors, the posterior densities in (4.5) are not guaranteed to exist. In section 4.3.1, we discuss conditions under which the posterior density is proper.

4.3.1 Geometric ergodicity of the block Gibbs sampler

In this case, the joint posterior density (up to a normalizing constant) of $\boldsymbol{\beta}, \boldsymbol{u}, \boldsymbol{v}, \boldsymbol{\tau}$, if it exists, is

$$\begin{aligned} \pi^*(\boldsymbol{\beta}, \boldsymbol{u}, \boldsymbol{v}, \boldsymbol{\tau} | \boldsymbol{y}) \propto & \left[\prod_{i=1}^{n} \exp\left\{ -\frac{1}{2} \left(v_i - \boldsymbol{x}_i^T \boldsymbol{\beta} - \boldsymbol{z}_i^T \boldsymbol{u} \right)^2 \right\} \left[1_{(0,\infty)}(v_i) \right]^{y_i} \left[1_{(-\infty,0]}(v_i) \right]^{1-y_i} \right] \\ & \times \prod_{j=1}^{r} \tau_j^{\frac{q_j}{2} + a_j - 1} \exp\left\{ -\tau_j \left(b_j + \frac{\boldsymbol{u}_j^T \boldsymbol{u}_j}{2} \right) \right\}. \end{aligned} \tag{4.21}$$

A similar two-block Gibbs sampler as in section 4.2.1 can be considered in this setting by alternating draws from the two conditional distributions, namely $\boldsymbol{\eta}$ given $\boldsymbol{v}, \boldsymbol{\tau}, \boldsymbol{y}$ and $\boldsymbol{v}$, $\boldsymbol{\tau}$ given $\boldsymbol{\eta}, \boldsymbol{y}$. From (4.21), it follows that

$$\boldsymbol{\eta} | \boldsymbol{v}, \boldsymbol{\tau}, \boldsymbol{y} \sim N_{p+q}\left(\boldsymbol{\Sigma}^{*-1} \boldsymbol{W}^T \boldsymbol{v}, \boldsymbol{\Sigma}^{*-1} \right), \tag{4.22}$$

where

$$\boldsymbol{\Sigma}^* = \begin{pmatrix} \boldsymbol{X}^T\boldsymbol{X} & \boldsymbol{X}^T\boldsymbol{Z} \\ \boldsymbol{Z}^T\boldsymbol{X} & \boldsymbol{Z}^T\boldsymbol{Z} + \boldsymbol{D}(\boldsymbol{\tau}) \end{pmatrix}. \tag{4.23}$$

The conditional distribution of v_i given $\boldsymbol{\eta}, \boldsymbol{y}$ is the same as in section 4.2.1. Also conditional on $\boldsymbol{\eta}, \boldsymbol{y}$, τ_j's are independent with $\tau_j \sim \text{Gamma}\left(a_j + q_j/2, b_j + \boldsymbol{u}_j^T\boldsymbol{u}_j/2\right)$ for $j = 1, \ldots, r$. Thus, one single iteration of the block Gibbs sampler $\{\boldsymbol{\eta}^{(m)}, \boldsymbol{v}^{(m)}, \boldsymbol{\tau}^{(m)}\}_{m=0}^{\infty}$ has the following two steps:

Algorithm 4.3 The $(m+1)$st iteration of the two-block Gibbs sampler

1: Draw $\tau_j^{(m+1)} \overset{\text{ind}}{\sim} \text{Gamma}\left(a_j + q_j/2, b_j + \boldsymbol{u}_j^{(m)T}\boldsymbol{u}_j^{(m)}/2\right)$ for $j = 1, \ldots, r$, and independently draw $v_i^{(m+1)} | \boldsymbol{\eta}^{(m)}, \boldsymbol{y} \overset{\text{ind}}{\sim} \text{TN}(\boldsymbol{w}_i^T\boldsymbol{\eta}^{(m)}, 1, y_i)$, $i = 1, \ldots, n$.

2: Draw $\boldsymbol{\eta}^{(m+1)} \sim N_{p+q}\left(\boldsymbol{\Sigma}^{*(m+1)-1}\boldsymbol{W}^T\boldsymbol{v}^{(m+1)}, \boldsymbol{\Sigma}^{*(m+1)-1}\right)$, where $\boldsymbol{\Sigma}^{*(m+1)}$ is evaluated at $\boldsymbol{\tau}^{(m+1)}$.

We now discuss conditions under which the posterior density (4.21) is proper. Let $c_i = 1$ if $y_i = 0$ and $c_i = -1$ if $y_i = 1$ for $i = 1, \ldots, n$. Suppose $\boldsymbol{W}^*_{n\times(p+q)}$ is a matrix whose ith row is $c_i(\boldsymbol{x}_i^T, \boldsymbol{z}_i^T)$. In the special case when $b_j = 0$, that is, when τ_j has the power prior $\pi(\tau_j) \propto \tau_j^{a_j - 1}$, Chen et al. (2002) (Theorem 4.2) showed that the corresponding posterior distribution is proper if the following conditions hold:

(A1) $\boldsymbol{W} = (\boldsymbol{X}, \boldsymbol{Z})$ is a full rank matrix;

(A2) There exists an $n \times 1$ positive vector $\boldsymbol{e} > 0$ such that $\boldsymbol{e}^T\boldsymbol{W}^* = 0$;

(A3) $\min\{2a_1 + q_1, \ldots, 2a_r + q_r\} > 0$;

(A4) $a_j < 0$ for $j = 1, \ldots, r$.

Roy and Hobert (2007) provided a simple method for checking the condition A2 using publicly available softwares.

Here we consider a general form of the prior distribution of τ_j as given in (4.20). Thus the parameters b_j's are not assumed to be zero. The following theorem gives the conditions for geometric ergodicity of the Markov chain underlying Algorithm 4.3. A proof of Theorem 4.2 is given in the Appendix C.

Theorem 4.2. *The Markov chain underlying the block Gibbs sampler is geometrically ergodic if the following conditions hold:*

(1) $a_j < b_j = 0$ *or* $b_j > 0$ *for* $j = 1, \ldots, r$*;*

(2) $(A1) - (A3)$ *hold.*

The condition A1 assumes that $\boldsymbol{W}$ is a full rank matrix. Unfortunately, when $\boldsymbol{Z}$ is a design matrix with elements 1's and 0's, which is pretty common in practice, this assumption may not hold. For example, we consider the following important probit two-way random effects model

$$\Phi^{-1}(P(Y_{ij} = 1)) = \beta + \alpha_i + \gamma_j, \tag{4.24}$$

for $i = 1, 2, \ldots, n_1$, $j = 1, 2, \ldots, n_2$. Here, the α_i's are i.i.d $N(0, 1/\tau_1)$, and the γ_j's are i.i.d $N(0, 1/\tau_2)$. There are total $n = n_1 \times n_2$ observations and we order them as $\boldsymbol{Y} = (Y_{11}, \ldots, Y_{1n_2}, \ldots, Y_{n_1 1}, \ldots, Y_{n_1 n_2})$. In this example, $p = 1$, and $\boldsymbol{X} = \mathbf{1}_n$ is an $n \times 1$ column vector of ones. Also there are $r = 2$ random effects with $q_1 = n_1$, $q_2 = n_2$, $q = q_1 + q_2 = n_1 + n_2$ and $\boldsymbol{Z} = (\boldsymbol{Z}_1, \boldsymbol{Z}_2)$, where $\boldsymbol{Z}_1 = \boldsymbol{I}_{n_1} \otimes \mathbf{1}_{n_2}$ and $\boldsymbol{Z}_2 = \mathbf{1}_{n_1} \otimes \boldsymbol{I}_{n_2}$ with $\otimes$ denoting the Kronecker product. It can be checked that the rank of $\boldsymbol{W} = (\boldsymbol{X}, \boldsymbol{Z})$ is $n_1 + n_2 - 1$. Thus $\boldsymbol{W}$ is not a full rank matrix and Theorem 4.2 cannot be used for this example.

We now provide Theorems 4.3 and 4.4 showing the posterior propriety and geometric convergence of the block Gibbs sampler without the assumption A1. We use certain transformations of the regression parameters $\boldsymbol{\beta}$ and random effects $\boldsymbol{u}$ to circumvent the problem with non-full rank matrix $\boldsymbol{W}$. Assume that the first column of $\boldsymbol{X}$ is a vector of 1's corresponding to an intercept term β_0 in $\boldsymbol{\beta} = (\beta_0, \beta_1, \ldots, \beta_{p-1})^T$. Let $\boldsymbol{Z} = (\boldsymbol{Z}_1, \ldots, \boldsymbol{Z}_r)$, where $\boldsymbol{Z}_j$ is an $n \times q_j$ matrix such that the (ik)th element is 1 if the observation i is observed at the kth level of the random effect $\boldsymbol{u}_j = \left(u_{j1}, \ldots, u_{jq_j}\right)^T$, 0 otherwise, for $i = 1, \ldots, n$, $k = 1, \ldots, q_j$ and $j = 1, \ldots, r$. Consider the following transformations,

$$\mu_0 = \beta_0 + \sum_{j=1}^{r} u_{j1}, \tag{4.25}$$

$$d_{jk} = u_{j,k+1} - u_{j1}, \text{for } k = 1, \ldots, q_j - 1, j = 1, \ldots, r. \tag{4.26}$$

Thus μ_0 is the sum of the intercept term and the first level effect of all r random effects. Also the (transformed) random effects d_{jk}'s denote the differences of the random effect compared to the first level effect.

Let $\tilde{\boldsymbol{\eta}} = (\mu_0, \beta_1, , \ldots, \beta_{p-1}, d_{11}, \ldots, d_{1,q_1-1}, \ldots d_{r1}, \ldots, d_{r,q_r-1})^T$. Define $\tilde{\boldsymbol{Z}} = (\tilde{\boldsymbol{Z}}_1, \ldots, \tilde{\boldsymbol{Z}}_r)$, where the $n \times (q_j - 1)$ matrix $\tilde{\boldsymbol{Z}}_j$ is $\boldsymbol{Z}_j$ without its first column. Thus, the vector $\boldsymbol{W}\boldsymbol{\eta}$ is the same as the vector $\tilde{\boldsymbol{W}}\tilde{\boldsymbol{\eta}}$, where $\tilde{\boldsymbol{W}} = \left(\boldsymbol{X}, \tilde{\boldsymbol{Z}}\right)$ with ith row $\tilde{\boldsymbol{w}}_i^T$. Let $\tilde{\boldsymbol{W}}^*$ be a matrix whose ith row is $\tilde{\boldsymbol{w}}_i^{*T} = c_i \tilde{\boldsymbol{w}}_i^T = c_i(\boldsymbol{x}_i^T, \tilde{\boldsymbol{z}}_i^T)$, where $\tilde{\boldsymbol{z}}_i^T$ is the ith row of $\tilde{\boldsymbol{Z}}$. For the example (4.24), the transformed parameters μ_0 and d_{jk}'s become

$$\begin{aligned} \mu_0 &= \beta + \alpha_1 + \gamma_1, \\ d_{1k} &= \alpha_{k+1} - \alpha_1 \text{ for } k = 1, \ldots, n_1 - 1, \\ d_{2k} &= \gamma_{k+1} - \gamma_1 \text{ for } k = 1, \ldots, n_2 - 1. \end{aligned}$$

Thus in this example, we have $\tilde{\boldsymbol{\eta}} = (\mu_0, d_{11}, \ldots, d_{1,n_1-1}, d_{21}, \ldots, d_{2,n_2-1})^T$. Also note that $\tilde{\boldsymbol{W}}$ is a full rank matrix in this example, although $\boldsymbol{W}$ is not.

Theorem 4.3. *Assume the following conditions hold,*

(B1) $a_j < b_j = 0$, $q_j \geq 2$ *or* $b_j > 0$ *for* $j = 1, \ldots, r$;

(B2) $2a_j + q_j - 1 > 0$ *for* $j = 1, \ldots, r$;

(B3) $\tilde{\boldsymbol{W}}$ *is a full rank matrix;*

(B4) There exists an $n \times 1$ *positive vector* $\boldsymbol{e} > 0$ *such that* $\boldsymbol{e}^T \tilde{\boldsymbol{W}}^* = 0$.

Then the joint posterior distribution (4.21) *is proper, i.e,*

$$\begin{aligned} &\int_{\mathbb{R}_+^r} \int_{\mathbb{R}^q} \int_{\mathbb{R}^p} \prod_{i=1}^{n} \Phi\left(\boldsymbol{x}_i^T\boldsymbol{\beta} + \boldsymbol{z}_i^T\boldsymbol{u}\right)^{y_i} \left[1 - \Phi\left(\boldsymbol{x}_i^T\boldsymbol{\beta} + \boldsymbol{z}_i^T\boldsymbol{u}\right)\right]^{1-y_i} \\ &\cdot \prod_{j=1}^{r} \tau_j^{\frac{q_j}{2} + a_j - 1} \exp\left[-\tau_j\left(b_j + \frac{1}{2}\boldsymbol{u}_j^T\boldsymbol{u}_j\right)\right] d\boldsymbol{\beta} d\boldsymbol{u} d\boldsymbol{\tau} < \infty. \end{aligned} \tag{4.27}$$

The following theorem provides the conditions for geometric convergence of the Markov chain underlying the Gibbs sampler given in Algorithm 4.3.

Theorem 4.4. *The block Gibbs sampler is geometrically ergodic under the following conditions:*

(1) $(B1) - (B4)$ *hold;*

(2) There exists an $s \in (0,1] \cap (0, \tilde{s})$ *such that*

$$2^{-s} \sum_{j=1}^{r} \frac{\Gamma(q_j/2 + a_j - s)}{\Gamma(q_j/2 + a_j)} \left[tr\left(R_j \left(\boldsymbol{I} - P_{\boldsymbol{Z}^T(\boldsymbol{I}-P_X)\boldsymbol{Z}} \right) R_j^T \right) \right]^s < 1, \tag{4.28}$$

where $\tilde{s} = \min\{a_1 + q_1/2, \ldots, a_r + q_r/2\}$, R_j *is a* $q_j \times q$ *matrix with 0's and 1's such that* $R_j \boldsymbol{u} = \boldsymbol{u}_j$ *and* $P_{\boldsymbol{Z}^T(\boldsymbol{I}-P_X)\boldsymbol{Z}}$ *is the projection matrix on the column space of* $\boldsymbol{Z}^T(\boldsymbol{I} - P_X)\boldsymbol{Z}$.

The proofs of Theorems 4.3 and 4.4 are given in Appendix D and Appendix E respectively.

Remark 4.3. *The extra condition (2) in Theorem 4.4 compared to Theorem 4.2 is due to the lack of the full rank assumption of* $\boldsymbol{W}$. *This condition is also used in Román and Hobert (2012), who provide some discussions on this. The left-hand side of (4.28) can be evaluated at values of* s *on a fine grid in the interval* $(0,1] \cap (0, \tilde{s})$ *to numerically check the condition. Note that,* R_j *is the matrix that extracts* $\boldsymbol{u}_j$ *out of* $\boldsymbol{u}$. *Thus when* $r > 1$, $tr\left(R_j \left(\boldsymbol{I} - P_{\boldsymbol{Z}^T(\boldsymbol{I}-P_X)\boldsymbol{Z}} \right) R_j^T \right)$ *is the sum of the* q_j *diagonal elements of* $\boldsymbol{I} - P_{\boldsymbol{Z}^T(\boldsymbol{I}-P_X)\boldsymbol{Z}}$ *corresponding to the* j*th random effect.*

4.3.2 A Haar PX-DA algorithm

Under improper priors, we can also construct a Haar PX-DA algorithm as in Section 4.2.3. From (4.21), we derive the marginal density of $\boldsymbol{v}, \boldsymbol{\tau}$ given by

$$\begin{aligned} \pi^*(\boldsymbol{v}, \boldsymbol{\tau}|\boldsymbol{y}) &= \int_{\mathbb{R}^{p+q}} \pi^*(\boldsymbol{\eta}, \boldsymbol{v}, \boldsymbol{\tau}|\boldsymbol{y}) d\boldsymbol{\eta} \\ &\propto \prod_{i=1}^{n} \left[1_{(0,\infty)}(v_i) \right]^{y_i} \left[1_{(-\infty,0]}(v_i) \right]^{1-y_i} \prod_{j=1}^{r} \tau_j^{\frac{q_j}{2}+a_j} e^{-b_j \tau_j} \\ &\quad \cdot |\boldsymbol{\Sigma}^*|^{-1/2} \exp\left\{ -\frac{1}{2} \boldsymbol{v}^T M_4 \boldsymbol{v} \right\}, \end{aligned} \tag{4.29}$$

where $M_4 = \boldsymbol{I} - \boldsymbol{W}\boldsymbol{\Sigma}^{*-1}\boldsymbol{W}^T$. As in section 4.2.3, we consider a probability density function $\vartheta^*(g)$ on G where

$$\begin{aligned} \vartheta^*(g)\, dg &\propto \pi^*(g\boldsymbol{v}, \boldsymbol{\tau}|\boldsymbol{y})\, \chi(g)\, \nu(dg) \\ &\propto g^{n-1} \exp\left\{ -\frac{1}{2} g^2 \boldsymbol{v}^T M_4 \boldsymbol{v} \right\} dg. \end{aligned} \tag{4.30}$$

Since $\vartheta^*(\cdot)$ is a log concave function, we can use the adaptive rejection sampling algorithm to effectively sample from it. Thus one step of the Haar PX-DA algorithm has the following 3 steps.

Algorithm 4.4 The $(m+1)$st iteration of the Haar PX-DA algorithm

1: $\tau_j \sim \text{Gamma}\left(a_j + q_j/2, b_j + \boldsymbol{u}_j^{(m)T}\boldsymbol{u}_j^{(m)}/2\right)$, for $j = 1, \ldots, r$ and independently draw $v_i|\boldsymbol{\eta}^{(m)}, \boldsymbol{y} \overset{\text{ind}}{\sim} \text{TN}(\boldsymbol{w}_i^T\boldsymbol{\eta}^{(m)}, 1, y_i)$ for $i = 1, \ldots, n$.

2: Draw g from (4.30).

3: Calculate $v_i' = gv_i$ and let $\boldsymbol{v}' = (v_1', \ldots, v_n')^T$. Draw

$$\boldsymbol{\eta}^{(m+1)} \sim N_{p+q}\left(\boldsymbol{\Sigma}\left(\boldsymbol{\tau}\right)^{*-1}\boldsymbol{W}^T\boldsymbol{v}', \boldsymbol{\Sigma}\left(\boldsymbol{\tau}\right)^{*-1}\right).$$

As in section 4.2.3, we have the following corollary in the case of improper priors.

Corollary 4.2. *Under the conditions of Theorem 4.2 or Theorem 4.4, the Markov chain underlying the Haar PX-DA algorithm described in Algorithm 4.4 is geometrically ergodic.*

4.4 An example

In this section, we use the *bacteria* data set from Venables and Ripley (2002) to compare the performance of the full Gibbs sampler, Algorithm 1 and Algorithm 2 presented in Appendix F, sections 4.2.1 and 4.2.3 respectively. The response variable here is a binary variable indicating the presence or absence of the bacteria *H.influenzae*. There are three covariates: week of test, three treatments (a placebo, and an active drug with and without extra effort to ensure that it is taken), and the subject ID. The total sample size is 220. Venables and Ripley (2002) used the logit linear mixed model to analyze this data. Instead of the logit link function, we use the probit link. The fixed week effect enters the model as $I(\text{week} > 2)$, where $I(\cdot)$ is an indicator function. The model we consider is

$$P(Y_{ij} = 1) = \Phi\left(\beta_0 + \beta_1 I(\text{week}_{ij} > 2) + \beta_2 x_{2i} + \beta_3 x_{3i} + u_i\right),$$

for $i = 1, \ldots, n = 50$, $j = 1, \ldots, n_i$, where n_i is the number of observations for subject i, x_2 and x_3 are binary variables corresponding to active drug treatment without and with extra effort to guarantee the drug is taken. Here $\boldsymbol{u} = (u_1, \ldots, u_n)^T$ is the random effect with 50 levels and we

assume that $\boldsymbol{u} \sim N(0, 1/\tau \boldsymbol{I}_{50})$. Using the method described in Roy and Hobert (2007), we see that the condition (B4) does not hold in this example. Thus we do not use improper flat prior for $\boldsymbol{\beta}$ here. We consider proper priors for both $\boldsymbol{\beta}$ and τ. We assume β_k's are apriori independent and the prior distribution of β_k is normal with mean 0 and variance 1000 for $k = 0, 1, 2, 3$. For the prior distribution of τ, we assume $\tau \sim$ truncated Gamma(a, b) with $a = b = 1$ and $\tau_0 = 10^{-10}$. (We also used two other values of τ_0, namely, 10^{-3} and 10^{-5}. The posterior mean estimates of the regression coefficients were exactly same as for $\tau_0 = 10^{-10}$.) For drawing from the truncated Gamma conditional distribution of τ, we simply used probability integral transformation with numerical approximations for the cdf and the quantile function of the Gamma distribution. We compare the two-block Gibbs sampler and the Haar PX-DA algorithm using the standard errors for the parameter estimates. We use the spectral variance estimator with Tukey-Hanning window (Flegal and Jones, 2010) for estimating the standard errors. We implement it using the R package *mcmcse* with default values for the lag window. Markov chains of length 2×10^6 after an initial burn-in of 2×10^6 iterations are used to calculate the parameter estimates and the standard error estimates. Table 4.1 shows posterior mean estimates of the parameters and the corresponding standard errors. The two algorithms have similar parameter estimates. We also calculate the ratio of asymptotic variance estimates ($\hat{\sigma}_h^2/\hat{\sigma}_h^{*2}$) for the DA algorithm ($\hat{\sigma}_h^2$, two-block Gibbs samplers) and the Haar PX-DA algorithm ($\hat{\sigma}_h^{*2}$). These ratios can be high as 2.3. Thus, the block Gibbs sampler needs about 2.3 times as many iterations as the Haar PX-DA algorithm in order to achieve the same level of precision. Since the two algorithms basically require the same amount of time to run per iteration, use of the Haar PX-DA algorithm can lead to significant gains in efficiency.

Table 4.1: Results for the block Gibbs sampler and the Haar PX-DA algorithm

	DA algorithm		PX-DA algorithm		
Parameter	estimate	s.e.	estimate	s.e	$\hat{\sigma}_h^2/\hat{\sigma}_h^{*2}$
β_0	2.2383	0.0015	2.2383	0.0010	2.3459
β_1	-0.9781	0.0007	-0.9780	0.0005	1.6918
β_2	-0.8502	0.0009	-0.8508	0.0008	1.3938
β_3	-0.5184	0.0009	-0.5181	0.0008	1.3346

We also compare the full Gibbs sampler given in Appendix F with the two-block Gibbs sampler and the Haar PX-DA algorithm. Figure 4.1 shows the auto-correlation plots (for the regression parameters) corresponding to these three algorithms. The plots show that the full Gibbs sampler always has the largest auto-correlation values. We also calculate the estimated effective sample sizes (Gong and Flegal, 2016) using the R package *mcmcse*. Table 4.2 shows the estimates of the effective sample sizes (ESS) per second, which are calculated by taking the ratio of the ESS and the total running times. We can see that the Haar PX-DA algorithm is the most efficient algorithm, and the full Gibbs sampler is the least efficient algorithm. Thus the Haar PX-DA needs less time and the full Gibbs sampler needs more time compared to the DA algorithm in order to have the same ESS.

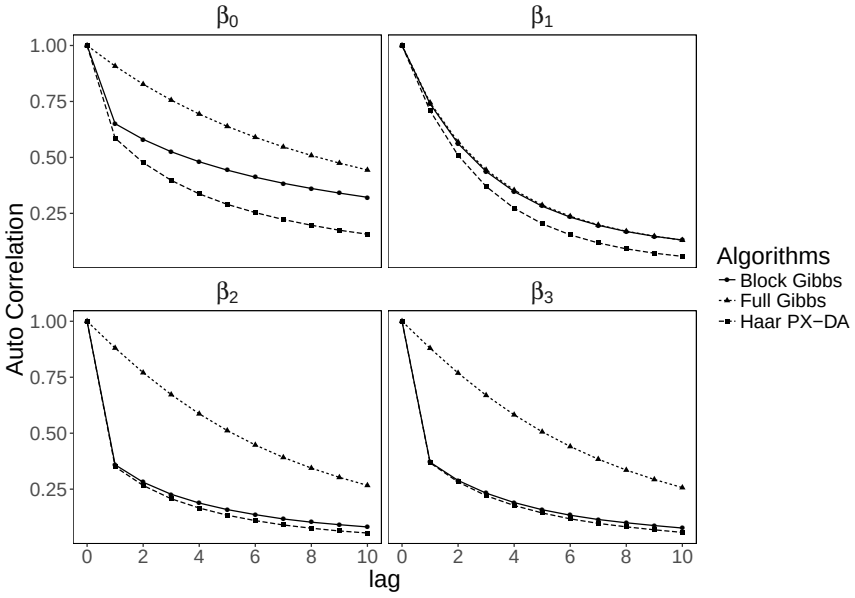

Figure 4.1: Auto-correlation plots of different regression parameters for the three algorithms

4.5 Discussion

We develop two-block Gibbs samplers for the Bayesian probit linear mixed models under both proper priors and improper priors. The block Gibbs algorithm samples the fixed effects and the random effects jointly. We prove the geometric ergodicity of the two-block Gibbs samplers, which

Table 4.2: Estimated effective sample sizes per second

Parameter	Block Gibbs	Haar PX-DA	Full Gibbs
β_0	6.31	12.65	5.29
β_1	13.15	19.15	13.91
β_2	21.97	26.26	9.45
β_3	23.06	26.39	10.12

guarantees the existence of central limit theorems for MCMC estimators under a finite second moment condition. This is the first ever theoretical analysis of a Gibbs sampler for a Bayesian generalized linear mixed model. We propose the corresponding Haar PX-DA algorithms for the two cases. These Haar PX-DA algorithms not only improve the efficiency of the Gibbs samplers, but also inherit their geometric convergence properties. Using an example, we show that the Haar PX-DA algorithm can lead to much efficiency gain compared to the block Gibbs sampler. We also compare the performance of the full Gibbs sampler and the block Gibbs samplers developed here.

Another popular link function is the logit link function. Polson et al. (2013) proposed a DA algorithm for the logistic regression model. Choi and Hobert (2013) proved the uniform ergodicity of this DA algorithm. As mentioned in Polson et al. (2013), their DA algorithm can be extended to the logistic linear mixed model. However, the convergence properties of the corresponding Markov chain have not been studied, and can be a topic for future research. Another future project can be deriving similar extensions of the results in Roy (2012a) for proving geometric convergence of Gibbs samplers for robit linear mixed models.

Appendices

A Proof of Theorem 1

Proof. We prove the geometric ergodicity of $\boldsymbol{\Psi}$ by establishing a drift condition. In particular, we consider the drift function

$$V(\boldsymbol{\eta}) \equiv \sum_{i=1}^{n} \left(\boldsymbol{x}_i^T \boldsymbol{\beta} + \boldsymbol{z}_i^T \boldsymbol{u} \right)^2 + \boldsymbol{\beta}^T \boldsymbol{Q} \boldsymbol{\beta} + \tau_0 \boldsymbol{u}^T \boldsymbol{u}, \tag{4.31}$$

and show that for any $\boldsymbol{\eta}, \boldsymbol{\eta}' \in \mathbb{R}^{p+q}$, there exist $\rho \in [0,1)$ and $L > 0$ such that

$$E\left[V(\boldsymbol{\eta})|\boldsymbol{\eta}'\right] \leq \rho V(\boldsymbol{\eta}') + L. \tag{4.32}$$

Let

$$\boldsymbol{M} = \begin{pmatrix} \boldsymbol{X}^T\boldsymbol{X} + \boldsymbol{Q} & \boldsymbol{X}^T\boldsymbol{Z} \\ \boldsymbol{Z}^T\boldsymbol{X} & \boldsymbol{Z}^T\boldsymbol{Z} + \tau_0\boldsymbol{I}_q \end{pmatrix}.$$

The drift function (4.31) can be written as $V(\boldsymbol{\eta}) = \boldsymbol{\eta}^T\boldsymbol{M}\boldsymbol{\eta}$. Now, we prove (4.32). By Fubini's theorem, we have

$$\begin{aligned} E\left[V\left(\boldsymbol{\eta}\right)|\boldsymbol{\eta}'\right] &= \int_{\mathbb{R}^{p+q}} V\left(\boldsymbol{\eta}\right) k\left(\boldsymbol{\eta}|\boldsymbol{\eta}'\right) d\boldsymbol{\eta} \\ &= \int_{\mathbb{R}^n}\int_{\mathbb{R}_+^r}\int_{\mathbb{R}^{p+q}} V\left(\boldsymbol{\eta}\right)\pi\left(\boldsymbol{\eta}|\boldsymbol{v},\boldsymbol{\tau},\boldsymbol{y}\right)\pi\left(\boldsymbol{v},\boldsymbol{\tau}|\boldsymbol{\eta}',\boldsymbol{y}\right) d\boldsymbol{\eta}d\boldsymbol{\tau}d\boldsymbol{v}. \end{aligned}$$

So the expectation can be calculated in two steps. The first step is to calculate $E\left(V\left(\boldsymbol{\eta}\right)|\boldsymbol{v},\boldsymbol{\tau},\boldsymbol{y}\right)$.

Note that

$$\boldsymbol{M} = \boldsymbol{W}^T\boldsymbol{W} + \boldsymbol{A}(\tau_0), \text{ where } \boldsymbol{A}(\tau_0) = \begin{pmatrix} \boldsymbol{Q} & \boldsymbol{0} \\ \boldsymbol{0} & \tau_0\boldsymbol{I}_q \end{pmatrix}.$$

Since the support of the density $\pi(\boldsymbol{\tau})$ is assumed to be truncated below at τ_0, we have $\boldsymbol{M} \preceq \boldsymbol{\Sigma}$, where $\boldsymbol{\Sigma}$ is defined in (4.9). Here "$\boldsymbol{M} \preceq \boldsymbol{\Sigma}$" means that $\boldsymbol{\Sigma} - \boldsymbol{M}$ is a positive semidefinite matrix. Thus, by (4.8) and (4.9), we have

$$\begin{aligned} E\left(\boldsymbol{\eta}^T\boldsymbol{M}\boldsymbol{\eta}|\boldsymbol{v},\boldsymbol{\tau},\boldsymbol{y}\right) &\leq E\left(\boldsymbol{\eta}^T\boldsymbol{\Sigma}\boldsymbol{\eta}|\boldsymbol{v},\boldsymbol{\tau},\boldsymbol{y}\right) \\ &= p+q+\left[E\left(\boldsymbol{\eta}|\boldsymbol{v},\boldsymbol{\tau},\boldsymbol{y}\right)\right]^T\boldsymbol{\Sigma}E\left(\boldsymbol{\eta}|\boldsymbol{v},\boldsymbol{\tau},\boldsymbol{y}\right) \\ &= p+q+\boldsymbol{\mu}^T\boldsymbol{\Sigma}^{-1}\boldsymbol{\mu} \\ &= p+q+\left(\boldsymbol{W}^T\boldsymbol{v}+\boldsymbol{l}\right)^T\boldsymbol{\Sigma}^{-1}\left(\boldsymbol{W}^T\boldsymbol{v}+\boldsymbol{l}\right) \\ &= p+q+\|\boldsymbol{\Sigma}^{-\frac{1}{2}}\left(\boldsymbol{W}^T\boldsymbol{v}+\boldsymbol{l}\right)\|^2, \end{aligned} \tag{4.33}$$

where $\|\cdot\|$ denotes the Euclidean norm. Using the inequality (Chakraborty and Khare, 2017)

$$\|\boldsymbol{a}+\boldsymbol{b}\|^2 \leq \left(1+c_0^2\right)\|\boldsymbol{a}\|^2 + \left(1+\frac{1}{c_0^2}\right)\|\boldsymbol{b}\|^2,$$

for any $\boldsymbol{a}, \boldsymbol{b} \in \mathbb{R}^{p+q}$ and $c_0 > 0$, we have

$$\begin{aligned} ||\boldsymbol{\Sigma}^{-\frac{1}{2}} \left(\boldsymbol{W}^T\boldsymbol{v} + \boldsymbol{l}\right)||^2 &\leq \left(1 + c_0^2\right)\boldsymbol{v}^T\boldsymbol{W}\boldsymbol{\Sigma}^{-1}\boldsymbol{W}^T\boldsymbol{v} + \left(1 + \frac{1}{c_0^2}\right)\boldsymbol{l}^T\boldsymbol{\Sigma}^{-1}\boldsymbol{l} \\ &= \left(1 + c_0^2\right)\boldsymbol{v}^T\boldsymbol{W}\left(\boldsymbol{W}^T\boldsymbol{W} + \boldsymbol{A}(\boldsymbol{\tau})\right)^{-1}\boldsymbol{W}^T\boldsymbol{v} \\ &+ \left(1 + \frac{1}{c_0^2}\right)\boldsymbol{l}^T\left(\boldsymbol{W}^T\boldsymbol{W} + \boldsymbol{A}(\boldsymbol{\tau})\right)^{-1}\boldsymbol{l}. \end{aligned} \tag{4.34}$$

Since $\boldsymbol{\Sigma}^{-1} = \left(\boldsymbol{W}^T\boldsymbol{W} + \boldsymbol{A}(\boldsymbol{\tau})\right)^{-1} \preceq \left(\boldsymbol{W}^T\boldsymbol{W} + \boldsymbol{A}(\tau_0)\right)^{-1} = \boldsymbol{M}^{-1}$(Proposition 8.6.6, Bernstein (2009)), we have

$$\boldsymbol{W}\left(\boldsymbol{W}^T\boldsymbol{W} + \boldsymbol{A}(\boldsymbol{\tau})\right)^{-1}\boldsymbol{W}^T \preceq \boldsymbol{W}\left(\boldsymbol{W}^T\boldsymbol{W} + \boldsymbol{A}(\boldsymbol{\tau}_0)\right)^{-1}\boldsymbol{W}^T,$$

and

$$\boldsymbol{l}^T\left(\boldsymbol{W}^T\boldsymbol{W} + \boldsymbol{A}(\boldsymbol{\tau})\right)^{-1}\boldsymbol{l} \leq \boldsymbol{l}^T\boldsymbol{M}^{-1}\boldsymbol{l}. \tag{4.35}$$

Let $\tilde{\boldsymbol{X}} = \boldsymbol{W}\boldsymbol{A}(\tau_0)^{-1/2}$, then

$$\boldsymbol{W}\left(\boldsymbol{W}^T\boldsymbol{W} + \boldsymbol{A}(\boldsymbol{\tau}_0)\right)^{-1}\boldsymbol{W}^T = \tilde{\boldsymbol{X}}\left(\tilde{\boldsymbol{X}}^T\tilde{\boldsymbol{X}} + \boldsymbol{I}_n\right)^{-1}\tilde{\boldsymbol{X}}^T.$$

From Chakraborty and Khare (2017)[Proposition A.1], we know that all eigenvalues of $\tilde{\boldsymbol{X}}\left(\tilde{\boldsymbol{X}}^T\tilde{\boldsymbol{X}} + \boldsymbol{I}_n\right)^{-1}\tilde{\boldsymbol{X}}^T$ lie in $[0, 1)$. Let $d_1, \ldots, d_{\tilde{r}}$ denote the nonzero singular values of $\tilde{\boldsymbol{X}}$, where $\tilde{r}$ is the rank of $\boldsymbol{W}$. Then from Chakraborty and Khare (2017)[Proposition A.1], it follows that $d_i^2/(d_i^2 + 1)$, $i = 1, \ldots, \tilde{r}$ are the nonzero eigenvalues of $\boldsymbol{W}\left(\boldsymbol{W}^T\boldsymbol{W} + \boldsymbol{A}(\boldsymbol{\tau}_0)\right)^{-1}\boldsymbol{W}^T$. Let $\lambda_{\max}(\boldsymbol{\tau}_0)$ denote $\max\{d_1^2/(d_1^2+1), \ldots, d_{\tilde{r}}^2/(d_{\tilde{r}}^2+1)\}$, we have $\lambda_{\max}(\tau_0) < 1$. Then

$$\boldsymbol{W}\left(\boldsymbol{W}^T\boldsymbol{W} + \boldsymbol{A}(\boldsymbol{\tau})\right)^{-1}\boldsymbol{W}^T \preceq \lambda_{\max}(\boldsymbol{\tau}_0)\boldsymbol{I}_n.$$

Hence,

$$\boldsymbol{v}^T\boldsymbol{W}\left(\boldsymbol{W}^T\boldsymbol{W} + \boldsymbol{A}(\boldsymbol{\tau})\right)^{-1}\boldsymbol{W}^T\boldsymbol{v} \leq \lambda_{\max}(\boldsymbol{\tau}_0)\sum_{i=1}^{n} v_i^2. \tag{4.36}$$

Combining (4.34), (4.35) and (4.36), from (4.33), we have

$$\begin{aligned} E\left(\boldsymbol{\eta}^T\boldsymbol{M}\boldsymbol{\eta}|\boldsymbol{v}, \boldsymbol{\tau}, \boldsymbol{y}\right) &\leq p + q + (1 + c_0^2)\lambda_{\max}(\boldsymbol{\tau}_0)\sum_{i=1}^{n} v_i^2 + \left(1 + \frac{1}{c_0^2}\right)\boldsymbol{l}^T\boldsymbol{M}^{-1}\boldsymbol{l} \\ &= A_1(c_0) + (1 + c_0^2)\lambda_{\max}(\boldsymbol{\tau}_0)\sum_{i=1}^{n} v_i^2, \end{aligned} \tag{4.37}$$

where $A_1(c_0) \equiv (1+c_0^{-2})\boldsymbol{l}^T\boldsymbol{M}^{-1}\boldsymbol{l} + p + q$.

Now, we consider the expectation related to the conditional distribution of $\boldsymbol{v}$ and $\boldsymbol{\tau}$ given $\boldsymbol{\eta}' \equiv (\boldsymbol{\beta}'^T, \boldsymbol{u}'^T)^T$ and $\boldsymbol{y}$. Using (10) from Roy and Hobert (2007), we have

$$E(v_i^2|\boldsymbol{\eta}', \boldsymbol{y}) = \begin{cases} 1 + (\boldsymbol{x}_i^T\boldsymbol{\beta}' + \boldsymbol{z}_i^T\boldsymbol{u}')^2 + \frac{(\boldsymbol{x}_i^T\boldsymbol{\beta}'+\boldsymbol{z}_i^T\boldsymbol{u}')\phi(\boldsymbol{x}_i^T\boldsymbol{\beta}'+\boldsymbol{z}_i^T\boldsymbol{u}')}{\Phi(\boldsymbol{x}_i^T\boldsymbol{\beta}'+\boldsymbol{z}_i^T\boldsymbol{u}')} & \text{if } y_i = 1 \\ 1 + (\boldsymbol{x}_i^T\boldsymbol{\beta}' + \boldsymbol{z}_i^T\boldsymbol{u}')^2 - \frac{(\boldsymbol{x}_i^T\boldsymbol{\beta}'+\boldsymbol{z}_i^T\boldsymbol{u}')\phi(\boldsymbol{x}_i^T\boldsymbol{\beta}'+\boldsymbol{z}_i^T\boldsymbol{u}')}{1-\Phi(\boldsymbol{x}_i^T\boldsymbol{\beta}'+\boldsymbol{z}_i^T\boldsymbol{u}')} & \text{if } y_i = 0 \end{cases}.$$

The above expectation can be written as,

$$E(v_i^2|\boldsymbol{\eta}', \boldsymbol{y}) = 1 + \left(\boldsymbol{w}_i^{*T}\boldsymbol{\eta}'\right)^2 - \frac{\left(\boldsymbol{w}_i^{*T}\boldsymbol{\eta}'\right)\phi\left(\boldsymbol{w}_i^{*T}\boldsymbol{\eta}'\right)}{1-\Phi\left(\boldsymbol{w}_i^{*T}\boldsymbol{\eta}'\right)}, \tag{4.38}$$

where $\boldsymbol{w}_i^* = c_i\boldsymbol{w}_i^T$ is the ith row of $\boldsymbol{W}^*$ defined in section 4.3.1. Also,

$$\begin{aligned} -\frac{\left(\boldsymbol{w}_i^{*T}\boldsymbol{\eta}'\right)\phi\left(\boldsymbol{w}_i^{*T}\boldsymbol{\eta}'\right)}{1-\Phi\left(\boldsymbol{w}_i^{*T}\boldsymbol{\eta}'\right)} &\leq \begin{cases} \left|\frac{(\boldsymbol{w}_i^{*T}\boldsymbol{\eta}')\phi(\boldsymbol{w}_i^{*T}\boldsymbol{\eta}')}{1-\Phi(\boldsymbol{w}_i^{*T}\boldsymbol{\eta}')}\right| & \text{if } \boldsymbol{w}_i^{*T}\boldsymbol{\eta}' \leq 0 \\ 0 & \text{if } \boldsymbol{w}_i^{*T}\boldsymbol{\eta}' > 0 \end{cases} \\ &\leq \sup_{u\in(-\infty,0]}\left|\frac{u\phi(u)}{1-\Phi(u)}\right| \equiv \Xi, \end{aligned} \tag{4.39}$$

where $\Xi \in (0,\infty)$. Thus from (4.38) we have $E(v_i^2|\boldsymbol{\eta}', \boldsymbol{y}) \leq 1 + \Xi + (\boldsymbol{x}_i^T\boldsymbol{\beta}' + \boldsymbol{z}_i^T\boldsymbol{u}')^2$ for $i = 1, \ldots, n$. From (4.37), it follows that

$$\begin{aligned} E\left(\boldsymbol{\eta}^T\boldsymbol{M}\boldsymbol{\eta}|\boldsymbol{\eta}', \boldsymbol{y}\right) &\leq A_1(c_0) + n(1+c_0^2)\lambda_{\max}(\tau_0)(1+\Xi) \\ &+ (1+c_0^2)\lambda_{\max}(\tau_0)\sum_{i=1}^n(\boldsymbol{x}_i^T\boldsymbol{\beta}' + \boldsymbol{z}_i^T\boldsymbol{u}')^2 \\ &\leq L + \rho(c_0)V(\boldsymbol{\eta}'), \end{aligned}$$

where $L = A_1(c_0) + n(1+c_0^2)\lambda_{\max}(\tau_0)(1+\Xi)$ and $\rho(c_0) = \lambda_{\max}(\tau_0)(1+c_0^2)$. Since $\lambda_{\max}(\tau_0) < 1$, there exists $c_0 \in (0, \sqrt{\lambda_{\max}(\tau_0)^{-1} - 1})$ such that $\rho(c_0) < 1$. That means there exist $\rho \in [0,1)$ and $L > 0$ such that (4.32) holds.

Since $\boldsymbol{M}$ is positive definite, $V(\boldsymbol{\eta})$ is unbounded off compact sets, that is, for any $a > 0$, the set $\{\boldsymbol{\eta} : V(\boldsymbol{\eta}) \leq a\}$ is compact. We now show that $\boldsymbol{\eta}$-chain is a Feller chain, which means that $K(\boldsymbol{\eta}, O)$ is a lower semi-continuous function on $\mathbb{R}^{p+q}$ for each fixed open set O. For a sequence $\{\boldsymbol{\eta}_m\}$ note

that,

$$\begin{aligned}\liminf_{m\to\infty} K(\boldsymbol{\eta}_m, O) &= \liminf_{m\to\infty} \int_O k(\boldsymbol{\eta}|\boldsymbol{\eta}_m)\, d\boldsymbol{\eta} \\ &= \liminf_{m\to\infty} \int_O \left[\int_{\mathbb{R}_+^r} \int_{\mathbb{R}^n} \pi(\boldsymbol{\eta}|\boldsymbol{v},\boldsymbol{\tau},\boldsymbol{y}) \pi(\boldsymbol{v},\boldsymbol{\tau}|\boldsymbol{\eta}_m,\boldsymbol{y}) d\boldsymbol{v} d\boldsymbol{\tau} \right] d\boldsymbol{\eta} \\ &\geq \int_O \int_{\mathbb{R}_+^r} \int_{\mathbb{R}^n} \pi(\boldsymbol{\eta}|\boldsymbol{v},\boldsymbol{\tau},\boldsymbol{y}) \liminf_{m\to\infty} \pi(\boldsymbol{v},\boldsymbol{\tau}|\boldsymbol{\eta}_m,\boldsymbol{y}) d\boldsymbol{v} d\boldsymbol{\tau} d\boldsymbol{\eta},\end{aligned}$$

where the inequality follows from Fatou's lemma. Recall that $\pi(\boldsymbol{v},\boldsymbol{\tau}|\boldsymbol{\eta},\boldsymbol{y}) = \pi(\boldsymbol{v}|\boldsymbol{\eta},\boldsymbol{y})\pi(\boldsymbol{\tau}|\boldsymbol{\eta},\boldsymbol{y})$. Since both $\pi(\boldsymbol{v}|\boldsymbol{\eta},\boldsymbol{y})$ and $\pi(\boldsymbol{\tau}|\boldsymbol{\eta},\boldsymbol{y})$ are continuous functions in $\boldsymbol{\eta}$, if $\boldsymbol{\eta}_m \to \boldsymbol{\eta}$,

$$\begin{aligned}\liminf_{m\to\infty} K(\boldsymbol{\eta}_m, O) &\geq \int_O \int_{\mathbb{R}_+^r} \int_{\mathbb{R}^n} \pi(\boldsymbol{\eta}|\boldsymbol{v},\boldsymbol{\tau},\boldsymbol{y}) \pi(\boldsymbol{v},\boldsymbol{\tau}|\boldsymbol{\eta},\boldsymbol{y}) d\boldsymbol{v} d\boldsymbol{\tau} d\boldsymbol{\eta} \\ &= K(\boldsymbol{\eta}, O).\end{aligned}$$

Thus by Meyn and Tweedie (1993)(chap. 15), (4.32) implies the Markov chain $\boldsymbol{\Psi}$ is geometrically ergodic. □

B Two Lemmas

In this section, we list some technical results. For $\boldsymbol{\Sigma}^*$ defined in (4.23), note that

$$\boldsymbol{\Sigma}^{*-1} = \begin{pmatrix} \left(\boldsymbol{X}^T\boldsymbol{X}\right)^{-1} + RS(\boldsymbol{\tau})^{-1}R^T & -RS(\boldsymbol{\tau})^{-1} \\ -S(\boldsymbol{\tau})^{-1}R^T & S(\boldsymbol{\tau})^{-1} \end{pmatrix}, \tag{4.40}$$

with $S(\boldsymbol{\tau})$ and R defined as

$$S(\boldsymbol{\tau}) = \boldsymbol{Z}^T(\boldsymbol{I} - P_X)\boldsymbol{Z} + \boldsymbol{D}(\boldsymbol{\tau}), \text{ and } R = \left(\boldsymbol{X}^T\boldsymbol{X}\right)^{-1}\boldsymbol{X}^T\boldsymbol{Z} \tag{4.41}$$

respectively, where

$$P_X = \boldsymbol{X}\left(\boldsymbol{X}^T\boldsymbol{X}\right)^{-1}\boldsymbol{X}^T. \tag{4.42}$$

Also the mean for the conditional distribution of $\boldsymbol{\eta}$ in (4.22) becomes

$$\boldsymbol{\Sigma}^{*-1}\boldsymbol{W}^T\boldsymbol{v} = \begin{pmatrix} \left(\boldsymbol{X}^T\boldsymbol{X}\right)^{-1}\boldsymbol{X}^T\left[\boldsymbol{I} - \boldsymbol{Z}S(\boldsymbol{\tau})^{-1}\boldsymbol{Z}^T(\boldsymbol{I} - P_X)\right]\boldsymbol{v} \\ S(\boldsymbol{\tau})^{-1}\boldsymbol{Z}^T(\boldsymbol{I} - P_X)\,\boldsymbol{v} \end{pmatrix}.$$

Let $U^T \Lambda U$ be the spectral decomposition of $\boldsymbol{Z}^T (\boldsymbol{I} - P_X) \boldsymbol{Z}$ and let λ_j's be the diagonal elements of Λ. Then $\left(\boldsymbol{Z}^T (\boldsymbol{I} - P_X) \boldsymbol{Z}\right)^+ \equiv U^T \Lambda^+ U$, where Λ^+ is a diagonal matrix whose jth diagonal element is $\lambda_j^+ = 1/\lambda_j$ if $\lambda_j \neq 0$, and 0 otherwise.

Lemma 4.1. *For the matrices $S(\boldsymbol{\tau})$ and P_X defined in (4.41) and (4.42), the following inequalities hold for all $\tau_j \in \mathbb{R}_+$, $j = 1, \ldots, r$:*

1. $S(\boldsymbol{\tau})^{-1} \preceq \left(\boldsymbol{Z}^T (\boldsymbol{I} - P_X) \boldsymbol{Z}\right)^+ + \sum_{j=1}^r 1/\tau_j \left(\boldsymbol{I} - P_{\boldsymbol{Z}^T (\boldsymbol{I} - P_X) \boldsymbol{Z}}\right)$.
2. $\left(R_j S(\boldsymbol{\tau})^{-1} R_j^T\right)^{-1} \preceq (\lambda_p + \tau_j) \boldsymbol{I}_{q_j}$, *where λ_p is the largest eigenvalue of $\boldsymbol{Z}^T (\boldsymbol{I} - P_X) \boldsymbol{Z}$ and R_j is a $q_j \times q$ matrix with 0's and 1's such that $R_j \boldsymbol{u} = \boldsymbol{u}_j$.*

The proof of the above result is similar to that of Lemma 1 in Román and Hobert (2012) and we omit it.

Lemma 4.2. *Let $S(\boldsymbol{\tau})$ and P_X be the two matrices as defined in (4.41) and (4.42). Let $\boldsymbol{l} = (l_1, \ldots, l_n)^T \in \mathbb{R}^n$. For any $\boldsymbol{\tau} \in \mathbb{R}_+^r$, we have,*

$$\left\| S(\boldsymbol{\tau})^{-1} \boldsymbol{Z}^T (\boldsymbol{I} - \boldsymbol{P}_X) \boldsymbol{l} \right\| \leq \hat{\varphi} \sum_{i=1}^n |l_i| ,$$

where $\hat{\varphi}$ is a finite number that depends on $\boldsymbol{W}$.

Proof. Let $\boldsymbol{Z}_P \equiv (\boldsymbol{I} - P_X) \boldsymbol{Z}$ and $\boldsymbol{z}_{Pi}^T$ be the ith row of $\boldsymbol{Z}_P$. Then

$$\begin{aligned}
&\left\| S(\boldsymbol{\tau})^{-1} \boldsymbol{Z}^T (\boldsymbol{I} - \boldsymbol{P}_X) \boldsymbol{l} \right\| = \left\| \left(\boldsymbol{Z}_P^T \boldsymbol{Z}_P + \boldsymbol{D}(\boldsymbol{\tau}) \right)^{-1} \boldsymbol{Z}_P^T \boldsymbol{l} \right\| \\
&= \left\| \sum_{i=1}^n \left(\boldsymbol{Z}_P^T \boldsymbol{Z}_P + \boldsymbol{D}(\boldsymbol{\tau}) \right)^{-1} \boldsymbol{z}_{Pi} l_i \right\| \leq \sum_{i=1}^n \left\| \left(\boldsymbol{Z}_P^T \boldsymbol{Z}_P + \boldsymbol{D}(\boldsymbol{\tau}) \right)^{-1} \boldsymbol{z}_{Pi} l_i \right\| \\
&= \sum_{i=1}^n \left\| \left(\sum_{k=1}^n \boldsymbol{z}_{Pk} \boldsymbol{z}_{Pk}^T + \boldsymbol{D}(\boldsymbol{\tau}) \right)^{-1} \boldsymbol{z}_{Pi} l_i \right\| \leq \sum_{i=1}^n |l_i| \, \varphi_i (\boldsymbol{\tau}) ,
\end{aligned}$$

where

$$\varphi_i^2 (\boldsymbol{\tau}) = \boldsymbol{z}_{Pi}^T \left(\boldsymbol{z}_{Pi} \boldsymbol{z}_{Pi}^T + \sum_{k \in \{1, \ldots, n\} \setminus \{i\}} \boldsymbol{z}_{Pk} \boldsymbol{z}_{Pk}^T + \boldsymbol{D}(\boldsymbol{\tau}) \right)^{-2} \boldsymbol{z}_{Pi} .$$

Note that for fixed $i \in \{1, 2 \ldots, n\}$,

$$\begin{aligned}
\varphi_i^2(\boldsymbol{\tau}) &= \boldsymbol{z}_{Pi}^T \left(\boldsymbol{z}_{Pi}\boldsymbol{z}_{Pi}^T + \sum_{k \in \{1,\ldots,n\}\setminus\{i\}} \boldsymbol{z}_{Pk}\boldsymbol{z}_{Pk}^T + \boldsymbol{D}(\boldsymbol{\tau}) - \frac{1}{\sum_{j=1}^r 1/\tau_j}\boldsymbol{I}_q + \frac{1}{\sum_{j=1}^r 1/\tau_j}\boldsymbol{I}_q \right)^{-2} \boldsymbol{z}_{Pi} \\
&\leq \sup_{\boldsymbol{\iota} \in \mathbb{R}_+^{n+q}} t_i^T \left(t_i t_i^T + \sum_{k \in \{1,\ldots n\}\setminus\{i\}} \iota_k t_k t_k^T + \sum_{k=n+1}^{n+q} \iota_k t_k t_k^T + \iota_1 \boldsymbol{I}_q \right)^{-2} t_i \\
&\equiv \hat{\varphi}_i^2,
\end{aligned}$$

where $\boldsymbol{\iota} = (\iota_1, \iota_2, \ldots, \iota_{n+q})$, $t_k = \boldsymbol{z}_{Pk}$ for $k \in \{1, \ldots, n\}$ and for $k = n+1, \ldots, n+q$, define t_k to be a $q \times 1$ unit vector with 1 on the $(k-n)$th position, 0 elsewhere. The inequality follows from the fact that $\sum_{j=1}^r 1/\tau_j > 1/\tau_j$. By Lemma 3 in Román and Hobert (2012), we know that $\hat{\varphi}_i^2$ is finite. Let $\hat{\varphi} = \max_{1 \leq i \leq n} \hat{\varphi}_i$, then

$$\left\| S(\boldsymbol{\tau})^{-1} \boldsymbol{Z}^T (\boldsymbol{I} - \boldsymbol{P}_X) \boldsymbol{l} \right\| \leq \sum_{i=1}^n |l_i| \hat{\varphi}_i \leq \hat{\varphi} \sum_{i=1}^n |l_i| .$$

□

C Proof of Theorem 2

The two-block Gibbs sampler $\{\boldsymbol{\eta}^{(m)}, (\boldsymbol{v}^{(m)}, \boldsymbol{\tau}^{(m)})\}_{m=0}^{\infty}$ in Algorithm 4.3 has the same rate of convergence as its two marginal chains, namely, the $\boldsymbol{\eta}$-chain and the $(\boldsymbol{v}, \boldsymbol{\tau})$-chain. Here as in the proof of Theorem 4.1, we work with the $\boldsymbol{\eta}$-chain, denoted as $\boldsymbol{\Psi}^* = \{\boldsymbol{\eta}^{(m)}\}_{m=0}^{\infty}$ and establish its geometric rate of convergence. Define $A \equiv \{j \in \{1, \ldots, r\} : b_j = 0\}$. Recall that given $\boldsymbol{\eta}$, the conditional distribution of $\boldsymbol{\tau}$ is given by independent Gamma$(a_j + q_j/2, b_j + \boldsymbol{u}_j^T \boldsymbol{u}_j/2)$, $j = 1, \ldots, r$, which is not defined when A is not empty and $\boldsymbol{\eta} \in \mathcal{N} = \left\{ \boldsymbol{\eta} \in \mathbb{R}^{p+q}; \prod_{j \in A} ||\boldsymbol{u}_j|| = 0 \right\}$. Since $\mathcal{N}$ is a set of measure zero, simulation of the Gibbs sampler is not affected by the fact that $\pi(\boldsymbol{\tau}|\boldsymbol{\eta}, \boldsymbol{y})$ is not defined on $\mathcal{N}$. But as mentioned in Román and Hobert (2012), for a theoretical analysis of the $\boldsymbol{\eta}$-chain, the Mtd of $\boldsymbol{\Psi}^*$ and hence $\pi(\boldsymbol{\tau}|\boldsymbol{\eta}, \boldsymbol{y})$ must be defined for *all* $\boldsymbol{\eta} \in \mathbb{R}^{p+q}$. Since $\mathcal{N}$ is a measure zero set, the Mtd of $\boldsymbol{\Psi}^*$ hence $\pi(\boldsymbol{\tau}|\boldsymbol{\eta}, \boldsymbol{y})$ can be defined arbitrarily on $\mathcal{N}$. If A is not empty

for all $\boldsymbol{\eta} \in \mathbb{R}^{p+q}$, we define $\pi(\boldsymbol{\tau}|\boldsymbol{\eta}, \boldsymbol{y})$ as follows,

$$\pi\left(\boldsymbol{\tau}|\boldsymbol{\eta}, \boldsymbol{y}\right) = \begin{cases} \prod_{j=1}^{r} f_G\left(\tau_j, \frac{q_j}{2} + a_j, \frac{\boldsymbol{u}_j^T \boldsymbol{u}_j}{2} + b_j\right) & \text{if } \boldsymbol{\eta} \notin \mathcal{N} \\ \prod_{j=1}^{r} f_G\left(\tau_j, 1, 1\right) & \text{if } \boldsymbol{\eta} \in \mathcal{N} \end{cases},$$

where f_G stands for the density of a Gamma random variable.

We denote the $\{\boldsymbol{\eta}^{(m)}\}_{m=0}^{\infty}$ Markov chain defined on $\mathbb{R}^{p+q}\backslash\mathcal{N}$ as $\tilde{\boldsymbol{\Psi}}^*$. The chain $\tilde{\boldsymbol{\Psi}}^*$ is Harris ergodic on $\mathbb{R}^{p+q}\backslash\mathcal{N}$. Our proof of geometric ergodicity of $\boldsymbol{\Psi}^*$ is through that of $\tilde{\boldsymbol{\Psi}}^*$. The following proof establishes the geometric ergodicity of $\tilde{\boldsymbol{\Psi}}^*$.

Proof. We prove the geometric ergodicity of $\tilde{\boldsymbol{\Psi}}^*$ by establishing a drift function, which has the following form,

$$V\left(\boldsymbol{\eta}\right) = \sum_{i=1}^{n} \left(\boldsymbol{x}_i^T \boldsymbol{\beta} + \boldsymbol{z}_i^T \boldsymbol{u}\right)^2 + \sum_{j=1}^{r} \left(\boldsymbol{u}_j^T \boldsymbol{u}_j\right)^{-c}, \tag{4.43}$$

where $c \in (0, 1/2)$ is a positive constant. Note that, since the condition A1 is in force, $V\left(\boldsymbol{\eta}\right) : \mathbb{R}^{p+q}\backslash\mathcal{N} \to [0, \infty)$ is unbounded off compact sets. We show that for any $\boldsymbol{\eta}, \boldsymbol{\eta}' \in \mathbb{R}^{p+q}\backslash\mathcal{N}$, there exists $\rho_1 \in [0, 1)$ and $L_1 > 0$ such that

$$E[V\left(\boldsymbol{\eta}\right)|\boldsymbol{\eta}'] \leq \rho_1 V(\boldsymbol{\eta}') + L_1. \tag{4.44}$$

The expectation on the left hand side of (4.44) can be evaluated using two steps by Fubini's theorem. First, we calculate the expectation with respect to the conditional distribution of $\boldsymbol{\eta}$ given $\boldsymbol{v}$, $\boldsymbol{\tau}$ and $\boldsymbol{y}$, that is $E[V(\boldsymbol{\eta})|\boldsymbol{v}, \boldsymbol{\tau}, \boldsymbol{y}]$.

From (4.40) and (4.41), we have $\boldsymbol{W}\boldsymbol{\Sigma}^{*-1}\boldsymbol{W}^T = P_X + \left(\boldsymbol{I} - P_X\right)\boldsymbol{Z}S(\boldsymbol{\tau})^{-1}\boldsymbol{Z}^T\left(\boldsymbol{I} - P_X\right)$. Also $\left(\boldsymbol{I} - P_X\right) = \left(\boldsymbol{I} - P_X\right)^2$. Let $\tilde{P} = \left(\boldsymbol{I} - P_X\right)\boldsymbol{Z}\boldsymbol{D}(\boldsymbol{\tau})^{-1/2}$, then

$$\begin{aligned} \left(\boldsymbol{I} - P_X\right)\boldsymbol{Z}S(\boldsymbol{\tau})^{-1}\boldsymbol{Z}^T\left(\boldsymbol{I} - P_X\right) &= \left(\boldsymbol{I} - P_X\right)^2\boldsymbol{Z}S(\boldsymbol{\tau})^{-1}\boldsymbol{Z}^T\left(\boldsymbol{I} - P_X\right)^2 \\ &= \left(\boldsymbol{I} - P_X\right)\tilde{P}\left(\tilde{P}^T\tilde{P} + \boldsymbol{I}\right)^{-1}\tilde{P}^T\left(\boldsymbol{I} - P_X\right) \preceq \boldsymbol{I} - P_X. \end{aligned}$$

Thus, $\boldsymbol{W}\boldsymbol{\Sigma}^{*-1}\boldsymbol{W}^T \preceq P_X + \boldsymbol{I} - P_X = \boldsymbol{I}$. From (4.22) and (4.23), it follows that

$$\begin{aligned} E\left[\sum_{i=1}^{n}\left(\boldsymbol{x}_i^T\boldsymbol{\beta} + \boldsymbol{z}_i^T\boldsymbol{u}\right)^2|\boldsymbol{v}, \boldsymbol{\tau}, \boldsymbol{y}\right] &\leq E\left[\boldsymbol{\eta}^T\boldsymbol{\Sigma}^*\boldsymbol{\eta}|\boldsymbol{\tau}, \boldsymbol{v}, \boldsymbol{y}\right] \\ = p + q + \boldsymbol{v}\boldsymbol{W}\boldsymbol{\Sigma}^{*-1}\boldsymbol{W}^T\boldsymbol{v} &\leq p + q + \boldsymbol{v}^T\boldsymbol{v}. \end{aligned} \tag{4.45}$$

According to Román and Hobert (2012), for $c \in (0, 1/2)$ we have

$$E\left[\left(\boldsymbol{u}_j^T \boldsymbol{u}_j\right)^{-c} | \boldsymbol{v}, \boldsymbol{\tau}, \boldsymbol{y}\right] \leq 2^{-c} \frac{\Gamma\left(q_j/2 - c\right)}{\Gamma\left(q_j/2\right)} \left[\lambda_p^c + \tau_j^c\right], \tag{4.46}$$

where λ_p is the largest eigenvalue of $\boldsymbol{Z}^T(\boldsymbol{I} - P_{\boldsymbol{X}})\boldsymbol{Z}$. Using (4.45) and (4.46) from (4.43), we have

$$E\left[V\left(\boldsymbol{\eta}\right) | \boldsymbol{\tau}, \boldsymbol{v}, \boldsymbol{y}\right] \leq \ \boldsymbol{v}^T \boldsymbol{v} + 2^{-c} \sum_{j=1}^{r} \frac{\Gamma\left(q_j/2 - c\right)}{\Gamma\left(q_j/2\right)} \tau_j^c + 2^{-c} \sum_{j=1}^{r} \frac{\Gamma\left(q_j/2 - c\right)}{\Gamma\left(q_j/2\right)} \lambda_p^c + p + q. \tag{4.47}$$

Now we consider the expectation corresponding to the conditional distribution of $\boldsymbol{v}$ and $\boldsymbol{\tau}$ given $\boldsymbol{\eta}'$ and $\boldsymbol{y}$.

We use $A_1, \ldots, A_{2^n}$ to denote all the subsets of $\mathbb{N}_n = \{1, 2 \ldots, n\}$. Following Roy and Hobert (2007), let

$$S_j = \left\{\boldsymbol{\eta}' \in \mathbb{R}^{p+q} \backslash \{\boldsymbol{0}\} : \boldsymbol{w}_i^T \boldsymbol{\eta}' \leq 0 \text{ for all } i \in A_j \text{ and } \boldsymbol{w}_i^T \boldsymbol{\eta}' > 0 \text{ for all } i \in \bar{A}_j\right\},$$

where $\bar{A}_j$ is the complement of A_j. As mentioned in Roy and Hobert (2007), the sets S_j's are disjoint, $\cup_{j=1}^{2^n} S_j = \mathbb{R}^{p+q} \backslash \{\boldsymbol{0}\}$ and some of the S_j's may be empty. For $j \in C \equiv \{i \in \mathbb{N}_{2^n} : S_i \neq \emptyset\}$, define

$$R_j\left(\boldsymbol{\eta}'\right) = \frac{\sum_{i \in A_j} \left(\boldsymbol{w}_i^{*T} \boldsymbol{\eta}'\right)^2}{\sum_{i=1}^{n} \left(\boldsymbol{w}_i^{*T} \boldsymbol{\eta}'\right)^2} = \frac{\sum_{i \in A_j} \left(\boldsymbol{w}_i^{*T} \boldsymbol{\eta}'\right)^2}{\sum_{i \in A_j} \left(\boldsymbol{w}_i^{*T} \boldsymbol{\eta}'\right)^2 + \sum_{i \in \bar{A}_j} \left(\boldsymbol{w}_i^{*T} \boldsymbol{\eta}'\right)^2}.$$

where $\boldsymbol{w}_i^*$'s are defined in the proof of Theorem 1. By (4.38), for $\boldsymbol{\eta} \in S_j$, $j \in C$, we have

$$\begin{aligned}
E\left[\sum_{i=1}^{n} v_i^2 | \boldsymbol{\eta}', \boldsymbol{y}\right] &= n + \sum_{i=1}^{n} \left(\boldsymbol{w}_i^{*T} \boldsymbol{\eta}'\right)^2 - \sum_{i \in A_j} \frac{\left(\boldsymbol{w}_i^{*T} \boldsymbol{\eta}'\right) \phi\left(\boldsymbol{w}_i^{*T} \boldsymbol{\eta}'\right)}{1 - \Phi\left(\boldsymbol{w}_i^{*T} \boldsymbol{\eta}'\right)} - \sum_{i \in \bar{A}_j} \frac{\left(\boldsymbol{w}_i^{*T} \boldsymbol{\eta}'\right) \phi\left(\boldsymbol{w}_i^{*T} \boldsymbol{\eta}'\right)}{1 - \Phi\left(\boldsymbol{w}_i^{*T} \boldsymbol{\eta}'\right)} \\
&= n + \sum_{i=1}^{n} \left(\boldsymbol{w}_i^{*T} \boldsymbol{\eta}'\right)^2 + \sum_{i \in A_j} \left| \frac{\left(\boldsymbol{w}_i^{*T} \boldsymbol{\eta}'\right) \phi\left(\boldsymbol{w}_i^{*T} \boldsymbol{\eta}'\right)}{1 - \Phi\left(\boldsymbol{w}_i^{*T} \boldsymbol{\eta}'\right)} \right| - \sum_{i \in \bar{A}_j} \frac{\left(\boldsymbol{w}_i^{*T} \boldsymbol{\eta}'\right) \phi\left(\boldsymbol{w}_i^{*T} \boldsymbol{\eta}'\right)}{1 - \Phi\left(\boldsymbol{w}_i^{*T} \boldsymbol{\eta}'\right)} \\
&\leq n + \sum_{i=1}^{n} \left(\boldsymbol{w}_i^{*T} \boldsymbol{\eta}'\right)^2 + n\Xi - \sum_{i \in \bar{A}_j} \left(\boldsymbol{w}_i^{*T} \boldsymbol{\eta}'\right)^2 \\
&= n\left(1 + \Xi\right) + R_j\left(\boldsymbol{\eta}'\right) \sum_{i=1}^{n} \left(\boldsymbol{w}_i^{*T} \boldsymbol{\eta}'\right)^2,
\end{aligned}$$

where Ξ is defined in (4.39) and the inequality is due to the fact that $u\phi\left(u\right) / \left[1 - \Phi\left(u\right)\right] \geq u^2$ for $u \geq 0$. Define $\lambda_j = \sup_{\boldsymbol{\eta}' \in S_j} \left\{R_j\left(\boldsymbol{\eta}'\right)\right\} \in [0, 1]$ and

$$\lambda_0 = \max_{j \in C} \lambda_j.$$

If $\boldsymbol{\eta}' = \mathbf{0}$, from (4.38), we have $E\left[\sum_{i=1}^{n} v_i^2 | \boldsymbol{\eta}', \boldsymbol{y}\right] = n$. Thus, for all $\boldsymbol{\eta}' \in \mathbb{R}^{p+q}$,

$$E\left[\sum_{i=1}^{n} v_i^2 | \boldsymbol{\eta}', \boldsymbol{y}\right] \leq \lambda_0 \sum_{i=1}^{n} \left(\boldsymbol{x}_i^T \boldsymbol{\beta}' + \boldsymbol{z}_i^T \boldsymbol{u}'\right)^2 + n\left(1 + \Xi\right). \tag{4.48}$$

Since conditions A1 and A2 are in force, using the techniques in Roy and Hobert (2007), it can be shown that $\lambda_0 < 1$.

For $c \in (0, 1/2)$, define

$$G_j(-c) = 2^c \frac{\Gamma(q_j/2 + a_j + c)}{\Gamma(q_j/2 + a_j)} \text{ for } j = 1, \ldots, r. \tag{4.49}$$

Since $\tau_j | \boldsymbol{\eta}', \boldsymbol{y} \sim \text{Gamma}(a_j + q_j/2, b_j + \boldsymbol{u}_j'^T \boldsymbol{u}_j'/2)$,

$$\begin{aligned} E\left[\tau_j^c | \boldsymbol{u}_j', \boldsymbol{y}\right] &= 2^{-c} G_j\left(-c\right) \left[b_j + \frac{\boldsymbol{u}_j'^T \boldsymbol{u}_j'}{2}\right]^{-c} \\ &\leq G_j\left(-c\right) \left[\left(2b_j\right)^{-c} I_{(0,\infty)}\left(b_j\right) + \left(\boldsymbol{u}_j'^T \boldsymbol{u}_j'\right)^{-c} I_{\{0\}}\left(b_j\right)\right]. \end{aligned} \tag{4.50}$$

Recall that $A = \{j \in \{1, 2, \ldots, r\} : b_j = 0\}$. We consider two cases, namely, when A is empty and A is not empty.

Case 1: A is not empty.

Then using (4.48) and (4.50), from (4.47) we have

$$E\left[V\left(\boldsymbol{\eta}\right) | \boldsymbol{\eta}'\right] \leq \lambda_0 \sum_{i=1}^{n} \left(\boldsymbol{x}_i^T \boldsymbol{\beta}' + \boldsymbol{z}_i^T \boldsymbol{u}'\right)^2 + \delta_1\left(c\right) \sum_{j \in A} \left(\boldsymbol{u}_j'^T \boldsymbol{u}_j'\right)^{-c} + L_1\left(c\right),$$

where

$$\begin{aligned} \delta_1\left(c\right) &\equiv 2^{-c} \max_{j \in A} G_j\left(-c\right) \frac{\Gamma\left(q_j/2 - c\right)}{\Gamma\left(q_j/2\right)}, \\ L_1\left(c\right) &\equiv n(1 + \Lambda) + p + q + 2^{-c} \lambda_p^c \sum_{j=1}^{r} \frac{\Gamma\left(q_j/2 - c\right)}{\Gamma\left(q_j/2\right)} + 2^{-c} \sum_{j \notin A} G_j\left(-c\right) \frac{\Gamma\left(q_j/2 - c\right)}{\Gamma\left(q_j/2\right)} \left(2b_j\right)^{-c}. \end{aligned} \tag{4.51}$$

By Román and Hobert (2012), there exists $c \in C_1 = (0, 1/2) \cap (0, -\max_{j \in A} a_j)$ such that $\delta_1(c) < 1$. Thus, taking $\rho_1 = \max(\lambda_0, \delta_1(c))$, and $L_1 = L_1(c)$, we have

$$E\left[V\left(\boldsymbol{\eta}\right) | \boldsymbol{\eta}'\right] \leq \rho_1 V\left(\boldsymbol{\eta}'\right) + L_1.$$

Case 2: A is empty.

In this case, the conditional expectation of τ_j^c can be bounded by a constant. Indeed from (4.50) we have

$$E\left[\tau_j^c|\boldsymbol{u}_j', \boldsymbol{y}\right] = 2^{-c}G_j\left(-c\right)\left[b_j + \frac{\boldsymbol{u}_j'^T\boldsymbol{u}_j'}{2}\right]^{-c} \leq G_j\left(-c\right)\left(2b_j\right)^{-c}.$$

Thus when A is empty, we have

$$E\left[V\left(\boldsymbol{\eta}\right)|\boldsymbol{\eta}'\right] \leq \lambda_0 \sum_{i=1}^{n}\left(\boldsymbol{x}_i^T\boldsymbol{\beta}' + \boldsymbol{z}_i^T\boldsymbol{u}'\right)^2 + L_1(c) \leq \lambda_0 V\left(\boldsymbol{\eta}'\right) + L_1(c).$$

Hence in both cases, (4.44) holds. Since $\tau_j|\boldsymbol{\eta}', \boldsymbol{y} \sim \text{Gamma}(a_j+q_j/2, b_j+\boldsymbol{u}_j'^T\boldsymbol{u}_j'/2)$ and condition A3 holds, for all $\boldsymbol{\eta}' \in \mathbb{R}^{p+q}\backslash\mathcal{N}$ the conditional distribution of τ_j is a Gamma distribution with positive shape and scale parameters even if $b_j = 0$. Hence as in the proof of Theorem 1, it follows that, the $\boldsymbol{\eta}$-chain is a Feller chain on $\mathbb{R}^{p+q}\backslash\mathcal{N}$. Thus (4.44) implies that $\boldsymbol{\eta}$-chain is geometrically ergodic on $\mathbb{R}^{p+q}\backslash\mathcal{N}$.

Next, we need to show that the original Markov chain $\boldsymbol{\Psi}^*$ is geometrically ergodic. The techniques of Lemma 12 in Román (2012) can be applied here for this purpose.

Let M and $\tilde{M}$ be the Mtfs of $\boldsymbol{\Psi}^*$ and $\tilde{\boldsymbol{\Psi}}^*$ respectively. Also, let M^m and $\tilde{M}^m$ be the corresponding m-step Mtfs, and $\mathsf{X} \equiv \mathbb{R}^{p+q}$, $\tilde{\mathsf{X}} \equiv \mathbb{R}^{p+q}\backslash\mathcal{N}$. Recall that $\mathscr{B}$ denotes the Borel σ-algebra of $\mathbb{R}^{p+q}$. Since the Lebesgue measure of $\mathcal{N}$ is 0, for any $\mathsf{x} \in \tilde{\mathsf{X}}$ and $\mathsf{B} \in \mathcal{B}_{\tilde{\mathsf{X}}} = \{\tilde{\mathsf{X}} \cap \mathsf{A} : \mathsf{A} \in \mathscr{B}\}$

$$\tilde{M}(\mathsf{x}, \mathsf{B}) = M(\mathsf{x}, \mathsf{B}).$$

Let μ and $\tilde{\mu}$ be the Lebesgue measures on X and $\tilde{\mathsf{X}}$ respectively. Then $\boldsymbol{\Psi}^*$ and $\tilde{\boldsymbol{\Psi}}^*$ are μ-irreducible and $\tilde{\mu}$-irreducible respectively. Also, μ and $\tilde{\mu}$ are the corresponding maximal irreducibility measures. These two Markov chains $\boldsymbol{\Psi}^*$ and $\tilde{\boldsymbol{\Psi}}^*$ are also aperiodic. According to Theorem 15.0.1 in Meyn and Tweedie (1993), there exists a ν-petite set $\mathsf{C} \in \mathcal{B}_{\tilde{\mathsf{X}}}$, $\rho_{\mathsf{C}} < 1$, $M_{\mathsf{C}} < \infty$, a number $\tilde{M}^{\infty}(\mathsf{C})$ such that $\tilde{\mu}(\mathsf{C}) > 0$ and

$$|\tilde{M}^m(\mathsf{x}, \mathsf{C}) - \tilde{M}^{\infty}(\mathsf{C})| < M_{\mathsf{C}}\rho_{\mathsf{C}}^m,$$

for all $\mathsf{x} \in \mathsf{C}$. Since the set C is a ν-petite set for $\tilde{\mathsf{X}}$, ν is a nontrivial measure on $\mathcal{B}_{\tilde{\mathsf{X}}}$ with,

$$\sum_{m=0}^{\infty} \tilde{M}^m(\mathsf{x}, \mathsf{B})\tilde{a}(m) \geq \nu(\mathsf{B})$$

for all $\mathsf{x} \in \mathsf{C}$ and $\mathsf{B} \in \mathcal{B}_{\tilde{\mathsf{X}}}$, where $\tilde{a}(m)$ is a mass function on $\{0, 1, 2, \ldots, \}$.

Since $\tilde{M}^m(\mathsf{x}, \mathsf{B}) = M^m(\mathsf{x}, \mathsf{B})$ for any $\mathsf{x} \in \tilde{\mathsf{X}}$ and $\mathsf{B} \in \mathcal{B}_{\tilde{\mathsf{X}}}$, we have $M^m(\mathsf{x}, \mathsf{C}) = \tilde{M}^m(\mathsf{x}, \mathsf{C})$. So for all $x \in \mathsf{C}$

$$|M^m(\mathsf{x}, \mathsf{C}) - \tilde{M}^\infty(\mathsf{C})| < M_{\mathsf{C}} \rho_{\mathsf{C}}^m.$$

Also, since $\mu(\mathcal{N}) = 0$, we know that $\mu(\mathsf{C}) > 0$. It can be checked that C is also petite for the original Markov chain $\mathbf{\Psi}^*$. Thus from Theorem 15.0.1 of Meyn and Tweedie (1993), it follows that $\mathbf{\Psi}^*$ is geometrically ergodic. □

D Proof of Theorem 3

Proof. Using the transformation $(\boldsymbol{\beta}^T, \boldsymbol{u}^T)^T \to (u_{11}, \ldots, u_{r1}, \tilde{\boldsymbol{\eta}}^T)^T$, the integral in (4.27) can be written as,

$$\begin{aligned} &\int_{\mathbb{R}^{p+q-r}} \int_{\mathbb{R}_+^r} \int_{\mathbb{R}^r} \prod_{i=1}^n \Phi\left(\tilde{\boldsymbol{w}}_i^T \tilde{\boldsymbol{\eta}}\right)^{y_i} \left[1 - \Phi\left(\tilde{\boldsymbol{w}}_i^T \tilde{\boldsymbol{\eta}}\right)\right]^{1-y_i} \\ &\prod_{j=1}^r \tau_j^{\frac{q_j}{2}+a_j-1} \exp\left[-\frac{\tau_j}{2}\left(u_{j1}^2 + \sum_{k=1}^{q_j-1}(d_{jk}+u_{j1})^2 + 2b_j\right)\right] du_{11}\cdots du_{r1} d\boldsymbol{\tau} d\tilde{\boldsymbol{\eta}}, \end{aligned} \tag{4.52}$$

where $\tilde{\boldsymbol{w}}_i$ is defined in section 4.3.1. Let $\bar{d}_j = \sum_{k=1}^{q_j-1} d_{jk}$. Then (4.52) becomes,

$$\begin{aligned} &\int_{\mathbb{R}^{p+q-r}} \int_{\mathbb{R}_+^r} \prod_{i=1}^n \Phi\left(\tilde{\boldsymbol{w}}_i^T \tilde{\boldsymbol{\eta}}\right)^{y_i} \left[1 - \Phi\left(\tilde{\boldsymbol{w}}_i^T \tilde{\boldsymbol{\eta}}\right)\right]^{1-y_i} \\ &\cdot (2\pi)^{\frac{r}{2}} \prod_{j=1}^r q_j^{-1/2} \tau_j^{\frac{q_j}{2}+a_j-\frac{3}{2}} \exp\left[-\frac{\tau_j}{2}\left(\sum_{k=1}^{q_j-1}\left(d_{jk}-\bar{d}_j\right)^2 + \frac{q_j-1}{q_j}\bar{d}_j^2 + 2b_j\right)\right] d\boldsymbol{\tau} d\tilde{\boldsymbol{\eta}} \\ =&\int_{\mathbb{R}^{p+q-r}} \prod_{i=1}^n \Phi\left(\tilde{\boldsymbol{w}}_i^T \tilde{\boldsymbol{\eta}}\right)^{y_i} \left[1 - \Phi\left(\tilde{\boldsymbol{w}}_i^T \tilde{\boldsymbol{\eta}}\right)\right]^{1-y_i} \\ &\cdot (2\pi)^{\frac{r}{2}} \prod_{j=1}^r q_j^{-1/2} \Gamma\left(q_j/2 + a_j - 1/2\right) 2^{\frac{q_j}{2}+a_j-\frac{1}{2}} \left(\sum_{k=1}^{q_j-1}\left(d_{jk}-\bar{d}_j\right)^2 + \frac{q_j-1}{q_j}\bar{d}_j^2 + 2b_j\right)^{-\frac{q_j}{2}-a_j+\frac{1}{2}} d\tilde{\boldsymbol{\eta}} \\ \leq&\varphi_1 \int_{\mathbb{R}^{p+q-r}} \prod_{i=1}^n \Phi\left(\tilde{\boldsymbol{w}}_i^T \tilde{\boldsymbol{\eta}}\right)^{y_i} \left[1 - \Phi\left(\tilde{\boldsymbol{w}}_i^T \tilde{\boldsymbol{\eta}}\right)\right]^{1-y_i} \prod_{j=1}^r \left(\sum_{k=1}^{q_j-1}\left(d_{jk}-\bar{d}_j\right)^2 + \frac{q_j-1}{q_j}\bar{d}_j^2 + 2b_j\right)^{-\frac{q_j}{2}-a_j+\frac{1}{2}} d\tilde{\boldsymbol{\eta}}, \end{aligned} \tag{4.53}$$

where φ_1 is a constant depending on r, q_j and a_j, $j = 1, \ldots, r$.

Let $\delta_i, i = 1, \ldots, n$ be n i.i.d standard normal random variables. Let $\boldsymbol{\delta}^* = (c_1\delta_1, \ldots, c_n\delta_n)^T$, where $c_i = 1$ if $y_i = 0$ and $c_i = -1$ if $y_i = 1$. We have $E\left[1\left\{c_i\tilde{\boldsymbol{w}}_i^T\tilde{\boldsymbol{\eta}} \le c_i\delta_i\right\}\right] = \left[\Phi\left(\tilde{\boldsymbol{w}}_i^T\tilde{\boldsymbol{\eta}}\right)\right]^{y_i}\left[1 - \Phi\left(\tilde{\boldsymbol{w}}_i^T\tilde{\boldsymbol{\eta}}\right)\right]^{1-y_i}$, for $i = 1, \ldots, n$. Thus

$$\prod_{i=1}^{n}\Phi\left(\tilde{\boldsymbol{w}}_i^T\tilde{\boldsymbol{\eta}}\right)^{y_i}\left[1 - \Phi\left(\tilde{\boldsymbol{w}}_i^T\tilde{\boldsymbol{\eta}}\right)\right]^{1-y_i} = E\left[1\left\{\tilde{\boldsymbol{W}}^*\tilde{\boldsymbol{\eta}} \le \boldsymbol{\delta}^*\right\}\right], \tag{4.54}$$

where $\tilde{\boldsymbol{W}}^*$ is the $n \times (p+q)$ matrix whose ith row is $c_i\tilde{\boldsymbol{w}}_i^T$.

Since conditions B3 and B4 are in force, according to Chen and Shao (2001) (Lemma 4.1), there exists a constant φ_0 depending on $\tilde{\boldsymbol{W}}$ and $\boldsymbol{y}$, such that $1\left\{\tilde{\boldsymbol{W}}^*\tilde{\boldsymbol{\eta}} \le \boldsymbol{\delta}^*\right\} \le 1\left\{\|\tilde{\boldsymbol{\eta}}\| \le \varphi_0\|\boldsymbol{\delta}^*\|\right\}$. Recall that $\tilde{\boldsymbol{\eta}} = (\mu_0, \beta_1, \ldots, \beta_{p-1}, d_{11}, \ldots, d_{1,q_1-1}, \ldots, d_{r1}, \ldots, d_{r,q_r-1})^T = (\mu_0, \beta_1, \ldots, \beta_{p-1}, \boldsymbol{d}_1^T, \ldots, \boldsymbol{d}_r^T)^T$, where $\boldsymbol{d}_j = (d_{j1}, \ldots, d_{j,q_j-1})^T$ for $j = 1, \ldots, r$. Thus from (4.53) and (4.54) it follows that (4.52) is bounded above by

$$\begin{aligned}
&\varphi_1 E\left[\int_{\mathbb{R}^{p+q-r}} 1\left\{\|\tilde{\boldsymbol{\eta}}\| \le \varphi_0\|\boldsymbol{\delta}^*\|\right\}\prod_{j=1}^{r}\left(\sum_{k=1}^{q_j-1}\left(d_{jk} - \bar{d}_j\right)^2 + \frac{q_j-1}{q_j}\bar{d}_j^2 + 2b_j\right)^{-\frac{q_j}{2}-a_j+\frac{1}{2}} d\tilde{\boldsymbol{\eta}}\right] \\
&\le 2^p\varphi_0^p\varphi_1 E\left[\|\boldsymbol{\delta}^*\|^p\int_{A_d}\prod_{j=1}^{r}\left(\sum_{k=1}^{q_j-1}\left(d_{jk} - \bar{d}_j\right)^2 + \frac{q_j-1}{q_j}\bar{d}_j^2 + 2b_j\right)^{-\frac{q_j}{2}-a_j+\frac{1}{2}} d\boldsymbol{d}_1\cdots, d\boldsymbol{d}_r\right] \\
&\le 2^p\varphi_0^p\varphi_1 E\left[\|\boldsymbol{\delta}^*\|^p\int_{A_d}\prod_{j=1}^{r}\left(\frac{q_j-1}{q_j}\bar{d}_j^2 + 2b_j\right)^{-\frac{q_j}{2}-a_j+\frac{1}{2}} d\boldsymbol{d}_1\cdots, d\boldsymbol{d}_r\right].
\end{aligned} \tag{4.55}$$

where $A_d = \{|d_{jk}| \le \varphi_0\|\boldsymbol{\delta}^*\|, j = 1, \ldots, r, k = 1, \ldots q_j - 1\}$.

We consider two cases of condition B1 separately.

Case 1: $a_j < b_j = 0$, $q_j \ge 2$. If $q_j = 2$, we have

$$\begin{aligned}
\int_{|d_{j1}|\le 1}\left[(d_{j1})^2\right]^{-a_j-\frac{1}{2}} dd_{j1} &= -\frac{1}{2a_j}\left[(d_{j1})^2\right]^{-a_j-\frac{1}{2}} d_{j1}\Big|_{-1}^{1} \\
&= -\frac{1}{2a_j}(1+1) = -\frac{1}{a_j} < \infty.
\end{aligned}$$

For $q_j > 2$, note that,

$$\int_{|d_{j1}|\le 1}\left[\left(\sum_{k=1}^{q_j-1} d_{jk}\right)^2\right]^{-\frac{q_j}{2}-a_j+\frac{1}{2}} dd_{j1} = \frac{1}{2-q_j-2a_j}\left[\left(\sum_{k=1}^{q_j-1} d_{jk}\right)^2\right]^{-\frac{q_j}{2}-a_j+\frac{1}{2}}\left(\sum_{k=1}^{q_j-1} d_{jk}\right)\Bigg|_{-1}^{1}$$

$$= \frac{1}{2-q_j-2a_j}\left[\left(1+\sum_{k=2}^{q_j-1} d_{jk}\right)^2\right]^{-\frac{q_j}{2}-a_j+\frac{1}{2}}\left(1+\sum_{k=2}^{q_j-1} d_{jk}\right)$$

$$- \frac{1}{2-q_j-2a_j}\left[\left(-1+\sum_{k=2}^{q_j-1} d_{jk}\right)^2\right]^{-\frac{q_j}{2}-a_j+\frac{1}{2}}\left(-1+\sum_{k=2}^{q_j-1} d_{jk}\right)$$

$$\le \frac{1}{2-q_j-2a_j}\left\{\left[\left(1+\sum_{k=2}^{q_j-1} d_{jk}\right)^2\right]^{-\frac{q_j}{2}-a_j+1} + \left[\left(-1+\sum_{k=2}^{q_j-1} d_{jk}\right)^2\right]^{-\frac{q_j}{2}-a_j+1}\right\}. \tag{4.56}$$

Ignoring the constant multiple, continuing integrating (4.56) with respect to $d_{j2},\ldots,d_{j,q_j-1}$ consecutively, we arrive at some linear combinations of terms

$$\left[\left(\alpha_0+d_{j,q_j-1}\right)^2\right]^{-\frac{q_j}{2}-a_j+\frac{q_j-1}{2}}\left(\alpha_0+d_{j,q_j-1}\right)\Big|_{-1}^{1}, \tag{4.57}$$

where α_0's are constants. Since $a_j < 0$, each of these terms in (4.57) is finite. Then

$$\int_{A_{dj}}\left(\frac{q_j-1}{q_j}\bar{d}_j^2+b_j\right)^{-\frac{q_j}{2}-a_j+\frac{1}{2}} d\boldsymbol{d}_j$$

$$= \left[q_j\left(q_j-1\right)\right]^{\frac{q_j}{2}+a_j-\frac{1}{2}}\left(\varphi_0\left\|\boldsymbol{\delta}^*\right\|\right)^{-2a_j}\int_{\{|d_{jk}|\le 1,k=1,\ldots,q_j-1\}}\left[\left(\sum_{k=1}^{q_j-1} d_{jk}\right)^2\right]^{-\frac{q_j}{2}-a_j+\frac{1}{2}} d\boldsymbol{d}_j$$

$$\le \varphi_{2j}\left\|\boldsymbol{\delta}^*\right\|^{-2a_j}, \tag{4.58}$$

where $A_{dj} = \{|d_{jk}| \le \varphi_0\|\boldsymbol{\delta}^*\|, k = 1,\ldots q_j-1\}$ and φ_{2j} is a finite positive constant.

Case 2: $b_j > 0$.

We have

$$\int_{A_{dj}}\left(\frac{q_j-1}{q_j}\bar{d}_j^2+2b_j\right)^{-\frac{q_j}{2}-a_j+\frac{1}{2}} d\boldsymbol{d}_j \le \int_{A_{dj}}(2b_j)^{-\frac{q_j}{2}-a_j+\frac{1}{2}} d\boldsymbol{d}_j$$

$$\le (2b_j)^{-\frac{q_j}{2}-a_j+\frac{1}{2}} 2^{q_j-1}\varphi_0^{q_j-1}\left\|\boldsymbol{\delta}^*\right\|^{q_j-1} \le \varphi_{3j}\left\|\boldsymbol{\delta}^*\right\|^{q_j-1}, \tag{4.59}$$

where φ_{3j} is a finite positive constant.

Using (4.58) and (4.59), it follows that (4.52) can be bounded above by

$$2^p\varphi_0^p\varphi_1 E\left[\|\boldsymbol{\delta}^*\|^p\prod_{j=1}^r\left\{\varphi_{2j}\|\boldsymbol{\delta}^*\|^{-2a_j}I(b_j=0)+\varphi_{3j}\|\boldsymbol{\delta}^*\|^{q_j-1}I(b_j>0)\right\}\right]$$
$$\leq 2^p\varphi_0^p\varphi_1\left[\prod_{j=1}^r\varphi_{2j}E\|\boldsymbol{\delta}^*\|^{p-2\sum_{j=1}^r a_j}I(b_j=0)+\prod_{j=1}^r\varphi_{3j}E\|\boldsymbol{\delta}^*\|^{p+q-r}I(b_j>0)\right]<\infty.$$

□

Remark .4. *If $q_j = 1$ and $b_j = 0$, (4.52) is ∞ since $\int_{\mathbb{R}_+}\tau_j^{q_j/2+a_j-3/2}d\tau_j=\infty$. If $b_j > 0$, the posterior density (4.21) can be proper even when $q_j = 1$.*

E Proof of Theorem 4

Proof. As in Appendix C, we study the convergence properties of the $\boldsymbol{\eta}$-chain. Recall that $\mathcal{N} = \left\{\boldsymbol{\eta}\in\mathbb{R}^{p+q};\prod_{j\in A}||\boldsymbol{u}_j||=0\right\}$. When A is nonempty and $\boldsymbol{\eta}\in\mathcal{N}$, we define the conditional distribution of $\boldsymbol{\tau}$ given $\boldsymbol{\eta},\boldsymbol{y}$ the same way as in Appendix C.

Consider the following drift function on $\mathbb{R}^{p+q}\backslash\mathcal{N}$,

$$V(\boldsymbol{\eta})=\alpha\sum_{i=1}^n\left(\boldsymbol{x}_i^T\boldsymbol{\beta}+\boldsymbol{z}_i^T\boldsymbol{u}\right)^2+\sum_{j=1}^r G_j(s)\left(\boldsymbol{u}_j^T\boldsymbol{u}_j\right)^s+\sum_{j=1}^r\left(\boldsymbol{u}_j^T\boldsymbol{u}_j\right)^{-c}.$$

where $G_j(\cdot)$ is defined in (4.49), α, $s\in\tilde{S}\equiv(0,1]\cap(0,\tilde{s})$ for $\tilde{s}$ defined in Theorem 4.4, and $c\in C_1=(0,1/2)\cap(0,-\max_{j\in A}a_j)$ are positive constants to be chosen later. We need to show that for any $\boldsymbol{\eta},\boldsymbol{\eta}'\in\mathbb{R}^{p+q}\backslash\mathcal{N}$, there exists a constant $\rho_2\in[0,1)$ and $L_2>0$ such that

$$E[V(\boldsymbol{\eta})|\boldsymbol{\eta}']=E\{E[V(\boldsymbol{\eta}|\boldsymbol{v},\boldsymbol{\tau},\boldsymbol{y})]|\boldsymbol{\eta}',\boldsymbol{y}\}\leq\rho_2V(\boldsymbol{\eta}')+L_2. \tag{4.60}$$

First, we calculate the expectation of $V(\boldsymbol{\eta})$ with respect to the $\boldsymbol{\eta}$ conditional distribution given $\boldsymbol{v},\boldsymbol{\tau}$ and $\boldsymbol{y}$. Same calculations as in the proof of Theorem 4.2 (see (4.45)) show that,

$$E\left[\sum_{i=1}^n\left(\boldsymbol{x}_i^T\boldsymbol{\beta}+\boldsymbol{z}_i^T\boldsymbol{u}\right)^2|\boldsymbol{v},\boldsymbol{\tau},\boldsymbol{y}\right]\leq p+q+\boldsymbol{v}^T\boldsymbol{v}. \tag{4.61}$$

For $s\in(0,1]$, by Jensen inequality,

$$E\left[\left(\boldsymbol{u}_j^T\boldsymbol{u}_j\right)^s|\boldsymbol{v},\boldsymbol{\tau},\boldsymbol{y}\right]\leq\left[E\left(\boldsymbol{u}_j^T\boldsymbol{u}_j|\boldsymbol{v},\boldsymbol{\tau},\boldsymbol{y}\right)\right]^s. \tag{4.62}$$

Also, from (4.22) and (4.23) it follows that

$$E\left(\boldsymbol{u}_j^T\boldsymbol{u}_j|\boldsymbol{v},\boldsymbol{\tau},\boldsymbol{y}\right)=tr\left(R_jS(\boldsymbol{\tau})^{-1}R_j\right)+\left[E\left(R_j\boldsymbol{u}|\boldsymbol{v},\boldsymbol{\tau},\boldsymbol{y}\right)\right]^T\left[E\left(R_j\boldsymbol{u}|\boldsymbol{v},\boldsymbol{\tau},\boldsymbol{y}\right)\right], \tag{4.63}$$

where R_j is defined in Lemma 4.1. For the first part on the right hand side of (4.63), we have

$$\begin{aligned} tr\left(R_jS(\boldsymbol{\tau})^{-1}R_j^T\right) &= tr\left[R_j\left(\boldsymbol{Z}^T\left(\boldsymbol{I}-P_X\right)\boldsymbol{Z}\right)^+R_j^T\right]+tr\left[R_j\left(\boldsymbol{I}-P_{\boldsymbol{Z}^T(\boldsymbol{I}-P_X)\boldsymbol{Z}}\right)R_j^T\right]\sum_{l=1}^r\tau_l^{-1} \\ &= \xi_j+\varsigma_j\sum_{l=1}^r\tau_l^{-1}, \end{aligned} \tag{4.64}$$

where $\xi_j=tr\left[R_j\left(\boldsymbol{Z}^T\left(\boldsymbol{I}-P_X\right)\boldsymbol{Z}\right)^+R_j^T\right]$ and $\varsigma_j=tr\left[R_j\left(\boldsymbol{I}-P_{\boldsymbol{Z}^T(\boldsymbol{I}-P_X)\boldsymbol{Z}}\right)R_j^T\right]$. For the second part, we have

$$\begin{aligned} \left[E\left(R_j\boldsymbol{u}|\boldsymbol{v},\boldsymbol{\tau},\boldsymbol{y}\right)\right]^T\left[E\left(R_j\boldsymbol{u}|\boldsymbol{v},\boldsymbol{\tau},\boldsymbol{y}\right)\right] &= \boldsymbol{v}^T\left(\boldsymbol{I}-P_X\right)\boldsymbol{Z}S(\boldsymbol{\tau})^{-1}R_j^TR_jS(\boldsymbol{\tau})^{-1}\boldsymbol{Z}^T\left(\boldsymbol{I}-P_X\right)\boldsymbol{v} \\ &\leq \boldsymbol{v}^T\left(\boldsymbol{I}-P_X\right)\boldsymbol{Z}S(\boldsymbol{\tau})^{-1}S(\boldsymbol{\tau})^{-1}\boldsymbol{Z}^T\left(\boldsymbol{I}-P_X\right)\boldsymbol{v} \\ &= \left\|S(\boldsymbol{\tau})^{-1}\boldsymbol{Z}^T\left(\boldsymbol{I}-P_X\right)\boldsymbol{v}\right\|^2 \\ &\leq \left(\hat{\varphi}\sum_{i=1}^n|v_i|\right)^2\leq\hat{\varphi}^2n\sum_{i=1}^nv_i^2, \end{aligned} \tag{4.65}$$

where the second inequality follows from Lemma 4.2 given in Appendix B. Combining (4.64) and (4.65), from (4.63) we have Then

$$\left[E\left(\boldsymbol{u}_j^T\boldsymbol{u}_j|\boldsymbol{v},\boldsymbol{\tau},\boldsymbol{y}\right)\right]^s\leq\left[\xi_j+\varsigma_j\sum_{j=1}^r\tau_j^{-1}+\hat{\varphi}^2n\sum_{i=1}^nv_i^2\right]^s\leq\xi_j^s+\varsigma_j^s\sum_{l=1}^r\tau_l^{-s}+\hat{\varphi}^{2s}n^s\sum_{i=1}^nv_i^{2s}.$$

Note that, if $v_i^2\leq1$, then $v_i^{2s}\leq1$, and if $v_i^{2s}>1$, then $v_i^{2s}<v_i^2$. So $v_i^{2s}\leq1+v_i^2$. Thus,

$$\left[E\left(\boldsymbol{u}_j^T\boldsymbol{u}_j|\boldsymbol{v},\boldsymbol{\tau},\boldsymbol{y}\right)\right]^s\leq\varsigma_j^s\sum_{l=1}^r\tau_l^{-s}+\hat{\varphi}^{2s}n^s\sum_{i=1}^nv_i^2+\hat{\varphi}^{2s}n^{1+s}+\xi_j^s. \tag{4.66}$$

Also recall from (4.46) that we also have,

$$E\left[\left(\boldsymbol{u}_j^T\boldsymbol{u}_j\right)^{-c}|\boldsymbol{v},\boldsymbol{\tau},\boldsymbol{y}\right]\leq2^{-c}\frac{\Gamma\left(q_j/2-c\right)}{\Gamma\left(q_j/2\right)}\left[\lambda_p^c+\tau_j^c\right].$$

Combining (4.46) , (4.61), (4.62) and (4.66) from (4.60) we have

$$E\left[V\left(\boldsymbol{\eta}\right)|\boldsymbol{v},\boldsymbol{\tau},\boldsymbol{y}\right]\leq\left(\alpha+\delta_2\left(s\right)\right)\sum_{i=1}^nv_i^2+\delta_3\left(s\right)\sum_{j=1}^r\tau_j^{-s}+2^{-c}\sum_{j=1}^r\frac{\Gamma\left(q_j/2-c\right)}{\Gamma\left(q_j/2\right)}\tau_j^c+\kappa_1\left(\alpha,s,c\right), \tag{4.67}$$

where

$$\delta_2(s) = \hat{\varphi}^{2s} n^s \sum_{j=1}^{r} G_j(s),$$

$$\delta_3(s) = \sum_{j=1}^{r} G_j(s) \varsigma_j^s, \text{ and}$$

$$\kappa_1(\alpha, s, c) = \alpha(p+q) + \sum_{j=1}^{r} G_j(s) \left(\hat{\varphi}^{2s} n^{1+s} + \xi_j^s\right) + 2^{-c} \lambda_p^c \sum_{j=1}^{r} \frac{\Gamma(q_j/2 - c)}{\Gamma(q_j/2)}.$$

Next we calculate the outer expectation in (4.60), that is, the expectation with respect to the conditional distribution of $\boldsymbol{v}$ and $\boldsymbol{\tau}$ given $\boldsymbol{\eta}'$ and $\boldsymbol{y}$.

When calculating the upper bound of $E(\sum_{i=1}^n v_i^2 | \boldsymbol{\eta}', \boldsymbol{y})$, we need to take into account the fact that $\boldsymbol{W}$ is not a full rank matrix in the current setting. But, $E(\sum_{i=1}^n v_i^2 | \boldsymbol{\eta}', \boldsymbol{y})$ can be written as,

$$E\left[\sum_{i=1}^{n} v_i^2 | \boldsymbol{\eta}', \boldsymbol{y}\right] = n + \sum_{i=1}^{n} \left(\tilde{\boldsymbol{w}}_i^{*T} \tilde{\boldsymbol{\eta}}'\right)^2 - \sum_{i=1}^{n} \frac{\left(\tilde{\boldsymbol{w}}_i^{*T} \tilde{\boldsymbol{\eta}}'\right) \phi\left(\tilde{\boldsymbol{w}}_i^{*T} \tilde{\boldsymbol{\eta}}'\right)}{1 - \Phi\left(\tilde{\boldsymbol{w}}_i^{*T} \tilde{\boldsymbol{\eta}}'\right)}.$$

where $\tilde{\boldsymbol{w}}_i^*$'s are defined in section 4.3.1.

Since the condition B3 is in force, we know that $\tilde{\boldsymbol{W}}$ is a full rank matrix. Then the same techniques (see (4.48)) as in the proof of Theorem 4.2 can be used to show that there exists $\lambda_0 \in [0, 1)$ such that

$$\begin{aligned} E\left[\sum_{i=1}^{n} v_i^2 | \boldsymbol{\eta}', \boldsymbol{y}\right] &\leq \lambda_0 \sum_{i=1}^{n} \left(\tilde{\boldsymbol{w}}_i^{*T} \tilde{\boldsymbol{\eta}}'\right)^2 + n(1 + \Xi) \\ &= \lambda_0 \sum_{i=1}^{n} \left(\boldsymbol{w}_i^T \boldsymbol{\eta}'\right)^2 + n(1 + \Xi) \\ &= \lambda_0 \sum_{i=1}^{n} \left(\boldsymbol{x}_i^T \boldsymbol{\beta}' + \boldsymbol{z}_i^T \boldsymbol{u}'\right)^2 + n(1 + \Xi). \end{aligned} \tag{4.68}$$

For $s \in \tilde{S}$, we have

$$E\left[\tau_j^{-s} | \boldsymbol{\eta}', \boldsymbol{y}\right] = 2^s G_j(s) \left(b_j + \frac{\boldsymbol{u}_j'^T \boldsymbol{u}_j'}{2}\right)^s \leq G_j(s) \left(\boldsymbol{u}_j'^T \boldsymbol{u}_j'\right)^s + 2^s G_j(s) b_j^s. \tag{4.69}$$

Also for $c \in C_1$ as in (4.50) we have

$$E\left[\tau_j^c | \boldsymbol{\eta}', \boldsymbol{y}\right] = 2^{-c} G_j(-c) \left[b_j + \frac{\boldsymbol{u}_j'^T \boldsymbol{u}_j'}{2}\right]^{-c} \leq G_j(-c) \left[(2b_j)^{-c} I_{(0,\infty)}(b_j) + \left(\boldsymbol{u}_j'^T \boldsymbol{u}_j'\right)^{-c} I_{\{0\}}(b_j)\right].$$

As in the proof of Theorem 4.2, we consider two cases, namely A is empty and A is not empty.

Case 1: A is not empty.

Using (4.50), (4.68) and (4.69) from (4.67), we have

$$E\left[V\left(\boldsymbol{\eta}\right)|\boldsymbol{\eta}'\right] = \alpha\lambda_0\left(1+\frac{\delta_2\left(s\right)}{\alpha}\right)\sum_{i=1}^{n}\left(\boldsymbol{x}_i^T\boldsymbol{\beta}'+\boldsymbol{z}_i^T\boldsymbol{u}'\right)^2+\delta_3\left(s\right)\sum_{j=1}^{r}G_j\left(s\right)\left(\boldsymbol{u}_j'^T\boldsymbol{u}_j'\right)^s$$
$$+\delta_1\left(c\right)\sum_{j\in A}\left(\boldsymbol{u}_j'^T\boldsymbol{u}_j'\right)^{-c}+L_2\left(\alpha,s,c\right), \tag{4.70}$$

where

$$L_2\left(\alpha,s,c\right)=\kappa_1\left(\alpha,s,c\right)+n\left(1+\Lambda\right)\left(\alpha+\delta_2\left(s\right)\right)+\delta_3\left(s\right)2^s\sum_{j=1}^{r}G_j\left(s\right)b_j^s$$
$$+2^{-c}\sum_{j\notin A}\frac{\Gamma\left(q_j/2-c\right)}{\Gamma\left(q_j/2\right)}G_j\left(-c\right)\left(2b_j\right)^{-c},$$

and $\delta_1(c)$ is defined as (4.51).

We know that for $c\in C_1$, $\delta_1(c)<1$ as in Theorem 4.2. Since condition 2 of Theorem 4.4 holds, we have $\delta_3(s)<1$. For a fixed s, $\lambda_0\left(1+\delta_2(s)/\alpha\right)<1$ iff $\alpha>\lambda_0\delta_2(s)/(1-\lambda_0)$. So there exists a $\rho_2\equiv\rho_2(\alpha,s,c)=\max\left\{\lambda_0\left(1+\delta_2(s)/\alpha\right),\delta_3(s),\delta_1(c)\right\}<1$ and $L_2\equiv L_2(\alpha,s,c)>0$ such that (4.60) holds.

Case 2: A is empty.

In this case, the conditional expectation of τ_j^c can be bounded by a constant. Thus we have

$$E\left[V\left(\boldsymbol{\eta}\right)|\boldsymbol{\eta}'\right] = \alpha\lambda_0\left(1+\frac{\delta_2\left(s\right)}{\alpha}\right)\sum_{i=1}^{n}\left(\boldsymbol{x}_i^T\boldsymbol{\beta}'+\boldsymbol{z}_i^T\boldsymbol{u}'\right)^2+\delta_3\left(s\right)\sum_{j=1}^{r}G_j\left(s\right)\left(\boldsymbol{u}_j'^T\boldsymbol{u}_j'\right)^s$$
$$+L_2\left(\alpha,s,c\right).$$

As in case 1, it follows that (4.60) holds.

Since $\boldsymbol{\eta}$-chain is a Feller chain on $\mathbb{R}^{p+q}\backslash\mathcal{N}$, and $V(\boldsymbol{\eta})$ is unbounded off compact sets on $\mathbb{R}^{p+q}\backslash\mathcal{N}$, the $\boldsymbol{\eta}$-chain is geometrically ergodic on $\mathbb{R}^{p+q}\backslash\mathcal{N}$. Using the same techniques as in Appendix C, it can be shown that the original $\{\boldsymbol{\eta}^{(m)}\}_{m=0}^{\infty}$ Markov chain defined on $\mathbb{R}^{p+q}$ is also geometrically ergodic. □

F The full Gibbs sampler

The difference between the full Gibbs sampler and the block Gibbs sampler developed in section 4.2.1 is that in the full Gibbs sampler, $\boldsymbol{\beta}$ and $\boldsymbol{u}$ are sampled sequentially instead of jointly in each iteration. The conditional distributions of $\boldsymbol{\beta}$ and $\boldsymbol{u}$ used in the full Gibbs sampler are

$$\boldsymbol{\beta}|\boldsymbol{u},\boldsymbol{\tau},\boldsymbol{v},\boldsymbol{y} \sim N\left(\left(\boldsymbol{X}^T\boldsymbol{X}+\boldsymbol{Q}\right)^{-1}\left(\boldsymbol{X}^T\left(\boldsymbol{v}-\boldsymbol{Z}\boldsymbol{u}\right)+\boldsymbol{\mu}_0\right),\left(\boldsymbol{X}^T\boldsymbol{X}+\boldsymbol{Q}\right)^{-1}\right),$$

and

$$\boldsymbol{u}|\boldsymbol{\beta},\boldsymbol{\tau},\boldsymbol{v},\boldsymbol{y} \sim N\left(\left(\boldsymbol{Z}^T\boldsymbol{Z}+\boldsymbol{D}\left(\boldsymbol{\tau}\right)\right)^{-1}\boldsymbol{Z}^T\left(\boldsymbol{v}-\boldsymbol{X}\boldsymbol{\beta}\right),\left(\boldsymbol{Z}^T\boldsymbol{Z}+\boldsymbol{D}\left(\boldsymbol{\tau}\right)\right)^{-1}\right).$$

The conditional distributions of $\boldsymbol{v}$ and $\boldsymbol{\tau}$ are the same as derived in section 4.2.1 for the block Gibbs sampler.

Bibliography

Albert, J. H. and Chib, S. (1993). Bayesian analysis of binary and polychotomous response data. *Journal of the American statistical Association*, 88(422):669–679.

Asmussen, S. and Glynn, P. W. (2011). A new proof of convergence of MCMC via the ergodic theorem. *Statistics and Probability Letters*, 81:1482–1485.

Baragatti, M. (2011). Bayesian variable selection for probit mixed models applied to gene selection. *Bayesian Analysis*, 6(2):209–229.

Bernstein, D. S. (2009). *Matrix mathematics: theory, facts, and formulas*. Princeton University Press.

Bhattacharya, A., Chakraborty, A., and Mallick, B. K. (2016). Fast sampling with gaussian scale mixture priors in high-dimensional regression. *Biometrika*, 103(4):985âĂŞ–991.

Breslow, N. E. and Clayton, D. G. (1993). Approximate inference in generalized linear mixed models. *Journal of the American statistical Association*, 88(421):9–25.

Chakraborty, S. and Khare, K. (2017). Convergence properties of Gibbs samplers for Bayesian probit regression with proper priors. *Electronic Journal of Statistics*, 11:177–210.

Chen, M.-H. and Shao, Q.-M. (2001). Propriety of posterior distribution for dichotomous quantal response models. *Proceedings of the American Mathematical Society*, 129(1):293–302.

Chen, M.-H., Shao, Q.-M., and Xu, D. (2002). Necessary and sufficient conditions on the properiety of posterior distributions for generalized linear mixed models. *Sankhyā: The Indian Journal of Statistics, Series A*, 64(1):57–85.

Choi, H. M. and Hobert, J. P. (2013). The Polya-Gamma Gibbs sampler for Bayesian logistic regression is uniformly ergodic. *Electronic Journal of Statistics*, 7:2054–2064.

Flegal, J. M. and Jones, G. L. (2010). Batch means and spectral variance estimators in Markov chain Monte Carlo. *The Annals of Statistics*, 38(2):1034–1070.

Gilks, W. R. and Wild, P. (1992). Adaptive rejection sampling for Gibbs sampling. *Applied Statistics*, 41(2):337–348.

Gong, L. and Flegal, J. M. (2016). A practical sequential stopping rule for high-dimensional markov chain monte carlo. *Journal of Computational and Graphical Statistics*, 25(3):684–700.

Hobert, J. P. and Marchev, D. (2008). A theoretical comparison of the data augmentation, marginal augmentation and PX-DA algorithms. *The Annals of Statistics*, 36(2):532–554.

Johnson, A. A. and Jones, G. L. (2010). Gibbs sampling for a bayesian hierarchical general linear model. *Electronic Journal of Statistics*, 4:313–333.

Jones, G. L. and Hobert, J. P. (2001). Honest exploration of intractable probability distributions via Markov chain Monte Carlo. *Statistical Science*, 16(4):312–334.

Jones, G. L. and Hobert, J. P. (2004). Sufficient burn-in for gibbs samplers for a hierarchical random effects model. *Annals of statistics*, 32(2):784–817.

Liu, J. S., Wong, W. H., and Kong, A. (1994). Covariance structure of the Gibbs sampler with applications to the comparisons of estimators and augmentation schemes. *Biometrika*, 81(1):27–40.

Liu, J. S. and Wu, Y. N. (1999). Parameter expansion for data augmentation. *Journal of the American Statistical Association*, 94(448):1264–1274.

McCulloch, C. E., Searle, S. R., and Neuhaus, J. M. (2011). *Generalized, Linear, and Mixed Models*. John Wiley & Sons.

Meng, X.-L. and Van Dyk, D. A. (1999). Seeking efficient data augmentation schemes via conditional and marginal augmentation. *Biometrika*, 86:301–320.

Meyn, S. P. and Tweedie, R. L. (1993). *Markov chains and stochastic stability*. Springer.

Polson, N. G., Scott, J. G., and Windle, J. (2013). Bayesian inference for logistic models using Pólya–Gamma latent variables. *Journal of the American statistical Association*, 108(504):1339–1349.

Roberts, G. O. and Rosenthal, J. S. (2001). Markov chains and de-initializing processes. *Scandinavian Journal of Statistics*, 28:489–504.

Roberts, G. O., Rosenthal, J. S., et al. (1997). Geometric ergodicity and hybrid Markov chains. *Electron. Comm. Probab*, 2(2):13–25.

Román, J. C. (2012). *Convergence analysis of block Gibbs samplers for Bayesian general linear mixed models*. PhD thesis, University of Florida.

Román, J. C. and Hobert, J. P. (2012). Convergence analysis of the Gibbs sampler for Bayesian general linear mixed models with improper priors. *The Annals of Statistics*, 40(6):2823–2849.

Román, J. C. and Hobert, J. P. (2015). Geometric ergodicity of Gibbs samplers for Bayesian general linear mixed models with proper priors. *Linear Algebra and its Applications*, 473:54–77.

Roy, V. (2012a). Convergence rates for MCMC algorithms for a robust Bayesian binary regression model. *Electronic Journal of Statistics*, 6:2463–2485.

Roy, V. (2012b). Spectral analytic comparisons for data augmentation. *Stat. and Prob. Letters*, 82:103–108.

Roy, V. (2014). Efficient estimation of the link function parameter in a robust Bayesian binary regression model. *Computational Statistics & Data Analysis*, 73:87–102.

Roy, V. and Hobert, J. P. (2007). Convergence rates and asymptotic standard errors for Markov chain Monte Carlo algorithms for Bayesian probit regression. *Journal of the Royal Statistical Society: Series B*, 69(4):607–623.

Tan, A. and Hobert, J. P. (2009). Block Gibbs sampling for Bayesian random effects models with improper priors: Convergence and regeneration. *Journal of Computational and Graphical Statistics*, 18(4):861–878.

Van Dyk, D. A. and Meng, X.-L. (2001). The art of data augmentation (with discussion). *Journal of Computational and Graphical Statistics*, 10:1–50.

Venables, W. N. and Ripley, B. D. (2002). *Modern applied statistics with S*. Springer.

CHAPTER 5. GEOMETRIC ERGODICITY OF PÓLYA-GAMMA GIBBS SAMPLER FOR BAYESIAN LOGISTIC REGRESSION WITH A FLAT PRIOR

Xin Wang and Vivekananda Roy

Department of Statistics, Iowa State University

Abstract

Logistic regression model is the most popular model for analyzing binary data. In the absence of any prior information, an improper flat prior is often used for the regression coefficients in Bayesian logistic regression models. The resulting intractable posterior density can be explored by running Polson et al.'s (2013) data augmentation (DA) algorithm. In this paper, we establish that the Markov chain underlying Polson et al.'s (2013) DA algorithm is geometrically ergodic. Proving this theoretical result is practically important as it ensures the existence of central limit theorems (CLTs) for sample averages under a finite second moment condition. The CLT in turn allows users of the DA algorithm to calculate standard errors for posterior estimates.

key words: Central Limit theorem, Data augmentation, Drift condition, Geometric rate, Markov chain, Posterior propriety

5.1 Introduction

Let $(Y_1, Y_2, \ldots, Y_n)$ denote the vector of Bernoulli random variables, $\boldsymbol{x}_i$ be the $p \times 1$ vector of known covariates associated with the ith observation for $i = 1, \ldots, n$. Let $\boldsymbol{\beta} \in \mathbb{R}^p$ be the unknown vector of regression coefficients. A generalized linear model can be built (McCulloch et al., 2011) with a link function that connects the expectation of Y_i with the covariate $\boldsymbol{x}_i$. One of the very popular link functions is the logit link function, $F^{-1}(\cdot)$, where F is cumulative distribution function

of the standard logistic random variable, that is $F(t) \equiv e^t/(1+e^t)$ for $t \in \mathbb{R}$. The logit link function leads to the logistic regression model,

$$F^{-1}\left(P(Y_i = 1)\right) = \log\left(\frac{P(Y_i = 1)}{1 - P(Y_i = 1)}\right) = \boldsymbol{x}_i^T \boldsymbol{\beta}.$$

The popularity of logistic regression model is due to the fact that $P(Y_i = 1)$ has a closed form as a function of $\boldsymbol{x}_i^T\boldsymbol{\beta}$, and also it is easy to interpret $\boldsymbol{\beta}$ in terms of odds ratio.

Let $\boldsymbol{y} = (y_1, y_2, \ldots, y_n)^T$ be the vector of observed Bernoulli response variables. The likelihood function for $\boldsymbol{\beta}$ is

$$L\left(\boldsymbol{\beta}|\boldsymbol{y}\right) = \prod_{i=1}^{n} \frac{\left[\exp\left(\boldsymbol{x}_i^T\boldsymbol{\beta}\right)\right]^{y_i}}{1 + \exp\left(\boldsymbol{x}_i^T\boldsymbol{\beta}\right)}.$$

In Bayesian framework, when there is no prior information available about the parameters, noninformative priors are generally used. A popular method of analyzing binary data is by fitting a Bayesian logistic regression model with a flat prior on $\boldsymbol{\beta}$, that is, $\pi\left(\boldsymbol{\beta}\right) \propto 1$. Then the posterior density of $\boldsymbol{\beta}$ is

$$\pi\left(\boldsymbol{\beta}|\boldsymbol{y}\right) = \frac{L\left(\boldsymbol{\beta}|\boldsymbol{y}\right)\pi\left(\boldsymbol{\beta}\right)}{c\left(\boldsymbol{y}\right)} = \frac{1}{c\left(\boldsymbol{y}\right)} \prod_{i=1}^{n} \frac{\left[\exp\left(\boldsymbol{x}_i^T\boldsymbol{\beta}\right)\right]^{y_i}}{1 + \exp\left(\boldsymbol{x}_i^T\boldsymbol{\beta}\right)}, \tag{5.1}$$

provided the marginal density

$$c\left(\boldsymbol{y}\right) = \int_{\mathbb{R}^p} \prod_{i=1}^{n} \frac{\left[\exp\left(\boldsymbol{x}_i^T\boldsymbol{\beta}\right)\right]^{y_i}}{1 + \exp\left(\boldsymbol{x}_i^T\boldsymbol{\beta}\right)} d\boldsymbol{\beta} < \infty.$$

Chen and Shao (2001) discussed necessary and sufficient conditions for propriety of the posterior density (5.1), that is, $c(\boldsymbol{y}) < \infty$. These conditions are given in Appendix A. Throughout this paper, we assume that the posterior density (5.1) is proper.

From (5.1), we know that the posterior density of $\boldsymbol{\beta}$, $\boldsymbol{\pi}(\boldsymbol{\beta}|\boldsymbol{y})$, is intractable in the sense that means with respect to this density is not available in a closed form. Markov chain Monte Carlo (MCMC) algorithms are generally used for exploring this posterior density. The data augmentation (DA) algorithm proposed in Albert and Chib (1993) for Bayesian probit regression model is widely used. For the logistic regression model, there have been many attempts without much success to produce such a DA algorithm (Holmes and Held, 2006; Frühwirth-Schnatter and Frühwirth, 2010) until recently, when Polson et al. (2013) (denoted as PS&W hereafter) proposed a new data

augmentation algorithm based on Pólya-Gamma (PG) distribution. As mentioned in Choi and Hobert (2013), PS&W's algorithm is the first ever DA algorithm for logistic regression which is truly analogous to Albert and Chib's (1993) popular DA algorithm for the probit model. PS&W's DA algorithm, like Albert and Chib's (1993) DA for probit model, in every iteration makes two draws — one draw from a $p-$dimensional normal distribution for $\boldsymbol{\beta}$ and the other draw for the latent variables. We now describe the two steps in every iteration of PS&W's DA algorithm.

Let $\boldsymbol{X}$ denote the $n\times p$ design matrix with ith row $\boldsymbol{x}_i^T$. Let $\mathbb{R}_+ = (0,\infty)$ and for $(\omega_1,\omega_2,\ldots,\omega_n) \in \mathbb{R}_+^n$, define $\boldsymbol{\Omega}$ to be the $n\times n$ diagonal matrix with ith diagonal element ω_i. Finally let $PG(1,b)$ denote the Pólya-Gamma distribution defined in Section 5.2 with parameters 1 and b. A single iteration of PS&W's algorithm uses the following two steps to move from $\boldsymbol{\beta}'$ to $\boldsymbol{\beta}$.

PS&W's algorithm:

1: Draw $\omega_1,\ldots,\omega_n$ independently with $\omega_i \sim \text{PG}\left(1, \left|\boldsymbol{x}_i^T\boldsymbol{\beta}'\right|\right)$.

2: Draw $\boldsymbol{\beta} \sim N\left(\left(\boldsymbol{X}^T\boldsymbol{\Omega}\boldsymbol{X}\right)^{-1}\boldsymbol{X}^T\boldsymbol{\kappa}, \left(\boldsymbol{X}^T\boldsymbol{\Omega}\boldsymbol{X}\right)^{-1}\right)$, where $\boldsymbol{\kappa} = (\kappa_1,\ldots,\kappa_n)^T$ with $\kappa_i = y_i - 1/2$.

PS&W provided an efficient method for sampling from the Pólya-Gamma distribution. It can be shown that the transition density of the underlying Markov chain of the above DA algorithm is strictly positive everywhere, which implies the chain is Harris ergodic (Asmussen and Glynn, 2011). Thus the sample averages based on the DA chain can be used to consistently estimate posterior means. However, in order to provide standard errors for these estimates one needs to show the existence of Markov chain central limit theorem (CLT) for these estimators. The only standard method of establishing Markov chain CLT is by proving the chain to be *geometrically ergodic* (Roberts and Rosenthal, 1997). The geometric ergodicity also allows consistent estimation of asymptotic variances in Markov chain CLT by the standard batch means or spectral variance methods (Flegal and Jones, 2010). This in turn allows the MCMC users to decide how long to run MCMC simulation (Jones and Hobert, 2001). Thus proving geometric ergodicity has important practical benefits. In this paper, we prove that the Markov chain underlying PS&W's DA algorithm converges at a geometric rate.

Choi and Hobert (2013) considered normal priors on the regression parameters and proved uniform ergodicity of the corresponding Pólya-Gamma DA Markov chain by establishing a minorization condition. Choi and Román (2017) considered the one-way logistic ANOVA model under a flat prior on group (treatment) main effects and showed that the Markov operator corresponding to Pólya-Gamma sampler is trace-class. The assumption of one-way logistic ANOVA model is very restrictive and has limited applications. Here, we analyze the convergence rate of PS&W's DA algorithm for Bayesian logistic regression models with general form of design matrix under a flat prior on regression coefficients. Our result provides the best result for constructing central limit theorem for Bayesian logistic regression models under improper priors. The conditions we need are only the conditions of Proposition 5.1 in Appendix A, which guarantee the posterior propriety. Since we use *drift condition* to prove geometric ergodicity of the DA algorithm and hence CLTs, the techniques used here are different from that of Choi and Hobert (2013) and Choi and Román (2017).

The rest of the paper is organized as follows. In section 5.2, we describe PS&W's Gibbs sampler. Section 5.3 contains a brief discussion on geometric rate of convergence for Markov chains and a proof of geometric ergodicity of PS&W's Gibbs sampler. Some concluding remarks are given in section 5.4. Finally, the appendices contain some technical results.

5.2 PS&W's Gibbs sampler

In PS&W's DA algorithm, latent variables with Pólya-Gamma distribution are introduced. The probability density function for a Pólya-Gamma random variable with parameters $a > 0$ and $b \geq 0$ is,

$$f(w|a,b) = \cosh^a(b/2)\frac{2^{a-1}}{\Gamma(a)}\sum_{n=0}^{\infty}(-1)^n\frac{\Gamma(n+a)}{\Gamma(n+1)}\frac{(2n+a)}{\sqrt{2\pi w^3}}e^{-\frac{(2n+a)^2}{8w}-\frac{b^2}{2}w}, w > 0. \tag{5.2}$$

We write $W \sim PG(a,b)$. (Recall that the hyperbolic cosine function cosh is defined in terms of the exponential function as $\cosh(t) = (e^t + e^{-t})/2$.)

Choi and Hobert (2013) developed a new way to formulate PS&W's DA algorithm, which we briefly describe now. Let $\boldsymbol{\omega} = (\omega_1, \ldots, \omega_n)^T$ be latent variables. Assume that, conditional on $\boldsymbol{\beta}$, Y_i

and ω_i are independent with $Y_i \sim \text{Bernoulli}(F(\boldsymbol{x}_i^T\boldsymbol{\beta}))$ and $\omega_i \sim PG(1, |\boldsymbol{x}_i^T\boldsymbol{\beta}|)$. Also, conditional on $\boldsymbol{\beta}$, let $\{(Y_i, \omega_i), i = 1, \ldots, n\}$ be n independent pairs. Then the *complete posterior* density of $\boldsymbol{\beta}$ and $\boldsymbol{\omega}$ is

$$\pi\left(\boldsymbol{\beta}, \boldsymbol{\omega}|\boldsymbol{y}\right) = \frac{\left[\prod_{i=1}^n P(Y_i = y_i|\boldsymbol{\beta})\right]\left[\prod_{i=1}^n f(\omega_i|1, |\boldsymbol{x}_i^T\boldsymbol{\beta}|)\right]\pi(\boldsymbol{\beta})}{c(\boldsymbol{y})}. \tag{5.3}$$

Clearly from (5.1) we see that,

$$\int_{\mathbb{R}^n} \pi\left(\boldsymbol{\beta}, \boldsymbol{\omega}|\boldsymbol{y}\right) d\boldsymbol{\omega} = \pi\left(\boldsymbol{\beta}|\boldsymbol{y}\right),$$

that is, the $\boldsymbol{\beta}$ marginal density of the augmented posterior density $\pi(\boldsymbol{\beta}, \boldsymbol{\omega}|\boldsymbol{y})$ is our target posterior density $\pi(\boldsymbol{\beta}|\boldsymbol{y})$.

Let $p\left(\omega_i\right)$ be the probability function of $PG(1, 0)$ and $\kappa_i = y_i - 1/2$, as defined before. It can be checked that,

$$\pi\left(\boldsymbol{\beta}, \boldsymbol{\omega}|\boldsymbol{y}\right) \propto \prod_{i=1}^n \exp\left[\kappa_i \boldsymbol{x}_i^T\boldsymbol{\beta} - \omega_i\left(\boldsymbol{x}_i^T\boldsymbol{\beta}\right)^2/2\right] p\left(\omega_i\right). \tag{5.4}$$

PS&W's DA algorithm is simply a two-variable Gibbs sampler that, in each iteration, alternates draws from the two conditional distributions of $\pi(\boldsymbol{\beta}, \boldsymbol{\omega}|\boldsymbol{y})$. Below we present the conditional densities of $\boldsymbol{\omega}$ given $\boldsymbol{\beta}$, $\boldsymbol{y}$ and $\boldsymbol{\beta}$ given $\boldsymbol{\omega}$, $\boldsymbol{y}$.

From (5.3) we see that

$$\omega_i|\boldsymbol{\beta}, \boldsymbol{y} \overset{ind}{\sim} \text{PG}\left(1, \left|\boldsymbol{x}_i^T\boldsymbol{\beta}\right|\right), \text{for } i = 1, \ldots, n, \tag{5.5}$$

that is, the conditional distribution of $\boldsymbol{\omega}$ given $\boldsymbol{\beta}$, $\boldsymbol{y}$ is independent of $\boldsymbol{y}$. Thus the conditional density of $\boldsymbol{\omega}$ given $\boldsymbol{\beta}$, $\boldsymbol{y}$ is

$$\pi\left(\boldsymbol{\omega}|\boldsymbol{\beta}, \boldsymbol{y}\right) \propto \prod_{i=1}^n \exp\left[-\omega_i\left(\boldsymbol{x}_i^T\boldsymbol{\beta}\right)^2/2\right] p\left(\omega_i\right). \tag{5.6}$$

From (5.4), it is easy to see that the conditional density of $\boldsymbol{\beta}$ is

$$\pi\left(\boldsymbol{\beta}|\boldsymbol{\omega}, \boldsymbol{y}\right) \propto \exp\left[-\frac{1}{2}\boldsymbol{\beta}^T\boldsymbol{X}^T\boldsymbol{\Omega}\boldsymbol{X}\boldsymbol{\beta} + \boldsymbol{\beta}^T\boldsymbol{X}^T\boldsymbol{\kappa}\right], \tag{5.7}$$

where $\boldsymbol{\kappa} = (\kappa_1, \ldots, \kappa_n)^T$. Thus the conditional distribution of $\boldsymbol{\beta}$ is multivariate normal. In particular,

$$\boldsymbol{\beta}|\boldsymbol{\omega}, \boldsymbol{y} \sim N\left(\left(\boldsymbol{X}^T\boldsymbol{\Omega}\boldsymbol{X}\right)^{-1}\boldsymbol{X}^T\boldsymbol{\kappa}, \left(\boldsymbol{X}^T\boldsymbol{\Omega}\boldsymbol{X}\right)^{-1}\right). \tag{5.8}$$

5.3 Geometric ergodicity of Pólya-Gamma Gibbs sampler

Let $\{\boldsymbol{\beta}^{(m)}, \boldsymbol{\omega}^{(m)}\}_{m=0}^{\infty}$ denote the Markov chain associated with PS&W's DA algorithm. In Bayesian logistic regression models, inference on $\boldsymbol{\beta}$ is made based on the $\{\boldsymbol{\beta}^{(m)}\}_{m=0}^{\infty}$ sub-chain. As mentioned in the introduction, the DA Markov chain is Harris ergodic. Let $h : \mathbb{R}^p \to \mathbb{R}$ with $\int_{\mathbb{R}^p} |h(\boldsymbol{\beta})|\pi(\boldsymbol{\beta}|\boldsymbol{y})d\boldsymbol{\beta} < \infty$, then $E(h(\boldsymbol{\beta})|\boldsymbol{y})$ can be consistently estimated by $\bar{h}_m = \sum_{i=0}^{m-1} h(\boldsymbol{\beta}^{(i)})/m$ for any starting value $\boldsymbol{\beta}^{(0)}$ (See Appendix A for a discussion on the existence of finite moments for (5.1).). We can build a CLT for $\bar{h}_m$ if there exists a constant $\sigma_h^2 \in (0, \infty)$ such that,

$$\sqrt{m}\left(\bar{h}_m - E(h(\boldsymbol{\beta})|\boldsymbol{y})\right) \xrightarrow{d} N\left(0, \sigma_h^2\right) \text{ as } m \to \infty. \tag{5.9}$$

Mere Harris ergodicity of the Markov chain does not ensure that CLT in (5.9) holds. It turns out that geometric rate of convergence defined below guarantees the CLT under a finite second moment condition (Roberts and Rosenthal, 1997). Also it turns out that all three Markov chains $\{\boldsymbol{\beta}^{(m)}, \boldsymbol{\omega}^{(m)}\}_{m=0}^{\infty}$, $\{\boldsymbol{\beta}^{(m)}\}_{m=0}^{\infty}$ and $\{\boldsymbol{\omega}^{(m)}\}_{m=0}^{\infty}$ have the same rate of convergence (Roberts and Rosenthal, 2001). In this article we analyze the $\{\boldsymbol{\omega}^{(m)}\}_{m=0}^{\infty}$ sub-chain denoted as $\boldsymbol{\Psi} = \{\boldsymbol{\omega}^{(m)}\}_{m=0}^{\infty}$. Let $\boldsymbol{\omega}'$ be the current state and $\boldsymbol{\omega}$ be the next state, then the Markov transition density (Mtd) of $\boldsymbol{\Psi}$ is

$$k\left(\boldsymbol{\omega}|\boldsymbol{\omega}'\right) = \int_{\mathbb{R}^p} \pi\left(\boldsymbol{\omega}|\boldsymbol{\beta}, \boldsymbol{y}\right) \pi\left(\boldsymbol{\beta}|\boldsymbol{\omega}', \boldsymbol{y}\right) d\boldsymbol{\beta}, \tag{5.10}$$

where $\pi(\cdot|\cdot, \boldsymbol{y})$'s are the conditional densities defined in (5.6) and (5.7). Let $\mathscr{B}$ denote the Borel σ-algebra of $\mathbb{R}_+^n$ and $K(\cdot, \cdot)$ be the Markov transition function corresponding to the Mtd $k(\cdot|\cdot)$ in (5.10), that is, for any set $A \in \mathscr{B}$, $\boldsymbol{\omega}' \in \mathbb{R}_+^n$ and any $j = 0, 1, \ldots,$

$$K(\boldsymbol{\omega}', A) = \Pr(\boldsymbol{\omega}^{(j+1)} \in A|\boldsymbol{\omega}^{(j)} = \boldsymbol{\omega}') = \int_A k(\boldsymbol{\omega}|\boldsymbol{\omega}')d\boldsymbol{\omega}. \tag{5.11}$$

Then the m-step Markov transition function is $K^m(\boldsymbol{\omega}', A) = \Pr(\boldsymbol{\omega}^{(m+j)} \in A|\boldsymbol{\omega}^{(j)} = \boldsymbol{\omega}')$. Let $\Pi(\cdot|\boldsymbol{y})$ be the probability measure with density $\pi(\boldsymbol{\omega}|\boldsymbol{y})$, where $\pi(\boldsymbol{\omega}|\boldsymbol{y}) = \int_{\mathbb{R}^p} \pi(\boldsymbol{\beta}, \boldsymbol{\omega}|\boldsymbol{y})d\boldsymbol{\beta}$ and $\pi(\boldsymbol{\beta}, \boldsymbol{\omega}|\boldsymbol{y})$ is the joint density defined in (5.3). The Markov chain $\boldsymbol{\Psi}$ is geometrically ergodic if there exist a constant $0 < t < 1$ and a function $H : \mathbb{R}_+^n \mapsto [0, \infty)$ such that for any $\boldsymbol{\omega} \in \mathbb{R}_+^n$, and $m \geq 1$,

$$||K^m(\boldsymbol{\omega}, \cdot) - \Pi(\cdot|\boldsymbol{y})||_{\text{TV}} := \sup_{A \in \mathscr{B}} |K^m(\boldsymbol{\omega}, A) - \Pi(A|\boldsymbol{y})| \leq H(\boldsymbol{\omega})t^m. \tag{5.12}$$

Harris ergodicity of $\boldsymbol{\Psi}$ implies that $||K^m(\boldsymbol{\omega}, \cdot) - \Pi(\cdot|\boldsymbol{y})||_{\text{TV}} \downarrow 0$ as $m \to \infty$, while (5.12) guarantees its exponential rate of convergence. Since the Markov chains $\{\boldsymbol{\beta}^{(m)}\}_{m=0}^{\infty}$ and $\{\boldsymbol{\omega}^{(m)}\}_{m=0}^{\infty}$ have the same rate of convergence, (5.12) implies $\{\boldsymbol{\beta}^{(m)}\}_{m=0}^{\infty}$ is geometrically ergodic. Roberts and Rosenthal (1997) show that since $\{\boldsymbol{\beta}^{(m)}\}_{m=0}^{\infty}$ is reversible, if (5.12) holds then there exists a CLT, that is, for any $h : \mathbb{R}^p \to \mathbb{R}$ with $E[h(\boldsymbol{\beta})^2|\boldsymbol{y}] < \infty$, (5.9) holds. Also, under (5.12) a consistent estimator of σ_h^2 can be found by batch means or spectral variance methods (Flegal and Jones, 2010). The following theorem shows that the Markov chain $\boldsymbol{\Psi}$ converges at a geometric rate.

Theorem 5.1. *The Markov chain $\boldsymbol{\Psi}$ is geometrically ergodic.*

Remark 5.1. *The conditions in Theorem 5.1 are the same as the necessary and sufficient conditions for posterior propriety given in Appendix A. Besides these two conditions, geometric ergodicity of the underlying Markov chain $\boldsymbol{\Psi}$ does not need any other conditions.*

Proof of Theorem 5.1. We prove the geometric ergodicity of $\boldsymbol{\Psi}$ by establishing a drift condition. In particular, we consider the drift function

$$V(\boldsymbol{\omega}) = \alpha \sum_{i=1}^{n} \frac{1}{\omega_i} + \sum_{i=1}^{n} \frac{1}{\sqrt{\omega_i}} + \sum_{i=1}^{n} \omega_i, \tag{5.13}$$

where α is a positive constant and show that for any $\boldsymbol{\omega}, \boldsymbol{\omega}' \in \mathbb{R}_+^n$, there exist some constants $\rho \in (0, 1)$ and $L > 0$ such that

$$E\left[V(\boldsymbol{\omega})\,|\boldsymbol{\omega}'\right] \leq \rho V(\boldsymbol{\omega}') + L. \tag{5.14}$$

In (5.14) the expectation is with respect to the Mtd $k(\boldsymbol{\omega}|\boldsymbol{\omega}')$ defined in (5.10). Note that $V(\boldsymbol{\omega})$ is unbounded off compact sets, that is, for any $a > 0$, the set $\{\boldsymbol{\omega} : V(\boldsymbol{\omega}) \leq a\}$ is compact. We now show that $\boldsymbol{\omega}$-chain is a Feller chain, which means $K(\boldsymbol{\omega}, O)$ is a lower semi-continuous function on $\mathbb{R}_+^n$ for each fixed open set O. Consider a sequence $\boldsymbol{\omega}_m$ with $\boldsymbol{\omega}_m \to \boldsymbol{\omega}$ as $m \to \infty$. Note that,

$$\begin{aligned}
\liminf_{m\to\infty} K(\boldsymbol{\omega}_m, O) &= \liminf_{m\to\infty} \int_O k(\boldsymbol{\omega}|\boldsymbol{\omega}_m)\, d\boldsymbol{\omega} \\
&= \liminf_{m\to\infty} \int_O \left[\int_{\mathbb{R}^p} \pi(\boldsymbol{\omega}|\boldsymbol{\beta}, \boldsymbol{y})\pi(\boldsymbol{\beta}|\boldsymbol{\omega}_m, \boldsymbol{y}) d\boldsymbol{\beta}\right] d\boldsymbol{\omega} \\
&\geq \int_O \int_{\mathbb{R}^p} \pi(\boldsymbol{\omega}|\boldsymbol{\beta}, \boldsymbol{y}) \liminf_{m\to\infty} \pi(\boldsymbol{\beta}|\boldsymbol{\omega}_m, \boldsymbol{y}) d\boldsymbol{\beta} d\boldsymbol{\omega},
\end{aligned}$$

where the inequality follows from Fatou's lemma. Since $\pi(\boldsymbol{\beta}|\boldsymbol{\omega}, \boldsymbol{y})$ is a continuous function in $\boldsymbol{\omega}$ and $\boldsymbol{\omega}_m \to \boldsymbol{\omega}$,

$$\begin{aligned}\liminf_{m\to\infty} K(\boldsymbol{\omega}_m, O) &\geq \int_O \int_{\mathbb{R}^p} \pi(\boldsymbol{\omega}|\boldsymbol{\beta}, \boldsymbol{y})\pi(\boldsymbol{\beta}|\boldsymbol{\omega}, \boldsymbol{y}) d\boldsymbol{\beta} d\boldsymbol{\omega} \\ &= K(\boldsymbol{\omega}, O).\end{aligned}$$

Thus by Meyn and Tweedie (1993)(chap. 15), (5.14) implies that the Markov chain $\boldsymbol{\Psi}$ is geometrically ergodic.

Now we establish (5.14). From the definition of the Mtd of $\boldsymbol{\Psi}$ in (5.10), it follows that

$$E\left[V(\boldsymbol{\omega})|\boldsymbol{\omega}'\right] = E\left\{E\left[V(\boldsymbol{\omega})|\boldsymbol{\beta}, \boldsymbol{y}\right]|\boldsymbol{\omega}', \boldsymbol{y}\right\}, \tag{5.15}$$

where $E[\cdot|\boldsymbol{\beta}, \boldsymbol{y}]$ denotes the expectation with respect to $\pi(\cdot|\boldsymbol{\beta}, \boldsymbol{y})$ given in (5.6) and $E[\cdot|\boldsymbol{\omega}', \boldsymbol{y}]$ denotes the expectation with respect to $\pi(\cdot|\boldsymbol{\omega}', \boldsymbol{y})$ given in (5.7) .

We first evaluate the inner expectation in (5.15), that is the expectation of $V(\boldsymbol{\omega})$ with respect to $\pi(\boldsymbol{\omega}|\boldsymbol{\beta}, \boldsymbol{y})$. From (5.5), we know that $\omega_i|\boldsymbol{\beta}, \boldsymbol{y} \sim PG\left(1, |\boldsymbol{x}_i^T\boldsymbol{\beta}|\right)$. Thus by Lemma 5.1 and Lemma 5.2 given in Appendix B, we have

$$E(\omega_i|\boldsymbol{\beta}, \boldsymbol{y}) = \frac{1}{2|\boldsymbol{x}_i^T\boldsymbol{\beta}|}\frac{\exp\left(\left|\boldsymbol{x}_i^T\boldsymbol{\beta}\right|\right) - 1}{\exp\left(|\boldsymbol{x}_i^T\boldsymbol{\beta}|\right) + 1} \leq \frac{1}{4},$$

$$E\left(\frac{1}{\omega_i} \mid \boldsymbol{\beta}, \boldsymbol{y}\right) \leq 2\left|\boldsymbol{x}_i^T\boldsymbol{\beta}\right| + L_1, \text{ and}$$

$$E\left(\frac{1}{\sqrt{\omega_i}} \mid \boldsymbol{\beta}, \boldsymbol{y}\right) \leq \sqrt{2}\left|\boldsymbol{x}_i^T\boldsymbol{\beta}\right|^{1/2} + L_2,$$

where $L_1 \equiv L(1)$ and $L_2 \equiv L(1/2)$. Then

$$E\left[V(\boldsymbol{\omega}) \mid \boldsymbol{\beta}, \boldsymbol{y}\right] \leq 2\alpha\sum_{i=1}^{n}\left|\boldsymbol{x}_i^T\boldsymbol{\beta}\right| + \sqrt{2}\sum_{i=1}^{n}\left|\boldsymbol{x}_i^T\boldsymbol{\beta}\right|^{1/2} + \alpha n L_1 + n L_2 + \frac{n}{4}. \tag{5.16}$$

Now we consider the outer expectation in (5.15), that is, the expectation with respect to $\pi(\boldsymbol{\beta}|\boldsymbol{\omega}', \boldsymbol{y})$. Let

$$\mu_i = \boldsymbol{x}_i^T\left(\boldsymbol{X}^T\boldsymbol{\Omega}'\boldsymbol{X}\right)^{-1}\boldsymbol{X}^T\boldsymbol{\kappa},$$

and

$$\sigma_i^2 = \boldsymbol{x}_i^T \left(\boldsymbol{X}^T \boldsymbol{\Omega}' \boldsymbol{X}\right)^{-1} \boldsymbol{x_i},$$

where $\boldsymbol{\Omega}'$ is the diagonal matrix with elements ω_i''s. From (5.8) we know that $\boldsymbol{x}_i^T\boldsymbol{\beta}|\boldsymbol{\omega}', \boldsymbol{y} \sim N(\mu_i, \sigma_i^2)$. Then $\left|\boldsymbol{x}_i^T\boldsymbol{\beta}\right|$ has a folded normal distribution. Let $G(\cdot)$ denote the distribution function of the standard normal random variable. So

$$E\left(\left|\boldsymbol{x}_i^T\boldsymbol{\beta}\right| \mid \boldsymbol{\omega}', \boldsymbol{y}\right) = \sigma_i\sqrt{\frac{2}{\pi}}e^{-\mu_i^2/2\sigma_i^2} + \mu_i\left(1 - 2G\left(-\frac{\mu_i}{\sigma_i}\right)\right) \leq \sigma_i\sqrt{\frac{2}{\pi}} + |\mu_i|\,. \tag{5.17}$$

By the inequality in Roy and Hobert (2010) [Lemma 3],

$$\sigma_i^2 = \boldsymbol{x}_i^T\left(\omega_i'\boldsymbol{x}_i\boldsymbol{x}_i^T + \sum_{j\neq i}\omega_j'\boldsymbol{x}_j\boldsymbol{x}_j^T\right)^{-1}\boldsymbol{x}_i = \frac{1}{\omega_i'}\boldsymbol{x}_i^T\left(\boldsymbol{x}_i\boldsymbol{x}_i^T + \sum_{j\neq i}\frac{\omega_j'}{\omega_i'}\boldsymbol{x}_j\boldsymbol{x}_j^T\right)^{-1}\boldsymbol{x}_i \leq \frac{1}{\omega_i'}. \tag{5.18}$$

Also,

$$\sum_{i=1}^n |\mu_i| = \sum_{i=1}^n \left|\boldsymbol{x}_i^T\left(\boldsymbol{X}^T\boldsymbol{\Omega}'\boldsymbol{X}\right)^{-1}\boldsymbol{X}^T\boldsymbol{\kappa}\right| = \boldsymbol{l}^T\boldsymbol{X}\left(\boldsymbol{X}^T\boldsymbol{\Omega}'\boldsymbol{X}\right)^{-1}\boldsymbol{X}^T\boldsymbol{\kappa},$$

where $\boldsymbol{l} = (l_1, \ldots, l_n)$ with $l_i = 1$ if $\mu_i \geq 0$ and $l_i = -1$ if $\mu_i < 0$. By Cauchy-Schwarz inequality, we have

$$\begin{aligned}\sum_{i=1}^n |\mu_i| &= \left|\boldsymbol{l}^T\boldsymbol{X}\left(\boldsymbol{X}^T\boldsymbol{\Omega}'\boldsymbol{X}\right)^{-1/2}\left(\boldsymbol{X}^T\boldsymbol{\Omega}'\boldsymbol{X}\right)^{-1/2}\boldsymbol{X}^T\boldsymbol{\kappa}\right| \\ &\leq \sqrt{\boldsymbol{l}^T\boldsymbol{X}\left(\boldsymbol{X}^T\boldsymbol{\Omega}'\boldsymbol{X}\right)^{-1}\boldsymbol{X}^T\boldsymbol{l}}\sqrt{\boldsymbol{\kappa}^T\boldsymbol{X}\left(\boldsymbol{X}^T\boldsymbol{\Omega}'\boldsymbol{X}\right)^{-1}\boldsymbol{X}^T\boldsymbol{\kappa}}\,.\end{aligned} \tag{5.19}$$

Now

$$\begin{aligned}\boldsymbol{l}^T\boldsymbol{X}\left(\boldsymbol{X}^T\boldsymbol{\Omega}'\boldsymbol{X}\right)^{-1}\boldsymbol{X}^T\boldsymbol{l} &= \boldsymbol{l}^T\left(\boldsymbol{\Omega}'\right)^{-1/2}\left(\boldsymbol{\Omega}'\right)^{1/2}\boldsymbol{X}\left(\boldsymbol{X}^T\boldsymbol{\Omega}'\boldsymbol{X}\right)^{-1}\boldsymbol{X}^T\left(\boldsymbol{\Omega}'\right)^{1/2}\left(\boldsymbol{\Omega}'\right)^{-1/2}\boldsymbol{l} \\ &\leq \boldsymbol{l}^T\left(\boldsymbol{\Omega}'\right)^{-1}\boldsymbol{l} = \sum_{i=1}^n\frac{1}{\omega_i'},\end{aligned} \tag{5.20}$$

where the inequality follows from the fact that $\boldsymbol{I} - \left(\boldsymbol{\Omega}'\right)^{1/2}\boldsymbol{X}\left(\boldsymbol{X}^T\boldsymbol{\Omega}'\boldsymbol{X}\right)^{-1}\boldsymbol{X}^T\left(\boldsymbol{\Omega}'\right)^{1/2}$ is a positive semidefinite matrix.

Since the posterior density (5.1) is assumed proper, the two conditions of Proposition 5.1 given in Appendix A hold. Thus by Lemma 5.3 presented in Appendix C and the facts $\boldsymbol{x}_i\boldsymbol{x}_i^T = \boldsymbol{z}_i\boldsymbol{z}_i^T$, $\kappa_i\boldsymbol{x}_i = -(1/2)\boldsymbol{z}_i$, there exists a constant $\rho_1 \in (0,1)$ such that

$$\boldsymbol{\kappa}^T\boldsymbol{X}\left(\boldsymbol{X}^T\boldsymbol{\Omega}'\boldsymbol{X}\right)^{-1}\boldsymbol{X}^T\boldsymbol{\kappa} = \frac{1}{4}\mathbf{1}^T\boldsymbol{Z}\left(\boldsymbol{Z}^T\boldsymbol{\Omega}'\boldsymbol{Z}\right)^{-1}\boldsymbol{Z}^T\mathbf{1} \leq \frac{1}{4}\rho_1\sum_{i=1}^n\frac{1}{\omega_i'}, \tag{5.21}$$

where $\boldsymbol{Z}$ is defined in Appendix A, and $\mathbf{1}$ is the $n \times 1$ vector of 1's.

Using (5.18) - (5.21), from (5.17) we have

$$E\left(\sum_{i=1}^{n}\left|\boldsymbol{x}_i^T\boldsymbol{\beta}\right|\left|\boldsymbol{\omega}', \boldsymbol{y}\right.\right) \leq \frac{1}{2}\sqrt{\rho_1}\sum_{i=1}^{n}\frac{1}{\omega_i'} + \sqrt{\frac{2}{\pi}}\sum_{i=1}^{n}\frac{1}{\sqrt{\omega_i'}}. \tag{5.22}$$

Using the inequality $2ab \leq a^2 + b^2$, we have for any $c_1 > 0$,

$$E\left(\sqrt{2}\left|\boldsymbol{x}_i^T\boldsymbol{\beta}\right|^{1/2}\left|\boldsymbol{\omega}', \boldsymbol{y}\right.\right) = E\left(2\frac{\sqrt{2}}{2c_1}c_1\left|\boldsymbol{x}_i^T\boldsymbol{\beta}\right|^{1/2}\left|\boldsymbol{\omega}', \boldsymbol{y}\right.\right) \leq c_1^2 E\left(\left|\boldsymbol{x}_i^T\boldsymbol{\beta}\right|\left|\boldsymbol{\omega}', \boldsymbol{y}\right.\right) + \frac{1}{2c_1^2}. \tag{5.23}$$

Using (5.22) and (5.23), we have

$$\begin{aligned} E\left(\sqrt{2}\sum_{i=1}^{n}\left|\boldsymbol{x}_i^T\boldsymbol{\beta}\right|^{1/2}\left|\boldsymbol{\omega}', \boldsymbol{y}\right.\right) &\leq c_1^2\sum_{i=1}^{n}E\left(\left|\boldsymbol{x}_i^T\boldsymbol{\beta}\right|\left|\boldsymbol{\omega}', \boldsymbol{y}\right.\right) + \frac{n}{2c_1^2} \\ &\leq \frac{1}{2}c_1^2\sqrt{\rho_1}\sum_{i=1}^{n}\frac{1}{\omega_i'} + c_1^2\sqrt{\frac{2}{\pi}}\sum_{i=1}^{n}\frac{1}{\sqrt{\omega_i'}} + \frac{n}{2c_1^2}. \end{aligned} \tag{5.24}$$

Combining (5.16), (5.22) and (5.24), from (5.15) we have

$$E\left[V\left(\boldsymbol{\omega}\right) \mid \boldsymbol{\omega}'\right] \leq \alpha\sqrt{\rho_1}\left(1 + \frac{c_1^2}{2\alpha}\right)\sum_{i=1}^{n}\frac{1}{\omega_i'} + \sqrt{\frac{2}{\pi}}\left(2\alpha + c_1^2\right)\sum_{i=1}^{n}\frac{1}{\sqrt{\omega_i'}} + \frac{n}{2c_1^2} + \alpha n L_1 + n L_2 + \frac{n}{4}.$$

We now show that there exist c_1 and α such that $\sqrt{\rho_1}\left(1 + c_1^2/\left(2\alpha\right)\right) < 1$ and $\sqrt{2/\pi}\left(2\alpha + c_1^2\right) < 1$, that is

$$\frac{c_1^2}{2}\frac{\sqrt{\rho_1}}{1 - \sqrt{\rho_1}} < \alpha < \frac{1}{2}\left(\sqrt{\frac{\pi}{2}} - c_1^2\right). \tag{5.25}$$

So we need to show there exists c_1 such that $\sqrt{\frac{\pi}{2}} - c_1^2 > c_1^2\sqrt{\rho_1}/\left(1 - \sqrt{\rho_1}\right)$. Thus for any c_1 with $c_1^2 < \sqrt{\pi/2}\left(1 - \sqrt{\rho_1}\right)$, we can choose α satisfying (5.25). So there exist c_1 and α such that

$$E\left[V\left(\boldsymbol{\omega}\right)\left|\boldsymbol{\omega}'\right.\right] \leq \rho V\left(\boldsymbol{\omega}'\right) + L,$$

where

$$\begin{aligned} \rho &= \max\left\{\sqrt{\rho_1}\left(1 + \frac{c_1^2}{2\alpha}\right), \sqrt{\frac{2}{\pi}}\left(2\alpha + c_1^2\right)\right\} < 1, \\ L &= \frac{n}{2c_1^2} + \alpha n L_1 + n L_2 + \frac{n}{4}. \end{aligned}$$

□

5.4 Discussion

In this article, we prove the geometric rate of convergence for the Polson et al.'s (2013) Pólya-Gamma Gibbs sampler for Bayesian logistic regression with a flat prior on regression coefficients $\boldsymbol{\beta}$. The conditions for geometric ergodicity are the same as the necessary and sufficient conditions for posterior propriety. That means, the Gibbs sampler is always geometrically ergodic if the posterior distribution is proper, which is one of the best possible results one could hope for MCMC convergence in the presence of improper priors. Roy and Hobert (2007) established a similar result for Albert and Chib's (1993) DA algorithm for Bayesian probit regression model with a flat prior on $\boldsymbol{\beta}$. The latent variables in Albert and Chib's (1993) DA algorithm are normal random variables and their conditional (posterior) distributions are truncated normal. Since the latent variables in Polson et al.'s (2013) DA algorithm have non-standard PG distribution, it turns out the drift function, inequalities, techniques used in our proof are quite different from those of Roy and Hobert (2007). One potential future work is to study the convergence properties of Pólya-Gamma Gibbs sampler for Bayesian logistic mixed models under improper priors for both regression coefficients and variance components.

Appendices

A Chen and Shao's (2001) conditions for posterior propriety

Let $\boldsymbol{X}$ denote the $n \times p$ design matrix with ith row $\boldsymbol{x}_i^T$, $\boldsymbol{Z}$ be the $n \times p$ matrix with the ith row $\boldsymbol{z}_i^T = c_i \boldsymbol{x}_i^T$, where $c_i = 1$ if $y_i = 0$ and $c_i = -1$ if $y_i = 1$ for $i = 1, \ldots, n$. The following proposition gives the necessary and sufficient conditions for propriety of the posterior density (5.1).

Proposition 5.1. *(Chen and Shao, 2001). The marginal density $c(\boldsymbol{y})$ is finite if and only if*

1. *$\boldsymbol{X}$ is a full rank matrix;*

2. *There exists a vector $\boldsymbol{e} = (e_1, \ldots, e_n)^T$ with strictly positive components such that $\boldsymbol{Z}^T \boldsymbol{e} = \boldsymbol{0}_p$.*

Remark .2. *Roy and Hobert (2007) provide a method for checking the second condition in Proposition 5.1. This method can be easily implemented using publicly available software packages.*

Remark .3. *Since the moment generating function of the logistic distribution exists from Chen and Shao (2001)[Theorem 2.3], it follows that under the two conditions of Proposition 5.1,* $\int_{\mathbb{R}^p} e^{\delta\|\boldsymbol{\beta}\|}\pi(\boldsymbol{\beta}|\boldsymbol{y})d\boldsymbol{\beta} < \infty$ *for some* $\delta > 0$ *and* $\int_{\mathbb{R}^p} \|\boldsymbol{\beta}\|^r \pi(\boldsymbol{\beta}|\boldsymbol{y})d\boldsymbol{y} < \infty$ *for all* $r \geq 0$.

B Some useful properties of Pólya-Gamma distribution

Lemma 5.1. *If* $\omega \sim PG(1, b)$, *then* $E(\omega) \leq \frac{1}{4}$.

Proof. From Polson et al. (2013), we know that

$$E(\omega) = \frac{1}{2b}\frac{e^b - 1}{e^b + 1}.$$

Consider the function $f(x) = (e^x - 1)/[x(e^x + 1)]$, then

$$f'(x) = \frac{2xe^x - e^{2x} + 1}{[x(e^x + 1)]^2}.$$

Consider another function $f_1(x) = 2xe^x - e^{2x} + 1$. We have $f_1'(x) = 2e^x(1 + x - e^x)$. And we know that $1 + x - e^x \leq 0$ for $x \geq 0$. So $f_1'(x) \leq 0$ for $x \geq 0$. Hence $f_1(x) \leq f_1(0) = 0$. Therefore, $f'(x) \leq 0$ for $x \geq 0$. Then for $x \geq 0$, $f(x) \leq \lim_{x\to 0} f(x) = 1/2$. So $E(\omega) \leq 1/4$. □

Lemma 5.2. *If* $\omega \sim PG(1, b)$, *then for* $0 < s \leq 1$,

$$E(\omega^{-s}) \leq 2^s b^s + L(s),$$

where $L(s)$ *is a constant.*

Proof. From (5.2), the probability density function of PG$(1, b)$ is,

$$f(x|1, b) = \cosh(b/2) \sum_{n=0}^{\infty} (-1)^n \frac{(2n + 1)}{\sqrt{2\pi x^3}} e^{-\frac{(2n+1)^2}{8x} - \frac{b^2}{2}x}.$$

We consider the two cases, $b = 0$ and $b \neq 0$ separately.

Case 1: $b = 0$. Since $0 < s \leq 1$, for any $x > 0$, $x^{-s} \leq x^{-1} + 1$. Thus

$$E(\omega^{-s}) \leq \int_0^{\infty} \left(x^{-1} + 1\right) f(x|1, 0)\, dx = \int_0^{\infty} x^{-1} f(x|1, 0)\, dx + 1.$$

Now

$$\begin{aligned}\int_0^\infty x^{-1} f\left(x|1,0\right) dx &= \sum_{n=0}^{\infty} \left(-1\right)^n \frac{\left(2n+1\right)}{\sqrt{2\pi}} \int_0^\infty x^{-5/2} e^{-\frac{(2n+1)^2}{8x}} dx \\ &= 2^3 \sum_{n=0}^{\infty} \left(-1\right)^n \frac{1}{\left(2n+1\right)^2} = 8C,\end{aligned}$$

where C is Catalan's constant. Hence $E\left(\omega^{-s}\right) \leq 8C + 1$.

Case 2: $b \neq 0$. Note that,

$$\begin{aligned}E\left(\omega^{-s}\right) &= \int_0^\infty x^{-s} f\left(x|1,b\right) dx \\ &= \cosh\left(b/2\right) \sum_{n=0}^{\infty} \left(-1\right)^n \frac{\left(2n+1\right)}{\sqrt{2\pi}} \int_0^\infty \frac{1}{\sqrt{x^3}} x^{-s} e^{-\frac{(2n+1)^2}{8x} - \frac{b^2}{2}x} dx.\end{aligned}$$

According to (Olver et al., 2010, 10.32.10), we have

$$\begin{aligned}\int_0^\infty \frac{1}{\sqrt{x^3}} x^{-s} e^{-\frac{(2n+1)^2}{8x} - \frac{b^2}{2}x} dx &= \int_0^\infty x^{-s-\frac{3}{2}} e^{-\frac{(2n+1)^2}{8x} - \frac{b^2}{2}x} dx \\ &= 2K_{s+\frac{1}{2}}\left(\frac{b\left(2n+1\right)}{2}\right) \cdot \left(\frac{2b}{2n+1}\right)^{s+\frac{1}{2}},\end{aligned}$$

where $K_\nu(x)$ is the modified Bessel function of the second kind. For $x > 0$, according to (Olver et al., 2010, 10.32.8),

$$\begin{aligned}K_{s+\frac{1}{2}}\left(x\right) &= \frac{\sqrt{\pi}\left(\frac{1}{2}x\right)^{s+1/2}}{\Gamma\left(s+1\right)} \int_1^\infty e^{-xt} \left(t^2-1\right)^s dt \\ &= \frac{\sqrt{\pi}\left(\frac{1}{2}x\right)^{s+1/2}}{\Gamma\left(s+1\right)} e^{-x} \int_0^\infty e^{-xt} \left(t^2+2t\right)^s dt \\ &\leq \frac{\sqrt{\pi}\left(\frac{1}{2}x\right)^{s+1/2}}{\Gamma\left(s+1\right)} e^{-x} \int_0^\infty e^{-xt} \left(t^{2s}+2^s t^s\right) dt \\ &= \frac{\sqrt{\pi}\left(\frac{1}{2}x\right)^{s+1/2}}{\Gamma\left(s+1\right)} e^{-x} \left(\frac{\Gamma\left(2s+1\right)}{x^{2s+1}} + 2^s \frac{\Gamma\left(s+1\right)}{x^{s+1}}\right) \\ &= \sqrt{\pi} e^{-x} \left[\frac{\Gamma\left(2s+1\right)}{\Gamma\left(s+1\right)} 2^{-s-1/2} x^{-s-1/2} + 2^{-1/2} x^{-1/2}\right].\end{aligned}$$

Thus

$$\begin{aligned}2K_{s+\frac{1}{2}}\left(\frac{b\left(2n+1\right)}{2}\right) \cdot \left(\frac{2b}{2n+1}\right)^{s+\frac{1}{2}} &= 2\sqrt{\pi}\exp\left(-nb - b/2\right) \\ &\quad \left[\frac{\Gamma\left(2s+1\right)}{\Gamma\left(s+1\right)} 2^{s+1/2} \frac{1}{\left(2n+1\right)^{2s+1}} + 2^{s+1/2} \frac{b^s}{\left(2n+1\right)^{s+1}}\right].\end{aligned}$$

Recall that $\cosh(b/2) = (e^{b/2} + e^{-b/2})/2$. Thus

$$E\left(\frac{1}{\omega^s}\right) = \frac{1+e^{-b}}{2}\sum_{n=0}^{\infty}(-1)^n e^{-nb}\left[\frac{\Gamma(2s+1)}{\Gamma(s+1)}2^{s+1}\frac{1}{(2n+1)^{2s}} + 2^{s+1}\frac{b^s}{(2n+1)^s}\right].$$

Also,

$$\sum_{n=0}^{\infty}\left(-e^{-b}\right)^n\frac{1}{(2n+1)^s} = 2^{-s}\Phi\left(-e^{-b}, s, \frac{1}{2}\right) = 2^{-s}\frac{1}{\Gamma(s)}\int_0^{\infty}\frac{t^{s-1}e^{-\frac{1}{2}t}}{1+e^{-b-t}}dt,$$

and

$$\sum_{n=0}^{\infty}\left(-e^{-b}\right)^n\frac{1}{(2n+1)^{2s}} = 2^{-2s}\Phi\left(-e^{-b}, 2s, \frac{1}{2}\right) = 2^{-2s}\frac{1}{\Gamma(2s)}\int_0^{\infty}\frac{t^{2s-1}e^{-\frac{1}{2}t}}{1+e^{-b-t}}dt \le 1. \tag{5.26}$$

where $\Phi(\cdot)$ is the Lerch transcendent function. The inequality in (5.26) follows from the fact that $1 + e^{-b-t} \ge 1$. Thus we have,

$$E\left(\frac{1}{\omega^s}\right) \le \left(1+e^{-b}\right)\frac{b^s}{\Gamma(s)}\int_0^{\infty}\frac{t^{s-1}e^{-\frac{1}{2}t}}{1+e^{-b-t}}dt + 2^{s+1}\frac{\Gamma(2s+1)}{\Gamma(s+1)}.$$

For fixed $s > 0$, let

$$f(b) \equiv \left(1+e^{-b}\right)\frac{b^s}{\Gamma(s)}\int_0^{\infty}\frac{t^{s-1}e^{-\frac{1}{2}t}}{1+e^{-b-t}}dt - 2^s b^s.$$

Using Dominated Convergence Theorem (DCT), we can show that $f(b)$ is a continuous function of b. DCT can also be used to show that $\lim_{b\to\infty} f(b) = 0$ and $f(0) = 0$. So $|f(b)|$ can be bounded by a positive constant value f_0. Thus we have

$$E\left(\frac{1}{\omega^s}\right) \le 2^s b^s + 2^{s+1}\frac{\Gamma(2s+1)}{\Gamma(s+1)} + f_0.$$

Combining the two cases $b = 0$ and $b \neq 0$, we have

$$E\left(\frac{1}{\omega^s}\right) \le 2^s b^s + L(s),$$

where $L(s) = \max\left\{2^{s+1}\frac{\Gamma(2s+1)}{\Gamma(s+1)} + f_0, 8C+1\right\}$. □

C A matrix result

Lemma 5.3. *For fixed $\boldsymbol{\omega} = (\omega_1, \ldots, \omega_n) \in \mathbb{R}_+^n$, define $\boldsymbol{\Omega}$ to be the $n \times n$ diagonal matrix whose ith diagonal element is ω_i. Let $\mathbf{1}$ be the $n \times 1$ vector of 1's. For a full rank $n \times p$ matrix $\boldsymbol{Z}$, if there*

exists a positive $n \times 1$ *vector* $\boldsymbol{e} = (e_1, e_2, \ldots, e_n)$ *such that* $\boldsymbol{Z}^T\boldsymbol{e} = \boldsymbol{0}$*, then there exists a constant* $\rho_1 \in [0, 1)$ *such that*

$$\mathbf{1}^T\boldsymbol{Z}\left(\boldsymbol{Z}^T\boldsymbol{\Omega}\boldsymbol{Z}\right)^{-1}\boldsymbol{Z}^T\mathbf{1} \leq \rho_1 \sum_{i=1}^{n} \frac{1}{\omega_i}.$$

Proof. Let $\boldsymbol{\lambda} = (\lambda_1, \ldots, \lambda_n)^T \in \mathbb{R}^n_+$, where $\lambda_i = (1/\sqrt{\omega_i})/\sqrt{\sum_{i=1}^n (1/\omega_i)}$, and $\boldsymbol{\Lambda} = \operatorname{diag}(\lambda_1, \ldots, \lambda_n)$. Define

$$S = \left\{\boldsymbol{x} = (x_1, \ldots, x_n)^T : x_i \in (0, \infty) \text{ for } i = 1, \ldots, n, \|\boldsymbol{x}\| = 1\right\},$$

and

$$S^* = \left\{\boldsymbol{x} = (x_1, \ldots, x_n)^T : x_i \in [0, \infty) \text{ for } i = 1, \ldots, n, \|\boldsymbol{x}\| = 1\right\}.$$

The set S^* is a compact set. Note that

$$\sup_{\boldsymbol{\omega} \in \mathbb{R}^n_+} \frac{\mathbf{1}^T\boldsymbol{Z}\left(\boldsymbol{Z}^T\boldsymbol{\Omega}\boldsymbol{Z}\right)^{-1}\boldsymbol{Z}^T\mathbf{1}}{\sum_{i=1}^n 1/\omega_i} = \sup_{\boldsymbol{\lambda} \in S} \mathbf{1}^T\boldsymbol{Z}\left(\boldsymbol{Z}^T\boldsymbol{\Lambda}^{-2}\boldsymbol{Z}\right)^{-1}\boldsymbol{Z}^T\mathbf{1}. \tag{5.27}$$

Now we study the supremum of $\mathbf{1}^T\boldsymbol{Z}\left(\boldsymbol{Z}^T\boldsymbol{\Lambda}^{-2}\boldsymbol{Z}\right)^{-1}\boldsymbol{Z}^T\mathbf{1}$ over $\boldsymbol{\lambda} \in S$. We know that $\mathbf{1}^T\boldsymbol{Z}\left(\boldsymbol{Z}^T\boldsymbol{\Lambda}^{-2}\boldsymbol{Z}\right)^{-1}\boldsymbol{Z}^T\mathbf{1}$ is a continuous function of $\boldsymbol{\lambda}$ in S. For $\boldsymbol{\lambda} \in S^* \backslash S$, there exists a sequence $\left\{\boldsymbol{\lambda}_m \equiv (\lambda_{1,m}, \ldots, \lambda_{n,m})^T \in S\right\}_{m=1}^{\infty}$ such that $\lim_{m\to\infty} \boldsymbol{\lambda}_m = \boldsymbol{\lambda}$. We define the function $f(\cdot)$ on S^* as

$$f(\boldsymbol{\lambda}) \equiv \begin{cases} \mathbf{1}^T\boldsymbol{Z}\left(\boldsymbol{Z}^T\boldsymbol{\Lambda}^{-2}\boldsymbol{Z}\right)^{-1}\boldsymbol{Z}^T\mathbf{1} & \boldsymbol{\lambda} \in S \\ \lim_{m\to\infty} \mathbf{1}^T\boldsymbol{Z}\left(\boldsymbol{Z}^T\boldsymbol{\Lambda}_m^{-2}\boldsymbol{Z}\right)^{-1}\boldsymbol{Z}^T\mathbf{1} & \boldsymbol{\lambda} \in S^* \backslash S, \end{cases}$$

where $\boldsymbol{\Lambda}_m = \operatorname{diag}(\lambda_{1,m}, \ldots, \lambda_{n,m})$ and $\lim_{m\to\infty} \boldsymbol{\lambda}_m = \boldsymbol{\lambda} \in S^* \backslash S$ with $\boldsymbol{\lambda}_m \in S$. Then $f(\boldsymbol{\lambda})$ is a continuous function on S^*. And

$$\sup_{\boldsymbol{\lambda} \in S} \mathbf{1}^T\boldsymbol{Z}\left(\boldsymbol{Z}^T\boldsymbol{\Lambda}^{-2}\boldsymbol{Z}\right)^{-1}\boldsymbol{Z}^T\mathbf{1} \leq \sup_{\boldsymbol{\lambda} \in S^*} f(\boldsymbol{\lambda}). \tag{5.28}$$

We will now show that $\sup_{\boldsymbol{\lambda} \in S^*} f(\boldsymbol{\lambda}) < 1$. First we show that for any $\boldsymbol{\lambda} \in S$, $f(\boldsymbol{\lambda}) < 1$. Define $\tilde{\boldsymbol{Z}} \equiv \boldsymbol{\Lambda}^{-1}\boldsymbol{Z}$, then

$$\begin{aligned} \mathbf{1}^T\boldsymbol{Z}\left(\boldsymbol{Z}^T\boldsymbol{\Lambda}^{-2}\boldsymbol{Z}\right)^{-1}\boldsymbol{Z}^T\mathbf{1} &= \mathbf{1}^T\boldsymbol{\Lambda}\boldsymbol{\Lambda}^{-1}\boldsymbol{Z}\left(\boldsymbol{Z}^T\boldsymbol{\Lambda}^{-2}\boldsymbol{Z}\right)^{-1}\boldsymbol{Z}^T\boldsymbol{\Lambda}^{-1}\boldsymbol{\Lambda}\mathbf{1} \\ &= \mathbf{1}^T\boldsymbol{\Lambda}\tilde{\boldsymbol{Z}}\left(\tilde{\boldsymbol{Z}}^T\tilde{\boldsymbol{Z}}\right)^{-1}\tilde{\boldsymbol{Z}}^T\boldsymbol{\Lambda}\mathbf{1} = \boldsymbol{\lambda}^T\tilde{\boldsymbol{Z}}\left(\tilde{\boldsymbol{Z}}^T\tilde{\boldsymbol{Z}}\right)^{-1}\tilde{\boldsymbol{Z}}^T\boldsymbol{\lambda}. \end{aligned} \tag{5.29}$$

Since by the assumption of Lemma 5.3, there exists a positive vector $\boldsymbol{e}$ such that $\boldsymbol{Z}^T\boldsymbol{e} = \boldsymbol{0}$, we have $\tilde{\boldsymbol{Z}}^T\boldsymbol{\Lambda}\boldsymbol{e} = \boldsymbol{Z}^T\boldsymbol{\Lambda}^{-1}\boldsymbol{\Lambda}e = \boldsymbol{Z}^T\boldsymbol{e} = \boldsymbol{0}$. Thus $\tilde{\boldsymbol{Z}}\left(\tilde{\boldsymbol{Z}}^T\tilde{\boldsymbol{Z}}\right)^{-1}\tilde{\boldsymbol{Z}}^T\boldsymbol{\Lambda}\boldsymbol{e} = \boldsymbol{0}$. In other words, $\boldsymbol{\Lambda}\boldsymbol{e}$ is an eigenvector of $\tilde{\boldsymbol{Z}}\left(\tilde{\boldsymbol{Z}}^T\tilde{\boldsymbol{Z}}\right)^{-1}\tilde{\boldsymbol{Z}}^T$ corresponding to eigenvalue zero. Since $\boldsymbol{e}^T\boldsymbol{\Lambda}\boldsymbol{\lambda} = \sum_{i=1}^n \lambda_i^2 e_i > 0$, and $\tilde{\boldsymbol{Z}}\left(\tilde{\boldsymbol{Z}}^T\tilde{\boldsymbol{Z}}\right)^{-1}\tilde{\boldsymbol{Z}}^T$ is an idempotent matrix, it implies that $\boldsymbol{\lambda}$ cannot be an eigenvector of $\tilde{\boldsymbol{Z}}\left(\tilde{\boldsymbol{Z}}^T\tilde{\boldsymbol{Z}}\right)^{-1}\tilde{\boldsymbol{Z}}^T$ corresponding to eigenvalue 1 (Bernstein, 2005, Proposition 4.5.4). Thus $\boldsymbol{\lambda}^T\tilde{\boldsymbol{Z}}\left(\tilde{\boldsymbol{Z}}^T\tilde{\boldsymbol{Z}}\right)^{-1}\tilde{\boldsymbol{Z}}^T\boldsymbol{\lambda} < 1$, that is by (5.29), $f(\boldsymbol{\lambda}) < 1$ for any $\boldsymbol{\lambda} \in S$.

Next we show that or any $\boldsymbol{\lambda} \in S^*\backslash S$, $f(\boldsymbol{\lambda}) < 1$. Define $\tilde{\boldsymbol{Z}}_m \equiv \boldsymbol{\Lambda}_m^{-1}\boldsymbol{Z}$. Now, we will show that $\lim_{m\to\infty}\tilde{\boldsymbol{Z}}_m\left(\tilde{\boldsymbol{Z}}_m^T\tilde{\boldsymbol{Z}}_m\right)^{-1}\tilde{\boldsymbol{Z}}_m^T$ exists. Define $\boldsymbol{P}_m \equiv \tilde{\boldsymbol{Z}}_m\left(\tilde{\boldsymbol{Z}}_m^T\tilde{\boldsymbol{Z}}_m\right)^{-1}\tilde{\boldsymbol{Z}}_m^T$. We will show that each element in $\boldsymbol{P}_m$ is bounded by 1. Let $\boldsymbol{Z} \equiv (\boldsymbol{z}_1, \ldots, \boldsymbol{z}_n)^T$, then $\tilde{\boldsymbol{Z}}_m = \left(\lambda_{1,m}^{-1}\boldsymbol{z}_1, \ldots, \lambda_{n,m}^{-1}\boldsymbol{z}_n\right)^T$. The (i,j)th element of $\boldsymbol{P}_m$ is $\lambda_{i,m}^{-1}\lambda_{j,m}^{-1}\boldsymbol{z}_i^T\left(\tilde{\boldsymbol{Z}}_m^T\tilde{\boldsymbol{Z}}_m\right)^{-1}\boldsymbol{z}_j$. For $i = j$, using the inequality in Roy and Hobert (2010) [Lemma 3], the ith diagonal element of $\boldsymbol{P}_m$ is

$$\lambda_{i,m}^{-2}\boldsymbol{z}_i^T\left(\tilde{\boldsymbol{Z}}_m^T\tilde{\boldsymbol{Z}}_m\right)^{-1}\boldsymbol{z}_i = \lambda_{i,m}^{-2}\boldsymbol{z}_i^T\left(\lambda_{i,m}^{-2}\boldsymbol{z}_i\boldsymbol{z}_i^T + \sum_{j=1,j\neq i}^{n}\lambda_{j,m}^{-2}\boldsymbol{z}_j\boldsymbol{z}_j^T\right)^{-1}\boldsymbol{z}_i \leq 1.$$

For $i \neq j$, by Cauchy–Schwartz inequality

$$\left|\lambda_{i,m}^{-1}\lambda_{j,m}^{-1}\boldsymbol{z}_i^T\left(\tilde{\boldsymbol{Z}}_m^T\tilde{\boldsymbol{Z}}_m\right)^{-1}\boldsymbol{z}_j\right| \leq \sqrt{\lambda_{i,m}^{-2}\boldsymbol{z}_i^T\left(\tilde{\boldsymbol{Z}}_m^T\tilde{\boldsymbol{Z}}_m\right)^{-1}\boldsymbol{z}_i}\sqrt{\lambda_{j,m}^{-2}\boldsymbol{z}_j^T\left(\tilde{\boldsymbol{Z}}_m^T\tilde{\boldsymbol{Z}}_m\right)^{-1}\boldsymbol{z}_j} \leq 1.$$

Since each element of $\boldsymbol{P}_m$ is a bounded, continuous function of $\boldsymbol{\lambda}_m$ over S, its limit as $m \to \infty$ exists and is bounded. Thus, $\lim_{m\to\infty}\tilde{\boldsymbol{Z}}_m\left(\tilde{\boldsymbol{Z}}_m^T\tilde{\boldsymbol{Z}}_m\right)^{-1}\tilde{\boldsymbol{Z}}_m^T$ exists, and we denote it as $\boldsymbol{P}$. For a matrix $\boldsymbol{A}$, define $\|\boldsymbol{A}\|_2 = \sup_{\boldsymbol{x}:\|\boldsymbol{x}\|=1}\|\boldsymbol{A}\boldsymbol{x}\|$. Since $\|\boldsymbol{P}_m\|_2 \leq \|\boldsymbol{P}\|_2 + \|\boldsymbol{P}_m - \boldsymbol{P}\|_2$ and $\|\boldsymbol{P}\|_2 \leq \|\boldsymbol{P}_m\|_2 + \|\boldsymbol{P}_m - \boldsymbol{P}\|_2$, we have

$$\left|\|\boldsymbol{P}_m\|_2 - \|\boldsymbol{P}\|_2\right| \leq \|\boldsymbol{P}_m - \boldsymbol{P}\|_2. \tag{5.30}$$

Since for all m, $\|\boldsymbol{P}_m\|_2 = 1$, being its largest eigenvalue and $\|\boldsymbol{P}_m - \boldsymbol{P}\|_2 \to 0$ as $m \to \infty$, (5.30) implies that $\|\boldsymbol{P}\|_2 = 1$. Thus the maximum eigenvalue of $\boldsymbol{P}$ is 1. Then for any $\boldsymbol{\lambda} \in S^*\backslash S$ with $\lim_{m\to\infty}\boldsymbol{\lambda}_m = \boldsymbol{\lambda}$, we have

$$\lim_{m\to\infty}\boldsymbol{1}^T\boldsymbol{Z}\left(\boldsymbol{Z}^T\boldsymbol{\Lambda}_m^{-2}\boldsymbol{Z}\right)^{-1}\boldsymbol{Z}^T\boldsymbol{1} = \lim_{m\to\infty}\boldsymbol{\lambda}_m^T\tilde{\boldsymbol{Z}}_m\left(\tilde{\boldsymbol{Z}}_m^T\tilde{\boldsymbol{Z}}_m\right)^{-1}\tilde{\boldsymbol{Z}}_m^T\boldsymbol{\lambda}_m = \boldsymbol{\lambda}^T\boldsymbol{P}\boldsymbol{\lambda}^T. \tag{5.31}$$

Since $\boldsymbol{Z}^T\boldsymbol{e} = \mathbf{0}$, then $\tilde{\boldsymbol{Z}}_m^T\boldsymbol{\Lambda}_m\boldsymbol{e} = \boldsymbol{Z}^T\boldsymbol{\Lambda}_m^{-1}\boldsymbol{\Lambda}_m\boldsymbol{e} = \mathbf{0}$. Define $\boldsymbol{\Lambda}_m\boldsymbol{e} = \tilde{\boldsymbol{e}}_m = (\tilde{e}_{m1}, \tilde{e}_{m2}, \ldots, \tilde{e}_{mn})^T$, where $\tilde{e}_{mi} = \lambda_{i,m}e_i$ and $\lim_{m\to\infty}\tilde{\boldsymbol{e}}_m = \tilde{\boldsymbol{e}} = (\lambda_1 e_1, \ldots, \lambda_n e_n)^T$. So we have

$$\boldsymbol{P}\tilde{\boldsymbol{e}} = \lim_{m\to\infty}\tilde{\boldsymbol{Z}}_m\left(\tilde{\boldsymbol{Z}}_m^T\tilde{\boldsymbol{Z}}_m\right)^{-1}\tilde{\boldsymbol{Z}}_m^T\boldsymbol{\Lambda}_m\boldsymbol{e} = \mathbf{0}.$$

Thus $\tilde{\boldsymbol{e}}$ is an eigenvector of $\boldsymbol{P}$ corresponding to eigenvalue 0. We also know that $\boldsymbol{\lambda}^T\tilde{\boldsymbol{e}} = \sum_{i=1}^n \lambda_i^2 e_i > 0$. So using similar arguments as before, $\boldsymbol{\lambda}$ cannot be an eigenvector for $\boldsymbol{P}$ corresponding to eigenvalue 1. Thus $\boldsymbol{\lambda}^T\boldsymbol{P}\boldsymbol{\lambda} < 1$, which by (5.31) implies $f(\boldsymbol{\lambda}) < 1$ for any $\boldsymbol{\lambda} \in S^*\backslash S$.

Therefore for any $\boldsymbol{\lambda} \in S^*$, $f(\boldsymbol{\lambda}) < 1$. Since S^* is a compact set, and $f(\boldsymbol{\lambda})$ is a continuous function of $\boldsymbol{\lambda}$ over S^*, we have

$$\sup_{\boldsymbol{\lambda}\in S^*} f(\boldsymbol{\lambda}) = f\left(\tilde{\boldsymbol{\lambda}}\right), \quad \text{for some } \tilde{\boldsymbol{\lambda}} \in S^*.$$

Therefore $\sup_{\boldsymbol{\lambda}\in S^*} f(\boldsymbol{\lambda}) < 1$, which by (5.27) and (5.28) in turn implies that

$$\sup_{\boldsymbol{\omega}\in\mathbb{R}_+^n} \frac{\mathbf{1}^T\boldsymbol{Z}\left(\boldsymbol{Z}^T\boldsymbol{\Omega}\boldsymbol{Z}\right)^{-1}\boldsymbol{Z}^T\mathbf{1}}{\sum_{i=1}^n 1/\omega_i} < 1.$$

Let $\rho_1 = \sup_{\boldsymbol{\omega}\in\mathbb{R}_+^n} \frac{\mathbf{1}^T\boldsymbol{Z}\left(\boldsymbol{Z}^T\boldsymbol{\Omega}\boldsymbol{Z}\right)^{-1}\boldsymbol{Z}^T\mathbf{1}}{\sum_{i=1}^n 1/\omega_i}$, so we have

$$\mathbf{1}^T\boldsymbol{Z}\left(\boldsymbol{Z}^T\boldsymbol{\Omega}\boldsymbol{Z}\right)^{-1}\boldsymbol{Z}^T\mathbf{1} \leq \rho_1\sum_{i=1}^n\frac{1}{\omega_i}.$$

□

Bibliography

Albert, J. H. and Chib, S. (1993). Bayesian analysis of binary and polychotomous response data. *Journal of the American statistical Association*, 88(422):669–679.

Asmussen, S. and Glynn, P. W. (2011). A new proof of convergence of MCMC via the ergodic theorem. *Statistics & Probability Letters*, 81(10):1482–1485.

Bernstein, D. S. (2005). *Matrix mathematics: Theory, facts, and formulas with application to linear systems theory*, volume 41. Princeton University Press.

Chen, M.-H. and Shao, Q.-M. (2001). Propriety of posterior distribution for dichotomous quantal response models. *Proceedings of the American Mathematical Society*, 129(1):293–302.

Choi, H. M. and Hobert, J. P. (2013). The Pólya-Gamma Gibbs sampler for Bayesian logistic regression is uniformly ergodic. *Electronic Journal of Statistics*, 7:2054–2064.

Choi, H. M. and Román, J. C. (2017). Analysis of Pólya-Gamma Gibbs sampler for Bayesian logistic analysis of variance. *Electronic Journal of Statistics*, 11(1):326–337.

Flegal, J. M. and Jones, G. L. (2010). Batch means and spectral variance estimators in Markov chain Monte Carlo. *The Annals of Statistics*, 38(2):1034–1070.

Frühwirth-Schnatter, S. and Frühwirth, R. (2010). Data augmentation and MCMC for binary and multinomial logit models. In *Statistical Modelling and Regression Structures*, pages 111–132. Springer.

Holmes, C. C. and Held, L. (2006). Bayesian auxiliary variable models for binary and multinomial regression. *Bayesian analysis*, 1(1):145–168.

Jones, G. L. and Hobert, J. P. (2001). Honest exploration of intractable probability distributions via Markov chain Monte Carlo. *Statistical Science*, 16(4):312–334.

McCulloch, C. E., Searle, S. R., and Neuhaus, J. M. (2011). *Generalized, Linear, and Mixed Models*. John Wiley & Sons.

Meyn, S. P. and Tweedie, R. L. (1993). *Markov chains and stochastic stability*. Springer.

Olver, F. W., Lozier, D. W., F., B. R., and Clark, C. W. (2010). *NIST Handbook of Mathematical Functions*. Cambridge University Press.

Polson, N. G., Scott, J. G., and Windle, J. (2013). Bayesian inference for logistic models using Pólya-Gamma latent variables. *Journal of the American statistical Association*, 108(504):1339–1349.

Roberts, G. O. and Rosenthal, J. S. (1997). Geometric ergodicity and hybrid Markov chains. *Electron. Comm. Probab*, 2(2):13–25.

Roberts, G. O. and Rosenthal, J. S. (2001). Markov chains and de-initializing processes. *Scandinavian Journal of Statistics*, 28(3):489–504.

Roy, V. and Hobert, J. P. (2007). Convergence rates and asymptotic standard errors for Markov chain Monte Carlo algorithms for Bayesian probit regression. *Journal of the Royal Statistical Society: Series B*, 69(4):607–623.

Roy, V. and Hobert, J. P. (2010). On Monte Carlo methods for Bayesian multivariate regression models with heavy-tailed errors. *Journal of Multivariate Analysis*, 101(5):1190–1202.

CHAPTER 6. ANALYSIS OF THE PÓLYA-GAMMA BLOCK GIBBS SAMPLER FOR BAYESIAN LOGISTIC LINEAR MIXED MODELS

Modified from a paper accepted by *Statistics and Probability Letters*

Xin Wang [1] and Vivekananda Roy

Department of Statistics, Iowa State University

Abstract

In this article, we construct a two-block Gibbs sampler using Polson et al.'s (2013) data augmentation technique for Bayesian logistic linear mixed models under proper priors. Furthermore, we prove the uniform ergodicity of this Gibbs sampler.

key words: Data augmentation; Markov Chain; Logit link; Pólya-Gamma distribution; Uniform ergodicity

6.1 Introduction

Consider the logistic linear mixed model set-up (Charles E. McCulloch and Neuhaus, 2008; McCulloch, 2003). Let $(Y_1, Y_2, \ldots, Y_N)$ denote the vector of Binomial(n_i, p_i) random variables, $\boldsymbol{x}_i$ and $\boldsymbol{z}_i$ be the $p \times 1$ and $q \times 1$ known covariates and random effect design vectors respectively associated with the ith observation for $i = 1, \ldots, N$. Let $\boldsymbol{\beta} \in \mathbb{R}^p$ be the unknown vector of regression coefficients and $\boldsymbol{u} \in \mathbb{R}^q$ be the random effects vector. Assume that $p_i = F(\boldsymbol{x}_i^T\boldsymbol{\beta} + \boldsymbol{z}_i^T\boldsymbol{u})$, where F is the standard logistic distribution function, that is $F(t) \equiv e^t/(1+e^t)$ for $t \in \mathbb{R}$. Suppose we have r random effects with $\boldsymbol{u} = (\boldsymbol{u}_1^T, \ldots, \boldsymbol{u}_r^T)^T$, where $\boldsymbol{u}_j$ is a $q_j \times 1$ vector with $q_j > 0$, $q_1 + \cdots + q_r = q$, and $\boldsymbol{u}_j \overset{\text{ind}}{\sim} N(0, \boldsymbol{I}_{q_j} 1/\tau_j)$, where $\tau_j \in \mathbb{R}_+ = (0, \infty)$ is the precision parameter associated with $\boldsymbol{u}_j$ for $j = 1, \ldots, r$. The joint distribution of $\boldsymbol{u}$ is $N\left(0, \boldsymbol{D}(\boldsymbol{\tau})^{-1}\right)$, where $\boldsymbol{D}(\boldsymbol{\tau}) = \oplus_{j=1}^r \tau_j \boldsymbol{I}_{q_j}$, $\boldsymbol{\tau} = (\tau_1, \ldots, \tau_r)$

[1] Corresponding author

and $\oplus$ denotes the direct sum. The data model for the logistic linear mixed model is

$$\begin{aligned} Y_i|\boldsymbol{\beta},\boldsymbol{u} &\overset{ind}{\sim} \text{Binomial}(n_i,p_i) \text{ for } i=1,\ldots,N \text{ with} \\ p_i &= F(\boldsymbol{x}_i^T\boldsymbol{\beta}+\boldsymbol{z}_i^T\boldsymbol{u}) \text{ for } i=1,\ldots,N, \\ \boldsymbol{u}_j|\tau_j &\overset{\text{ind}}{\sim} N\Big(0,\frac{1}{\tau_j}\boldsymbol{I}_{q_j}\Big),\ j=1,\ldots,r. \end{aligned} \tag{6.1}$$

Let $\boldsymbol{y}=(y_1,y_2,\ldots,y_N)^T$ be the observed Binomial response variables. The likelihood function for $(\boldsymbol{\beta},\boldsymbol{\tau})$ is

$$L\left(\boldsymbol{\beta},\boldsymbol{\tau}|\boldsymbol{y}\right)=\int_{\mathbb{R}^q}\prod_{i=1}^{N}\binom{n_i}{y_i}\frac{\left[\exp\left(\boldsymbol{x}_i^T\boldsymbol{\beta}+\boldsymbol{z}_i^T\boldsymbol{u}\right)\right]^{y_i}}{\left[1+\exp\left(\boldsymbol{x}_i^T\boldsymbol{\beta}+\boldsymbol{z}_i^T\boldsymbol{u}\right)\right]^{n_i}}\phi_q\left(\boldsymbol{u};\boldsymbol{0},\boldsymbol{D}(\boldsymbol{\tau})^{-1}\right)d\boldsymbol{u}, \tag{6.2}$$

where $\phi_q(s;a,B)$ is the probability density function of the q-dimensional normal distribution with mean vector a and covariance matrix B evaluated at s. In Bayesian framework, let $\pi\left(\boldsymbol{\beta}\right)$ and $\pi\left(\boldsymbol{\tau}\right)$ be the prior densities for $\boldsymbol{\beta}$ and $\boldsymbol{\tau}$ respectively. Assume that $\boldsymbol{\beta}$ and $\boldsymbol{\tau}$ are apriori independent. The joint posterior density of $(\boldsymbol{\beta},\boldsymbol{\tau})$ is

$$\pi\left(\boldsymbol{\beta},\boldsymbol{\tau}|\boldsymbol{y}\right)=\frac{1}{c_0\left(\boldsymbol{y}\right)}L\left(\boldsymbol{\beta},\boldsymbol{\tau}|\boldsymbol{y}\right)\pi\left(\boldsymbol{\beta}\right)\pi\left(\boldsymbol{\tau}\right), \tag{6.3}$$

where $c_0(\boldsymbol{y})$ is the marginal density of $\boldsymbol{y}$ with $c_0\left(\boldsymbol{y}\right)=\int_{\mathbb{R}_+^r}\int_{\mathbb{R}^p}L\left(\boldsymbol{\beta},\boldsymbol{\tau}|\boldsymbol{y}\right)\pi\left(\boldsymbol{\beta}\right)\pi\left(\boldsymbol{\tau}\right)d\boldsymbol{\beta}d\boldsymbol{\tau}$.

The posterior density (6.3) is intractable for any choice of the prior distributions of $\boldsymbol{\beta}$ and $\boldsymbol{\tau}$. Generally, Markov chain Monte Carlo (MCMC) algorithms are used for exploring these posterior densities. Even in the absence of random effects, for generalized linear models, MCMC algorithms are needed to summarize the associated posterior densities. For probit regression models, Albert and Chib (1993) proposed a widely used data augmentation (DA) algorithm to sample from the corresponding posterior distributions. Roy and Hobert (2007) and Chakraborty and Khare (2017) proved the geometric ergodicity of this DA algorithm for Bayesian probit regression model under improper and proper priors respectively. Wang and Roy (2017) recently extended the convergence rate analysis of the block Gibbs samplers based on this DA technique for Bayesian probit linear mixed models under both proper and improper priors.

For logistic regression models, there have been several attempts for producing a DA algorithm similar to Albert and Chib's (1993) algorithm for the probit regression model (see e.g. Holmes and

Held (2006) and Frühwirth-Schnatter and Frühwirth (2010)). Unfortunately, these algorithms are far more complex than Albert and Chib's (1993) algorithm. Only recently, Polson et al. (2013) produced such a DA algorithm for logistic regression models using Pólya-Gamma latent variables. Choi and Hobert (2013) proved uniform ergodicity of the Pólya-Gamma DA Markov chain under normal priors on the regression parameters. Choi and Román (2017) showed that the Markov operator based on Polson et al.'s (2013) DA algorithm for one-way logistic ANOVA model is trace-class, which implies that the associated Markov Chain is geometrically ergodic. Both Choi and Hobert (2013) and Choi and Román (2017) considered the special case when the data are binary, that is $n_i = 1$ for all i. However, there is no result in the literature about convergence analysis of any Gibbs samplers for Bayesian logistic linear mixed models. In this article, we construct a two-block Gibbs sampler for Bayesian logistic linear mixed models with normal priors on regression parameters and truncated Gamma priors on precision parameters. We further establish uniform ergodicity of this Gibbs sampler.

The article is organized as follows. In section 6.2, we construct the two-block Gibbs sampler for the Bayesian logistic linear mixed model under proper priors. In section 6.3, we prove the uniform ergodicity of the underlying Markov chain. Finally, we have some discussions in section 6.4.

6.2 Two-block Gibbs sampler

In Polson et al. (2013), a logistic linear mixed model example is introduced. In their example, normal distribution is used as the prior for regression coefficients and Gamma distribution is used as the prior for precision parameters. We assume the following priors: $\boldsymbol{\beta} \sim N_p(\boldsymbol{Q}^{-1}\boldsymbol{\mu}_0, \boldsymbol{Q}^{-1})$ for some $p \times p$ positive definite matrix $\boldsymbol{Q}$ and $\boldsymbol{\mu}_0 \in \mathbb{R}^p$, $\tau_j \overset{ind}{\sim}$ truncated Gamma(a_j, b_j, τ_0), $j = 1, \ldots, r$, where $b_j > 0$ for $j = 1, \ldots, r$. The density function of truncated Gamma(a_j, b_j, τ_0) is

$$f(\tau_j | a_j, b_j, \tau_0) = [c(\tau_0, a_j, b_j)]^{-1} \tau_j^{a_j - 1} \exp(-b_j \tau_j) I(\tau_j \geq \tau_0), \tag{6.4}$$

where $c(\tau_0, a_j, b_j) = \int_{\tau_0}^{\infty} \tau^{a_j - 1} \exp(-b_j \tau) d\tau$ and $\tau_0 > 0$ is a known constant.

By Theorem 6.1 in Polson et al. (2013),

$$\frac{\left[\exp\left(\boldsymbol{x}_i^T\boldsymbol{\beta}+\boldsymbol{z}_i^T\boldsymbol{u}\right)\right]^{y_i}}{\left[1+\exp\left(\boldsymbol{x}_i^T\boldsymbol{\beta}+\boldsymbol{z}_i^T\boldsymbol{u}\right)\right]^{n_i}} = 2^{-n_i}\exp\left[\kappa_i\left(\boldsymbol{x}_i^T\boldsymbol{\beta}+\boldsymbol{z}_i^T\boldsymbol{u}\right)\right] \times\int_0^\infty \exp\left[-\omega_i\left(\boldsymbol{x}_i^T\boldsymbol{\beta}+\boldsymbol{z}_i^T\boldsymbol{u}\right)^2/2\right]p\left(\omega_i\right)d\omega_i, \tag{6.5}$$

where $p\left(\omega_i\right)$ is the probability density function of the random variable $\omega_i \sim \mathrm{PG}\left(n_i,0\right)$ and $\kappa_i = y_i - n_i/2$ for $i=1,\ldots,N$. Here, $\mathrm{PG}(n_i,0)$ denotes the Pólya-Gamma distribution with parameters n_i and 0 with density

$$f(x|n_i,0) = \frac{2^{n_i-1}}{\Gamma(n_i)}\sum_{n=0}^{\infty}(-1)^n\frac{\Gamma(n+n_i)}{\Gamma(n+1)}\frac{(2n+n_i)}{\sqrt{2\pi x^3}}e^{-\frac{(2n+n_i)^2}{8x}},\ x>0.$$

Let $\boldsymbol{\omega}=(\omega_1,\ldots,\omega_N)$ and the joint (posterior) density of $\boldsymbol{\beta},\boldsymbol{u},\boldsymbol{\omega}$ and $\boldsymbol{\tau}$ be

$$\pi\left(\boldsymbol{\beta},\boldsymbol{u},\boldsymbol{\omega},\boldsymbol{\tau}|\boldsymbol{y}\right)\propto\prod_{i=1}^{N}\exp\left[\kappa_i\left(\boldsymbol{x}_i^T\boldsymbol{\beta}+\boldsymbol{z}_i^T\boldsymbol{u}\right)-\omega_i\left(\boldsymbol{x}_i^T\boldsymbol{\beta}+\boldsymbol{z}_i^T\boldsymbol{u}\right)^2/2\right]p\left(\omega_i\right) \times\phi_q\left(\boldsymbol{u};\boldsymbol{0},\boldsymbol{D}(\boldsymbol{\tau})^{-1}\right)\phi_p\left(\boldsymbol{\beta};\boldsymbol{Q}^{-1}\boldsymbol{\mu}_0,\boldsymbol{Q}^{-1}\right)\prod_{j=1}^{r}\tau_j^{a_j-1}e^{-b_j\tau_j}I(\tau_j\geq\tau_0). \tag{6.6}$$

From (6.2), (6.3) and (6.5), it follows that $\int_{\mathbb{R}^q}\int_{\mathbb{R}_+^N}\pi(\boldsymbol{\beta},\boldsymbol{u},\boldsymbol{\omega},\boldsymbol{\tau}|\boldsymbol{y})d\boldsymbol{\omega}d\boldsymbol{u}=\pi(\boldsymbol{\beta},\boldsymbol{\tau}|\boldsymbol{y})$, which is our target posterior density. Using draws from all full conditional distribution distributions of (6.6), we can run a Gibbs sampler with stationary density (6.6). It is known that by combining and simultaneously drawing multiple parameters, the convergence of the Gibbs sampler can be improved (Liu et al., 1994). Here we construct a two-block Gibbs sampler for (6.6). Let $\boldsymbol{\eta}=\left(\boldsymbol{\beta}^T,\boldsymbol{u}^T\right)^T$, $\boldsymbol{\kappa}=(\kappa_1,\ldots,\kappa_n)$ and $\boldsymbol{M}=(\boldsymbol{X},\boldsymbol{Z})$ with ith row $\boldsymbol{m}_i^T$ and $\boldsymbol{\Omega}$ be the $n\times n$ diagonal matrix with ith diagonal element ω_i. Standard calculations show that the conditional density of $\boldsymbol{\eta}$ is

$$\pi\left(\boldsymbol{\eta}|\boldsymbol{\omega},\boldsymbol{\tau},\boldsymbol{y}\right)\propto\exp\left[-\frac{1}{2}\boldsymbol{\eta}^T\boldsymbol{M}^T\boldsymbol{\Omega}\boldsymbol{M}\boldsymbol{\eta}+\boldsymbol{\eta}^T\boldsymbol{M}^T\boldsymbol{\kappa}\right]\exp\left[-\frac{1}{2}\boldsymbol{\eta}^T\boldsymbol{A}\left(\boldsymbol{\tau}\right)\boldsymbol{\eta}+\boldsymbol{\eta}^T\boldsymbol{l}\right],$$

where $\boldsymbol{l}=\left(\boldsymbol{\mu}_0^T,\boldsymbol{0}_{1\times q}\right)^T$, and $\boldsymbol{A}\left(\boldsymbol{\tau}\right)=\boldsymbol{Q}\oplus\boldsymbol{D}(\boldsymbol{\tau})$. That is,

$$\boldsymbol{\eta}|\boldsymbol{\omega},\boldsymbol{\tau},\boldsymbol{y}\sim N\left(\boldsymbol{\Sigma}^{-1}\boldsymbol{\mu},\boldsymbol{\Sigma}^{-1}\right) \tag{6.7}$$

$$\text{where }\boldsymbol{\Sigma}=\begin{pmatrix}\boldsymbol{X}^T\boldsymbol{\Omega}\boldsymbol{X}+\boldsymbol{Q} & \boldsymbol{X}^T\boldsymbol{\Omega}\boldsymbol{Z}\\ \boldsymbol{Z}^T\boldsymbol{\Omega}\boldsymbol{X} & \boldsymbol{Z}^T\boldsymbol{\Omega}\boldsymbol{Z}+\boldsymbol{D}(\boldsymbol{\tau})\end{pmatrix}=\boldsymbol{M}^T\boldsymbol{\Omega}\boldsymbol{M}+\boldsymbol{A}\left(\boldsymbol{\tau}\right),\quad\boldsymbol{\mu}=\boldsymbol{M}^T\boldsymbol{\kappa}+\boldsymbol{l}.$$

Similarly, the conditional density of $(\boldsymbol{\omega}, \boldsymbol{\tau})$ is

$$\pi(\boldsymbol{\omega}, \boldsymbol{\tau}|\boldsymbol{\beta}, \boldsymbol{u}, \boldsymbol{y}) \propto \prod_{i=1}^{N} \exp\left[-\omega_i \left(\boldsymbol{x}_i^T\boldsymbol{\beta} + \boldsymbol{z}_i^T\boldsymbol{u}\right)^2/2\right] p(\omega_i) \times \prod_{j=1}^{r} \tau_j^{a_j+q_j/2-1} \exp\left[-\left(\boldsymbol{u}_j^T\boldsymbol{u}_j/2 + b_j\right)\tau_j\right] I(\tau_j \geq \tau_0).$$

So, given $\boldsymbol{\beta}, \boldsymbol{u}, \boldsymbol{y}$, we have that $\boldsymbol{\omega}$ and $\boldsymbol{\tau}$ are conditionally independent with

$$\omega_i|\boldsymbol{\eta}, \boldsymbol{y} \overset{ind}{\sim} PG\left(n_i, |\boldsymbol{m}_i^T\boldsymbol{\eta}|\right), \; i = 1, \ldots, N,$$
$$\tau_j|\boldsymbol{\eta}, \boldsymbol{y} \overset{ind}{\sim} \text{truncated Gamma}\left(a_j + \frac{q_j}{2}, b_j + \frac{\boldsymbol{u}_j^T\boldsymbol{u}_j}{2}, \tau_0\right), \; j = 1, \ldots, r.$$

Remark 6.1. *As in Wang and Roy (2017), we assume that the prior distribution for τ_j is a truncated Gamma distribution. However, while implementing the block Gibbs sampler in practice, a number slightly larger than the machine precision zero can be treated as τ_0, practically avoiding the need to use any rejection sampling algorithms to draw from the truncated conditional distribution of $\boldsymbol{\tau}$.*

Thus, one single iteration of the block Gibbs sampler $\{\boldsymbol{\eta}^{(m)}, \boldsymbol{\omega}^{(m)}, \boldsymbol{\tau}^{(m)}\}_{m=0}^{\infty}$ has the following two steps:

Algorithm: The $(m+1)$st iteration for the two-block Gibbs sampler

1: Draw $\boldsymbol{\tau}_j^{(m+1)}$ from truncated Gamma $\left(a_j + q_j/2, b_j + \boldsymbol{u}_j^T\boldsymbol{u}_j/2, \tau_0\right)$ with $\boldsymbol{u} = \boldsymbol{u}^{(m)}$ for $j = 1, \ldots, r$, and independently draw $\omega_i^{(m+1)} \overset{\text{ind}}{\sim} PG\left(n_i, |\boldsymbol{m}_i^T\boldsymbol{\eta}^{(m)}|\right)$ for $i = 1, \ldots, N$.

2: Draw $\boldsymbol{\eta}^{(m+1)}$ from (6.7), $\boldsymbol{\eta}^{(m+1)} \sim N_{p+q}\left(\boldsymbol{\Sigma}^{(m)-1}\left(\boldsymbol{M}^T\boldsymbol{\kappa} + \boldsymbol{l}\right), \boldsymbol{\Sigma}^{(m)-1}\right)$, where $\boldsymbol{\Sigma}^{(m)} = \boldsymbol{M}^T\boldsymbol{\Omega}^{(m+1)}\boldsymbol{M} + \boldsymbol{A}(\boldsymbol{\tau}^{(m+1)})$ and the diagonal elements of $\boldsymbol{\Omega}^{(m+1)}$ are $\omega_i^{(m+1)}$, $i = 1, \ldots, N$.

Polson et al. (2013) developed an efficient method for sampling from PG distribution, which is the only nonstandard distribution involved in the above Gibbs sampler.

6.3 Uniform ergodicity of the two-block Gibbs sampler

In this section, we prove the uniform ergodicity of the two-block Gibbs sampler $\{\boldsymbol{\eta}^{(m)}, \boldsymbol{\omega}^{(m)}, \boldsymbol{\tau}^{(m)}\}_{m=0}^{\infty}$, which has the same rate of convergence as the $\boldsymbol{\eta}$-marginal Markov chain $\{\boldsymbol{\eta}^{(m)}\}_{m=0}^{\infty}$ (Roberts and Rosenthal, 2001). Below we analyze the $\boldsymbol{\Psi} \equiv \{\boldsymbol{\eta}^{(m)}\}_{m=0}^{\infty}$ chain.

Let $\boldsymbol{\eta}'$ be the current state and $\boldsymbol{\eta}$ be the next state, then the Markov transition density (Mtd) of $\boldsymbol{\Psi}$ is

$$k(\boldsymbol{\eta}|\boldsymbol{\eta}') = \int_{\mathbb{R}_+^r} \int_{\mathbb{R}_+^N} \pi(\boldsymbol{\eta}|\boldsymbol{\omega}, \boldsymbol{\tau}, \boldsymbol{y}) \pi(\boldsymbol{\omega}, \boldsymbol{\tau}|\boldsymbol{\eta}', \boldsymbol{y}) d\boldsymbol{\omega} d\boldsymbol{\tau}, \tag{6.8}$$

where $\pi(\cdot|\cdot, \boldsymbol{y})$'s are the conditional densities from section 6.2. Routine calculations show that $k(\boldsymbol{\eta}|\boldsymbol{\eta}')$ is reversible and thus invariant with respect to the marginal density of $\boldsymbol{\eta}$ denoted as $\pi(\boldsymbol{\eta}|\boldsymbol{y}) \equiv \int_{\mathbb{R}_+^r} \int_{\mathbb{R}_+^N} \pi(\boldsymbol{\eta}, \boldsymbol{\omega}, \boldsymbol{\tau}|\boldsymbol{y}) d\boldsymbol{\omega} d\boldsymbol{\tau}$, where $\pi(\boldsymbol{\eta}, \boldsymbol{\omega}, \boldsymbol{\tau}|\boldsymbol{y})$ is defined in (6.6). Since $k(\boldsymbol{\eta}|\boldsymbol{\eta}')$ is strictly positive, the Markov chain $\boldsymbol{\Psi}$ is Harris ergodic (Hobert, 2011).

Let $\mathscr{B}$ denote the Borel σ-algebra of $\mathbb{R}^{p+q}$ and $K(\cdot, \cdot)$ be the Markov transition function corresponding to the Mtd $k(\cdot, \cdot)$ in (6.8), that is, for any set $A \in \mathscr{B}$, $\boldsymbol{\eta}' \in \mathbb{R}^{p+q}$ and any $j = 0, 1, \ldots,$

$$K(\boldsymbol{\eta}', A) = \Pr(\boldsymbol{\eta}^{(j+1)} \in A | \boldsymbol{\eta}^{(j)} = \boldsymbol{\eta}') = \int_A k(\boldsymbol{\eta}|\boldsymbol{\eta}') d\boldsymbol{\eta}. \tag{6.9}$$

Then the m-step Markov transition function is $K^m(\boldsymbol{\eta}', A) = \Pr(\boldsymbol{\eta}^{(m+j)} \in A | \boldsymbol{\eta}^{(j)} = \boldsymbol{\eta}')$. Let $\Pi(\cdot|\boldsymbol{y})$ be the probability measure with density $\pi(\boldsymbol{\eta}|\boldsymbol{y})$. The Markov chain $\boldsymbol{\Psi}$ is geometrically ergodic if there exists a constant $0 < t < 1$ and a function $G : \mathbb{R}^{p+q} \mapsto \mathbb{R}^+$ such that for any $\boldsymbol{\eta} \in \mathbb{R}^{p+q}$,

$$||K^m(\boldsymbol{\eta}, \cdot) - \Pi(\cdot|\boldsymbol{y})|| := \sup_{A \in \mathscr{B}} |K^m(\boldsymbol{\eta}, A) - \Pi(A|\boldsymbol{y})| \leq G(\boldsymbol{\eta}) t^m. \tag{6.10}$$

If $G(\boldsymbol{\eta})$ is bounded above, then the corresponding Markov chain is uniformly ergodic. The following theorem establishes uniform ergodicity of the Markov chain $\boldsymbol{\Psi}$ by constructing a minorization condition.

Theorem 6.1. *Assume that $a_j + q_j/2 \geq 1$ and $b_j > 0$ for all j, then the Markov chain $\boldsymbol{\Psi}$ is uniformly ergodic.*

Proof. We show that there exists a $\delta > 0$ and a density function $h : \mathbb{R}^{p+q} \to [0, \infty)$ such that, for all $\boldsymbol{\eta}', \boldsymbol{\eta} \in \mathbb{R}^{p+q}$,

$$k(\boldsymbol{\eta}|\boldsymbol{\eta}') \geq \delta h(\boldsymbol{\eta}). \tag{6.11}$$

By Roberts and Rosenthal (2004)[Theorem 8], (6.11) implies that the Markov chain $\boldsymbol{\Psi}$ is uniformly ergodic. Furthermore, under (6.11), (6.10) holds with $G = 1$ and $t = 1 - \delta$.

For $\tau_j \geq \tau_0$, $j = 1, \ldots, q$, $\boldsymbol{\Sigma} \geq \boldsymbol{M}^T \boldsymbol{\Omega} \boldsymbol{M} + \boldsymbol{A}(\tau_0)$, that is $\boldsymbol{\Sigma} - (\boldsymbol{M}^T \boldsymbol{\Omega} \boldsymbol{M} + \boldsymbol{A}(\tau_0))$ is positive semidefinite. So $|\boldsymbol{\Sigma}| \geq \left|\boldsymbol{M}^T \boldsymbol{\Omega} \boldsymbol{M} + \boldsymbol{A}(\tau_0)\right| = |\boldsymbol{A}(\tau_0)| \left|\tilde{\boldsymbol{M}}^T \boldsymbol{\Omega} \tilde{\boldsymbol{M}} + \boldsymbol{I}\right| \geq |\boldsymbol{A}(\tau_0)|$, where $\tilde{\boldsymbol{M}} = \boldsymbol{M}\boldsymbol{A}(\tau_0)^{-1/2}$. And $\boldsymbol{\mu}^T \boldsymbol{\Sigma}^{-1} \boldsymbol{\mu} \leq \boldsymbol{\mu}^T \left(\boldsymbol{M}^T \boldsymbol{\Omega} \boldsymbol{M} + \boldsymbol{A}(\tau_0)\right)^{-1} \boldsymbol{\mu} \leq \boldsymbol{\mu}^T \boldsymbol{A}(\tau_0)^{-1} \boldsymbol{\mu}$. Then,

$$
\begin{aligned}
\pi(\boldsymbol{\eta}|\boldsymbol{\omega}, \boldsymbol{\tau}, \boldsymbol{y}) &= (2\pi)^{-\frac{p+q}{2}} |\boldsymbol{\Sigma}|^{\frac{1}{2}} \exp\left[-\frac{1}{2}\left(\boldsymbol{\eta} - \boldsymbol{\Sigma}^{-1}\boldsymbol{\mu}\right)^T \boldsymbol{\Sigma} \left(\boldsymbol{\eta} - \boldsymbol{\Sigma}^{-1}\boldsymbol{\mu}\right)\right] \\
&\geq (2\pi)^{-\frac{p+q}{2}} |\boldsymbol{A}(\tau_0)|^{1/2} \exp\left[-\frac{1}{2}\left(\boldsymbol{\eta}^T \boldsymbol{\Sigma} \boldsymbol{\eta} - 2\boldsymbol{\eta}^T \boldsymbol{\mu}\right) - \frac{1}{2}\boldsymbol{\mu}^T \boldsymbol{A}(\tau_0)^{-1} \boldsymbol{\mu}\right] \\
&= (2\pi)^{-\frac{p+q}{2}} |\boldsymbol{A}(\tau_0)|^{1/2} \exp\left[-\frac{1}{2}\boldsymbol{\beta}^T \boldsymbol{Q} \boldsymbol{\beta} - \frac{1}{2}\boldsymbol{u}^T \boldsymbol{D}(\boldsymbol{\tau}) \boldsymbol{u} + \boldsymbol{\eta}^T \boldsymbol{\mu} - \frac{1}{2}\boldsymbol{\mu}^T \boldsymbol{A}(\tau_0)^{-1} \boldsymbol{\mu}\right] \\
&\times \exp\left[-\frac{1}{2}\sum_{i=1}^{N} \omega_i \left(\boldsymbol{m}_i^T \boldsymbol{\eta}\right)^2\right].
\end{aligned}
$$

Therefore,

$$
\begin{aligned}
&\pi(\boldsymbol{\eta}|\boldsymbol{\omega}, \boldsymbol{\tau}, \boldsymbol{y}) \pi(\boldsymbol{\omega}, \boldsymbol{\tau}|\boldsymbol{\eta}', \boldsymbol{y}) \\
&\geq (2\pi)^{-\frac{p+q}{2}} |\boldsymbol{A}(\tau_0)|^{1/2} \exp\left[-\frac{1}{2}\boldsymbol{\beta}^T \boldsymbol{Q} \boldsymbol{\beta} - \frac{1}{2}\boldsymbol{u}^T \boldsymbol{D}(\boldsymbol{\tau}) \boldsymbol{u} + \boldsymbol{\eta}^T \boldsymbol{\mu} - \frac{1}{2}\boldsymbol{\mu}^T \boldsymbol{A}(\tau_0)^{-1} \boldsymbol{\mu}\right] \\
&\times \prod_{j=1}^{r} \frac{1}{c\left(\tau_0, a_j + q_j/2, b_j + \boldsymbol{u}_j'^T \boldsymbol{u}_j'/2\right)} \tau_j^{a_j + q_j/2 - 1} \exp\left[-\left(b_j + \boldsymbol{u}_j'^T \boldsymbol{u}_j'/2\right)\tau_j\right] I(\tau_j \geq \tau_0) \\
&\times \prod_{i=1}^{N} \cosh^{n_i}\left(\frac{\left|\boldsymbol{m}_i^T \boldsymbol{\eta}'\right|}{2}\right) \exp\left[-\frac{\left(\boldsymbol{m}_i^T \boldsymbol{\eta}'\right)^2 + \left(\boldsymbol{m}_i^T \boldsymbol{\eta}\right)^2}{2}\omega_i\right] p(\omega_i).
\end{aligned}
$$

According to Polson et al. (2013) and Choi and Hobert (2013),

$$
\begin{aligned}
&\int_{\mathbb{R}_+} \exp\left[-\frac{\left(\boldsymbol{m}_i^T \boldsymbol{\eta}'\right)^2 + \left(\boldsymbol{m}_i^T \boldsymbol{\eta}\right)^2}{2}\omega_i\right] p(\omega_i)\, d\omega_i = \left[\cosh\left(\frac{\sqrt{\left(\boldsymbol{m}_i^T \boldsymbol{\eta}'\right)^2 + \left(\boldsymbol{m}_i^T \boldsymbol{\eta}\right)^2}}{2}\right)\right]^{-n_i} \\
&\geq \left[\cosh\left(\frac{\left|\boldsymbol{m}_i^T \boldsymbol{\eta}'\right|}{2} + \frac{\left|\boldsymbol{m}_i^T \boldsymbol{\eta}\right|}{2}\right)\right]^{-n_i} \geq \left[2\cosh\left(\frac{\left|\boldsymbol{m}_i^T \boldsymbol{\eta}'\right|}{2}\right)\cosh\left(\frac{\left|\boldsymbol{m}_i^T \boldsymbol{\eta}\right|}{2}\right)\right]^{-n_i},
\end{aligned}
$$

implying

$$
\begin{aligned}
&\cosh^{n_i}\left(\frac{\left|\boldsymbol{m}_i^T \boldsymbol{\eta}'\right|}{2}\right) \int_{\mathbb{R}_+} \exp\left[-\frac{\left(\boldsymbol{m}_i^T \boldsymbol{\eta}'\right)^2 + \left(\boldsymbol{m}_i^T \boldsymbol{\eta}\right)^2}{2}\omega_i\right] p(\omega_i)\, d\omega_i \geq 2^{-n_i} \cosh^{-n_i}\left(\frac{\left|\boldsymbol{m}_i^T \boldsymbol{\eta}\right|}{2}\right) \\
&\geq 2^{-n_i}\left[\exp\left(\frac{\left|\boldsymbol{m}_i^T \boldsymbol{\eta}\right|}{2}\right)\right]^{-n_i} \geq 2^{-n_i}\left[\exp\left(\frac{\left(\boldsymbol{m}_i^T \boldsymbol{\eta}\right)^2 + 1}{4}\right)\right]^{-n_i} = 2^{-n_i} e^{-n_i/4} \exp\left[-\frac{n_i}{4}\left(\boldsymbol{m}_i^T \boldsymbol{\eta}\right)^2\right].
\end{aligned}
$$

So we have,

$$\begin{aligned}
&\int_{\mathbb{R}_+^N} \pi(\boldsymbol{\eta}|\boldsymbol{\omega},\boldsymbol{\tau},\boldsymbol{y})\pi(\boldsymbol{\omega},\boldsymbol{\tau}|\boldsymbol{\eta}',\boldsymbol{y})d\boldsymbol{\omega} \\
&\geq (2\pi)^{-\frac{p+q}{2}} \left|\boldsymbol{A}\left(\tau_0\right)\right|^{1/2} \exp\left[-\frac{1}{2}\boldsymbol{\beta}^T\boldsymbol{Q}\boldsymbol{\beta}+\boldsymbol{\eta}^T\boldsymbol{\mu}-\frac{1}{2}\boldsymbol{\mu}^T\boldsymbol{A}\left(\tau_0\right)^{-1}\boldsymbol{\mu}\right] \\
&\times 2^{-n}e^{-\frac{n}{4}} \exp\left[-\frac{1}{4}\boldsymbol{\eta}^T\boldsymbol{M}^T\boldsymbol{\Lambda}\boldsymbol{M}\boldsymbol{\eta}\right] \\
&\times \prod_{j=1}^{r}[c\left(\tau_0, a_j+q_j/2, b_j+\boldsymbol{u}_j'^T\boldsymbol{u}_j'/2\right)]^{-1}\tau_j^{a_j+q_j/2-1}\exp\left[-\left(b_j+\boldsymbol{u}_j'^T\boldsymbol{u}_j'/2+\boldsymbol{u}_j^T\boldsymbol{u}_j/2\right)\tau_j\right] I(\tau_j\geq\tau_0),
\end{aligned}$$

where $n=\sum_{i=1}^N n_i$ and $\boldsymbol{\Lambda}$ is the $N\times N$ diagonal matrix with ith diagonal element n_i. Thus,

$$\begin{aligned}
&k(\boldsymbol{\eta}|\boldsymbol{\eta}') = \int_{\mathbb{R}_+^r}\int_{\mathbb{R}_+^N} \pi(\boldsymbol{\eta}|\boldsymbol{\omega},\boldsymbol{\tau},\boldsymbol{y})\pi(\boldsymbol{\omega},\boldsymbol{\tau}|\boldsymbol{\eta}',\boldsymbol{y})d\boldsymbol{\omega}d\boldsymbol{\tau} \\
&\geq (2\pi)^{-\frac{p+q}{2}} \left|\boldsymbol{A}\left(\tau_0\right)\right|^{1/2} \exp\left[-\frac{1}{2}\boldsymbol{\beta}^T\boldsymbol{Q}\boldsymbol{\beta}+\boldsymbol{\eta}^T\boldsymbol{\mu}-\frac{1}{2}\boldsymbol{\mu}^T\boldsymbol{A}\left(\tau_0\right)^{-1}\boldsymbol{\mu}\right] \times 2^{-n}e^{-\frac{n}{4}} \exp\left[-\frac{1}{4}\boldsymbol{\eta}^T\boldsymbol{M}^T\boldsymbol{\Lambda}\boldsymbol{M}\boldsymbol{\eta}\right] \\
&\times \prod_{j=1}^{r}\frac{1}{c\left(\tau_0, a_j+q_j/2, b_j+\boldsymbol{u}_j'^T\boldsymbol{u}_j'/2\right)}\int_{\tau_0}^{\infty}\tau_j^{a_j+q_j/2-1}\exp\left[-\left(b_j+\boldsymbol{u}_j'^T\boldsymbol{u}_j'/2+\boldsymbol{u}_j^T\boldsymbol{u}_j/2\right)\tau_j\right]d\tau_j.
\end{aligned}$$

Now consider

$$\begin{aligned}
&\frac{1}{c\left(\tau_0, a_j+q_j/2, b_j+\boldsymbol{u}_j'^T\boldsymbol{u}_j'/2\right)}\int_{\tau_0}^{\infty}\tau_j^{a_j+q_j/2-1}\exp\left[-\left(b_j+\boldsymbol{u}_j'^T\boldsymbol{u}_j'/2+\boldsymbol{u}_j^T\boldsymbol{u}_j/2\right)\tau_j\right]d\tau_j \\
=&\frac{\left(b_j+\boldsymbol{u}_j'^T\boldsymbol{u}_j'/2\right)^{a_j+q_j/2}}{\left(b_j+\boldsymbol{u}_j'^T\boldsymbol{u}_j'/2+\boldsymbol{u}_j^T\boldsymbol{u}_j/2\right)^{a_j+q_j/2}}\cdot\frac{\int_{\left(b_j+\boldsymbol{u}_j'^T\boldsymbol{u}_j'/2+\boldsymbol{u}_j^T\boldsymbol{u}_j/2\right)\tau_0}^{\infty}x^{a_j+q_j/2-1}\exp\left(-x\right)dx,}{\int_{\left(b_j+\boldsymbol{u}_j'^T\boldsymbol{u}_j'/2\right)\tau_0}^{\infty}x^{a_j+q_j/2-1}\exp\left(-x\right)dx}
\end{aligned}$$

For $x\geq 0$, define, $f_1\left(x\right)=\int_{\left(b_j+x+\boldsymbol{u}_j^T\boldsymbol{u}_j/2\right)\tau_0}^{\infty}t^{a_j+q_j/2-1}\exp\left(-t\right)dt$, $f_2\left(x\right)=\int_{\left(b_j+x\right)\tau_0}^{\infty}t^{a_j+q_j/2-1}\exp\left(-t\right)dt$ and $g\left(x\right)=f_1\left(x\right)-\exp\left(-\tau_0\boldsymbol{u}_j^T\boldsymbol{u}_j/2\right)f_2\left(x\right)$. Since $a_j+q_j/2-1\geq 0$ by assumption, it can be shown that $g'\left(x\right)\leq 0$. And $g\left(x\right)\geq\lim_{x\to\infty}g\left(x\right)=0$. Thus $f_1\left(x\right)/f_2\left(x\right)\geq\exp\left[-\tau_0\boldsymbol{u}_j^T\boldsymbol{u}_j/2\right]$. Also $\left(b_j+\boldsymbol{u}_j'^T\boldsymbol{u}_j'/2\right)/\left(b_j+\boldsymbol{u}_j'^T\boldsymbol{u}_j'/2+\boldsymbol{u}_j^T\boldsymbol{u}_j/2\right)\geq b_j/\left(b_j+\boldsymbol{u}_j^T\boldsymbol{u}_j/2\right)$, So

$$\begin{aligned}
\kappa(\boldsymbol{\eta}|\boldsymbol{\eta}') \geq{}& (2\pi)^{-\frac{p+q}{2}} \left|\boldsymbol{A}\left(\tau_0\right)\right|^{1/2} \exp\left[-\frac{1}{2}\boldsymbol{\beta}^T\boldsymbol{Q}\boldsymbol{\beta}+\boldsymbol{\eta}^T\boldsymbol{\mu}-\frac{1}{2}\boldsymbol{\mu}^T\boldsymbol{A}\left(\tau_0\right)^{-1}\boldsymbol{\mu}\right] \\
&\times 2^{-n}e^{-\frac{n}{4}} \exp\left[-\frac{1}{4}\boldsymbol{\eta}^T\boldsymbol{M}^T\boldsymbol{\Lambda}\boldsymbol{M}\boldsymbol{\eta}\right] \times \prod_{j=1}^{r}\left(\frac{b_j}{b_j+\boldsymbol{u}_j^T\boldsymbol{u}_j/2}\right)^{a_j+q_j/2}\exp\left(-\tau_0\boldsymbol{u}_j^T\boldsymbol{u}_j/2\right).
\end{aligned}$$

Let

$$
\begin{aligned}
c_1(\boldsymbol{M},\boldsymbol{y}) &= \int_{\mathbb{R}^{p+q}} \exp\left[-\frac{1}{2}\boldsymbol{\beta}^T\boldsymbol{Q}\boldsymbol{\beta}+\boldsymbol{\eta}^T\boldsymbol{\mu}-\frac{1}{4}\boldsymbol{\eta}^T\boldsymbol{M}^T\boldsymbol{\Lambda}\boldsymbol{M}\boldsymbol{\eta}\right] \\
&\quad\times\prod_{j=1}^{r}\left(\frac{b_j}{b_j+\boldsymbol{u}_j^T\boldsymbol{u}_j/2}\right)^{a_j+q_j/2}\exp\left(-\tau_0\boldsymbol{u}_j^T\boldsymbol{u}_j/2\right)d\boldsymbol{\eta} \\
&\le (2\pi)^{\frac{p+q}{2}}\left|\boldsymbol{A}(\tau_0)\right|^{-1/2}\exp\left(\frac{1}{2}\boldsymbol{\mu}^T\boldsymbol{A}(\tau_0)\boldsymbol{\mu}\right)2^n e^{\frac{n}{4}}<\infty.
\end{aligned}
$$

So there exists a density function $h(\boldsymbol{\eta})$ and $\delta>0$ such that,

$$
k(\boldsymbol{\eta}|\boldsymbol{\eta}')=\int_{\mathbb{R}_+^r}\int_{\mathbb{R}_+^n}\pi(\boldsymbol{\eta}|\boldsymbol{\omega},\boldsymbol{\tau},\boldsymbol{y})\pi(\boldsymbol{\omega},\boldsymbol{\tau}|\boldsymbol{\eta}',\boldsymbol{y})d\boldsymbol{\omega}d\boldsymbol{\tau}\ge\delta h(\boldsymbol{\eta}),
$$

where

$$
\begin{aligned}
h(\boldsymbol{\eta}) &= \frac{1}{c_1(\boldsymbol{M},\boldsymbol{y})}\exp\left[-\frac{1}{2}\boldsymbol{\beta}^T\boldsymbol{Q}\boldsymbol{\beta}+\boldsymbol{\eta}^T\boldsymbol{\mu}-\frac{1}{4}\boldsymbol{\eta}^T\boldsymbol{M}^T\boldsymbol{\Lambda}\boldsymbol{M}\boldsymbol{\eta}\right] \\
&\quad\times\prod_{j=1}^{r}\left[b_j/(b_j+\boldsymbol{u}_j^T\boldsymbol{u}_j/2)\right]^{a_j+q_j/2}\exp\left(-\tau_0\boldsymbol{u}_j^T\boldsymbol{u}_j/2\right), \\
\text{and } \delta &= (2\pi)^{-\frac{p+q}{2}}\left|\boldsymbol{A}(\tau_0)\right|^{1/2}2^{-n}e^{-\frac{n}{4}}\cdot\exp\left[-\frac{1}{2}\boldsymbol{\mu}^T\boldsymbol{A}(\tau_0)^{-1}\boldsymbol{\mu}\right]c_1(\boldsymbol{M},\boldsymbol{y}).
\end{aligned}
$$

Hence the Markov chain is uniformly ergodic.

□

Remark 6.2. *Since Theorem 6.1 does not put any conditions on* $\boldsymbol{y}$, $\boldsymbol{X}$, $\boldsymbol{Z}$, N, p *and* q, *it is applicable in high dimensional situations where* p *(or* q*) can be much larger than* N.

Remark 6.3. *Following the proof of Theorem 6.1, the uniform ergodicity result in Choi and Hobert (2013) can be extended to binomial data.*

Remark 6.4. *Since* $1/(x+1)\ge\exp(-x)$, *we have* $b_j/(b_j+\boldsymbol{u}_j^T\boldsymbol{u}_j/2)\ge\exp\left[-\boldsymbol{u}_j^T\boldsymbol{u}_j/(2b_j)\right]$. *Using this inequality, we have*

$$
\delta\ge 2^{-n}e^{-\frac{n}{4}}\left|\boldsymbol{A}(\tau_0)\right|^{1/2}\left|\boldsymbol{\Sigma}_1\right|^{-1/2}\exp\left[-\frac{1}{2}\boldsymbol{\mu}^T\boldsymbol{A}(\tau_0)^{-1}\boldsymbol{\mu}+\frac{1}{2}\boldsymbol{\mu}^T\boldsymbol{\Sigma}_1^{-1}\boldsymbol{\mu}\right],
$$

where $\boldsymbol{\Sigma}_1=\frac{1}{2}\boldsymbol{M}^T\boldsymbol{\Lambda}\boldsymbol{M}+\boldsymbol{Q}\oplus\left[\oplus_{j=1}^r\{\tau_0+(a_j+q_j)/(2b_j)\}\boldsymbol{I}_{q_j}\right]$. *This in turn, gives a computable upper bound to the total variation distance to the stationary in* (6.10).

6.4 Discussion

We prove uniform ergodicity of the two-block Gibbs sampler for Bayesian logistic linear mixed models, which guarantees the existence of central limit theorem for MCMC estimators under a finite second moment condition (Jones, 2004). Thus, our result has important practical implications as it allows for obtaining valid asymptotic standard errors for the posterior estimates (Flegal and Jones, 2010). Convergence rates analysis of Gibbs samplers for Bayesian logistic linear mixed models with improper priors is a potential future project.

Bibliography

Albert, J. H. and Chib, S. (1993). Bayesian analysis of binary and polychotomous response data. *Journal of the American statistical Association*, 88(422):669–679.

Chakraborty, S. and Khare, K. (2017). Convergence properties of Gibbs samplers for Bayesian probit regression with proper priors. *Electronic Journal of Statistics*, 11:177–210.

Charles E. McCulloch, S. R. S. and Neuhaus, J. M. (2008). *Generalized, linear, and mixed models*. Wiley, 2nd ed edition.

Choi, H. M. and Hobert, J. P. (2013). The Pólya-Gamma Gibbs sampler for Bayesian logistic regression is uniformly ergodic. *Electronic Journal of Statistics*, 7:2054–2064.

Choi, H. M. and Román, J. C. (2017). Analysis of Pólya-Gamma Gibbs sampler for Bayesian logistic analysis of variance. *Electronic Journal of Statistics*, 11(1):326–337.

Flegal, J. M. and Jones, G. L. (2010). Batch means and spectral variance estimators in Markov chain Monte Carlo. *The Annals of Statistics*, 38(2):1034–1070.

Frühwirth-Schnatter, S. and Frühwirth, R. (2010). Data augmentation and MCMC for binary and multinomial logit models. In *Statistical Modelling and Regression Structures*, pages 111–132. Springer.

Hobert, J. P. (2011). The data augmentation algorithm: Theory and methodology. In Brooks, S., Gelman, A., Jones, G., and Meng, X.-L., editors, *Handbook of Markov Chain Monte Carlo*. Chapman & Hall/CRC Press.

Holmes, C. C. and Held, L. (2006). Bayesian auxiliary variable models for binary and multinomial regression. *Bayesian analysis*, 1(1):145–168.

Jones, G. L. (2004). On the markov chain central limit theorem. *Probability surveys*, 1:299âĂŞ–320.

Liu, J. S., Wong, W. H., and Kong, A. (1994). Covariance structure of the Gibbs sampler with applications to the comparisons of estimators and augmentation schemes. *Biometrika*, 81(1):27–40.

McCulloch, C. E. (2003). Generalized linear mixed models. *NSF-CBMS regional conference series in probability and statistics*, 7:i–84.

Polson, N. G., Scott, J. G., and Windle, J. (2013). Bayesian inference for logistic models using Pólya-Gamma latent variables. *Journal of the American statistical Association*, 108(504):1339–1349.

Roberts, G. O. and Rosenthal, J. S. (2001). Markov chains and de-initializing processes. *Scandinavian Journal of Statistics*, 28:489–504.

Roberts, G. O. and Rosenthal, J. S. (2004). General state space markov chains and MCMC algorithms. *Probability Surveys*, 1:20–71.

Roy, V. and Hobert, J. P. (2007). Convergence rates and asymptotic standard errors for Markov chain Monte Carlo algorithms for Bayesian probit regression. *Journal of the Royal Statistical Society: Series B*, 69(4):607–623.

Wang, X. and Roy, V. (2017). Convergence analysis of block Gibbs samplers for Bayesian probit linear mixed models. *arXiv preprint arXiv:1706.01846*.

CHAPTER 7. ESTIMATING SUBGROUPS FOR SPATIAL AREAL DATA WITH REPEATED MEASURES

Xin Wang [1],Zhengyuan Zhu [1] and Hao Helen Zhang[2]

[1]Department of Statistics, Iowa State University

[2]Department of Mathematics, University of Arizona

Abstract

We consider the subgroup analysis problem for spatial areal data with repeated measures. We use a concave pairwise fusion method with an objective function having both weighted least squares and pairwise penalty. Each paired penalty has its associated weight based on the corresponding spatial information. Alternating direction method of multiplier algorithm (ADMM) is applied to obtain estimates. We show that the oracle estimator based on weighted least squares is a local minimizer of the objective function with probability approaching 1 under some conditions. In simulation studies, we compare the performances of different weights as well as equal weights according to the estimated number of groups, root mean square error and adjusted Rand index. The results show that the spatial information will help when the minimal group difference is small or the number of repeated measures is small. We also apply the proposed method to find the relationship between two surveys.

key words: Areal data; Linear regression; Penalization; Repeated measures; Spatial clustering; Subgroup analysis

7.1 Introduction

Spatial clustering or spatial boundaries detection is an important problem in disease mapping, spatial epidemiology and population genetics (Hegarty and Barry, 2008; Reich and Bondell, 2011;

Lawson, 2013; Li et al., 2015). Lu and Carlin (2005) and Lu et al. (2007) considered areal boundary detection using a Bayesian hierarchical model based on the conditional autoregressive model (Banerjee et al., 2014). The boundaries were determined by the posterior distribution of the corresponding spatial process or spatial weights. These boundary detections focused on the clustering of observations instead of regression coefficients. Li et al. (2011) proposed a method based on Bayesian information criteria combined with spatial neighborhood information for boundary detection in spatial areal data. Li et al. (2015) used Dirichlet process and false discovery rate to detect the boundaries under a hierarchical model setting. These models detected the boundaries through modeling the spatial random effect with the same regression coefficients for all areas. Dirichlet process was also involved in modeling spatial dependence in genetics data to identify homogeneous groups (Reich and Bondell, 2011). Hegarty and Barry (2008) applied the product partition model (Hartigan, 1990) in a disease mapping problem without considering covariates and spatial information. Page and Quintana (2016) proposed the spatial product partition model with covariates, which put priors on the partitions according to the spatial locations of observations, but the exact number of groups cannot be obtained.

A clustering problem can also be solved through an optimization problem. Chi and Lange (2015) developed a method for the convex clustering problem through alternating direction method of multiplier algorithm (ADMM, Boyd et al. (2011)) with pairwise $L_p(p \geq 1)$ penalty. Nonnegative weights are considered to reduce bias for pairwise penalties. Fan and Guan (2018) considered a clustering problem with l_0 penalty on graphs. These two methods are developed for clustering based on observations. Besides clustering for observations, another problem is to obtain clusters or homogeneous groups based on regression coefficients. Ma and Huang (2016) and Ma and Huang (2017) extended the problem to linear regression settings and used the smoothly clipped absolute deviation (SCAD) penalty (Fan and Li, 2001) and the minimax concave penalty (MCP) (Zhang, 2010). They also showed theoretical properties of their estimators.

In spatial data analysis, observations near each other could share similar patterns, so spatial dependence information should be considered in models to find homogeneous groups. In this article,

we consider a spatial clustering or spatial subgroup analysis problem based on regression coefficients for spatial areal data with repeated measures. As in Ma and Huang (2016), we use pairwise concave penalties for the differences among group (cluster) regression coefficients. We also consider pairwise weights associated with each paired penalty based on spatial information. Several different pairwise weights are studied in simulation studies, which shows that the spatial information will help when the minimal group difference is small, or the number of repeated measures is small.

The article is organized as follows. In section 7.2, we describe the model and the corresponding ADMM algorithm. In section 7.3, we show the theoretical properties of the proposed estimator. The simulation study is conducted in section 7.4 under several scenarios to show the performances of the proposed estimator. We use an example to illustrate our proposed estimator in section 7.5. Finally, some discussions are given in section 7.6.

7.2 The model and the algorithm

In section 7.2.1, the model and the corresponding objective function are introduced. In section 7.2.2, we describe the ADMM algorithm to optimize the objective function.

7.2.1 The model with repeated measures

Let y_{ih} , $i = 1, \ldots, n$, $h = 1, \ldots, n_i$ be the response variable for the ith subject hth observation observed at location $\boldsymbol{s}_i$. Let $\boldsymbol{z}_{ih}$ and $\boldsymbol{x}_{ih}$ be the corresponding covariate vectors with dimension q and p respectively. The linear regression model with individual regression parameter $\boldsymbol{\beta}_i$ is

$$y_{ih} = \boldsymbol{z}_{ih}^T \boldsymbol{\eta} + \boldsymbol{x}_{ih}^T \boldsymbol{\beta}_{ih} + \epsilon_{ih}, \tag{7.1}$$

where ϵ_{ih}'s are i.i.d random errors with $E(\epsilon_{ih}) = 0$ and $Var(\epsilon_{ih}) = \sigma^2$. Assume there are K mutually exclusive subgroups and the corresponding partition of $\{1, \ldots, n\}$ is denoted as $\mathcal{G} = \{\mathcal{G}_1, \ldots, \mathcal{G}_K\}$. In the kth group, the regression parameter is denoted as $\boldsymbol{\alpha}_k$. The goal is to find a partition such that subjects in the same group have the same regression coefficients. That is, we want to find an estimated partition $\hat{\mathcal{G}} = \{\hat{\mathcal{G}}_1, \ldots, \hat{\mathcal{G}}_{\hat{K}}\}$, where $\hat{\mathcal{G}}_k = \{i : \hat{\boldsymbol{\beta}}_i = \hat{\boldsymbol{\alpha}}_k, 1 \leq i \leq n\}$. To

achieve this goal, we use the following objective function with pairwise penalty

$$Q_n\left(\boldsymbol{\eta}, \boldsymbol{\beta}; \lambda, \psi\right) = \frac{1}{2}\sum_{i=1}^{n}\frac{1}{n_i}\sum_{h=1}^{n_i}\left(y_{ih} - \boldsymbol{z}_{ih}^T\boldsymbol{\eta} - \boldsymbol{x}_{ih}^T\boldsymbol{\beta}_i\right)^2 + \sum_{1\le i<j\le n} p_\gamma\left(\left\|\boldsymbol{\beta}_i - \boldsymbol{\beta}_j\right\|, c_{ij}\lambda\right), \tag{7.2}$$

where, $\boldsymbol{\beta} = \left(\boldsymbol{\beta}_1^T, \ldots, \boldsymbol{\beta}_n^T\right)^T$, $\|\cdot\|$ denotes the Euclidean norm and $p_\gamma\left(\cdot, \lambda\right)$ is a penalty function with tuning parameter $\lambda \ge 0$. In the penalty term, we also incorporate weights c_{ij}'s associated with location $\boldsymbol{s}_i$ and $\boldsymbol{s}_j$.

In general, c_{ij} can be defined as

$$c_{ij} = \exp\left(-\psi\left\|\boldsymbol{s}_i - \boldsymbol{s}_j\right\| \cdot \left\|\hat{\boldsymbol{\beta}}_i - \hat{\boldsymbol{\beta}}_j\right\|\right),$$

where $\hat{\boldsymbol{\beta}}_i$ is an initial estimate of $\boldsymbol{\beta}_i$ and ψ is a tuning parameter. In areal data, c_{ij} can be defined as

$$c_{ij} = \exp\left(\psi\left(1 - a_{ij}\right) \cdot \left\|\hat{\boldsymbol{\beta}}_i - \hat{\boldsymbol{\beta}}_j\right\|\right), \tag{7.3}$$

where a_{ij} is the neighbor order between subject i and subject j, which means that if i and j are neighbors, $a_{ij} = 1$. If i and j are not neighbors, but they have at least one same neighbor, $a_{ij} = 2$. Similarly, we can have all the neighborhood order for all subjects or locations. The weights can also involve only regression coefficients or spatial information. If only regression coefficients are included, the corresponding weight is defined as

$$c_{ij} = \exp\left(-\psi\left\|\hat{\boldsymbol{\beta}}_i - \hat{\boldsymbol{\beta}}_j\right\|\right). \tag{7.4}$$

If only spatial information is considered, we have

$$c_{ij} = \exp\left(\psi(1 - a_{ij})\right). \tag{7.5}$$

For large λ, some $\|\boldsymbol{\beta}_i - \boldsymbol{\beta}_j\|$ can be shrank to be zeros. Furthermore, since we have an associated weight for each pair, $\|\boldsymbol{\beta}_i - \boldsymbol{\beta}_j\|$ with large weights tend to shrink faster than pairs with smaller weights. For spatial data, observations near each other tend to have similar trends. Thus, larger weights are used for closer locations. Besides that, if we have good initial estimates based on the replicates, we could also put more weights for pairs with similar initial estimates.

L_1 penalty (lasso) is a popular penalty function (Tibshirani, 1996) with form $p_\gamma(t,\lambda) = \lambda|t|$. But as in Ma and Huang (2017) shows, L_1 penalty tends to have too many estimated groups without pairwise weights, so they focused on SCAD and MCP. Here, we only consider SCAD penalty, which is defined as

$$p_\gamma(t,\lambda) = \lambda \int_0^{|t|} \min\{1, (\gamma - x/\lambda)_+/(\gamma-1)\}dx. \tag{7.6}$$

Here we treat γ as a fixed value as in Fan and Li (2001), Zhang (2010) and Ma and Huang (2016).

7.2.2 The algorithm

In this section, we show the ADMM algorithm to solve (7.7) in section 7.2.1, which is similar to Ma and Huang's (2017) algorithm.

Let $\hat{\lambda}$ and $\hat{\psi}$ be the selected tuning parameters, $\hat{K}$ be the estimated groups, $\hat{\boldsymbol{\beta}}$ and $\hat{\boldsymbol{\eta}}$ be the estimates of $\boldsymbol{\beta}$ and $\boldsymbol{\eta}$ based on selected $\hat{\lambda}$ and $\hat{\psi}$. For given λ and ψ, the solution for (7.2) is

$$\left(\hat{\boldsymbol{\eta}}, \hat{\boldsymbol{\beta}}\right) = \underset{\boldsymbol{\eta}\in\mathbb{R}^q, \boldsymbol{\beta}\in\mathbb{R}^{np}}{\arg\min}\, Q_n\left(\boldsymbol{\eta}, \boldsymbol{\beta}, \lambda, \psi\right). \tag{7.7}$$

In the ADMM algorithm, let $\boldsymbol{\delta}_{ij} = \boldsymbol{\beta}_i - \boldsymbol{\beta}_j$, the problem becomes minimization of following objective function

$$L_0\left(\boldsymbol{\eta}, \boldsymbol{\beta}, \boldsymbol{\delta}\right) = \frac{1}{2}\sum_{i=1}^{n}\frac{1}{n_i}\sum_{h=1}^{n_i}\left(y_{ih} - \boldsymbol{z}_{ih}^T\boldsymbol{\eta} - \boldsymbol{x}_{ih}^T\boldsymbol{\beta}_i\right)^2 + \sum_{1\le i<j\le n} p_\gamma\left(\left\|\boldsymbol{\delta}_{ij}\right\|, c_{ij}\lambda\right),$$

$$\text{subject to } \boldsymbol{\beta}_i - \boldsymbol{\beta}_j - \boldsymbol{\delta}_{ij} = \mathbf{0}.$$

where $\boldsymbol{\delta} = \left(\boldsymbol{\delta}_{ij}^T, i<j\right)^T$. The augmented Lagrangian is

$$L\left(\boldsymbol{\eta}, \boldsymbol{\beta}, \boldsymbol{\delta}, \boldsymbol{v}\right) = L_0\left(\boldsymbol{\eta}, \boldsymbol{\beta}, \boldsymbol{\delta}\right) + \sum_{i<j}\left\langle \boldsymbol{v}_{ij}, \boldsymbol{\beta}_i - \boldsymbol{\beta}_j - \boldsymbol{\delta}_{ij}\right\rangle + \frac{\vartheta}{2}\sum_{i<j}\left\|\boldsymbol{\beta}_i - \boldsymbol{\beta}_j - \boldsymbol{\delta}_{ij}\right\|^2,$$

where $\boldsymbol{v} = \left(\boldsymbol{v}_{ij}^T, i<j\right)^T$ are Lagrange multipliers and ϑ is the penalty parameter. Given $\boldsymbol{\delta}^m$ and $\boldsymbol{v}^m$, the updates of $\boldsymbol{\eta}, \boldsymbol{\beta}, \boldsymbol{\delta}, \boldsymbol{v}$ are

$$\begin{aligned}
\left(\boldsymbol{\eta}^{m+1}, \boldsymbol{\beta}^{m+1}\right) &= \underset{\boldsymbol{\eta},\boldsymbol{\beta}}{\arg\min}\, L\left(\boldsymbol{\eta}, \boldsymbol{\beta}, \boldsymbol{\delta}^m, \boldsymbol{v}^m\right), \\
\boldsymbol{\delta}^{m+1} &= \underset{\boldsymbol{\delta}}{\arg\min}\, L\left(\boldsymbol{\eta}^{m+1}, \boldsymbol{\beta}^{m+1}, \boldsymbol{\delta}, \boldsymbol{v}^m\right), \\
\boldsymbol{v}_{ij}^{m+1} &= \boldsymbol{v}_{ij}^m + \vartheta\left(\boldsymbol{\beta}_i^{m+1} - \boldsymbol{\beta}_j^{m+1} - \boldsymbol{\delta}_{ij}^{m+1}\right).
\end{aligned} \tag{7.8}$$

To update $\boldsymbol{\eta}$ and $\boldsymbol{\beta}$, the problem becomes minimization of the following objective function

$$f(\boldsymbol{\beta},\boldsymbol{\eta}) = \left\|\boldsymbol{\Omega}^{1/2}(\boldsymbol{y}-\boldsymbol{Z}\boldsymbol{\eta}-\boldsymbol{X}\boldsymbol{\beta})\right\|^2 + \vartheta\left\|\boldsymbol{A}\boldsymbol{\beta}-\boldsymbol{\delta}^m+\vartheta^{-1}\boldsymbol{v}^m\right\|^2,$$

where $\boldsymbol{y} = (y_{11},\ldots,y_{1n_1},\ldots,y_{n1},\ldots,y_{n,n_n})^T$, $\boldsymbol{Z} = (\boldsymbol{z}_{11},\ldots,\boldsymbol{z}_{1n_1},\ldots,\boldsymbol{z}_{n1},\ldots,\boldsymbol{z}_{n,n_n})^T$, $\boldsymbol{X} = \mathrm{diag}(\boldsymbol{X}_1,\ldots,\boldsymbol{X}_n)$ with $\boldsymbol{X}_i = (\boldsymbol{x}_{i1},\ldots,\boldsymbol{x}_{i,n_i})^T$, $\boldsymbol{\Omega} = \mathrm{diag}(1/n_1\boldsymbol{I}_{n_1},\ldots,1/n_n\boldsymbol{I}_{n_n})$ and $\boldsymbol{A} = \boldsymbol{D}\otimes\boldsymbol{I}_p$ with an $n(n-1)/2\times$ n matrix $\boldsymbol{D} = \{(\boldsymbol{e}_i-\boldsymbol{e}_j)\}^T$, where e_i is an $n\times 1$ vector with ith element 1 and other elements 0. Then the solutions for $\boldsymbol{\beta}$ and $\boldsymbol{\eta}$ are

$$\boldsymbol{\beta}^{(m+1)} = \left(\boldsymbol{X}^T\boldsymbol{Q}_{Z,\Omega}\boldsymbol{X}+\vartheta\boldsymbol{A}^T\boldsymbol{A}\right)^{-1}\left[\boldsymbol{X}^T\boldsymbol{Q}_{Z,\Omega}\boldsymbol{y}+\vartheta\mathrm{vec}\left(\left(\boldsymbol{\Delta}^m-\vartheta^{-1}\boldsymbol{\Upsilon}^m\right)\boldsymbol{D}\right)\right], \tag{7.9}$$

$$\boldsymbol{\eta}^{(m+1)} = \left(\boldsymbol{Z}^T\boldsymbol{\Omega}\boldsymbol{Z}\right)^{-1}\boldsymbol{Z}^T\boldsymbol{\Omega}\left(\boldsymbol{y}-\boldsymbol{X}\boldsymbol{\beta}^{(m+1)}\right), \tag{7.10}$$

where $\boldsymbol{\Delta}^m = \left(\boldsymbol{\delta}_{ij}^m, i<j\right)_{p\times n(n-1)/2}$, $\boldsymbol{\Upsilon}^m = \left(\boldsymbol{v}_{ij}^m, i<j\right)_{p\times n(n-1)/2}$ and

$$\boldsymbol{Q}_{Z,\Omega} = \boldsymbol{\Omega}-\boldsymbol{\Omega}\boldsymbol{Z}\left(\boldsymbol{Z}^T\boldsymbol{\Omega}\boldsymbol{Z}\right)^{-1}\boldsymbol{Z}^T\boldsymbol{\Omega} = \boldsymbol{\Omega}^{1/2}\left(\boldsymbol{I}-\boldsymbol{P}_{\boldsymbol{\Omega}^{1/2}\boldsymbol{Z}}\right)\boldsymbol{\Omega}^{1/2}.$$

Updating $\boldsymbol{\delta}$ is equivalent to minimize

$$\frac{\vartheta}{2}\left\|\boldsymbol{\varsigma}_{ij}^m-\boldsymbol{\delta}_{ij}\right\|^2 + p_\gamma\left(\|\boldsymbol{\delta}_{ij}\|, c_{ij}\lambda\right),$$

where $\boldsymbol{\varsigma}_{ij}^m = \left(\boldsymbol{\beta}_i^{m+1}-\boldsymbol{\beta}_j^{m+1}\right)+\vartheta^{-1}\boldsymbol{v}_{ij}^m$. The solution based on SCAD penalty is

$$\boldsymbol{\delta}_{ij}^{m+1} = \begin{cases} S\left(\boldsymbol{\varsigma}_{ij}^m, \lambda c_{ij}/\vartheta\right) & \text{if } \left\|\boldsymbol{\varsigma}_{ij}^m\right\| \le \lambda c_{ij}+\lambda c_{ij}/\vartheta, \\ \frac{S\left(\boldsymbol{\varsigma}_{ij}^m,\gamma\lambda c_{ij}/((\gamma-1)\vartheta)\right)}{1-1/((\gamma-1)\vartheta)} & \text{if } \lambda c_{ij}+\lambda c_{ij}/\vartheta < \left\|\boldsymbol{\varsigma}_{ij}^m\right\| \le \gamma\lambda c_{ij}, \\ \boldsymbol{\varsigma}_{ij}^m & \text{if } \left\|\boldsymbol{\varsigma}_{ij}^m\right\| > \gamma\lambda c_{ij}, \end{cases} \tag{7.11}$$

where $\gamma > c_{ij}+c_{ij}/\vartheta$ and $S(\boldsymbol{w},t) = (1-t/\|\boldsymbol{w}\|)_+\boldsymbol{w}$, and $(t)_+ = t$ if $t>0$, 0 otherwise.

The algorithm can be summarized as follows.

If $n_i = 1$ or small, the initial values can be set using the procedure in Ma and Huang (2016). If the size of n_i is reasonable, such as 10 or lager. We start with n groups with $\hat{\boldsymbol{\beta}}_i$ estimated from fitting a linear regression model $y_{ih} = \boldsymbol{z}_{ih}^T\boldsymbol{\eta}_i+\boldsymbol{x}_{ih}^T\boldsymbol{\beta}_i+\epsilon_{ih}$ for each $i=1,\ldots,n$. Then set

Algorithm: ADMM algorithm

Require: : Initialize $\boldsymbol{\beta}_0$, $\boldsymbol{\delta}_0$ and $\boldsymbol{v}_0$.

for $m = 0, 1, 2, \ldots$ **do**
  Update $\boldsymbol{\beta}$ by (7.9).
  Update $\boldsymbol{\eta}$ by (7.10).
  Update $\boldsymbol{\delta}$ by (7.11)
  Update $\boldsymbol{v}$ by (7.8).
  if convergence criterion is met **then**
    Stop and get the estimates
  else
    $m = m + 1$
  end if
end for

$\boldsymbol{\delta}_{ij}^0 = \boldsymbol{\beta}_i^0 - \boldsymbol{\beta}_j^0$ and $\boldsymbol{v}^0 = \mathbf{0}$. We use three or four values for tuning parameter ψ, such as 0.1, 0.5, 1, 3. For each ψ, we use the warm start and continuation strategy as in Ma and Huang (2016) to select tuning parameter λ.

If $\hat{\boldsymbol{\delta}}_{ij} = \mathbf{0}$, then the subject i and j are in the same group. The we can obtain the corresponding estimated partition $\hat{\mathcal{G}}$ and the estimated number of groups $\hat{K}(\lambda, \psi)$. The estimated group parameter vector is $\hat{\boldsymbol{\alpha}}_k = 1/|\hat{\mathcal{G}}_k| \sum_{i \in \hat{\mathcal{G}}_k} \hat{\boldsymbol{\beta}}_i$.

Remark 7.1. *If the the model is* $y_{ih} = \boldsymbol{x}_{ih}^T \boldsymbol{\beta}_i + \epsilon_{ih}$, $\boldsymbol{\eta}$ *is not needed to update. When updating* $\boldsymbol{\beta}$, *set* $\boldsymbol{Q}_{Z,\Omega} = \boldsymbol{\Omega}$.

Remark 7.2. *The convergence criterion used is the same as Ma and Huang (2017), which is based on the primal residual* $\boldsymbol{r}^{(m+1)} = \boldsymbol{A}\boldsymbol{\beta}^{(m+1)} - \boldsymbol{\delta}^{(m+1)}$. *The algorithm is stopped if* $\|\boldsymbol{r}^{(m+1)}\| < \varepsilon$, *where* ε *is a small positive value.*

7.3 Theoretical properties

In this section, we study the theoretical properties of the proposed estimator.

Let $\widetilde{\boldsymbol{W}}$ be an $n \times K$ matrix with element w_{ik} and $w_{ik} = 1$ if $i \in \mathcal{G}_k$, $w_{ik} = 0$, otherwise. Denote $\boldsymbol{W} = \widetilde{\boldsymbol{W}} \otimes \boldsymbol{I}_p$, which is an $np \times Kp$ matrix and $\boldsymbol{U} = (\boldsymbol{Z}, \boldsymbol{X}\boldsymbol{W})$. Define $\mathcal{M}_{\mathcal{G}} = \{\boldsymbol{\beta} \in \mathbb{R}^{np} : \boldsymbol{\beta}_i = \boldsymbol{\beta}_j, \text{ for } i, j \in \mathcal{G}_k, 1 \le k \le K\}$. Thus, $\boldsymbol{\beta}$ can be written as $\boldsymbol{\beta} = \boldsymbol{W}\boldsymbol{\alpha}$ if $\boldsymbol{\beta} \in \mathcal{M}_{\mathcal{G}}$, where

$\boldsymbol{\alpha} = \left(\boldsymbol{\alpha}_1^T, \ldots, \boldsymbol{\alpha}_K^T\right)^T$. Let $|\mathcal{G}_k|$ be the number of subjects in group $\mathcal{G}_k$ for $k = 1, \ldots, K$, $|\mathcal{G}_{\min}|$ and $|\mathcal{G}_{\max}|$ be the minimum and maximum group sizes respectively. For any positive numbers, x_n and y_n, $x_n \gg y_n$ means that $x_n^{-1} y_n = o(1)$. Define the scaled penalty function by

$$\rho_\gamma(t) = \lambda^{-1} p_\gamma(t, \lambda). \tag{7.12}$$

Below are our assupmtions, where (C1), (C3) follows those in Ma and Huang (2016).

(C1) The function $\rho_\gamma(t)$ is a symmetric, non-decreasing and concave on $[0, \infty)$. It is constant for $t \geq a\lambda$ for some constant $a > 0$, and $\rho_\gamma(0) = 0$. Also, $\rho'(t)$ exists and is continuous except for a finite number values of t and $\rho'(0+) = 1$.

(C2) There exist finite positive constants $M_1, M_2, M_3 > 0$ such that $|x_{ih,l}| \leq M_1$, $|z_{ih,l}| \leq M_1$ for $j = 1, \ldots, n_i$ and $i = 1, \ldots, n$ and $M_2 \leq \max_i n_i / \min_i n_i \leq M_3$. Also, assume that $\lambda_{\min}\left(\boldsymbol{U}^T \boldsymbol{\Omega} \boldsymbol{U}\right) \geq C_1 |\mathcal{G}_{\min}|$, $\lambda_{\max}\left(\boldsymbol{U}^T \boldsymbol{\Omega} \boldsymbol{U}\right) \leq C_1' n$ for some constant $0 < C_1 < \infty$ and $0 < C_1' < \infty$, where $\lambda_{\min}$ and $\lambda_{\max}$ are the corresponding minimum and maximum eigenvalues respectively. Besides that, we also assume that $\sup_{i,h} \|\boldsymbol{x}_{ih}\| \leq C_2\sqrt{p}$ and $\sup_{i,h} \|\boldsymbol{z}_{ih}\| \leq C_3\sqrt{q}$ for some constants $0 < C_2 < \infty$ and $0 < C_3 < \infty$.

(C3) The random error vector $\boldsymbol{\epsilon} = (\epsilon_{11}, \ldots, \epsilon_{1n_1}, \epsilon_{21}, \ldots, \epsilon_{2n_2}, \ldots, \epsilon_{n1}, \ldots, \epsilon_{nn_n})^T$ has sub-Gaussian tails such that $P\left(\left|\boldsymbol{a}^T \boldsymbol{\epsilon}\right| > \|\boldsymbol{a}\| x\right) \leq 2\exp\left(-c_1 x^2\right)$ for any vector $\boldsymbol{a} \in \mathbb{R}^m$ and $x > 0$, where $0 < c_1 < \infty$ and $m = \sum_{i=1}^n n_i$.

(C4) The pairwise weights c_{ij}'s are bounded if i and j are in the same group.

We first study the properties of the oracle estimator, which is the weighted least squares estimator assuming that the underlying group structure is known. The oracle estimator of $(\boldsymbol{\eta}, \boldsymbol{\alpha})$ is

$$\begin{aligned}(\hat{\boldsymbol{\eta}}^{or}, \hat{\boldsymbol{\alpha}}^{or}) &= \underset{\boldsymbol{\eta} \in \mathbb{R}^q, \boldsymbol{\alpha} \in \mathbb{R}^{Kp}}{\arg\min} \frac{1}{2} \left\| \boldsymbol{\Omega}^{1/2} \left(\boldsymbol{y} - \boldsymbol{Z}\boldsymbol{\eta} - \boldsymbol{X}\boldsymbol{W}\boldsymbol{\alpha}\right) \right\|^2 \\ &= \left(\boldsymbol{U}^T \boldsymbol{\Omega} \boldsymbol{U}\right)^{-1} \boldsymbol{U}^T \boldsymbol{\Omega} \boldsymbol{y}. \end{aligned} \tag{7.13}$$

Thus, the corresponding oracle estimator of $\boldsymbol{\beta}$ is $\hat{\boldsymbol{\beta}}^{or} = \boldsymbol{W}\hat{\boldsymbol{\alpha}}^{or}$. Let $\boldsymbol{\alpha}_k^0$ be the true coefficient vector for group k, $k = 1, \ldots, K$ and $\boldsymbol{\alpha}^0 = ((\boldsymbol{\alpha}_1^0)^T, \ldots, (\boldsymbol{\alpha}_K^0)^T)^T$, and let $\boldsymbol{\eta}^0$ be the true common coefficient vector. The following theorem shows the properties of the oracle estimator.

Theorem 7.1. *Suppose*

$$|\mathcal{G}_{\min}| \gg (q + Kp)^{1/2} \max\left(\sqrt{\frac{n}{\min_i n_i}\log n}, (q + Kp)^{1/2}\right).$$

Under conditions (C1)-(C3), $q = o(n)$ and $Kp = o(n)$, we have with probability at least $1 - 2(q + Kp)n^{-1}$,

$$\left\| \begin{pmatrix} \hat{\boldsymbol{\eta}}^{or} - \boldsymbol{\eta}^0 \\ \hat{\boldsymbol{\alpha}}^{or} - \boldsymbol{\alpha}^0 \end{pmatrix} \right\| \leq \phi_n,$$

and

$$\left\|\hat{\boldsymbol{\beta}}^{or} - \boldsymbol{\beta}^0\right\| \leq \sqrt{|\mathcal{G}_{\max}|}\phi_n; \sup_i \left\|\hat{\boldsymbol{\beta}}_i^{or} - \boldsymbol{\beta}_i^0\right\| \leq \phi_n,$$

where

$$\phi_n = c_1^{-1/2} C_1^{-1} M_1 \sqrt{q + Kp}\, |\mathcal{G}_{\min}|^{-1} \sqrt{\frac{n}{\min n_i}\log n}.$$

Furthermore, for any vector $\boldsymbol{a}_n \in \mathbb{R}^{q+Kp}$, we have as $n \to \infty$

$$\sigma_n(\boldsymbol{a}_n)^{-1}\boldsymbol{a}_n^T \left(\left(\hat{\boldsymbol{\eta}}^{or} - \boldsymbol{\eta}^0\right)^T, \left(\hat{\boldsymbol{\alpha}}^{or} - \hat{\boldsymbol{\alpha}}^0\right)^T\right)^T \xrightarrow{d} N(0, 1), \tag{7.14}$$

where

$$\sigma_n(\boldsymbol{a}_n) = \sigma\left[\boldsymbol{a}_n^T \left(\boldsymbol{U}^T\boldsymbol{\Omega}\boldsymbol{U}\right)^{-1} \boldsymbol{U}^T\boldsymbol{\Omega}\boldsymbol{\Omega}\boldsymbol{U} \left(\boldsymbol{U}^T\boldsymbol{\Omega}\boldsymbol{U}\right)^{-1} \boldsymbol{a}_n\right]^{1/2}. \tag{7.15}$$

Remark 7.3. *If $\min n_i \ll \frac{n}{q+Kp}\log n$, or $\min n_i = O\left(\frac{n}{q+Kp}\log n\right)$, we have $|\mathcal{G}_{\min}| \gg (q + Kp)^{1/2}\sqrt{\frac{n}{\min n_i}\log n}$. If $\min n_i \gg \frac{n}{q+Kp}\log n$, we have $|\mathcal{G}_{\min}| \gg q + Kp$. In this case, if q, p and K are fixed values, what we need is only $1/|\mathcal{G}_{\min}| = o(1)$.*

Remark 7.4. *If $n_i = 1$, for $i = 1, \ldots, n$, we have the same model as Ma and Huang (2016). Our condition is*

$$|\mathcal{G}_{\min}| \gg (q + Kp)^{1/2}\sqrt{n \log n}. \tag{7.16}$$

In general, if n_i is bounded, we also have the above condition in (7.16). Our condition has lower rate than Ma and Huang (2016) with $|\mathcal{G}_{\min}| \gg (q+Kp)^{1/2} n^{3/4}$.

Remark 7.5. *If let $|\mathcal{G}_{\min}| = \delta n/K$ for some constant $0 < \delta \leq 1$, then*

$$\phi_n = c_1^{-1/2} C_1^{-1} M_1 \delta^{-1} K \sqrt{q+Kp} \sqrt{\log n/(n \min n_i)}.$$

Moreover, if q, p and K are fixed values, then $\phi_n = C^* \sqrt{\log n/(n \min n_i)}$ for some constant $0 < C^* < \infty$.

Next, we study the properties of our proposed estimator. Let

$$b_n = \min_{i \in \mathcal{G}_k, j \in \mathcal{G}_{k'}} \left\| \boldsymbol{\beta}_i^0 - \boldsymbol{\beta}_j^0 \right\| = \min_{k \neq k'} \left\| \boldsymbol{\alpha}_k^0 - \boldsymbol{\alpha}_{k'}^0 \right\| \tag{7.17}$$

be the minimal difference among different groups.

Theorem 7.2. *Suppose the conditions of Theorem 7.1 hold and (C4) holds. If $b_n > a\lambda$ and $\lambda \gg \phi_n$ for some constant $a > 0$, then there exists a local minimizer $\left(\hat{\boldsymbol{\eta}}(\lambda,\psi)^T, \hat{\boldsymbol{\beta}}(\lambda,\psi)^T\right)^T$ of the objective function $Q_n(\boldsymbol{\eta}, \boldsymbol{\beta})$ given in (7.2) such that*

$$P\left(\left(\hat{\boldsymbol{\eta}}(\lambda,\psi)^T, \hat{\boldsymbol{\beta}}(\lambda,\psi)^T\right)^T = \left((\hat{\boldsymbol{\eta}}(\lambda,\psi)^{or})^T, (\hat{\boldsymbol{\beta}}(\lambda,\psi)^{or})^T\right)^T\right) \to 1. \tag{7.18}$$

Remark 7.6. *Theorem 7.2 implies that true group structure can be recovered with probability approaching 1. It also implies that the estimated number of groups $\hat{K}$ satisfies*

$$P\left(\hat{K} = K\right) \to 1. \tag{7.19}$$

Given that the group structure is recovered in probability approaching 1, let $\hat{\boldsymbol{\alpha}}(\lambda,\psi)$ be the distinct group vectors of $\hat{\boldsymbol{\beta}}(\lambda,\psi)$. According to Theorem 7.1 and Theorem 7.2, we have the following result.

Corollary 7.1. *Suppose the conditions in Theorem 7.2 hold, for any vector $\boldsymbol{a}_n \in \mathbb{R}^{q+Kp}$, we have as $n \to \infty$*

$$\sigma_n(\boldsymbol{a}_n)^{-1} \boldsymbol{a}_n^T \left(\left(\hat{\boldsymbol{\eta}}(\lambda,\psi) - \boldsymbol{\eta}^0\right)^T, \left(\hat{\boldsymbol{\alpha}}(\lambda,\psi) - \hat{\boldsymbol{\alpha}}^0\right)^T\right)^T \xrightarrow{d} N(0,1). \tag{7.20}$$

Remark 7.7. *The variance parameter σ^2 can be estimated by*

$$\sigma^2 = \frac{1}{m - q - \hat{K}p} \sum_{i=1}^{n} \sum_{h=1}^{n_i} \left(y_{ih} - \boldsymbol{z}_{ih}^T \hat{\boldsymbol{\eta}} - \boldsymbol{x}_{ih}^T \hat{\boldsymbol{\beta}}_i\right)^2 \tag{7.21}$$

7.4 Simulation studies

In this section, we compare the performances of the proposed estimators with different pairwise weights $c_{ij} = 1$, (7.3), (7.4) and (7.5) based on 100 simulations.

$\boldsymbol{z}_{ih} = (z_{ih,1}, \ldots, z_{ih,5})^T$ with $z_{ih,1} = 1$ and $(z_{ih,2}, \ldots, z_{ih,5})^T$ are simulated from multivariate normal distribution with mean 0, variance 1 and correlation $\rho = 0.3$. $\boldsymbol{x}_{ih} = (x_{ih,1}, x_{ih,2})^T$, where $x_{ih,1}$ is simulated from standard normal distribution and $x_{ih,2}$ is simulated from centered and standardized binomial $(n, 0.7)$. $\boldsymbol{\eta} = (\eta_1, \ldots, \eta_5)^T$ with η_k simulated from Uniform $[1, 2]$ and $\sigma = 0.5$. In the algorithm, we set $\vartheta = 1$ and $\gamma = 3$ and the penalty function is SCAD.

We use the modified Bayes Information Criterion (BIC, Wang et al. (2007)), which is defined as

$$\text{BIC}\,(\lambda, \psi) = \log\left[\frac{1}{n}\sum_{i=1}^{n}\frac{1}{n_i}\left(y_{ih} - \boldsymbol{z}_{ih}^T\hat{\boldsymbol{\eta}}(\lambda,\psi) - \boldsymbol{x}_{ih}^T\hat{\boldsymbol{\beta}}_i(\lambda,\psi)\right)^2\right] + C_n\frac{\log n}{n}\left(\hat{K}(\lambda,\psi)p + q\right), \quad (7.22)$$

where C_n is a positive number which can depend on n. Here we use $C_n = c_0 \log(\log(np + q))$ (Ma and Huang, 2017) with $c_0 = 0.2$.

We calculate the estimated group numbers $\hat{K}(\lambda, \psi)$, adjusted Rand index (ARI) (Rand, 1971; Hubert and Arabie, 1985; Vinh et al., 2010) and root mean square error (RMSE) for $\boldsymbol{\beta}$. The largest value of ARI is 1 and a larger ARI value means that the two partitions agree a lot. RMSE is calculated for $\boldsymbol{\beta}$, which is defined as

$$\sqrt{\frac{1}{n}\sum_{i=1}^{n}\|\hat{\boldsymbol{\beta}}_i - \boldsymbol{\beta}_i\|^2}. \quad (7.23)$$

We consider the simulations in several scenarios.

7.4.1 Balanced group

We assume there are three true groups $\mathcal{G}_1, \mathcal{G}_2$ and $\mathcal{G}_3$. Two sets of group parameters are considered. One set is $\boldsymbol{\beta}_i = (1, 1)^T$ if $i \in \mathcal{G}_1$, $\boldsymbol{\beta}_i = (1.5, 1.5)^T$ if $i \in \mathcal{G}_2$ and $\boldsymbol{\beta}_i = (2, 2)^T$ if $i \in \mathcal{G}_3$. The other set is $\boldsymbol{\beta}_i = (1, 1)^T$ if $i \in \mathcal{G}_1$, $\boldsymbol{\beta}_i = (1.25, 1.25)^T$ if $i \in \mathcal{G}_2$ and $\boldsymbol{\beta}_i = (1.5, 1.5)^T$ if $i \in \mathcal{G}_3$. We simulate data sets on two sizes of regular lattice, one is7×7 grid and the other one is 10×10.

Figure 7.1 shows two lattices and the group distributions. The left one is a 7×7 regular lattice and the right one is a 10×10 regular lattice.

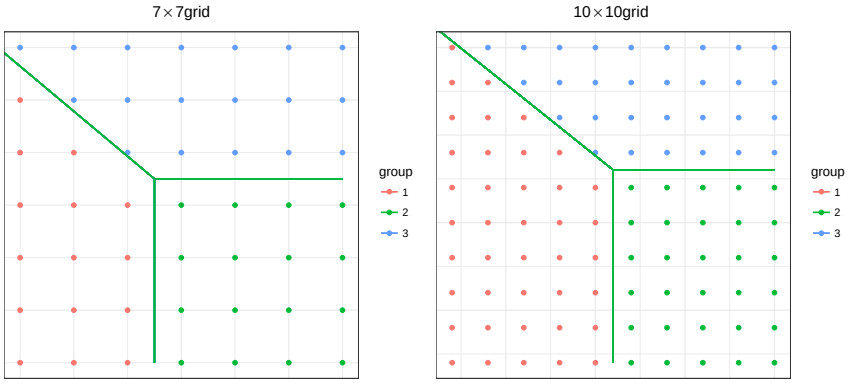

Figure 7.1: Two spatial settings

The first set of parameters: $\boldsymbol{\beta}_i = (1,1)^T$ if $i \in \mathcal{G}_1$, $\boldsymbol{\beta}_i = (1.5,1.5)^T$ if $i \in \mathcal{G}_2$ and $\boldsymbol{\beta}_i = (2,2)^T$ if $i \in \mathcal{G}_3$.

Tables 7.1 , 7.2 and 7.3 show the results of number of estimated groups and ARI, where "per" is the percentage of $\hat{K}$ equaling to the true number of groups $K = 3$. Figure 7.2 and Figure 7.3 show the RMSE of different weights under the first set of parameters. Here, "equal" corresponds to $c_{ij} = 1$, and "reg_sp" corresponds to weight in (7.3). Also, "reg" corresponds to weight in (7.4) and "sp" corresponds to weight in (7.5). For $n_i = 10$ with the 7×7 grid, we also consider cross validation to select tuning parameters. For a 10-fold cross validation, the repeated measures of subject i are divided into 10 parts. The jth part of each subject is combined as the test data set, the remaining data are considered as the training data set. "cv" represents the results based on cross validation. After we have the group information, we can estimate parameters $\boldsymbol{\eta}$ and $\boldsymbol{\beta}$ assuming the group information is known, which is denoted as "refit". From the following results, we can see that when $n_i = 30$ for the 7×7 grid, different weights do not have much differences. When $n_i = 10$, weight "sp" performs the best. Cross validation tends to have more estimated groups, but it does not perform bad in terms of RMSE. This is because that cross validation focuses on

the prediction behavior, the estimates of some groups are close to the true groups but they are not shrank together.

Table 7.1: Summary of $\hat{K}$ for the first set of parameters under the 7×7 grid

	$n_i = 10$					$n_i = 30$			
	equal	reg_sp	reg	sp	cv	equal	reg_sp	reg	sp
mean	3.340	3.150	3.330	3.130	3.820	3.000	3.000	3.000	3.000
median	3.000	3.000	3.000	3.000	3.000	3.000	3.000	3.000	3.000
sd	0.536	0.386	0.514	0.338	1.274	0.000	0.000	0.000	0.000
per	0.690	0.860	0.690	0.870	0.560	1.000	1.000	1.000	1.000

Table 7.2: ARI for the first set of parameters under the 7×7 grid

	$n_i = 10$					$n_i = 30$			
	equal	reg_sp	reg	sp	cv	equal	reg_sp	reg	sp
mean	0.798	0.917	0.818	0.920	0.947	0.998	0.999	0.998	0.999
median	0.818	0.936	0.827	0.936	0.970	1.000	1.000	1.000	1.000
sd	0.105	0.077	0.098	0.074	0.068	0.010	0.006	0.010	0.006

Table 7.3: Summary of $\hat{K}$ and ARI for the first set of parameters under the 10×10 grid

	$\hat{K}$				ARI			
	$n_i = 10$		$n_i = 30$		$n_i = 10$		$n_i = 30$	
	equal	sp	equal	sp	equal	sp	equal	sp
mean	3.590	3.370	3.000	3.000	0.697	0.970	0.996	1.000
median	3.000	3.000	3.000	3.000	0.697	0.973	1.000	1.000
sd	0.726	0.646	0.000	0.000	0.092	0.030	0.011	0.000
per	0.530	0.710	1.000	1.000	-	-	-	-

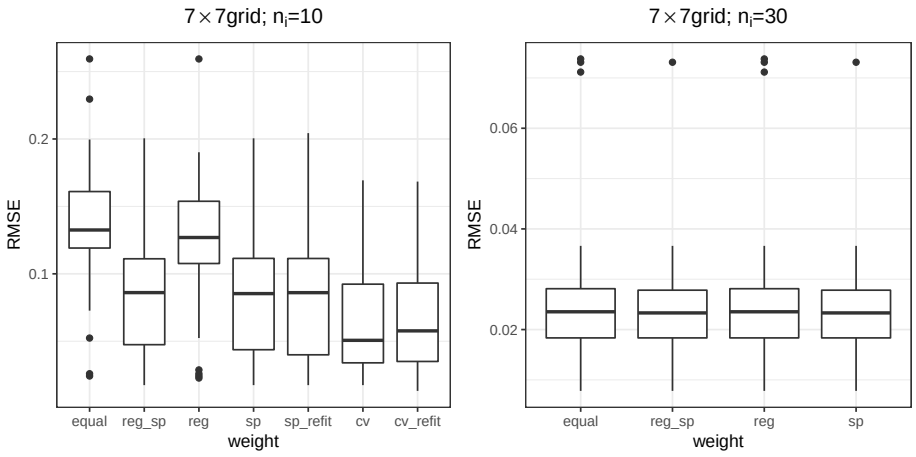

Figure 7.2: RMSE for the first set of parameters under the 7×7 grid

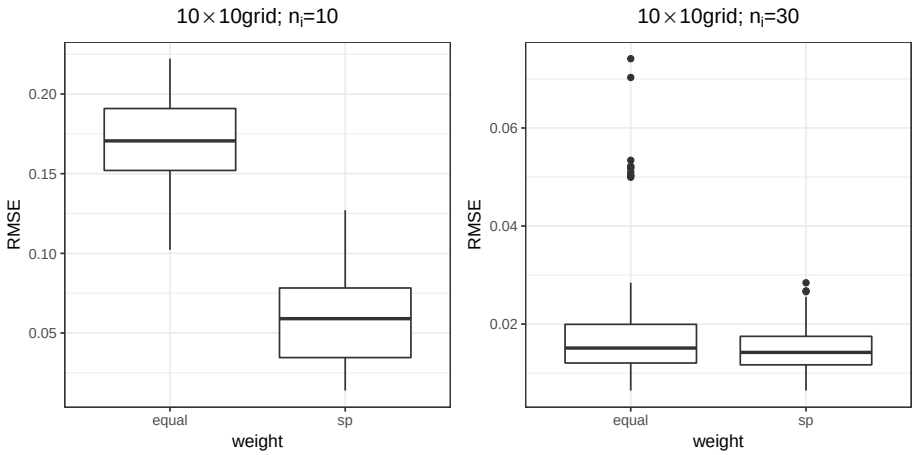

Figure 7.3: RMSE for the first set of parameters under the 10×10 grid

The second set of parameters: $\boldsymbol{\beta}_i = (1,1)^T$ if $i \in \mathcal{G}_1$, $\boldsymbol{\beta}_i = (1.25, 1.25)^T$ if $i \in \mathcal{G}_2$ and $\boldsymbol{\beta}_i = (1.5, 1.5)^T$ if $i \in \mathcal{G}_3$.

Tables 7.4, 7.5 and 7.6 show the results for $\hat{K}$ and ARI based on the second set of parameters setting. And Figures 7.4 and 7.5 show the corresponding values of RMSE for $\boldsymbol{\beta}$. We can see that,

when the difference among groups becomes smaller, even with $n_i = 30$, the model with spatial weight is superior to other models.

Table 7.4: Summary of $\hat{K}$ for the second set of parameters under the 7×7 grid

	$n_i = 10$				$n_i = 30$			
	equal	reg_sp	reg	sp	equal	reg_sp	reg	sp
mean	3.250	3.010	3.140	2.880	2.700	2.900	2.760	2.950
median	3.000	3.000	3.000	3.000	3.000	3.000	3.000	3.000
sd	1.192	0.927	1.073	0.671	0.461	0.302	0.429	0.219
per	0.340	0.450	0.330	0.600	0.700	0.900	0.760	0.950

Table 7.5: ARI for the second set of parameters under the 7×7 grid

	$n_i = 10$				$n_i = 30$			
	equal	reg_sp	reg	sp	equal	reg_sp	reg	sp
mean	0.319	0.504	0.330	0.608	0.723	0.860	0.751	0.902
median	0.310	0.438	0.331	0.519	0.766	0.936	0.803	0.936
sd	0.107	0.225	0.097	0.257	0.182	0.148	0.170	0.120

Table 7.6: Summary of $\hat{K}$ and ARI for the second set of parameters under the 10×10 grid

	$\hat{K}$				ARI			
	$n_i = 10$		$n_i = 30$		$n_i = 10$		$n_i = 30$	
	equal	sp	equal	sp	equal	sp	equal	sp
mean	3.820	3.350	3.100	3.000	0.320	0.814	0.793	0.942
median	3.500	3.000	3.000	3.000	0.322	0.907	0.821	0.947
sd	1.466	0.783	0.595	0.000	0.085	0.220	0.121	0.052
per	0.320	0.620	0.640	1.000	-	-	-	-

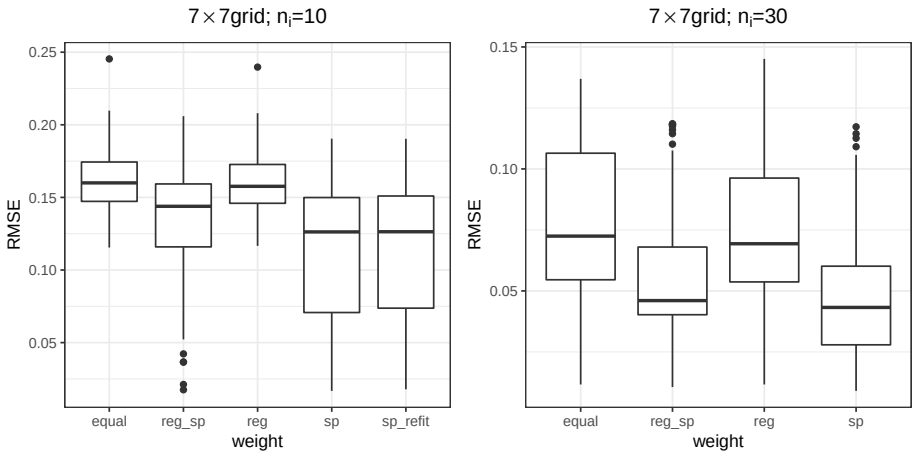

Figure 7.4: RMSE under the second set of parameters under the 7×7 grid

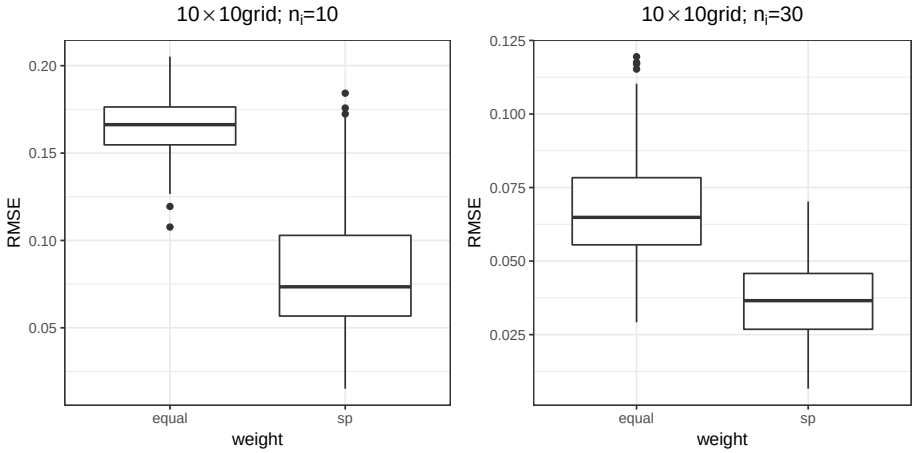

Figure 7.5: RMSE under the second set of parameters under the 10×10 grid

7.4.2 Unbalanced group

We also consider an unbalanced group setting as shown in Figure 7.6. In this setting, there are four groups, denoted as $\mathcal{G}_1, \mathcal{G}_2, \mathcal{G}_3$ and $\mathcal{G}_4$. Two groups have 9 subjects and the other two groups have 41 subjects. The group parameters are $\boldsymbol{\beta}_i = (1,1)^T$ if $i \in \mathcal{G}_1$, $\boldsymbol{\beta}_i = (1.5,1.5)^T$ if $i \in \mathcal{G}_2$, $\boldsymbol{\beta}_i = (2,2)^T$ if $i \in \mathcal{G}_3$ and $\boldsymbol{\beta}_i = (2.5,2.5)^T$ if $i \in \mathcal{G}_4$.

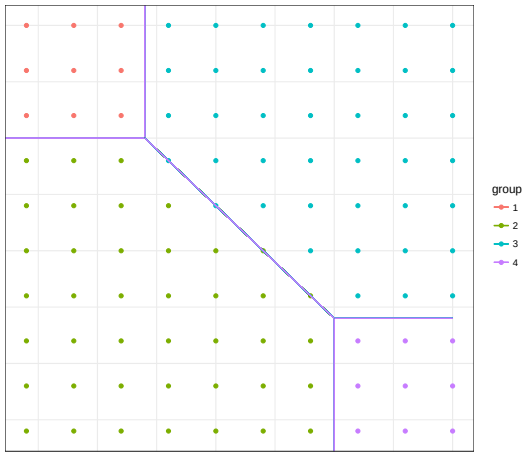

Figure 7.6: Unbalanced simulation setting

Table 7.7 and Figure 7.7 show the summaries of $\hat{K}$, ARI and RMSE for $\boldsymbol{\beta}$. Under this case, the model with weights "reg_sp" and "sp" perform better than the other two.

Table 7.7: Summary of $\hat{K}$ and ARI based on unbalanced setting with $n_i = 10$

	$\hat{K}$				ARI			
	equal	reg_sp	reg	sp	equal	reg_sp	reg	sp
mean	4.580	4.230	5.170	4.350	0.618	0.940	0.670	0.963
median	4.000	4.000	5.000	4.000	0.615	0.953	0.673	0.964
sd	0.934	0.489	1.064	0.592	0.102	0.061	0.093	0.037
per	0.570	0.800	0.300	0.710	-	-	-	-

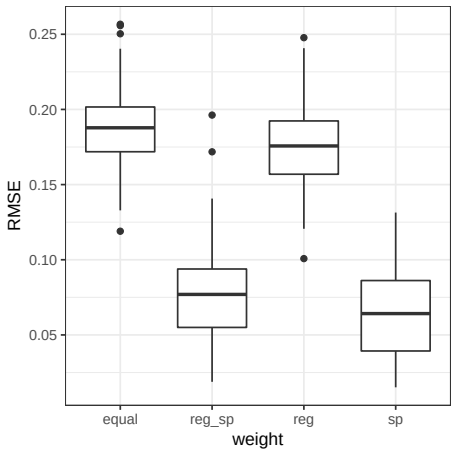

Figure 7.7: RMSE for unbalanced setting

7.4.3 Random group

We also consider a setting without specified location group information. For each subject, it has equal probability to three groups. The group parameters are $\boldsymbol{\beta}_i = (1,1)^T$ if $i \in \mathcal{G}_1$, $\boldsymbol{\beta}_i = (1.5,1.5)^T$ if $i \in \mathcal{G}_2$ and $\boldsymbol{\beta}_i = (2,2)^T$ if $i \in \mathcal{G}_3$. From Tables 7.8, 7.9 and Figure 7.8, we can see that different weights have similar performances.

Table 7.8: Summary of $\hat{K}$ and ARI under the 7×7 grid with $n_i = 10$

	$\hat{K}$				ARI			
	equal	reg_sp	reg	sp	equal	reg_sp	reg	sp
mean	3.420	3.450	3.400	3.450	0.778	0.819	0.813	0.817
median	3.000	3.000	3.000	3.000	0.781	0.821	0.822	0.821
sd	0.638	0.626	0.586	0.626	0.107	0.099	0.096	0.109
per	0.660	0.620	0.650	0.620	-	-	-	-

Table 7.9: Summary of $\hat{K}$ and ARI under the 7×7 grid with $n_i = 30$

	$\hat{K}$				ARI			
	equal	reg_sp	reg	sp	equal	reg_sp	reg	sp
mean	2.770	2.770	2.830	2.730	0.744	0.761	0.774	0.744
median	3.000	3.000	3.000	3.000	0.776	0.800	0.810	0.785
sd	0.446	0.446	0.403	0.468	0.153	0.157	0.142	0.167
per	0.750	0.750	0.810	0.710	-	-	-	-

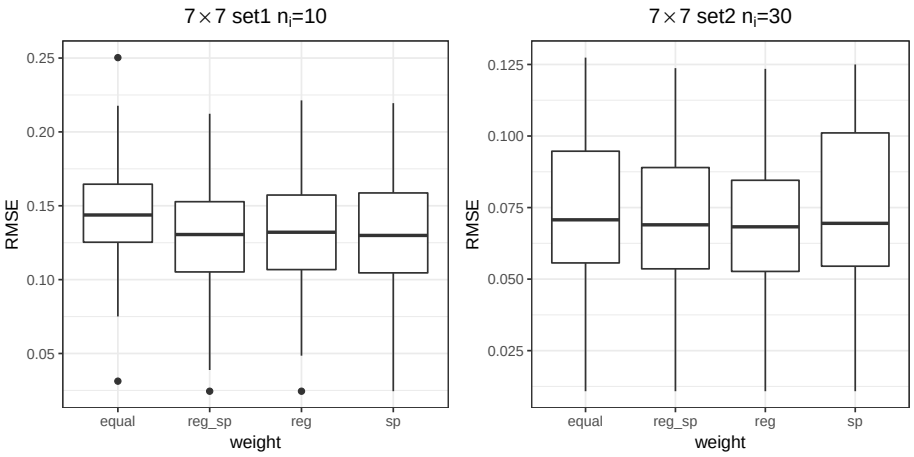

Figure 7.8: RMSE for random groups under the 7×7 grid

7.5 Application

In this section, we apply our method to an example. In the National Resources Inventory survey (NRI) [1], one of the problem is to estimate county level estimates of different landcovers. Since the NRI county level estimates usually have larger values of coefficient of variation, it would be helpful to include auxiliary information to improve the estimator. One of the available auxiliary covariate is Cropland Data Layer (CDL), which a classification of square pixels into several mutually exclusive and exhaustive land cover categories. We want to investigate the relationship between NRI forest proportion and CDL forest proportion among 48 states. In NRI, forest belonging to federal land,

[1] https://www.nrcs.usda.gov/wps/portal/nrcs/main/national/technical/nra/nri/

such as national parks, is not included in the forest category. For states with more forest federal land, NRI estimates would be smaller than the CDL estimates.

The model we consider is,

$$y_{ih} = \beta_{0,i} + \beta_{1,i} x_{ih} + \epsilon_{ih} \tag{7.24}$$

where y_{ih} is the NRI forest proportion of hth county in ith state, x_{ih} is the CDL forest proportion of hth county in ith state. $\beta_{0,i}$ and $\beta_{1,i}$ are the unknown coefficients. Both x and y are standardized. Instead of using the estimated linear regression coefficients as the initial values directly, we use five sets of initial values, which are simulated from the multivariate normal distribution with estimated coefficients as the mean vector and estimated covariance matrix as the covariance matrix. The models with the smallest modified BIC values are selected for equal weight and spatial weight respectively.

Figure 7.10 shows the estimated groups based on 2011 NRI data sets. The left figure is about the estimated groups with equal weight, and the right one is about the estimated groups with spatial weight. We find that the two different weights give two different estimated groups. Tables 7.10 and 7.11 are the corresponding estimates of regression coefficients in different groups. We also fit the two models on 2010 data sets, the group estimates based on equal weight change a lot, however, the group estimates based on spatial weight does not change, which means that the model with spatial weight is more stable.

Table 7.10: Estimated coefficients of different groups for equal weight

group	1	2
β_0	-0.029(0.006)	0.003(0.008)
β_1	0.885(0.011)	0.241(0.026)

Table 7.11: Estimated coefficients of different groups for spatial weight

group	1	2	3	4	5	6	7
β_0	-0.041(0.016)	-0.032(0.006)	0.003(0.007)	0.023(0.015)	-0.108(0.293)	0.275(0.038)	0.376 (0.309)
β_1	1.018(0.028)	0.867(0.012)	0.241(0.024)	0.608(0.033)	1.148 (0.377)	0.332(0.064)	0.341(0.384)

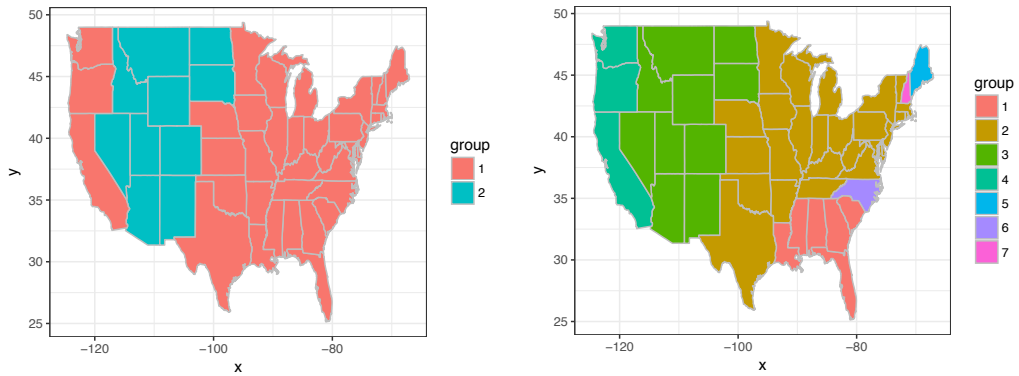

(a) Estimated groups based on equal weights

(b) Estimated groups based on spatial weights

Figure 7.10: Estimated groups for both equal weight and spatial weight

We also consider changing the tuning parameter in the model with equal weight to have similar estimated number of groups to the right figure in Figure 7.10. Figure 7.11 shows the results, which has seven estimated number of groups. But "WA", "OR" and "CA" are not separated from other states. However, we can separate the three states with other states by using spatial weight, which is more reasonable and respect the nature from the estimates of coefficients.

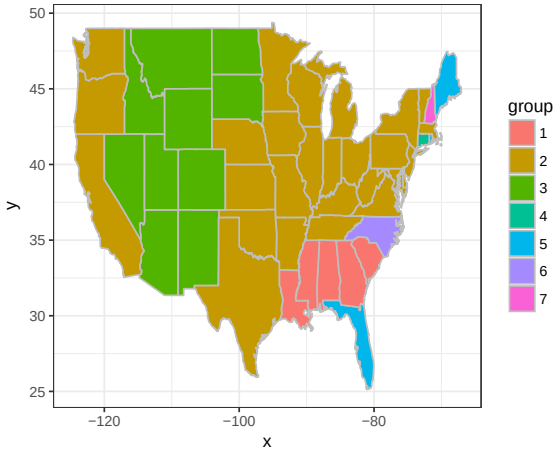

Figure 7.11: Estimated groups by changing tuning parameter with equal weights

Besides that, we consider K-means clustering based on the initial estimates. Figure 7.12 shows the maps for 2 clusters and 7 clusters. The map with 2 clusters is almost the same as the map based on equal weights. However, the map with 7 clusters is not interpretable compared to the result based on spatial weight.

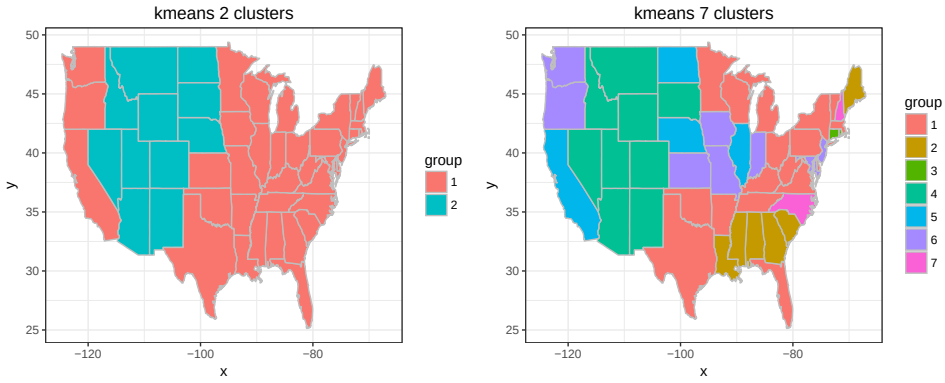

Figure 7.12: Estimated groups based on K-means

7.6 Discussion

In this article, we consider the spatial clustering problem based on subgroup analysis framework with repeated measures. Since in spatial data locations near each other usually have similar patterns, spatial information is included in pairwise penalty to control the shrinkage. Pairs near each other will have larger weights, which will shrink faster. In the simulation study, we use several examples to compare the performances of different weights, which show that the spatial information helps when the minimal group difference is small or the number of repeated measures is small. We also prove the theoretical properties of the proposed estimator, which shows that the oracle estimator is a local minimizer of the objective function with probability approaching 1.

In the empirical example, we consider state as subject and counties as repeated measures. Another way to look at this problem is to consider counties individually, since one state could have counties with two different features. Then, the algorithm will involve a matrix inverse with

dimension more than 3000, which could be expressed as Woodbury's formula. A further study is needed to compare these two models for application.

Appendices

A Proof of Theorem 7.1

In this section, we prove Theorem 7.1 . When proving the central limit theorem (CLT) we use the technique in Huang et al. (2004).

The oracle estimator is define in (7.13), which has the following form

$$\begin{pmatrix} \hat{\boldsymbol{\eta}}^{or} \\ \hat{\boldsymbol{\alpha}}^{or} \end{pmatrix} = \left(\boldsymbol{U}^T\boldsymbol{\Omega}\boldsymbol{U}\right)^{-1}\boldsymbol{U}^T\boldsymbol{\Omega}\boldsymbol{y}.$$

Thus, we have

$$\begin{pmatrix} \hat{\boldsymbol{\eta}}^{or} - \boldsymbol{\eta}^0 \\ \hat{\boldsymbol{\alpha}}^{or} - \boldsymbol{\alpha}^0 \end{pmatrix} = \left(\boldsymbol{U}^T\boldsymbol{\Omega}\boldsymbol{U}\right)^{-1}\boldsymbol{U}^T\boldsymbol{\Omega}\boldsymbol{\epsilon},$$

where $\boldsymbol{\epsilon} = (\boldsymbol{\epsilon}_i^T, \ldots, \boldsymbol{\epsilon}_n^T)^T$ with $\boldsymbol{\epsilon}_i = (\epsilon_{i1}, \ldots, \epsilon_{i,n_i})^T$. Therefore,

$$\left\| \begin{pmatrix} \hat{\boldsymbol{\eta}}^{or} - \boldsymbol{\eta}^0 \\ \hat{\boldsymbol{\alpha}}^{or} - \boldsymbol{\alpha}^0 \end{pmatrix} \right\| \leq \left\| \left(\boldsymbol{U}^T\boldsymbol{\Omega}\boldsymbol{U}\right)^{-1} \right\|_2 \left\| \boldsymbol{U}^T\boldsymbol{\Omega}\boldsymbol{\epsilon} \right\|, \tag{7.25}$$

where $\|\cdot\|_2$ is matrix norm, which is defined as, for a matrix $\boldsymbol{A}$, $\|\boldsymbol{A}\|_2 = \sup_{\|\boldsymbol{x}\|=1} \|\boldsymbol{A}\boldsymbol{x}\|$.

We know that

$$\begin{aligned} P\left(\left\|\boldsymbol{U}^T\boldsymbol{\Omega}\boldsymbol{\epsilon}\right\|_\infty > C\sqrt{\frac{n}{\min n_i}\log n}\right) \leq\ & P\left(\left\|(\boldsymbol{X}\boldsymbol{W})^T\boldsymbol{\Omega}\boldsymbol{\epsilon}\right\|_\infty > C\sqrt{\frac{n}{\min n_i}\log n}\right) \\ & + P\left(\left\|\boldsymbol{Z}^T\boldsymbol{\Omega}\boldsymbol{\epsilon}\right\|_\infty > C\sqrt{\frac{n}{\min n_i}\log n}\right), \end{aligned} \tag{7.26}$$

where C is a finite positive constant and $\|\cdot\|_\infty$ is defined as, for a vector $\boldsymbol{x} \in \mathbb{R}^m$, $\|\boldsymbol{x}\|_\infty = \max_{1\leq i\leq m} x_i$. By condition (C2), we have

$$\sqrt{\sum_{i=1}^{n}\sum_{h=1}^{n_i}\frac{x_{ih,l}^2}{n_i^2}1\left\{i \in \mathcal{G}_k\right\}} \leq M_1\sqrt{\sum_{i=1}^{n}\frac{1}{n_i}\left\{i \in \mathcal{G}_k\right\}} \leq M_1\sqrt{\sum_{i=1}^{n}\frac{1}{n_i}} \leq M_1\sqrt{\frac{n}{\min n_i}}.$$

Since

$$\left\|(\boldsymbol{XW})^T\boldsymbol{\Omega\epsilon}\right\|_\infty = \sup_{k,l}\left|\sum_{i=1}^{n}\frac{1}{n_i}\sum_{h=1}^{n_i}x_{ih,l}\epsilon_{ih}1\left\{i\in\mathcal{G}_k\right\}\right|,$$

from condition (C3), it follows that

$$\begin{aligned}
&P\left(\left\|(\boldsymbol{XW})^T\boldsymbol{\Omega\epsilon}\right\|_\infty > C\sqrt{\frac{n}{\min n_i}\log n}\right)\\
\leq&\sum_{l=1}^{p}\sum_{k=1}^{K}P\left(\left|\sum_{i=1}^{n}\sum_{j=1}^{n_i}\frac{1}{n_i}x_{ih,l}\epsilon_{ih}1\left\{i\in\mathcal{G}_k\right\}\right| > C\sqrt{\frac{n}{\min n_i}\log n}\right)\\
=&\sum_{l=1}^{p}\sum_{k=1}^{K}P\left(\left|\sum_{i=1}^{n}\sum_{h=1}^{n_i}\frac{1}{n_i}x_{ih,l}\epsilon_{ih}1\left\{i\in\mathcal{G}_k\right\}\right| > \frac{\sqrt{\sum_{i=1}^{n}\sum_{h=1}^{n_i}\frac{x_{ih,l}^2}{n_i^2}1\left\{i\in\mathcal{G}_k\right\}}}{\sqrt{\sum_{i=1}^{n}\sum_{h=1}^{n_i}\frac{x_{ih,l}^2}{n_i^2}1\left\{i\in\mathcal{G}_k\right\}}}C\sqrt{\frac{n}{\min n_i}\log n}\right)\\
\leq&\sum_{l=1}^{p}\sum_{k=1}^{K}P\left(\left|\sum_{i=1}^{n}\sum_{h=1}^{n_i}\frac{1}{n_i}x_{ih,l}\epsilon_{ih}1\left\{i\in\mathcal{G}_k\right\}\right| > \sqrt{\sum_{i=1}^{n}\sum_{h=1}^{n_i}\frac{x_{ih,l}^2}{n_i^2}1\left\{i\in\mathcal{G}_k\right\}}\frac{C}{M_1}\sqrt{\log n}\right)\\
\leq&2Kp\exp\left(-c_1\frac{C^2}{M_1^2}\log n\right) = 2Kpn^{-c_1C^2/M_1^2}.
\end{aligned}$$

Similarly, $\left|\sum_{i=1}^{n}\sum_{h=1}^{n_i}\frac{z_{ih,l}^2}{n_i^2}\right| \leq M_1^2\sum_{i=1}^{n}1/n_i \leq M_1^2\frac{n}{\min n_i}$. Again, by condition (C3), we have

$$\begin{aligned}
&P\left(\left\|\boldsymbol{Z}^T\boldsymbol{\Omega\epsilon}\right\|_\infty > C\sqrt{\frac{n}{\min n_i}\log n}\right)\\
\leq&\sum_{l=1}^{q}P\left(\left|\sum_{i=1}^{n}\sum_{h=1}^{n_i}\frac{1}{n_i}z_{ih,l}\epsilon_{ih}\right| > C\sqrt{\frac{n}{\min n_i}\log n}\right)\\
\leq&\sum_{l=1}^{q}P\left(\left|\sum_{i=1}^{n}\sum_{h=1}^{n_i}\frac{1}{n_i}z_{ih,l}\epsilon_{ih}\right| > \sqrt{\sum_{i=1}^{n}\sum_{h=1}^{n_i}\frac{z_{ih,l}^2}{n_i^2}}\frac{C}{M_1}\sqrt{\log n}\right)\\
\leq&2q\exp\left(-c_1\frac{C^2}{M_1^2}\log n\right) = 2qn^{-c_1C^2/M_1^2}.
\end{aligned}$$

Thus, (7.26) can be bounded by

$$P\left(\left\|\boldsymbol{U}^T\boldsymbol{\Omega\epsilon}\right\|_\infty > C\sqrt{\frac{n}{\min n_i}\log n}\right) \leq 2\left(Kp+q\right)n^{-c_1C^2/M_1^2}.$$

Since $\left\|\boldsymbol{U}^T\boldsymbol{\Omega\epsilon}\right\| \leq \sqrt{q+Kp}\left\|\boldsymbol{U}^T\boldsymbol{\Omega\epsilon}\right\|_\infty$,

$$P\left(\left\|\boldsymbol{U}^T\boldsymbol{\Omega\epsilon}\right\| > C\sqrt{q+Kp}\sqrt{\frac{n}{\min n_i}\log n}\right) \leq 2\left(Kp+q\right)n^{-c_1C^2/M_1^2}.$$

Let $C = c_1^{-1/2}M_1$, thus

$$P\left(\left\|\boldsymbol{U}^T\boldsymbol{\Omega\epsilon}\right\| > C\sqrt{q+Kp}\sqrt{\frac{n}{\min n_i}\log n}\right) \leq 2\left(Kp+q\right)n^{-1}. \tag{7.27}$$

Also, according to condition (C2), we have

$$\left\|\left(\boldsymbol{U}^T\boldsymbol{\Omega}\boldsymbol{U}\right)^{-1}\right\|_2 \leq C_1^{-1}\left|\mathcal{G}_{\min}\right|^{-1}. \tag{7.28}$$

Combining (7.25), (7.27) and (7.28), with probability at least $1-2\left(Kp+q\right)n^{-1}$, we have

$$\left\|\begin{pmatrix}\hat{\boldsymbol{\eta}}^{or}-\boldsymbol{\eta}^0\\ \hat{\boldsymbol{\alpha}}^{or}-\boldsymbol{\alpha}^0\end{pmatrix}\right\| \leq CC_1^{-1}\sqrt{q+Kp}\left|\mathcal{G}_{\min}\right|^{-1}\sqrt{\frac{n}{\min n_i}\log n}.$$

Let

$$\phi_n = c_1^{-1/2}C_1^{-1}M_1\sqrt{q+Kp}\left|\mathcal{G}_{\min}\right|^{-1}\sqrt{\frac{n}{\min n_i}\log n}.$$

Furthermore,

$$\begin{aligned}\left\|\hat{\boldsymbol{\beta}}^{or}-\boldsymbol{\beta}^0\right\|^2 &= \sum_{k=1}^{K}\sum_{i\in\mathcal{G}_k}\left\|\hat{\boldsymbol{\alpha}}_k^{or}-\boldsymbol{\alpha}_k^0\right\|^2 \leq \left|\mathcal{G}_{\max}\right|\sum_{k=1}^{K}\left\|\hat{\boldsymbol{\alpha}}_k^{or}-\boldsymbol{\alpha}_k^0\right\|^2\\ &= \left|\mathcal{G}_{\max}\right|\left\|\hat{\boldsymbol{\alpha}}^{or}-\boldsymbol{\alpha}^0\right\|^2 \leq \left|\mathcal{G}_{\max}\right|\phi_n^2,\end{aligned}$$

and

$$\sup_i\left\|\hat{\boldsymbol{\beta}}_i^{or}-\boldsymbol{\beta}_i^0\right\| = \sup_k\left\|\hat{\boldsymbol{\alpha}}_k^{or}-\boldsymbol{\alpha}_k^0\right\| \leq \left\|\hat{\boldsymbol{\alpha}}^{or}-\boldsymbol{\alpha}^0\right\| \leq \phi_n.$$

Next, we consider the central limit theorem. Let $\boldsymbol{U}=\left(\boldsymbol{U}_1^T,\ldots,\boldsymbol{U}_n^T\right)^T$ with $\boldsymbol{U}_i=(\boldsymbol{U}_{i1},\ldots,\boldsymbol{U}_{i,n_i})^T$ for $i=1,\ldots,n$. Consider

$$\boldsymbol{a}_n^T\left(\left(\hat{\boldsymbol{\eta}}^{or}-\boldsymbol{\eta}^0\right)^T,\left(\hat{\boldsymbol{\alpha}}^{or}-\hat{\boldsymbol{\alpha}}^0\right)^T\right)^T = \sum_{i=1}^{n}\boldsymbol{a}_n^T\left(\sum_{i=1}^{n}\boldsymbol{U}_i^T\boldsymbol{\Omega}_i\boldsymbol{U}_i\right)^{-1}\boldsymbol{U}_i^T\boldsymbol{\Omega}_i\boldsymbol{\epsilon}_i,$$

where $\boldsymbol{\Omega}_i = 1/n_i\boldsymbol{I}_{n_i}$. By the assumption of $\boldsymbol{\epsilon}_i$ in the model (7.1), we have

$$E\left[\boldsymbol{a}_n^T\left(\left(\hat{\boldsymbol{\eta}}^{or}-\boldsymbol{\eta}^0\right)^T,\left(\hat{\boldsymbol{\alpha}}^{or}-\hat{\boldsymbol{\alpha}}^0\right)^T\right)^T\right]=0.$$

The variance of $\boldsymbol{a}_n^T\left(\left(\hat{\boldsymbol{\eta}}^{or}-\boldsymbol{\eta}^0\right)^T,\left(\hat{\boldsymbol{\alpha}}^{or}-\hat{\boldsymbol{\alpha}}^0\right)^T\right)^T$ can be written as

$$\begin{aligned}&Var\left\{\boldsymbol{a}_n^T\left(\left(\hat{\boldsymbol{\eta}}^{or}-\boldsymbol{\eta}^0\right)^T,\left(\hat{\boldsymbol{\alpha}}^{or}-\hat{\boldsymbol{\alpha}}^0\right)^T\right)^T\right\}\\ =&\sigma^2\left[\boldsymbol{a}_n^T\left(\boldsymbol{U}^T\boldsymbol{\Omega}\boldsymbol{U}\right)^{-1}\boldsymbol{U}^T\boldsymbol{\Omega}\boldsymbol{\Omega}\boldsymbol{U}\left(\boldsymbol{U}^T\boldsymbol{\Omega}\boldsymbol{U}\right)^{-1}\boldsymbol{a}_n\right]\\ =&\sigma^2\left[\boldsymbol{a}_n^T\left(\boldsymbol{U}^T\boldsymbol{\Omega}\boldsymbol{U}\right)^{-1}\sum_{i=1}^{n}\boldsymbol{U}_i^T\boldsymbol{\Omega}_i\boldsymbol{\Omega}_i\boldsymbol{U}_i\left(\boldsymbol{U}^T\boldsymbol{\Omega}\boldsymbol{U}\right)^{-1}\boldsymbol{a}_n\right].\end{aligned}$$

We use the technique of Huang et al. (2004) in the proof of their Theorem 3. That is, $\boldsymbol{a}_n^T \left(\left(\hat{\boldsymbol{\eta}}^{or} - \boldsymbol{\eta}^0\right)^T, \left(\hat{\boldsymbol{\alpha}}^{or} - \hat{\boldsymbol{\alpha}}^0\right)^T \right)^T$ can be written as $\sum_{i=1}^n a_i \xi_i$ with

$$a_i^2 = \boldsymbol{a}_n^T \left(\boldsymbol{U}^T \boldsymbol{\Omega} \boldsymbol{U} \right)^{-1} \boldsymbol{U}_i^T \boldsymbol{\Omega}_i \boldsymbol{\Omega}_i \boldsymbol{U}_i \left(\boldsymbol{U}^T \boldsymbol{\Omega} \boldsymbol{U} \right)^{-1} \boldsymbol{a}_{\boldsymbol{n}},$$

where ξ_i's are independent with mean zero and variance one. If

$$\frac{\max_i a_i^2}{\sum_{i=1}^n a_i^2} \to 0,$$

then $\sum_{i=1}^n a_i \xi_i / \sqrt{\sum_{i=1}^n a_i^2}$ is asymptotically $N(0,1)$.

For any $\boldsymbol{\lambda} = (\lambda_1, \ldots, \lambda_{q+Kp})^T$, we have

$$\begin{aligned}
\boldsymbol{\lambda}^T \boldsymbol{U}_i^T \boldsymbol{\Omega}_i \boldsymbol{\Omega}_i \boldsymbol{U}_i \boldsymbol{\lambda} &= \frac{1}{n_i^2} \boldsymbol{\lambda}^T \boldsymbol{U}_i^T \boldsymbol{U}_i \boldsymbol{\lambda} = \frac{1}{n_i^2} \sum_{h=1}^{n_i} \boldsymbol{\lambda}^T \boldsymbol{U}_{ih} \boldsymbol{U}_{ih}^T \boldsymbol{\lambda} \\
&= \frac{1}{n_i^2} \sum_{h=1}^{n_i} \left(\sum_{l=1}^{q+Kp} U_{ih,l} \lambda_l \right)^2 \\
&\leq \frac{1}{n_i^2} \sum_{h=1}^{n_i} \left(\sum_{l=1}^{q+Kp} U_{ih,l}^2 \right) \left(\sum_{l=1}^{q+Kp} \lambda_l^2 \right) \leq \frac{M_1^2}{n_i} (q + Kp) \|\boldsymbol{\lambda}\|^2 .
\end{aligned}$$

$$\begin{aligned}
\boldsymbol{\lambda}^T \left(\sum_{i=1}^n \boldsymbol{U}_i^T \boldsymbol{\Omega}_i \boldsymbol{\Omega}_i \boldsymbol{U}_i \right) \boldsymbol{\lambda} &\geq \frac{1}{\max_i n_i} \boldsymbol{\lambda}^T \left(\sum_{i=1}^n \boldsymbol{U}_i^T \boldsymbol{\Omega}_i \boldsymbol{U}_i \right) \boldsymbol{\lambda} \geq \frac{1}{\max_i n_i} \boldsymbol{\lambda}^T \boldsymbol{U}^T \boldsymbol{\Omega} \boldsymbol{U} \boldsymbol{\lambda} \\
&\geq \frac{1}{\max_i n_i} C_1 |\mathcal{G}_{\min}| \|\boldsymbol{\lambda}\|^2 ,
\end{aligned}$$

where the last inequality is by condition (C2). So,

$$\begin{aligned}
\frac{\max_i \boldsymbol{\lambda}^T \boldsymbol{U}_i^T \boldsymbol{\Omega}_i \boldsymbol{\Omega}_i \boldsymbol{U}_i \boldsymbol{\lambda}}{\boldsymbol{\lambda}^T \left(\sum_{i=1}^n \boldsymbol{U}_i^T \boldsymbol{\Omega}_i \boldsymbol{\Omega}_i \boldsymbol{U}_i \right) \boldsymbol{\lambda}} &\leq \left(\max_i n_i \right) \left(\max_i \frac{1}{n_i} \right) M_1^2 C_1^{-1} |\mathcal{G}_{\min}|^{-1} (q + Kp) \\
&= M_1^2 C_1^{-1} \frac{\max_i n_i}{\min_i n_i} |\mathcal{G}_{\min}|^{-1} (q + Kp) \to 0, \qquad (7.29)
\end{aligned}$$

by assumption.

By (7.29), we have that $\max_i a_i^2 / \sum_{i=1}^n a_i^2 \to 0$, so (7.14) exists.

B Proof of Theorem 7.2

In this section, we prove Theorem 7.2. As in Ma and Huang (2016) and Ma and Huang (2017), we define $T : \mathcal{M}_{\mathcal{G}} \to \mathbb{R}^{Kp}$ to be the mapping that $T(\boldsymbol{\beta}) = \boldsymbol{\alpha}$ and $T^* : \mathbb{R}^{np} \to \mathbb{R}^{Kp}$ to be the mapping that $T^*(\boldsymbol{\beta}) = \left(|\mathcal{G}_k|^{-1} \sum_{i \in \mathcal{G}_k} \boldsymbol{\beta}_i^T, \, k = 1, \ldots, K \right)^T$.

Consider the following neighborhood of $(\boldsymbol{\eta}^0, \boldsymbol{\beta}^0)$,

$$\Theta = \left\{ \boldsymbol{\eta} \in \mathbb{R}^q, \boldsymbol{\beta} \in \mathbb{R}^{np} : \left\| \boldsymbol{\eta} - \boldsymbol{\eta}^0 \right\| \leq \phi_n, \sup_i \left\| \boldsymbol{\beta}_i - \boldsymbol{\beta}_i^0 \right\| \leq \phi_n \right\}.$$

According to Theorem 7.1, there exists an event E_1 where $\|\boldsymbol{\eta} - \boldsymbol{\eta}^0\| \leq \phi_n$ and $\sup_i \|\boldsymbol{\beta}_i - \boldsymbol{\beta}_i^0\| \leq \phi_n$ such that $P(E_1) \geq 1 - 2(q + Kp) n^{-1}$.

Recall that the objective function to minimize is given in 7.2, which has the following form

$$Q_n(\boldsymbol{\eta}, \boldsymbol{\beta}; \lambda, \psi) = \frac{1}{2} \sum_{i=1}^{n} \frac{1}{n_i} \sum_{h=1}^{n_i} \left(y_{ih} - \boldsymbol{z}_{ih}^T \boldsymbol{\eta} - \boldsymbol{x}_{ih}^T \boldsymbol{\beta}_i \right)^2 + \sum_{1 \leq i < j \leq n} p_\gamma \left(\|\boldsymbol{\beta}_i - \boldsymbol{\beta}_j\|, c_{ij} \lambda \right). \tag{7.30}$$

Here we show that $\left((\hat{\boldsymbol{\eta}}^{or})^T, (\hat{\boldsymbol{\beta}}^{or})^T \right)^T$ is a strict local minimizer of the above objective function with probability approaching 1 by two steps as in Ma and Huang (2016). The first step is to show that in event E_1, $Q_n(\boldsymbol{\eta}, \boldsymbol{\beta}^*) > Q_n(\hat{\boldsymbol{\eta}}^{or}, \hat{\boldsymbol{\beta}}^{or})$ for any $(\boldsymbol{\eta}^T, \boldsymbol{\beta}^T)^T \in \Theta$ and $(\boldsymbol{\eta}^T, \boldsymbol{\beta}^{*T})^T \neq ((\hat{\boldsymbol{\eta}}^{or})^T, (\hat{\boldsymbol{\beta}}^{or})^T)^T$, where $\boldsymbol{\beta}^* = T^{-1}(T^*(\boldsymbol{\beta}))$ and $\boldsymbol{\beta} \in \mathbb{R}^{np}$. The proof of this step is almost the same as the first step in Ma and Huang (2016) , which is omitted here.

Here we show the second step, that is, there exists an event E_2 such that $P(E_2) \geq 1 - 2n^{-1}$. In the event $E_1 \cap E_2$, there is a neighborhood Θ_n of $\left((\hat{\boldsymbol{\eta}}^{or})^T, \left(\hat{\boldsymbol{\beta}}^{or} \right)^T \right)^T$, such that $Q_n(\boldsymbol{\eta}, \boldsymbol{\beta}) \geq Q_n(\boldsymbol{\eta}, \boldsymbol{\beta}^*)$ for any $\left(\boldsymbol{\eta}^T, \boldsymbol{\beta}^T \right)^T \in \Theta_n \cap \Theta$ for sufficiently large n.

Let $\Theta_n = \left\{ \boldsymbol{\beta}_i : \sup_i \left\| \boldsymbol{\beta}_i - \hat{\boldsymbol{\beta}}_i^{or} \right\| \leq t_n \right\}$, where t_n is a positive sequence with $t_n = o(1)$. By Taylor's expansion, for $\left(\boldsymbol{\eta}^T, \boldsymbol{\beta}^T \right)^T \in \Theta_n \cap \Theta$,

$$Q_n(\boldsymbol{\eta}, \boldsymbol{\beta}) - Q_n(\boldsymbol{\eta}, \boldsymbol{\beta}^*) = \Gamma_1 + \Gamma_2, \tag{7.31}$$

where

$$\begin{aligned}
\Gamma_1 &= -(\boldsymbol{y} - \boldsymbol{Z}\boldsymbol{\eta} - \boldsymbol{X}\boldsymbol{\beta}^m)^T \boldsymbol{\Omega} \boldsymbol{X} (\boldsymbol{\beta} - \boldsymbol{\beta}^*), \\
\Gamma_2 &= \sum_{i=1}^{n} \frac{\partial \left[\lambda \sum_{l<j} c_{lj} \rho_\gamma \left(\left\| \boldsymbol{\beta}_l^m - \boldsymbol{\beta}_j^m \right\| \right) \right]}{\partial \boldsymbol{\beta}_i^T} (\boldsymbol{\beta}_i - \boldsymbol{\beta}_i^*),
\end{aligned}$$

with $\boldsymbol{\beta}^m = \alpha \boldsymbol{\beta} + (1 - \alpha) \boldsymbol{\beta}^*$ for some constant $\alpha \in (0, 1)$.

We have Γ_2 as follows,

$$\Gamma_2 = \lambda \sum_{i<j} c_{ij} \rho_\gamma' \left(\left\| \boldsymbol{\beta}_i^m - \boldsymbol{\beta}_j^m \right\| \right) \left\| \boldsymbol{\beta}_i^m - \boldsymbol{\beta}_j^m \right\|^{-1} \left(\boldsymbol{\beta}_i^m - \boldsymbol{\beta}_j^m \right)^T \left\{ (\boldsymbol{\beta}_i - \boldsymbol{\beta}_i^*) - \left(\boldsymbol{\beta}_j - \boldsymbol{\beta}_j^* \right) \right\}.$$

For $i,j \in \mathcal{G}_k$, $\boldsymbol{\beta}_i^* = \boldsymbol{\beta}_j^*$ and $\boldsymbol{\beta}_i^m - \boldsymbol{\beta}_j^m = \alpha\left(\boldsymbol{\beta}_i - \boldsymbol{\beta}_j\right)$, then

$$\begin{aligned}\Gamma_2 = &\lambda \sum_{k=1}^{K} \sum_{\{i,j\in\mathcal{G}_k, i<j\}} c_{ij}\rho_\gamma'\left(\left\|\boldsymbol{\beta}_i^m - \boldsymbol{\beta}_j^m\right\|\right)\left\|\boldsymbol{\beta}_i^m - \boldsymbol{\beta}_j^m\right\|^{-1}\left(\boldsymbol{\beta}_i^m - \boldsymbol{\beta}_j^m\right)^T\left(\boldsymbol{\beta}_i - \boldsymbol{\beta}_j\right)\\ &+\lambda \sum_{k=1}^{K} \sum_{\{i\in\mathcal{G}_k, j\in\mathcal{G}_{k'}\}} c_{ij}\rho_\gamma'\left(\left\|\boldsymbol{\beta}_i^m - \boldsymbol{\beta}_j^m\right\|\right)\left\|\boldsymbol{\beta}_i^m - \boldsymbol{\beta}_j^m\right\|^{-1}\left(\boldsymbol{\beta}_i^m - \boldsymbol{\beta}_j^m\right)^T\left\{\left(\boldsymbol{\beta}_i - \boldsymbol{\beta}_i^*\right) - \left(\boldsymbol{\beta}_j - \boldsymbol{\beta}_j^*\right)\right\}.\end{aligned}$$

Since $\sup_i \left\|\boldsymbol{\beta}_i^m - \boldsymbol{\beta}_i^0\right\| \le \phi_n$, for $k \neq k'$, $i \in \mathcal{G}_k$,$j \in \mathcal{G}_{k'}$,

$$\left\|\boldsymbol{\beta}_i^m - \boldsymbol{\beta}_j^m\right\| \ge \min_{i\in\mathcal{G}_k, j\in\mathcal{G}_{k'}} \left\|\boldsymbol{\beta}_i^0 - \boldsymbol{\beta}_j^0\right\| - 2\max_i \left\|\boldsymbol{\beta}_i^m - \boldsymbol{\beta}_i^0\right\| \ge b_n - 2\phi_n > a\lambda.$$

Thus, $\rho_\gamma'(\left\|\boldsymbol{\beta}_i^m - \boldsymbol{\beta}_j^m\right\|) = 0$ by assumption (C1). Therefore,

$$\Gamma_2 = \lambda \sum_{i=1}^{K} \sum_{\{i,j\in\mathcal{G}_k, i<j\}} c_{ij}\rho_\gamma'\left(\left\|\boldsymbol{\beta}_i^m - \boldsymbol{\beta}_j^m\right\|\right)\left\|\boldsymbol{\beta}_i - \boldsymbol{\beta}_j\right\|. \tag{7.32}$$

Also, for $i,j \in \mathcal{G}_k$, $\sup_i \left\|\boldsymbol{\beta}_i^m - \boldsymbol{\beta}_j^m\right\| \le 4t_n$, so $\rho_\gamma'\left(\left\|\boldsymbol{\beta}_i^m - \boldsymbol{\beta}_j^m\right\|\right) \ge \rho'\left(4t_n\right)$ by assumption (C1). Thus, we have

$$\Gamma_2 \ge \sum_{k=1}^{K} \sum_{\{i,j\in\mathcal{G}_k, i<j\}} \lambda c_{ij}\rho_\gamma'\left(4t_n\right)\left\|\boldsymbol{\beta}_i - \boldsymbol{\beta}_j\right\|.$$

Let $\boldsymbol{Q} = \left(\boldsymbol{Q}_1^T, \ldots, \boldsymbol{Q}_n^T\right)^T = \left[\left(\boldsymbol{y} - \boldsymbol{Z}\boldsymbol{\eta} - \boldsymbol{X}\boldsymbol{\beta}^m\right)^T \boldsymbol{\Omega}\boldsymbol{X}\right]^T$ with

$$\boldsymbol{Q}_i = \frac{1}{n_i}\sum_{h=1}^{n_i}\left(y_{ih} - \boldsymbol{z}_{ih}^T\boldsymbol{\eta} - \boldsymbol{x}_{ih}^T\boldsymbol{\beta}_i^m\right)\boldsymbol{x}_{ih}.$$

We have,

$$\begin{aligned}\Gamma_1 &= -\left(\boldsymbol{y} - \boldsymbol{Z}\boldsymbol{\eta} - \boldsymbol{X}\boldsymbol{\beta}^m\right)^T \boldsymbol{\Omega}\boldsymbol{X}\left(\boldsymbol{\beta} - \boldsymbol{\beta}^*\right)\\ &= -\boldsymbol{Q}^T\left(\boldsymbol{\beta} - \boldsymbol{\beta}^*\right)\\ &= -\sum_{k=1}^{K}\sum_{\{i,j\in\mathcal{G}_k, i<j\}} \frac{\left(\boldsymbol{Q}_i - \boldsymbol{Q}_j\right)^T\left(\boldsymbol{\beta}_i - \boldsymbol{\beta}_j\right)}{|\mathcal{G}_k|}.\end{aligned} \tag{7.33}$$

Moreover,

$$\boldsymbol{Q}_i = \frac{1}{n_i}\sum_{h=1}^{n_i}\left(\epsilon_{ih} + \boldsymbol{z}_{ih}^T\left(\boldsymbol{\eta}^0 - \boldsymbol{\eta}\right) + \boldsymbol{x}_{ih}^T\left(\boldsymbol{\beta}_i^0 - \boldsymbol{\beta}_i^m\right)\right)\boldsymbol{x}_{ih},$$

so

$$\begin{aligned}\sup_i \|\boldsymbol{Q}_i\| &\leq \sup_{i,h} \|\boldsymbol{x}_{ih}\| \left(\|\boldsymbol{\xi}\|_\infty + \sup_{i,h} \|\boldsymbol{z}_{ih}\| \left\|\boldsymbol{\eta}^0 - \boldsymbol{\eta}\right\| + \sup_{i,h} \|\boldsymbol{x}_{ih}\| \left\|\boldsymbol{\beta}_i^0 - \boldsymbol{\beta}_i^m\right\| \right) \\ &\leq C_2\sqrt{p}\left(\|\boldsymbol{\xi}\|_\infty + C_3\sqrt{q}\phi_n + C_2\sqrt{p}\phi_n \right),\end{aligned}$$

where $\boldsymbol{\xi} = (\xi_1, \ldots, \xi_n)^T$ with $\xi_i = \frac{1}{n_i}\sum_{h=1}^{n} \epsilon_{ih}$. According to Condition (C3),

$$\begin{aligned}P\left(\|\boldsymbol{\xi}\|_\infty > \sqrt{2c_1^{-1}}\sqrt{\log n / \min n_i} \right) &\leq \sum_{i=1}^{n} P\left(|\xi_i| > \sqrt{2c_1^{-1}}\sqrt{\log n / \min n_i} \right) \\ &= \sum_{i=1}^{n} P\left(\left| \frac{1}{n_i}\sum_{j=1}^{n_i} \epsilon_{ij} \right| > \sqrt{2c_1^{-1}}\sqrt{\log n / \min n_i} \right) \\ &\leq \sum_{i=1}^{n} P\left(\left| \frac{1}{n_i}\sum_{j=1}^{n_i} \epsilon_{ij} \right| > \sqrt{2c_1^{-1}}\sqrt{\log n / n_i} \right) \\ &\leq 2\sum_{i=1}^{n} \exp\left\{ -c_1 2c_1^{-1} \log n \right\} \leq \frac{2}{n}.\end{aligned}$$

Thus, there exists an event E_2 such that $P(E_2) \geq 1 - 2n^{-1}$ and

$$\sup_i \|\boldsymbol{Q}_i\| \leq C_2\sqrt{p}\left(\sqrt{2c_1^{-1}}\sqrt{\log n / \min_i n_i} + C_3\sqrt{q}\phi_n + C_2\sqrt{p}\phi_n \right).$$

Thus,

$$\begin{aligned}&\left| \frac{(\boldsymbol{Q}_i - \boldsymbol{Q}_j)^T (\boldsymbol{\beta}_i - \boldsymbol{\beta}_j)}{|\mathcal{G}_k|} \right| \\ \leq& 2\left|\mathcal{G}_{\min}\right|^{-1} \sup_i \|\boldsymbol{Q}_i\| \, \|\boldsymbol{\beta}_i - \boldsymbol{\beta}_j\| \\ \leq& 2C_2\left|\mathcal{G}_{\min}\right|^{-1}\sqrt{p}\left(\sqrt{2c_1^{-1}}\sqrt{\log n / \min_i n_i} + C_3\sqrt{q}\phi_n + C_2\sqrt{p}\phi_n \right) \|\boldsymbol{\beta}_i - \boldsymbol{\beta}_j\|. \end{aligned} \tag{7.34}$$

Combining (7.32), (7.33) and (7.34), (7.31) follows that

$$\begin{aligned}&Q_n(\boldsymbol{\eta}, \boldsymbol{\beta}) - Q_n(\boldsymbol{\eta}, \boldsymbol{\beta}^*) \\ \geq& \sum_{k=1}^{K} \sum_{\{i,j\in\mathcal{G}_k, i<j\}} \left\{ \lambda c_{ij}\rho'(4t_n) - 2C_2\left|\mathcal{G}_{\min}\right|^{-1}\sqrt{p}\left(\sqrt{2c_1^{-1}}\sqrt{\frac{\log n}{\min_i n_i}} + C_3\sqrt{q}\phi_n + C_2\sqrt{p}\phi_n \right) \right\} \|\boldsymbol{\beta}_i - \boldsymbol{\beta}_j\|.\end{aligned}$$

As $t_n = o(1)$, $\rho'(4t_n) \to 1$. Since $|\mathcal{G}_{\min}| \gg (q + Kp)^{1/2} \max\left(\sqrt{\frac{n}{\min_i n_i}\log n}, (q + Kp)^{1/2} \right)$, $p = o(n)$ and $q = o(n)$, then $|\mathcal{G}_{\min}|^{-1} p = o(1)$ and $|\mathcal{G}_{\min}|^{-1}\sqrt{pq} = o(1)$. Thus, $\lambda \gg |\mathcal{G}_{\min}|^{-1}\sqrt{p}\sqrt{\frac{\log n}{\min n_i}}$,

$\lambda \gg |\mathcal{G}_{\min}|^{-1}\sqrt{pq}\phi_n$ and $\lambda \gg |\mathcal{G}_{\min}|^{-1} p\phi_n$. Therefore, $Q_n(\boldsymbol{\eta}, \boldsymbol{\beta}) - Q_n(\boldsymbol{\eta}, \boldsymbol{\beta}^*) \geq 0$ for sufficiently large n by the assumption (C4) that c_{ij}'s are bounded if i and j are in the same group.

Therefore, combining the two steps, we will have that $Q_n(\boldsymbol{\eta}, \boldsymbol{\beta}) > Q_n(\hat{\boldsymbol{\eta}}^{or}, \hat{\boldsymbol{\beta}}^{or})$ for any $\left(\boldsymbol{\eta}^T, \boldsymbol{\beta}^T\right)^T \in \Theta_n \cap \Theta$ and $(\boldsymbol{\eta}^T, \boldsymbol{\beta}^T)^T \neq ((\hat{\boldsymbol{\eta}}^{or})^T, (\hat{\boldsymbol{\beta}}^{or})^T)^T$. This shows that $((\hat{\boldsymbol{\eta}}^{or})^T, (\hat{\boldsymbol{\beta}}^{or})^T)^T$ is a strict local minimizer of the objective function (7.2) on $E_1 \cap E_2$ with probability at least $1 - 2(K + p + 1)n^{-1}$ for sufficiently large n.

Bibliography

Banerjee, S., Carlin, B. P., and Gelfand, A. E. (2014). *Hierarchical modeling and analysis for spatial data*. Crc Press.

Boyd, S., Parikh, N., Chu, E., Peleato, B., and Eckstein, J. (2011). Distributed optimization and statistical learning via the alternating direction method of multipliers. *Foundations and Trends in Machine Learning*, 3(1):1–122.

Chi, E. C. and Lange, K. (2015). Splitting methods for convex clustering. *Journal of Computational and Graphical Statistics*, 24(4):994–1013.

Fan, J. and Li, R. (2001). Variable selection via nonconcave penalized likelihood and its oracle properties. *Journal of the American statistical Association*, 96(456):1348–1360.

Fan, Z. and Guan, L. (2018). Approximate l_0-estimation of piecewise-constant signals on graphs. *The Annals of Statistics (to appear)*.

Hartigan, J. A. (1990). Partition models. *Communications in statistics-Theory and methods*, 19(8):2745–2756.

Hegarty, A. and Barry, D. (2008). Bayesian disease mapping using product partition models. *Statistics in medicine*, 27(19):3868–3893.

Huang, J. Z., Wu, C. O., and Zhou, L. (2004). Polynomial spline estimation and inference for varying coefficient models with longitudinal data. *Statistica Sinica*, 14(3):763–788.

Hubert, L. and Arabie, P. (1985). Comparing partitions. *Journal of classification*, 2(1):193–218.

Lawson, A. B. (2013). *Bayesian disease mapping: hierarchical modeling in spatial epidemiology*. CRC press.

Li, P., Banerjee, S., Hanson, T. A., and McBean, A. M. (2015). Bayesian models for detecting difference boundaries in areal data. *Statistica Sinica*, 25(1):385–402.

Li, P., Banerjee, S., and McBean, A. M. (2011). Mining boundary effects in areally referenced spatial data using the Bayesian information criterion. *Geoinformatica*, 15(3):435–454.

Lu, H. and Carlin, B. P. (2005). Bayesian areal wombling for geographical boundary analysis. *Geographical Analysis*, 37(3):265–285.

Lu, H., Reilly, C. S., Banerjee, S., and Carlin, B. P. (2007). Bayesian areal wombling via adjacency modeling. *Environmental and Ecological Statistics*, 14(4):433–452.

Ma, S. and Huang, J. (2016). Estimating subgroup-specific treatment effects via concave fusion. *arXiv preprint arXiv:1607.03717*.

Ma, S. and Huang, J. (2017). A concave pairwise fusion approach to subgroup analysis. *Journal of the American Statistical Association*, 112(517):410–423.

Page, G. L. and Quintana, F. A. (2016). Spatial product partition models. *Bayesian Analysis*, 11(1):265–298.

Rand, W. M. (1971). Objective criteria for the evaluation of clustering methods. *Journal of the American Statistical association*, 66(336):846–850.

Reich, B. J. and Bondell, H. D. (2011). A spatial Dirichlet process mixture model for clustering population genetics data. *Biometrics*, 67(2):381–390.

Tibshirani, R. (1996). Regression shrinkage and selection via the lasso. *Journal of the Royal Statistical Society. Series B (Methodological)*, 58(1):267–288.

Vinh, N. X., Epps, J., and Bailey, J. (2010). Information theoretic measures for clusterings comparison: Variants, properties, normalization and correction for chance. *Journal of Machine Learning Research*, 11:2837–2854.

Wang, H., Li, R., and Tsai, C.-L. (2007). Tuning parameter selectors for the smoothly clipped absolute deviation method. *Biometrika*, 94(3):553–568.

Zhang, C.-H. (2010). Nearly unbiased variable selection under minimax concave penalty. *The Annals of statistics*, 38(2):894–942.

CHAPTER 8. SUMMARY AND DISCUSSION

Several problems in GLMs and GLMMs are studied, including link function estimation, small area estimation for compositional data and convergence analysis of Gibbs samplers for Bayesian probit linear mixed models, Bayesian logistic linear regression models and Bayesian logistic linear mixed models. We also consider the spatial subgroup analysis problem.

In Chapter 2, we propose a new algorithm estimating the unknown monotone link function in GLMs by P-spline. It guarantees that the estimated link function is monotone and it can handle multiple covariates. In the simulation study, we compare several symmetric and asymmetric parametric link functions with nonparametric link functions estimated by our proposed algorithm. The results show that the nonparametric link function, fitted using the proposed algorithm, can approximate the true link functions very well in most cases. If the sample size is not very small, in the absence of prior knowledge on the true link function, we recommend the use of the nonparametric link function, which provides a robust alternative for fitting GLMs.

In Chapter 3, we use the generalized Dirichlet distribution to model design based estimates of compositional proportions and obtain small area estimators of compositional proportions. The proposed model allows incorporating auxiliary information, spatial random effects, as well as sampling variance. In a design based Monte Carlo study that represents the NRI data, the model based estimators are superior to design based estimators and multinomial model estimators in terms of RMSE and relative RMSE. The use of the posterior predictive distribution validates the use of the variance model for the NRI application. The GD distribution allows greater flexibility than both the multinomial distribution and the Dirichlet distribution. The variance model allows us to incorporate auxiliary information in the design based variance estimators. The model also allows different covariate, regression parameters and spatial effects for different categories.

In Chapter 4, Chapter 5 and Chapter 6, we study the convergence properties of MCMC algorithms for GLMs and GLMMs in Bayesian framework. We develop two-block Gibbs samplers for the Bayesian probit linear mixed models under both proper priors and improper priors in Chapter 4. We prove the geometric ergodicity of the two-block Gibbs samplers, which guarantee the existence of central limit theorems for MCMC estimators under a finite second moment condition. This is the first ever theoretical analysis of Gibbs samplers for any Bayesian generalized linear mixed model. We propose the corresponding Haar PX-DA algorithms for the two cases, which not only improves the efficiency of the Gibbs samplers, but also inherits their geometric convergence property. In Chapter 5, we prove the geometric rate of convergence for the Polson et al.'s (2013) Pólya-Gamma Gibbs sampler for Bayesian logistic regression with a flat prior on regression coefficients $\boldsymbol{\beta}$. The conditions for geometric ergodicity are the same as the necessary and sufficient conditions for posterior propriety. That means, the Gibbs sampler is always geometrically ergodic if the posterior distribution is proper, which is one of the best possible results one could hope for MCMC convergence in the presence of improper priors. We also prove uniform ergodicity of the two-block Gibbs sampler for Bayesian logistic linear mixed models under truncated Gamma priors in Chapter 6.

In Chapter 7, we consider the spatial clustering problem based on subgroup analysis framework with repeated measures. Spatial information is included in pairwise penalty to control the shrinkage since locations near each other usually have similar patterns. We prove the theoretical properties of the proposed estimator, which shows that the oracle estimator is a local minimizer of the objective function with probability approaching 1. In the simulation study, we use several examples to compare the performances of different weights, which show that the spatial information helps when the minimal group difference is small or the number of repeated measures is small.